THE OFFICIAL MAGAZINE OF THE OCEANOGRAPHY SOCIETY

Oceanography

VOL. 39, NO. 2, JUNE 2026

IN THIS ISSUE

SEA·BIRD
SCIENTIFIC

POWERING SCIENCE-BASED DECISIONS

FOR A BETTER OCEAN.

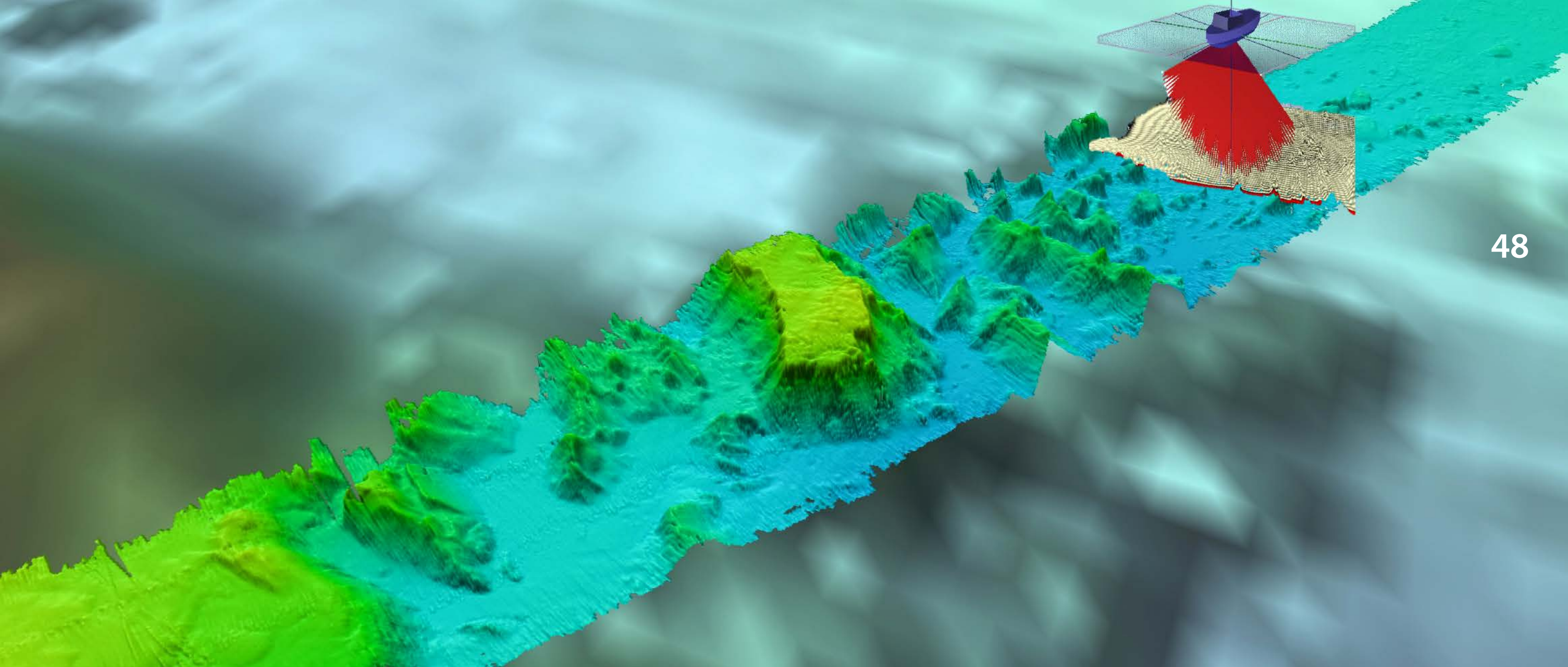

contents

VOL. 39, NO. 2, JUNE 2026

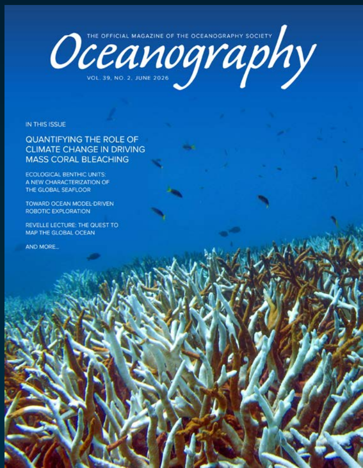

ON THE COVER
Acropora coral, Howland Island, central Pacific Ocean, affected by a global bleaching event in 2010. *Image credit: Kevin Lino, NOAA Fisheries*

CONTACT US
The Oceanography Society
1 Research Court, Suite 450-117
Rockville, MD 20850 USA
t: (1) 301-251-7708
info@tos.org

HAVE YOU MOVED?
Send changes of address to info@tos.org or go to https://tosmc.memberclicks.net, click on Login, and update your profile.

ADVERTISING INFO
Please send advertising inquiries to info@tos.org or go to https://tos.org/oceanography/advertise.

CORRECTIONS
Please send corrections to magazine@tos.org.

SUBMIT A MANUSCRIPT TO *Oceanography*

PUBLISH WITH US

- **EXPAND YOUR AUDIENCE** beyond your subdiscipline.
- **SHARE YOUR WORK** with high-quality graphics that readers can use in classrooms.
- **NO TEMPLATES:** We design the pages for you.
- **FLEXIBLE MANUSCRIPT STRUCTURE** accommodates different article types.
- **BRING YOUR SCIENCE TO LIFE** with videos, animations, audio, and photo galleries.
- **MOVE QUICKLY:** Our goal is to publish papers within six months of submission.

WHAT GETS OUR ATTENTION

FEATURE ARTICLES (<7,000 words) provide an outlet for making significant advances in oceanography accessible to a broad readership. They can include review or synthesis papers, papers that discuss new findings and how they significantly revise our thinking about a topic, or more traditional scientific research papers.

BREAKING WAVES (<3,500 words) articles describe novel approaches to multidisciplinary problems in oceanography. These provocative papers present findings that have the potential to move the field of oceanography forward or in new directions.

OCEAN EDUCATION (<3,500 words) articles should inspire teachers in higher education to try new active, student-centered instruction (ranging from short activities to curricula) and provide ideas/materials to do so.

DIY OCEANOGRAPHY (<3,500 words) articles share all of the relevant information on a homemade sensor, instrument, or software tool(s) so that others can build, or build upon, it. These articles also showcase how this technology was used successfully in the field.

MEETING/WORKSHOP/CONFERENCE REPORTS (<3,500 words) describe the goals, activities, and accomplishments of meetings/workshops/conferences in all aspects of ocean science.

COMMENTARIES (<3,500 words) present analyses of issue of interest to *Oceanography* readers, written by experts in the field.

RIP CURRENT – NEWS IN OCEANOGRAPHY (<1,500 words) articles describe newsworthy items in the field of oceanography.

LEARN MORE

See the online *Oceanography* Author Guidelines for a full listing of manuscript categories and descriptions, publication fees, and details of the manuscript submission process.

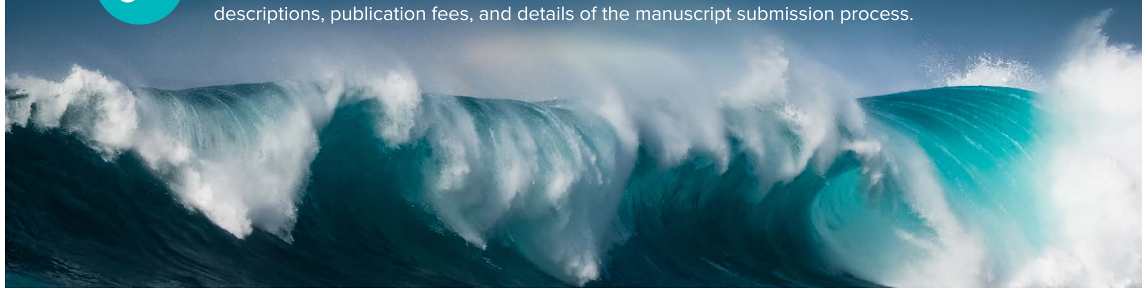

Oceanography

tos.org/oceanography

Oceanography is an open-access, peer-reviewed journal published quarterly by The Oceanography Society. Its articles present significant research, noteworthy achievements, and emerging tools and technologies, and connect ocean science with public policy and education. By publishing articles that are accessible to a broad audience, *Oceanography* promotes cross-disciplinary communication in the ocean sciences.

Oceanography (Print ISSN 1042-8275; Online ISSN 2377-617X) is published by The Oceanography Society, 1 Research Court, Suite 450-117, Rockville, MD 20850 USA.

CELEBRATING 27 YEARS OF

ROGER REVELLE COMMEMORATIVE LECTURES

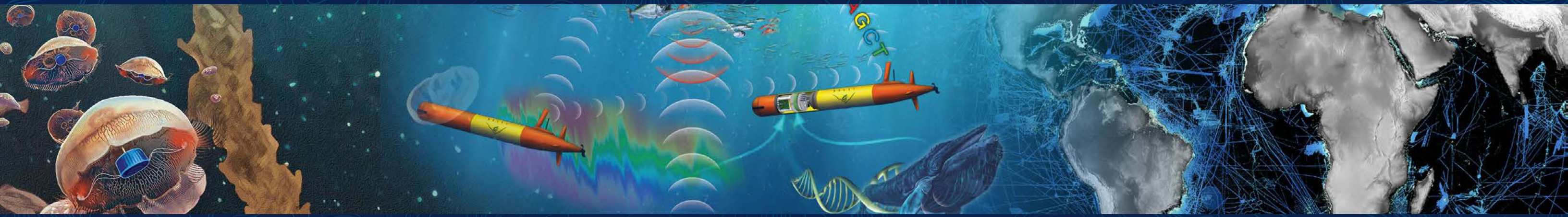

The **Roger Revelle Commemorative Lecture Series** was created by the Ocean Studies Board of the National Academies of Sciences, Engineering, and Medicine to highlight the important links between ocean sciences and public policy. The series was named in honor of the late Roger Revelle, a leader in the field of oceanography for over 50 years who spearheaded efforts to investigate the mechanisms and consequences of climate change.

Oceanography has published these lectures annually, beginning with the first lecture in 1999. Links to the articles are provided below.

2026. The Quest to Map the Global Ocean — by Larry Mayer

2025. Oceanography in the Age of Intelligent Robots and a Changing Climate — by Chris Scholin

2023. Making Waves and Charting New Paths: A Fireside Chat with Kathy Sullivan and Margaret Leinen — by Taylor Goelz

2022. Bio-Inspired Ocean Exploration — by Nicole W. Xu and John O. Dabiri

2021. A Generational Shift in Ocean Stewardship — by Alfredo Giron-Nava and Harriet Harden-Davies

2020. The Story of Plastic Pollution: From the Distant Ocean Gyres to the Global Policy Stage — by Chelsea M. Rochman

2019. Sustainability in Deep Water: Climate Change, Human Pressures, and Biodiversity Conservation — by Lisa A. Levin

2018. Distress Signals: Historical Waypoints in Northwest Atlantic Fisheries Since 1850 — by W. Jeffrey Bolster

2017. Swells, Soundings, and Sustainability, but…"Here Be Monsters" — by Dawn J. Wright

2016. Managing Leviathan: Conservation Challenges for the Great Whales in a Post-Whaling World — by Phillip J. Clapham

2015. Overturning Assumptions: Past, Present, and Future Concerns about the Ocean's Circulation — by M. Susan Lozier

2014. The Contemporary Challenge of the Sea: Science, Society, and Sustainability — by David M. Karl

2013. Melting Ice: What is Happening to Arctic Sea Ice, and What Does It Mean for Us? — by John E. Walsh

2012. Tsunamis: Are We Underestimating the Risk? — by Eddie Bernard

2011. Troubled Waters of the Gulf of Mexico — by Nancy N. Rabalais

2010. The Interconnected Biosphere: Science at the Ocean's Tipping Points — by Jane Lubchenco and Laura E. Petes

2009. The Once and Future Ocean — by Paul G. Falkowski

2008. Looking Down on the Seas: How Satellites Are Revolutionizing Our Understanding of the Ocean — by Michael H. Frielich

2007. What Corals are Dying to Tell Us About CO_2 and Ocean Acidification — by Ken Caldeira

2006. Disasters, Death, and Destruction—Making Sense of Recent Calamities — by Roger A. Pielke, Jr.

2004. Abrupt Climate Changes: Oceans, Ice, and Us — by Richard B. Alley

2003. Sustaining Our Oceans: A Public Resource, A Public Trust — by Admiral James D. Watkins

2002. Beyond the Freedom of the Seas: Ocean Policy for the Third Millennium — by Michael Orbach

2001. Ocean Exploration — by Marcia McNutt

2000. The Oceans and Human Health: The Discovery and Development of Marine-Derived Drugs — by Shirley A. Pomponi

1999. Contemplating Action: Storing Carbon Dioxide in the Ocean — by Peter G. Brewer

RULE CHANGES RELATED TO PUBLICATIONS PROPOSED BY THE US OFFICE OF MANAGEMENT AND BUDGET

In the United States, it has been difficult for scientists to ignore the proposed new Office of Management and Budget (OMB) rules related to scientific awards, international collaboration, conference attendance, and publication fees, among other activities. If implemented as scheduled on October 1, 2026, the proposed rules would significantly affect scientists' ability to carry out work effectively and efficiently. The Oceanography Society (TOS) has shared these proposed rules with our membership, and TOS's president, Paula Bontempi, has urged everyone to submit public comments by July 13 (see https://tos.org/omb-2026-0034). I certainly have.

Here, I focus on the proposed rules' potential consequences for publications.

From the Federal Register (v. 91, n. 103, May 29, 2026, p. 32232): "OMB is revising the section to make publication costs unallowable unless such costs are expressly required by statute or approved in advance by the Federal agency on a case-by-case basis."

This is a fundamental change to the current rules, which state: "Page charges, article processing charges (APCs), or similar fees such as open access fees for professional journal publications and other peer-reviewed publications resulting from a Federal award are allowable where the publications report work supported by the Federal Government," and the charges are levied impartially by the journal, whether or not the research was supported under a Federal award.

The ambiguous language makes the consequences of the proposed change a bit unclear. On the one hand, it could mean that as long as APCs are an approved item within the grant's budget ("approved in advance"), then authors can, as in the past, charge the APC to their grant without needing to seek further approval. On the other hand, the "case-by-case" wording suggests that for every paper scientists wish to publish, they would need to ask their agency program manager for permission to use grant funds. If that is the government's intent, then this requirement imposes a huge new burden on the authors—and their program managers. Without knowing how favorably such requests will be received, and how quickly the program manager will respond, is it worth the time and effort to submit such requests? Will there be a simple form and portal to submit publication requests? Will agencies require letters containing detailed justification for publishing? Can that letter contain a request for a budget supplement to support APCs, or will the grantee need to use funds budgeted for something else? Will program managers need approval from a political appointee before responding positively? If APCs cannot be paid from grants, where will the funds to publish come from? If the burden of paying APCs is shifted to universities, how much support will universities (and other institutions) be able to provide to their researchers?

And, of course, if APCs are no longer permitted in federal grants, will journals like *Oceanography*, which is published by a small nonprofit society, be able to survive? Our APCs cover the cost of humans doing work (editing, design, and web posting, among other tasks), plus they allow us to make your work publicly and openly accessible on the web. We do not have an advertising base nor large donors to cover the costs of publishing and maintaining an archive of past issues.

The text of the proposed new rule also provides OMB's rationale for this rule change: "Publication costs are not inherently necessary to carry out the core programmatic objectives of most Federal awards. In many cases, such activities are discretionary, vary widely in scope and costs, and may serve institutional, professional, or reputational interests rather than the specific objectives of the Federal program."

That statement represents a fundamental misunderstanding of how science advances or an intentional misrepresentation of the need for grants to support scientific publishing. As any scientist knows, good experimental design relies on what you and your colleagues around the globe have learned from previous research, as laid out in the peer-reviewed literature and as discussed at conferences and elsewhere. Advancing the science also relies on your colleagues' evaluation of your experimental design and findings, as shared in the peer-reviewed literature and at conferences. Publishing results offers transparency in scientific background, methodology, and results, and permits others to duplicate your experiment to ensure its validity (reproducibility). Peer review and sharing our results simply makes our science better. Importantly, supporting APCs (and conference attendance) also allows program managers and other agency representatives to see and evaluate the results of the grants they supported.

If you haven't already, I urge you to use this public comment period to submit your thoughts on these proposed OMB rules, whether you pick one or a few rules that are particularly meaningful to you or you take on the whole batch of changes. With more voices, perhaps we can make a difference.

Ellen S Kappel

Ellen S. Kappel, Editor

ARTICLE DOI. https://doi.org/10.5670/oceanog.2026.e206

Argo AT A CROSSROADS

ACHIEVEMENTS, IMPACTS, AND THE IMPERATIVE FOR SUSTAINED GLOBAL OCEAN OBSERVATIONS

By Lilian A. Dove, Gaël Forget, Momme Hell, Verena Hormann, Irina Marinov, Monique Messié, Anastasia Romanou, Jacob Steinberg, and Lynne D. Talley

ABSTRACT. Over the past 25 years, the international Argo program has become the backbone of subsurface ocean observation and a prime example of a highly successful, sustained global scientific collaboration. Through evolving technology, the program has become more efficient while also expanding its suite of observations, with a subset of floats equipped with biogeochemical sensors or the ability to sample below 2,000 m water depth. By delivering continuous, global measurements essential for climate science and national security operations, Argo observations underpin advances in understanding ocean heat uptake, circulation, carbon cycling, deoxygenation, and marine ecosystem variability, while also supporting operational forecasting, ocean reanalysis, and coupled Earth system prediction. Here, we synthesize Argo's scientific, operational, and societal contributions while emphasizing the importance of sustained continuity and expansion of the observing system. We, members of the US CLIVAR Phenomena, Observations, and Synthesis Panel, argue that Argo has become an indispensable global infrastructure whose long-term value depends on maintaining consistent global coverage and data quality. Emerging advances in biogeochemical sensing, deep-ocean observations, artificial intelligence, and data systems provide opportunities to further strengthen the network, but continued investment and international coordination are essential to preserve and expand humanity's capacity to monitor and predict a changing ocean and climate system.

The ocean, covering more than two-thirds of our planet, exerts a profound influence on Earth's climate system by regulating regional climates, driving weather patterns, and absorbing and redistributing vast amounts of heat and carbon dioxide from the atmosphere. Despite its central role, the global ocean remains largely unexplored, owing both to its immense scale and to the opacity of seawater to the electromagnetic signals commonly used in atmospheric and space-based observations. As a result, satellite coverage is largely restricted to the ocean's surface and upper tens of meters. In this context, the Argo program, through an extraordinary international collaboration, has emerged as a transformative force over the past 25 years, deploying a global fleet of autonomous underwater profilers that have delivered sustained, frequent, and widespread measurements of the ocean's interior dynamics and properties (Roemmich et al., 1999, 2019; Thierry et al., 2025).

As members of the Phenomena, Observations, and Synthesis (POS) Panel of the US Climate Variability and Predictability Program (US CLIVAR), we are inspired to highlight Argo as a remarkable international success story. The mission of the POS Panel is to improve understanding of climate phenomena, inform the needs for a sustained global climate observing system, and guide the development of global climate-relevant datasets and model synthesis. Our range of expertise in ocean and climate science enables us to assert that Argo affects virtually everyone who depends on or cares about weather prediction, ecosystem health, and national security, both in the United States and globally. Argo's impact resonates across various sectors, from academic research to practical applications in industries and government, making it a fundamental piece of modern Earth system science.

Here, we spotlight a critical juncture regarding the future of monitoring Earth's biosphere with Argo. We champion continued investment in this critical infrastructure that advances and directly supports US federal research priorities while serving as a model for sustained multinational scientific cooperation. Through partnerships between governments, academia, nonprofit research institutions, and industry, Argo supports ocean data assimilation and modeling, workforce development in data sciences, and ongoing exploration of the ocean and polar regions. Together, these efforts accelerate technological and scientific innovation and result in the delivery of applied science products to stakeholders.

KEY OUTCOMES FROM 25 YEARS OF ARGO

For over two decades, Argo has been a core component of the Global Ocean Observing System (GOOS), coordinated internationally through the United Nations Educational, Scientific, and Cultural Organization (UNESCO). The Argo program has transformed oceanography from a data-sparse discipline into one grounded in sustained, global observations of the ocean's interior

(Figure 1). Numerous comprehensive reviews (e.g., Riser et al., 2016; Roemmich et al., 2019; Wong et al., 2020; G.C. Johnson et al., 2022; Thierry et al., 2025) have documented these advances in detail. Rather than reiterating individual findings, we synthesize Argo's principal outcomes across three domains: scientific discovery, operational capability, and education (Figure 2).

Argo has fundamentally reshaped understanding of the ocean's role in the climate system by providing continuous, global measurements of temperature and salinity in the upper 2,000 m of the ocean. These observations underpin quantification of key climate indicators, including ocean heat content, sea level rise, and changes in the global hydrological cycle. More recently, through the Biogeochemical-Argo (BGC-Argo; Claustre et al., 2020) and Deep Argo (Zilberman et al., 2023) expansions, data coverage has been extended to include biogeochemical parameters and the full ocean depth. Together, the core observations of temperature and salinity, BGC-Argo, Deep Argo, and proposed polar expansions of Argo are referred to as "OneArgo" (Thierry et al., 2025). With its expanded capabilities, Argo has enabled advances in understanding full-depth ocean circulation and mixing, while also transforming observation of the ocean carbon system, biological productivity, and oxygen distribution (Claustre et al., 2020; G.C. Johnson et al., 2022). As highlighted in prior review articles, Argo now provides the dominant share of global subsurface observations for many essential climate variables (Figure 1), establishing an internally consistent benchmark for evaluating Earth system variability and change.

Beyond its scientific contributions, Argo provides a cornerstone for climatology, operational oceanography, and environmental prediction. Argo profiles are routinely assimilated into ocean and coupled Earth system models to constrain initial conditions, reduce uncertainty, and improve forecasts spanning short-range weather to seasonal and decadal climate variability (Figure 3). These observations enhance prediction of phenomena such as the El Niño-Southern Oscillation (ENSO), marine heatwaves, and tropical cyclone intensity, and are operationally integrated into forecasting systems at US agencies that include the National Hurricane Center of the National Oceanic and Atmospheric Administration (NOAA; Halliwell et al., 2017) and the US Navy (Chen et al., 2017), as well as those at international modeling centers (Balmaseda et al., 2024). Argo data are also central to ocean reanalyses, providing coherent reconstructions of the evolving ocean state and

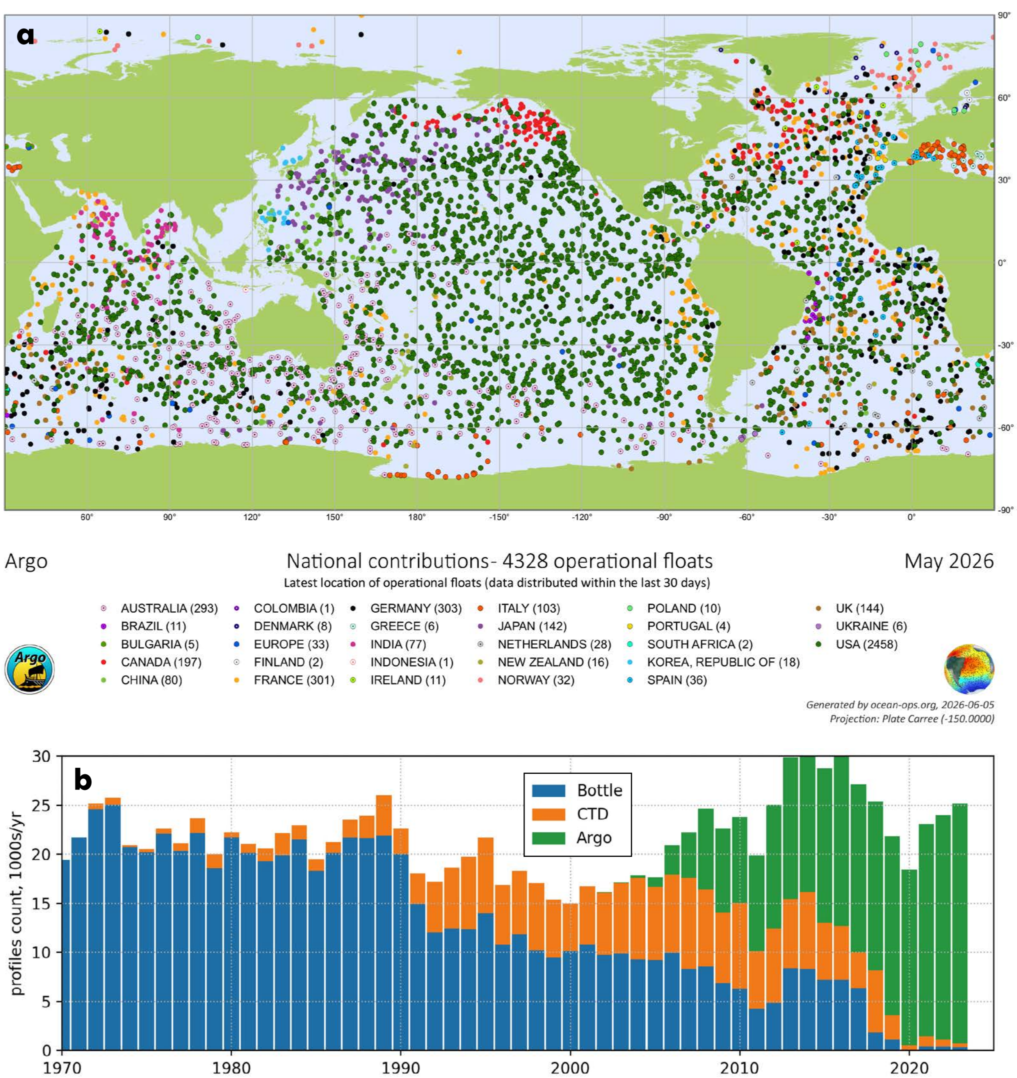

FIGURE 1. Status and contribution of the Argo network. (a) Dots represent operating floats contributed to the Argo network by various countries as of May 2026. (b) Oxygen profiles are plotted per year in the NOAA World Ocean Database collected by Argo as opposed to traditional observation methods (bottle, CTD). *Panel (a) reproduced from ocean-ops.org. Panel (b) reproduced from Thierry et al. (2025), under CC BY license*

critical benchmarks for climate models; in many regions, Argo is the dominant source of subsurface ocean observations for these systems. Its global, internally consistent data record further supports emerging essential satellite measurement calibration and bias correction efforts, as well as artificial intelligence and machine learning (AI/ML) approaches that rely on large training datasets to improve prediction of ocean and climate variability (Forget, et al., 2015; Jiménez-Esteve et al., 2025). At the same time, the growing biogeochemical Argo record enables detection of declining ocean oxygen and hypoxic regions, with implications for marine ecosystems, fisheries management, and nitrogen cycling (Claustre et al., 2020; Thierry et al., 2025).

Finally, Argo's openly accessible, near-real-time data have also had a profound impact on education and workforce development. The program has supported hundreds of graduate theses across oceanography, climate science, and related fields (Argo, 2024) while also serving as a widely used resource in undergraduate curricula. At the K–12 level, initiatives such as Adopt-a-Float and curated educational materials have enabled primary and secondary school students worldwide to engage directly with real ocean data, fostering early interest in Earth science, engineering, and data literacy. More broadly, Argo exemplifies the value of open, international scientific infrastructure, providing equitable access to high-quality environmental data and enabling participation from a global community of researchers, educators, and students.

ARGO'S RETURN ON INVESTMENT

Given its immense and wide-ranging impacts (Figure 2), Argo delivers unparalleled value for its cost. In the last 25 years, Argo floats have collected over three million temperature and salinity profiles, greatly exceeding the number of subsurface (>1,000 m) observations available from the historical record prior to Argo (Wong et al., 2020; Thierry et al., 2025). BGC-Argo has helped fill the gap in oxygen data created by declining shipboard measurements (Figure 1b). This prolific output is achieved at a fraction of the traditional cost: producing one core Argo profile costs less than $250 (in present-day US dollars) compared to over $10,000 for one ship-based temperature and salinity profile (Jayne et al., 2017). Likewise, a biogeochemical profile by BGC-Argo costs between $800 and $900, while collecting an equivalent suite of biogeochemical observations from a research vessel typically costs orders of magnitude more due to ship time and analytical expenses (K.S. Johnson and Claustre, 2026).

The value of these observations extends across sectors, supporting applications in weather forecasting, fisheries, shipping, and national security. While difficult to quantify precisely, Argo's central role in GOOS implies economic benefits on the order of hundreds of millions of dollars annually (Kite-Powell, 2009). Crucially, no other observing system provides sustained, global subsurface coverage at comparable scale and cost. Satellite (Barale et al., 2010) and ship-based (Sloyan et al., 2019) observations are complementary but cannot replace this capability; a resilient ocean observing enterprise depends on the integration of all these observational data types.

Argo's commitment to free and open data further amplifies its impact, ensuring that these observations are immediately accessible worldwide and fully utilized across scientific, operational, and societal applications (Roemmich et al., 1999). The freely available data guide actionable science such as detection of extreme weather and early warning signals for disaster response, maritime safety, and global shipping route optimization, as well as aquaculture and fisheries management. Open access to high-quality ocean observations also helps expand scientific capacity in developing countries, where freely available data are essential for advancing research programs, supporting education and workforce development, and enabling participation in the global ocean observing community.

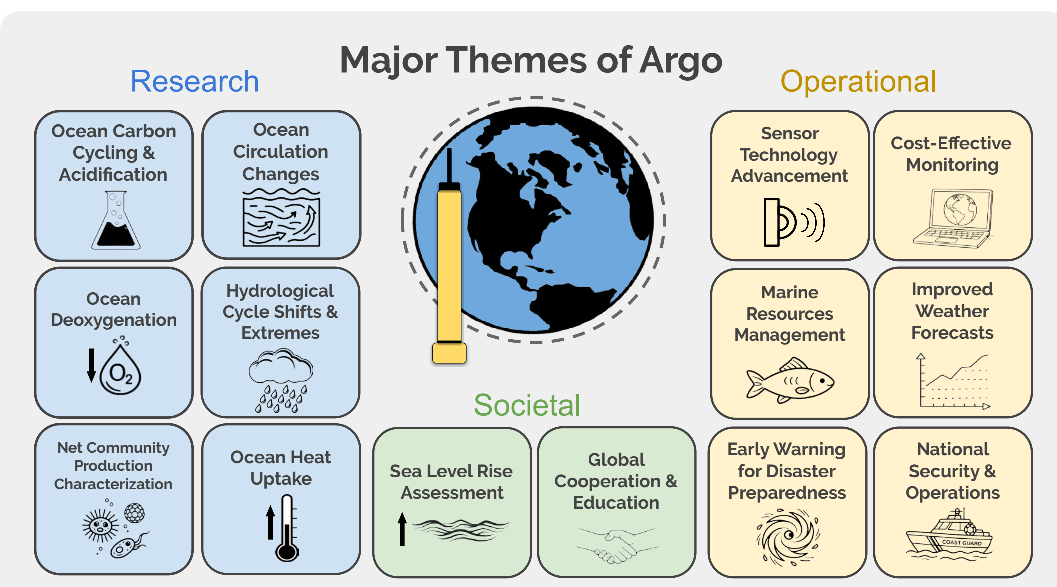

FIGURE 2. Operational, societal, and scientific goals and approaches enabled by Argo. Research themes include measurements of essential Earth system variables, both those directly observed and those calculated. Operational themes include capacity building and technological breakthrough potentials. Societal themes include international and national priorities for safety, security, and cooperation.

THE NECESSITY OF CONTINUITY TO THE ARGO MISSION

Sustained continuity is essential to Argo's value. The program's impact depends on not only global coverage but also the consistency of its long-term record. Interruptions in sampling or shifts in measurement systems risk degrading the climate data record in ways that cannot be recovered retrospectively (Lidström and Wickberg, 2025). Reduced coverage below scientifically determined targets for the Argo program—Core Argo (2,500 floats), Biogeochemical Argo (1,000 floats), and Deep Argo (1,200 floats)—will diminish the system's ability to resolve seasonal-to-interannual variability, including early warning signals for extreme events. It will also weaken constraints on ocean heat and carbon uptake and increase uncertainty in estimates of large-scale circulation and water mass changes (G.C. Johnson et al., 2015; Chamberlain et al., 2023). Because the configuration of the Argo array is already minimal for meeting climate-scale objectives (Roemmich et al. 2009), further reduction would not only degrade resolution but also risk crossing thresholds beyond which key signals become aliased or undetectable (Sivareddy et al., 2017; Gasparin et al., 2023). Maintaining full coverage is not an aspirational goal but a requirement for preserving the integrity, usability, and long-term societal value of GOOS. Reduction of the Argo program would undermine basic as well as actionable research and their critical roles in protecting ecosystems and societies.

The continuity of Argo is critical because systems, such as forecasting and reanalysis, and emerging AI/ML applications, depend on Argo as their primary source of subsurface observations (Forget et al., 2015; Lellouche et al., 2021). Disruptions would propagate directly into reduced forecast skill and increased uncertainty. The implications of a reduced Argo program extend beyond science to economic stability and national security. Given the reliance on Argo data across a wide range of economic sectors, from shipping and fisheries to disaster preparedness and national defense, gaps in coverage represent a form of strategic vulnerability. Argo provides not only observations of the ocean but also the basis for decisions that affect billions of dollars in economic activity and public safety. Ensuring continuity is therefore essential to maintaining reliable environmental intelligence in a changing climate.

The continued development and deployment of new technologies, including improved sensors that can expand observational capabilities, increase accuracy, and reduce costs, are key aspects of the Argo system. However, given the importance of data continuity, advances in sensor technology must be integrated carefully. The strength of the Argo program lies in the stability and comparability of its long-term record, which depends on consistent measurement practices across decades (Roemmich et al., 1999; Riser et al., 2016; Thierry et al., 2025). Introducing new sensors inevitably risks introducing biases, calibration offsets, or shifts in data characteristics that can mask real climate signals. To avoid this, sensor evolution must be accompanied by careful cross calibration, overlap between old and new technologies, and rigorous validation against reference standards (World Meteorological Organization, 2015; Biogeochemical-Argo Planning Group, 2016). At the same time, failing to adopt improved sensors would limit the system's ability to address emerging risk factors and scientific questions, from ocean carbon uptake to deoxygenation (Ito et al., 2026). The challenge, therefore, is not to choose between consistency and innovation, but to manage their coexistence and intensify effort, ensuring that technological progress strengthens the observing system without compromising sustainability or the integrity of the environmental record it is designed to sustain.

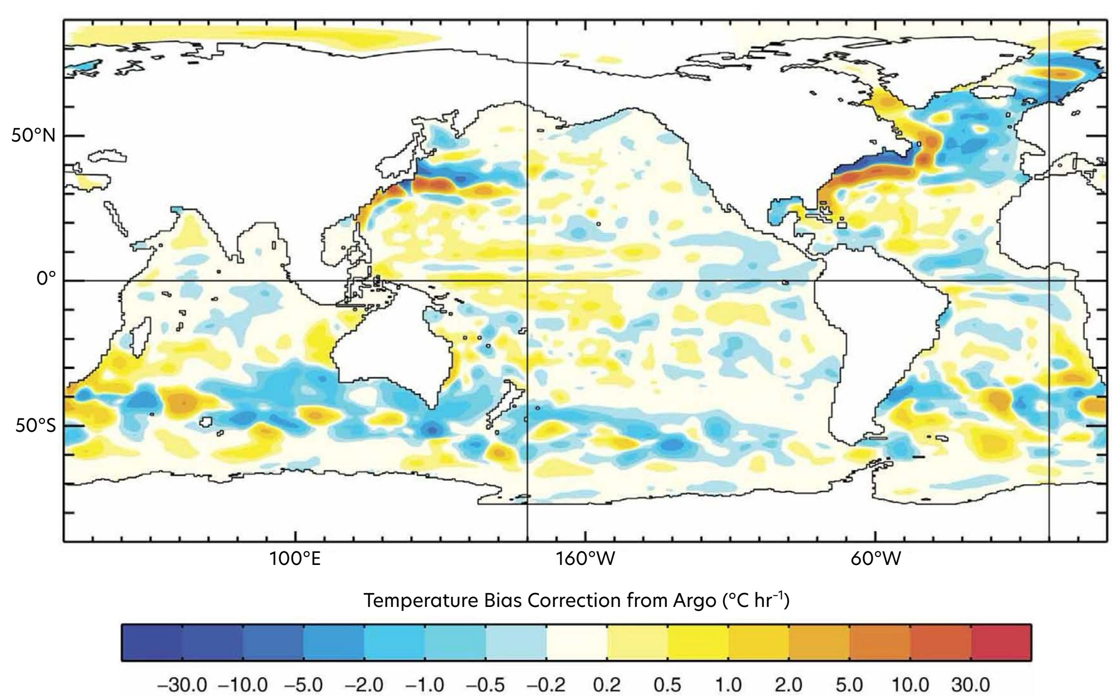

FIGURE 3. Temperature correction estimated from Argo float observations for depths of 300–700 m. This correction represents how model temperatures are adjusted over time to better match real-world ocean measurements, as applied within the ORAS4 ocean reanalysis (a combined model-observation ocean reconstruction). *Figure reproduced from Balmaseda et al. (2013)*

NEW FRAMEWORKS FOR AN INDISPENSABLE PROGRAM

Meeting the research, operational, and educational demands of the coming decades may require rethinking Argo not simply as a research program, but as an enduring infrastructure. Currently, in the United States, which funds half of the international Argo program, it is funded through National Science Foundation (NSF), National Aeronautics and Space Administration (NASA), and NOAA research programs rather than through a dedicated long-term operational infrastructure line. As reliance on Argo data grows across forecasting, climate monitoring, and decision-making systems, its sustained operation must be treated with the same priority as other core environmental observing networks. This shift in framing from project-based funding toward long-term infrastructure investment would provide the stability needed to maintain continuity while enabling strategic and sustainable innovation (NASEM, 2017; European Marine Board, 2021).

Recognizing the need for a more scalable global observing network, the Argo community is advancing efforts to streamline technical infrastructure and operations. Argo-affiliated international partners, data system developers, and observing system engineers have already begun to develop new technical frameworks to improve efficiency and scalability. These efforts include modernizing data management pipelines, integrating cloud-based and AI-enabled workflows, improving interoperability across observing platforms, and developing more autonomous quality control systems to accommodate the rapidly growing volume and complexity of ocean observations. Efforts to standardize communication interfaces and data systems across float platforms are reducing operational complexity and lowering costs while also improving interoperability and data accessibility within the broader GOOS program. These advances position Argo to more seamlessly incorporate new technologies without fragmenting the observing network.

Emerging AI/ML approaches in data assimilation and ocean modeling are creating new pathways for scientific and operational advances, with Argo positioned as a primary source of the observations needed to train, constrain, and evaluate these next-generation systems. Throughout the program's life, Argo observations have been routinely integrated into operational and research forecasting frameworks, underpinning ocean reanalyses and coupled climate predictions. Advances in AI/ML therefore build on an already mature assimilation infrastructure, offering pathways to improve how Argo data are used, potentially through more efficient data assimilation, model optimization, improved error characterization, and the capacity for adaptive sampling strategies that respond to evolving ocean conditions. Looking ahead, developments in high-performance computing systems and increased use of graphics processing units (GPUs) may further enhance weather prediction and ocean state estimation systems that already rely heavily on Argo. Rather than requiring a fundamental shift, these innovations position Argo to remain central to a new generation of forecasting systems that will support a more flexible and responsive observing network while preserving the continuity and reliability that make it indispensable.

MAINTAINING UNITED STATES LEADERSHIP IN A GLOBAL SUCCESS STORY

Argo's path has been one of remarkable success and collaboration, but the journey ahead demands critical decisions, renewed commitment, and potentially new organizational frameworks. In our view, augmenting Argo, not just maintaining it, is of the utmost importance for science and society. By extending observations to the full depth of the ocean, sustaining the newly built global BGC float array, and enhancing coverage in polar regions, the proposed expansion to a complete OneArgo by 2030 (Thierry et al., 2025) would transform our mechanistic and quantitative understanding of the world ocean as well as our ability to predict its future evolution. This evolution is not merely an enhancement of existing capabilities but a necessary leap to address emerging scientific questions and environmental risks while continuing to support existing data-assimilating and machine-learning infrastructure.

Recently in the United States, leaders of the ocean science and technology agencies on the National Science and Technology Council have reaffirmed the value that data from Argo floats bring to all agency missions (National Science and Technology Council Subcommittee on Ocean Science and Technology, 2024). This reaffirmation presents an opportunity for the United States to strengthen its commitment, for fellow leaders in the Argo community (the European Union, United Kingdom, Japan, Canada, India, Australia) to expand their investment in the program, and for emerging leaders to play a larger role in this global initiative.

As we look ahead, the future of Argo presents several possible paths. In an optimistic scenario, sustained and reliable funding would support a technologically advanced, publicly accessible network that delivers unparalleled insights into our ocean and its societal impacts. By contrast, maintaining the status quo with flat or even decreased funding risks stagnation and an erosion of scientific and operational capacities. Because Argo is already deeply embedded in operational forecasting and climate monitoring frameworks, such degradation would directly reduce predictive skill for weather, climate, and ocean hazards, thus increasing the risk to humanity, societies, and individuals. If the United States does not rise to the challenge, international partners will need to shoulder the responsibility of sustaining momentum and shaping the next era of global ocean observations.

At this critical juncture, Argo represents a story of great past achievements through strong US involvement and international collaboration as well as expected future accomplishments with renewed dedication and financial support. The path we choose will determine not only the future of global ocean measurements but also our ability to understand and respond to the challenges posed by a changing climate and environment.

REFERENCES

Argo. 2024. "Thesis Citations," https://argo.ucsd.edu/outreach/publications/thesis-citations.

Balmaseda, M.A., K. Mogensen, and A.T. Weaver. 2013. Evaluation of the ECMWF ocean reanalysis system ORAS4. *Quarterly Journal of the Royal Meteorological Society* 139(674):1,132–1,161, https://doi.org/10.1002/qj.2063.

Balmaseda, M.A., B. Balan Sarojini, M. Mayer, S. Tietsche, H. Zuo, F. Vitart, and T.N. Stockdale. 2024. Impact of the ocean in-situ observations on the ECMWF seasonal forecasting system. *Frontiers in Marine Science* 11:1456013, https://doi.org/10.3389/fmars.2024.1456013.

Barale, V., J. Gower, and L. Alberotanza, eds. 2010. *Oceanography from Space*. Springer, Dordrecht, 374 pp., https://doi.org/10.1007/978-90-481-8681-5.

Biogeochemical-Argo Planning Group. 2016. The scientific rationale, design and implementation plan for a Biogeochemical-Argo float array. Ifremer, https://doi.org/10.13155/46601.

Chamberlain, P., L.D. Talley, B. Cornuelle, M. Mazloff, and S.T. Gille. 2023. Optimizing the Biogeochemical Argo float distribution. *Journal of Atmospheric and Oceanic Technology* 40(11):1,355–1,379, https://doi.org/10.1175/JTECH-D-22-0093.1.

Chen, S., J.A. Cummings, J.M. Schmidt, E.R. Sanabia, and S.R. Jayne. 2017. Targeted ocean sampling guidance for tropical cyclones. *Journal of Geophysical Research: Oceans* 122(5):3,505–3,518, https://doi.org/10.1002/2017JC012727.

Claustre, H., K.S. Johnson, and Y. Takeshita. 2020. Observing the global ocean with Biogeochemical-Argo. *Annual Review of Marine Science* 12:23–48, https://doi.org/10.1146/annurev-marine-010419-010956.

European Marine Board. 2021. *Sustaining in situ Ocean Observations in the Age of the Digital Ocean.* European Marine Board, 15 pp., https://www.marineboard.eu/sites/marineboard.eu/files/public/publication/EMB_PB9_Sustaining_OO_web_HQ.pdf.

Forget, G., J.-M. Campin, P. Heimbach, C.N. Hill, R.M. Ponte, and C. Wunsch. 2015. ECCO version 4: An integrated framework for non-linear inverse modeling and global ocean state estimation. *Geoscientific Model Development* 8(10):3,071–3,104, https://doi.org/10.5194/gmd-8-3071-2015.

Forget, G., D. Ferreira, and X. Liang. 2015. On the observability of turbulent transport rates by Argo: Supporting evidence from an inversion experiment. *Ocean Science* 11(5):839–853, https://doi.org/10.5194/os-11-839-2015.

Gasparin, F., J.-M. Lellouche, S.E. Cravatte, G. Ruggiero, B. Rohith, P.Y. Le Traon, and E. Rémy. 2023. On the control of spatial and temporal oceanic scales by existing and future observing systems: An observing system simulation experiment approach. *Frontiers in Marine Science* 10:1021650, https://doi.org/10.3389/fmars.2023.1021650.

Halliwell, G.R. Jr., M.F. Mehari, M. Le Hénaff, V.H. Kourafalou, I.S. Androulidakis, H.S. Kang, and R. Atlas. 2017. North Atlantic Ocean OSSE system: Evaluation of operational ocean observing system components and supplemental seasonal observations for potentially improving tropical cyclone prediction in coupled systems. *Journal of Operational Oceanography* 10(2):154–175, https://doi.org/10.1080/1755876X.2017.1322770.

Ito, T., Y. Takano, Y.A. Eddebbar, J.F. Tiputra, Z. Wang, S. Minobe, L. Cheng, J. Du, and Y. Abe. 2026. Are simulated ocean deoxygenation rates consistent with the observational reconstructions? *Annual Review of Earth and Planetary Sciences* 54:239–267, https://doi.org/10.1146/annurev-earth-032524-123111.

Jayne, S.R., D. Roemmich, N. Zilberman, S.C. Riser, K.S. Johnson, G.C. Johnson, and S.R. Piotrowicz. 2017. The Argo Program: Present and future. *Oceanography* 30(2):18–28, https://doi.org/10.5670/oceanog.2017.213.

Jiménez-Esteve, B., D. Barriopedro, J.E. Johnson, and R. García-Herrera. 2025. AI-driven weather forecasts to accelerate climate change attribution of heatwaves. *Earth's Future* 13(8):e2025EF006453, https://doi.org/10.1029/2025EF006453.

Johnson, G.C., J.M. Lyman, and S.G. Purkey. 2015. Informing Deep Argo array design using Argo and full-depth hydrographic section data. *Journal of Atmospheric and Oceanic Technology* 32(11):2,187–2,198, https://doi.org/10.1175/JTECH-D-15-0139.1.

Johnson, G.C., S. Hosoda, S.R. Jayne, P.R. Oke, S.C. Riser, D. Roemmich, T. Suga, V. Thierry, S.E. Wijffels, and J. Xu. 2022. Argo—Two decades: Global oceanography, revolutionized. *Annual Review of Marine Science* 14:379–403, https://doi.org/10.1146/annurev-marine-022521-102008.

Johnson, K.S., and H. Claustre. 2026. Overview of BGC-Argo: Accomplishments & capabilities. Presentation to the National Academies of Sciences, Engineering, and Medicine, https://www.nationalacademies.org/cdn/materials/a1cfc50f-a505-49b6-9c5a-32ebfbfc220f.

Kite-Powell, H.L. 2009. Economic considerations in the design of ocean observing systems. *Oceanography* 22(2):44–49, https://doi.org/10.5670/oceanog.2009.37.

Lellouche, J.-M., E. Greiner, R. Bourdallé-Badie, G. Garric, A. Melet, M. Drévillon, C. Bricaud, M. Hamon, O. Le Galloudec, C. Regnier, and others. 2021. The Copernicus global 1/12° oceanic and sea ice GLORYS12 reanalysis. *Frontiers in Earth Science* 9:698876, https://doi.org/10.3389/feart.2021.698876.

Lidström, S., and A. Wickberg. 2025. Co-environing the ocean and climate: The Argo program. *Environment and Planning E: Nature and Space* 8(6):2,002–2,017, https://doi.org/10.1177/25148486251377704.

NASEM (National Academies of Sciences, Engineering, and Medicine). 2017. *Sustaining Ocean Observations to Understand Future Changes in Earth's Climate*. The National Academies Press, Washington, DC, 150 pp., https://doi.org/10.17226/24919.

National Science and Technology Council Subcommittee on Ocean Science and Technology. 2024. Statement of Support for OneArgo, June 27, 2024, https://www.noaa.gov/sites/default/files/2024-07/SOST Statement of Support for OneArgo (1).pdf.

Riser, S.C., H.J. Freeland, D. Roemmich, S. Wijffels, A. Troisi, M. Belbéoch, and S.R. Jayne. 2016. Fifteen years of ocean observations with the global Argo array. *Nature Climate Change*, 6(2):145–153, https://doi.org/10.1038/nclimate2872.

Roemmich, D., O. Boebel, Y. Desaubies, H. Freeland, B. King, P.-Y. LeTraon, R. Molinari, B. Owens, S. Riser, U. Send, and others. 1999. Argo: The global array of profiling floats. *CLIVAR Exchanges* 4(3):4–5.

Roemmich, D., G.C. Johnson, S. Riser, R. Davis, J. Gilson, W.B. Owens, S.L. Garzoli, C. Schmid, and M. Ignaszewski. 2009. The Argo Program: Observing the global ocean with profiling floats. *Oceanography* 22(2):34–43, https://doi.org/10.5670/oceanog.2009.36.

Roemmich, D., M.H. Alford, H. Claustre, K. Johnson, B. King, J. Moum, P. Oke, W.B. Owens, S. Pouliquen, S. Purkey, and others. 2019. On the future of Argo: A global, full-depth, multi-disciplinary array. *Frontiers in Marine Science* 6:439, https://doi.org/10.3389/fmars.2019.00439.

Sivareddy, S., A. Paul, T. Sluka, M. Ravichandran, and E. Kalnay. 2017. The pre-Argo ocean reanalyses may be seriously affected by the spatial coverage of moored buoys. *Scientific Reports* 7(1):46685, https://doi.org/10.1038/srep46685.

Sloyan, B.M., R. Wanninkhof, M. Kramp, G.C. Johnson, L.D. Talley, T. Tanhua, E. McDonagh, C. Cusack, E. O'Rourke, E. McGovern, and others. 2019. The Global Ocean Ship-Based Hydrographic Investigations Program (GO-SHIP): A platform for integrated multidisciplinary ocean science. *Frontiers in Marine Science* 6:445, https://doi.org/10.3389/fmars.2019.00445.

Thierry, V., H. Claustre, O. Pasqueron de Fommervault, N. Zilberman, K.S. Johnson, B.A. King, S.E. Wijffels, U.T.V.S. Baskar, M.A. Balmaseda, M. Belbeoch, and others. 2025. Advancing ocean monitoring and knowledge for societal benefit: The urgency to expand Argo to OneArgo by 2030. *Frontiers in Marine Science* 12:1593904, https://doi.org/10.3389/fmars.2025.1593904.

Wong, A.P.S., S.E. Wijffels, S.C. Riser, S. Pouliquen, S. Hosoda, D. Roemmich, J. Gilson, G.C. Johnson, K. Martini, D.J. Murphy, and others. 2020. Argo data 1999–2019: Two million temperature-salinity profiles and subsurface velocity observations from a global array of profiling floats. *Frontiers in Marine Science* 7:700, https://doi.org/10.3389/fmars.2020.00700.

World Meteorological Organization. 2015. *Status of the Global Observing System for Climate*. World Meteorological Organization, Geneva, 373 pp., https://library.wmo.int/records/item/54812-status-of-the-global-observing-system-for-climate.

Zilberman, N.V., V. Thierry, B. King, M. Alford, X. André, K. Balem, N. Briggs, Z. Chen, C. Cabanes, L. Coppola, and others. 2023. Observing the full ocean volume using Deep Argo floats. *Frontiers in Marine Science* 10:1287867, https://doi.org/10.3389/fmars.2023.1287867.

ACKNOWLEDGMENTS

Any opinions or views expressed or implied herein are those of the authors and do not necessarily reflect the views of NASA, NOAA, the Department of Commerce, or their individual employers. The authors thank Alyssa Johnson, Alyssa Cannistraci, and Mike Patterson of the US CLIVAR program office for their assistance in the preparation of this manuscript.

AUTHORS

Lilian A. Dove (dove@gatech.edu), School of Earth and Atmospheric Sciences, Georgia Institute of Technology, Atlanta, GA, USA. **Gaël Forget**, Department of Earth, Atmospheric and Planetary Sciences, Massachusetts Institute of Technology, Cambridge, MA, USA. **Momme Hell**, Woods Hole Oceanographic Institution, Woods Hole, MA, USA. **Verena Hormann**, Scripps Institution of Oceanography, University of California San Diego, La Jolla, CA, USA. **Irina Marinov**, Department of Earth and Environmental Science, University of Pennsylvania, Philadelphia, PA, USA. **Monique Messié**, Monterey Bay Aquarium Research Institute, Moss Landing, CA, USA. **Anastasia Romanou**, NASA-Goddard Institute for Space Studies, New York, NY, USA. **Jacob Steinberg**, NOAA/Geophysical Fluid Dynamics Laboratory, Princeton, NJ, USA. **Lynne D. Talley**, Scripps Institution of Oceanography, University of California San Diego, La Jolla, CA, USA.

ARTICLE CITATION

Dove, L.A., G. Forget, M. Hell, V. Hormann, I. Marinov, M. Messié, A. Romanou, J. Steinberg, and L.D. Talley. 2026. Argo at a crossroads: Achievements, impacts, and the imperative for sustained global ocean observations. *Oceanography* 39(2):6–11, https://doi.org/10.5670/oceanog.2026.e207.

QUANTIFYING THE ROLE OF CLIMATE CHANGE IN DRIVING MASS CORAL BLEACHING

By Andrew J. Pershing, John F. Bruno, Joseph Giguere, and Alexandra Khrizman

ABSTRACT. Four global mass coral bleaching events have now been recorded. The first, in 1998, was associated with that year's strong El Niño. Subsequent global-scale bleaching occurred in 2010 and then over the periods 2014–2017 and 2018–2025 (and likely ongoing). All these events also coincided with El Niños for at least part of the period. While El Niño is an important factor, each event has also occurred during a period of rising global temperatures. Here, we use attribution of daily sea surface temperatures to show that the most recent global coral bleaching event is entirely due to human-caused warming. Furthermore, all previous events, including the original one in 1998, had strong fingerprints of anthropogenic climate change. Our analysis shows that global warming is the main driver of bleaching and that global coral bleaching simply would not occur without human-caused climate change.

Coral reefs are the most diverse marine ecosystems, housing approximately 32% of all named marine species (Fisher et al., 2015). Reef-building corals have adapted to their local annual cycle of environmental temperature, but when temperatures exceed these conditions for several weeks, bleaching or even death can occur (Hoegh-Guldberg, 1999). Extensive mortality leads to a transformation in the ecosystem from one dominated by coral to one dominated by algae, sponges, or other taxa (Norström et al., 2009), and this is typically accompanied by a loss of species richness and diversity (Bellwood et al., 2004).

Global mass coral bleaching events—coincident bleaching across many reefs around the world—have occurred periodically since 1998 (Goreau et al., 2000). These events, which also occurred in 2010, 2014–2017, and 2018–2025 (Spady et al., 2026), all coincided wholly or in part with El Niño conditions, making it difficult to isolate the influence of climate change. Here, we use attribution of daily ocean temperatures to quantify the role of anthropogenic ocean warming in driving global mass bleaching of the world's coral reefs.

ISOLATING THE SIGNAL OF CLIMATE CHANGE IN OCEAN TEMPERATURE RECORDS

Our ability to detect climate change at finer spatial and temporal scales has increased in the last decade. This is most apparent in the advent of extreme event attribution (Otto, 2017; Swain et al., 2020), which has been used to diagnose the contribution of climate change to individual heatwaves on land (Stott et al., 2004) and in the ocean (Hope et al., 2024), extreme rainfall events (Van Oldenborgh et al., 2017; Reed et al., 2022), and economic damages from coastal flooding (Strauss et al., 2021).

Gilford et al. (2022), extended extreme event attribution methods (e.g., Otto, 2017; Swain et al., 2020) to daily air temperatures. Their approach integrates information from climate models run with and without anthropogenic greenhouse gas forcing and from the observed local response to changing global temperatures. Giguere et al. (2024) applied this same multi-method approach to sea surface temperatures from NOAA's Optimum Interpolation Sea Surface Temperature (OISST) long-term Climate Data Record (Reynolds et al., 2007). The Gilford-Giguere approach reaches similar conclusions about how climate change increased the likelihood of terrestrial heatwaves (Gilford et al., 2024b) and marine heatwaves (Giguere et al., 2024) as did other studies (e.g., Laufkötter et al.'s [2020] attribution of marine heatwaves). This approach has an additional advantage in that it can be easily automated and applied to any day's temperature, not just extremes.

This daily, local-scale perspective provides new capabilities for considering that climate change has and is impacting marine ecosystems such as coral reefs. For this study, we use Giguere et al.'s (2024) approach to assess the influence of climate change on sea surface temperatures, specifically using NOAA's OISST (Reynolds et al., 2007). This approach is built around a statistical reconstruction of the distribution of daily temperatures expected at a location and time of year under a specific global climate condition (detailed methods are provided in the online supplementary material). We use a smoothed version of HadCRUT5 (Morice et al., 2021) global mean temperature (GMT) as our estimate of the global conditions. We refer to this as GMT15 because it approximates a centered 15-year running average. Global temperatures are reported relative to the 1850–1900 baseline used by the Intergovernmental Panel on Climate Change (IPCC). For example, assessing a temperature in 2025 would contrast the distribution under GMT15 = 1.35°C with the counterfactual (no global warming) distribution represented by GMT15 = 0°C.

We divide the year into 24 periods. We then use output from 13 climate simulations and two empirical approaches to characterize the local temperature distributions for each period and how they change with GMT15. We downscale and debias each climate model dataset based on the 1991–2020 period. We then fit a skew-normal distribution to the 30 years of daily output when each model's global temperature anomaly first crosses the desired GMT15 value. We also fit a distribution to the model's control run without anthropogenic greenhouse gas forcing. This produces 13 paired distributions.

The Gilford-Giguere approach also uses two empirical methods to estimate how local temperatures respond to changes in GMT. The first empirical method uses linear regression to estimate how the median daily temperature responds to a change in GMT. The slope of this regression, called the scale factor, is used to shift the skew-normal distribution built with data from 1991 to 2020 (GMT15 = 0.88°C) to the climate of the observations and to the counterfactual climate. The second empirical method calculates the scale factor for 21 evenly spaced quantiles between 0.01 and 0.99. This allows for the variance and skewness of the distribution to change in response to global forcing.

For impact studies, we need to estimate the counterfactual temperature, not the probability. Following Giguere et al. (2024), we define the counterfactual temperature (T_{cf}) as the temperature with the same exceedance probability in the GMT15 = 0° distribution as the observed temperature (T) has in its climate. We calculate T_{cf} for each of the 13 climate models and average them. We then calculate T_{cf} for the two empirical models and average. Finally, we average the two averages. This gives us two sets of temperatures, one corresponding to the observations and another corresponding to the observations but with the influence of climate change removed. These can then be used to drive a process model, allowing us to estimate how climate change has influenced that process. For example, Gilford et al. (2024a) applied a model of hurricane maximum intensity to daily sea surface temperature counterfactuals to identify the role of climate change in increasing Atlantic hurricane intensity.

ATTRIBUTION OF CORAL BLEACHING

For this study, our process of interest is the risk of coral bleaching. We applied the bleaching risk model developed by NOAA's Coral Reef Watch (CRW) program (Liu et al., 2014; Skirving et al., 2019) to both the observed and the counterfactual temperatures. This model is based on degree heating week (DHW) accumulation above a local maximum monthly mean climatological temperature. We calculated the maximum monthly mean climatology for OISST using the same years (centered on the year 1998.5) as CRW. We mapped the 12-week DHW onto risk levels (Heron et al., 2016; Manzello et al., 2025): moderate (DHW ≥4°-week) implies a risk of reef-wide bleaching, severe (DHW ≥ 8°-week) translates to a risk of mortality of sensitive species, and extreme (DHW ≥ 12°-week) indicates risk of multi-species mortality. To highlight patterns at lower DWH, we split NOAA's "low" category into two bins: very low (DHW < 1°-week) and low (1°-week ≤ DHW < 4°-week) correspond to a risk of possible bleaching. For 100 coral reef containing regions, we calculated the annual maximum value (DHW_{max}) for the years 1982–2025.

Spady et al. (2026) aggregated reports of bleaching during the most recent global bleaching event. For each of the 71 regions where they determined that bleaching had occurred, we found the maximum DHW_{max} over the period 2018–2025. Consistent with their analysis, we find that bleaching risk was elevated in all the regions they identified (Figure 1a). Risk was most intense in the southern Caribbean and along the Central and South American coasts. Throughout this region, DHW_{max} reached extreme levels (DHW_{max} ≥ 12°C-weeks) at which large-scale mortality is expected and has been documented in some regions (Manzello et al., 2025).

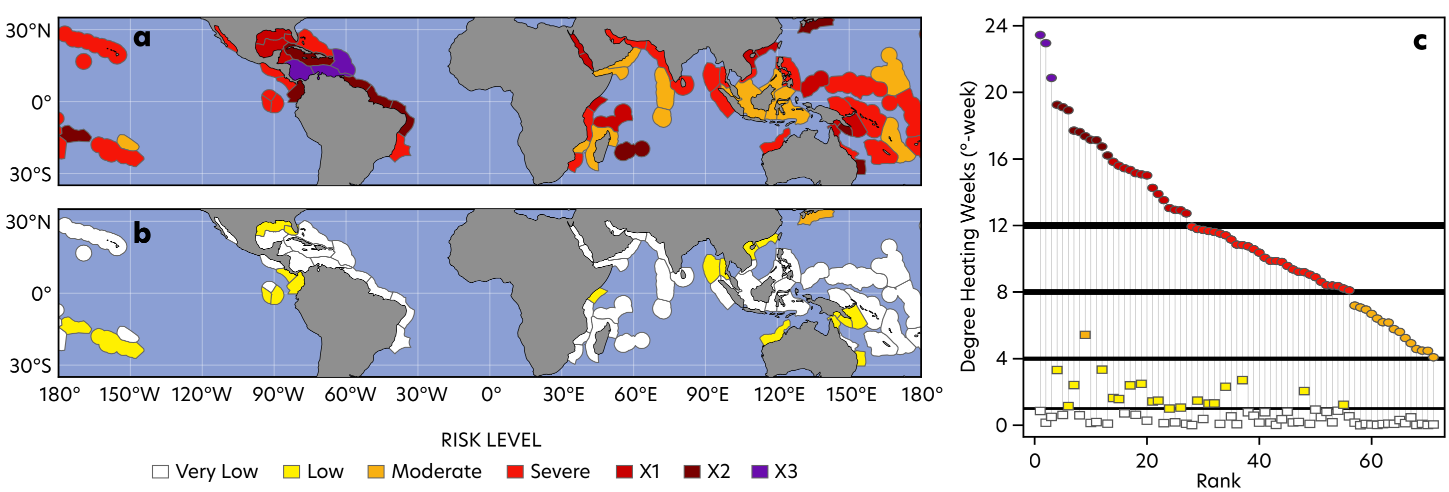

FIGURE 1. Bleaching risk attributable to anthropogenic climate change for the fourth global mass coral bleaching event. (a) Risk levels based on maximum degree heating weeks (DHW_{max}) for 71 regions where bleaching was reported during 2018–2025 (Spady et al., 2026). The extreme risk level is split into three sublevels to highlight the gradation. (b) Risk levels calculated using counterfactual temperatures. (c) Plot of observed (circles) and counterfactual (squares) DHW_{max}. The regions are ranked based on the observed values and colored according to risk levels as in panel a. The DHW_{max} values for each region are in online supplementary Table S1.

Other regions that reached the extreme level include the Red Sea, central and eastern Polynesia, and the coast of Japan. Risk reached at least moderate levels (DHW_{max} > 4°C-weeks) in all other regions, a risk level associated with reef-wide bleaching.

Our analysis indicates there would be essentially no coral bleaching and certainly not a global-scale event without human-caused climate change. Based on DHW_{max} calculated with counterfactual temperatures, we find a substantial reduction in the risk of bleaching (Figure 1b). Only one region, the central Kuroshio, had moderate bleaching risk in the counterfactual climate. This region had an observed DHW_{max} value exceeding 17.4°C-weeks, well above the extreme risk threshold (Figure 1c). All the remaining regions had little temperature-based risk, including 51 regions with DHW_{max} < 1°C-week.

The influence of climate change is also apparent in previous global coral bleaching events. During each of these events, at least 40 regions were at moderate risk (Figure 2). In 1998, only one of these regions had bleaching risk that was not attributable, meaning that the region reached the moderate risk level under the counterfactual conditions (in the absence of global warming). For all other global events, the other regions would not have had this level of risk in the counterfactual climate. The rising trend in the number of regions experiencing each risk level suggests that many regions are now experiencing stressful temperatures multiple times in a decade.

GLOBAL WARMING VS. EL NIÑO

The attributability of the 1998 event is especially noteworthy given the perceived importance of El Niño in that event (Hoegh-Guldberg, 1999; Bruno et al., 2001). Our approach to calculating the counterfactual temperature is designed to account for natural variability from the El Niño-Southern Oscillation (ENSO) and other sources. It does this by characterizing the distribution of temperatures during a 30-year reference period (in this case, 1991–2020) and then shifting that distribution using the observed trends and climate models (Giguere et al., 2024). This means that the counterfactual temperatures for 1998 or any El Niño year would reflect El Niño conditions in the absence of warming.

To further explore the hypothesis that global warming and not El Niño is the main driver of large-scale bleaching, we use linear regression to fit a statistical model of DHW_{max} for each region:

$$DHW_{max}(\text{year}) = a^{*}\text{GMT15}(\text{year}) + b^{*}\text{ONI}(\text{year-L}) + c,$$

where ONI(year) is the monthly Oceanic Niño Index (Glantz and Ramirez, 2020; NOAA, 2025) from the month when the region's maximum monthly climatological temperature occurs. The parameter L is the lag in months (from 0 to 12) that gives the best fit. We found 23 regions where only the temperature term was significant and 74 out of 100 regions where both the global temperature and ONI effects were significant (Figure S1 in the online supplementary material). For the regions where both factors were significant, we calculated $GMT_{eqiv} = 2^{*}b/a$ (i.e., the global mean temperature that leads to a change in DHW_{max} comparable to a strong El Niño; ONI = 2).

According to the statistical modeling, the effect of global temperature became stronger than El Niño in half the regions where both factors are significant when global mean temperature was only 0.5°C above the preindustrial (Figure 3a, blue curve). These conditions occurred in the year 1989. In 1998, during the first global bleaching event, the global mean temperature was 0.72° above preindustrial conditions, and warming was stronger in 61 out of 74 regions. Under current conditions in 2025 (GMT15 = 1.35°), only three regions, Cocos Islands, Northern Galápagos Islands, and Line Islands, have a stronger El Niño effect (Figure 3b). Under current warming rates (SSP3-7.0), warming will outweigh ENSO in all regions where both factors are significant by 2028.

The statistical models also demonstrate that climate change has been the main driver of coral bleaching risk over the last 40 years. By 2000, when GMT15 = 0.77°C, the effect of warming emerged from natural variability in half of the 95 regions with significant GMT15 terms (Figure 3a). In the current climate of 1.35°C, forcing from global temperature exceeds natural variability in 93% of regions (90/97). All regions are expected to exceed their natural variability by 2040 (Figure 3c).

DISCUSSION

Both the attribution analysis and the linear modeling indicate that rising greenhouse gas emissions and the ensuing rise in global temperatures are the main drivers of mass coral bleaching. Without human-induced climate change, reef-wide bleaching would be exceedingly rare, and global bleaching events simply would not occur. According to our analysis, large El Niño events add to the risk from long-term warming, but temperature changes

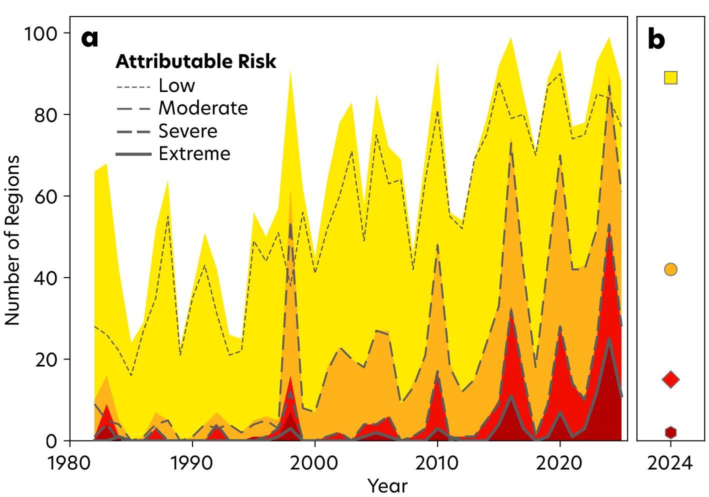

FIGURE 2. Number of coral regions exposed to elevated risk of bleaching. (a) Number of regions reaching a particular bleaching risk level (indicated by colors as in Figure 1a). The dashed lines show the number of regions where the risk is attributable to human-induced warming, meaning that the region's DHW_{max} calculated with observed temperatures is above the threshold but the value using the counterfactual temperatures is below the threshold. (b) The number of regions at each risk level in 2024 re-calculated using the 1992–2023 baseline.

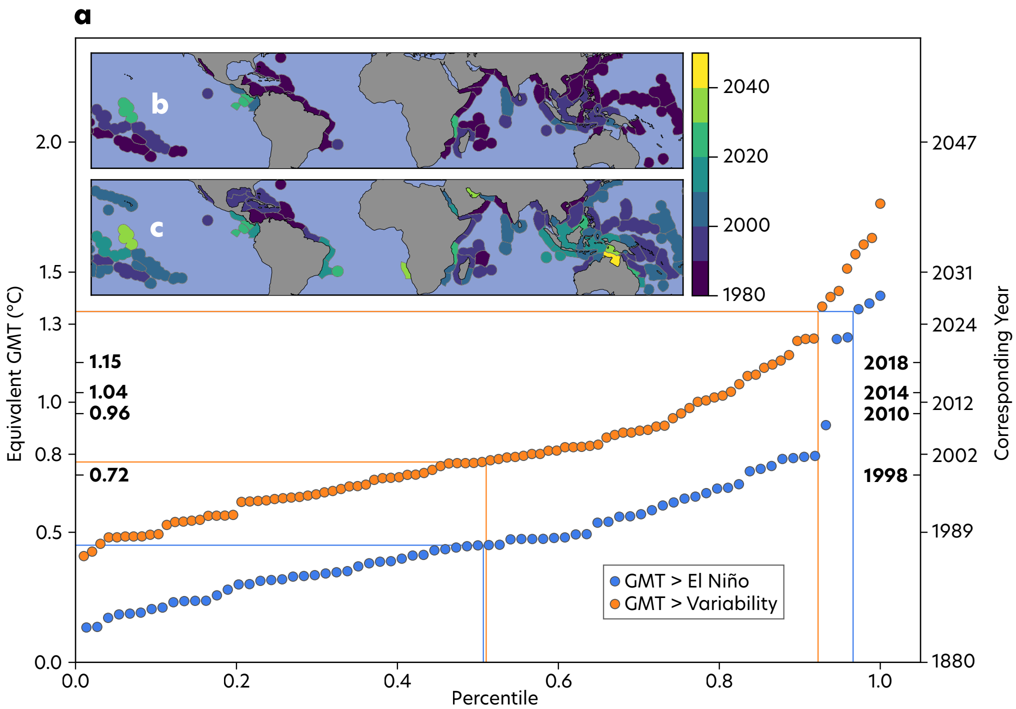

FIGURE 3. Drivers of bleaching risk. (a) The number of regions (expressed as a percentile) for which the influence of global mean temperature (GMT) on DHW_{max} exceeds that of a strong El Niño (blue dots) or natural variability (orange dots). The year when the equivalent GMT value was or is expected to be reached is indicated on the right. The GMT values for the start of the four global mass bleaching events are indicated in bold. One set of thin lines indicates the equivalent GMT when the GMT effect is stronger in 50% of regions. The other set highlights the proportion of regions where GMT is stronger in 2025 (current climate of 1.35°C). The maps show the decade in which the effect of GMT exceeds that of El Niño (b) or natural variability (c).

from El Niño would not be strong enough on their own to result in widespread bleaching.

The main advance in our study is the ability to quantify the influence of global warming and to isolate it from natural climate variability, including El Niño events. The multi-method, daily approach developed by Giguere et al. (2024) is currently being used to provide operational assessments of the influence of climate change on sea surface temperatures (see https://csi.climatecentral.org/ocean). This approach provides a convenient pathway for generating time series of counterfactual temperatures that can be used for impact attribution. The main requirement for impact attribution is a model linking sea surface temperature with the process of interest. Marine species distributions (e.g., Morley et al., 2018) and fishery population dynamics (e.g., Pershing et al., 2015) have all been modeled using sea surface temperature and would be particularly suited to attribution studies.

The DHW risk model follows from the understanding that reef-building corals are adapted to the prevailing conditions in their regions. Exposure to stressful temperatures can cause bleaching; however, it can also lead to physiological acclimatization and genetic adaptation, and at the community level, to the loss of the species most sensitive to warming. This may explain why some reefs do not bleach when exposed to conditions that they have previously experienced. For example, in the Chagos Archipelago, high DHW values in 2005 and 2010 were comparable in magnitude to the 1998 event, yet coral cover did not decline and instead increased until 2015 (Sheppard et al., 2017).

Ultimately, a region will only be able to retain a coral reef ecosystem if the rate of adaptation (defined broadly to include processes ranging from acclimatization and genetic changes to species replacement) is faster than the rate of warming (Pershing et al., 2019). Understanding the process of adaptation to rising temperatures is the defining goal of climate change ecology (Witman et al., 2023). The rate of adaptation in coral reef communities should be slow due to the long lifespan and slow growth of most reef-building corals and will be further exacerbated in isolated reefs where species replacement is slower.

Defining bleaching risk relative to the original baseline period echoes the fixed-baseline definition of marine heatwaves (Hobday et al., 2016). Jacox (2019) argued for defining marine heatwaves after removing the long-term trend. From the perspective of marine ecology, removing the trend assumes that adaptation processes are fast enough to keep pace with the trend. Coral communities lie somewhere between these perspectives. If we shift the baseline period for the DHW calculations from the standard NOAA period (mean year = 1982.3) to the most recent 30 years (mean year = 2008.5), there is a reduction in the number of reefs at each risk level (Figure 2b); however, the number of reefs exposed in each category remains high and is similar to 1998 and 2010. In other words, we would still expect a significant global mass bleaching event.

Our analysis suggests that anthropogenic warming was already driving coral bleaching in the 1990s, the period when the scientific consensus on human-caused climate change was coming into focus. The failure to reduce greenhouse gas emissions after that time led to an additional 0.7° of warming, increasing the exposure of reef ecosystems to dangerously warm temperatures. The International Union for Conservation of Nature (IUCN) has documented that 1,008 species have gone extinct since 1600, most due to human activities (IUCN, 2025). Continued emissions and additional warming raise the potential that human actions may soon eliminate coral reef ecosystems as we know them from the planet.

SUPPLEMENTARY MATERIALS

The supplementary materials are available online at https://doi.org/10.5670/oceanog.2026.e210.

REFERENCES

Bellwood, D.R., T.P. Hughes, C. Folke, and M. Nyström. 2004. Confronting the coral reef crisis. *Nature* 429(6994):827–833, https://doi.org/10.1038/nature02691.

Bruno, J., C. Siddon, J. Witman, P. Colin, and M. Toscano. 2001. El Niño related coral bleaching in Palau, western Caroline Islands. *Coral Reefs* 20(2):127–136, https://doi.org/10.1007/s003380100151

Fisher, R., R.A. O'Leary, S. Low-Choy, K. Mengersen, N. Knowlton, R.E. Brainard, and M.J. Caley. 2015. Species richness on coral reefs and the pursuit of convergent global estimates. *Current Biology* 25(4):500–505, https://doi.org/10.1016/j.cub.2014.12.022.

Giguere, J., D.M. Gilford, and A.J. Pershing. 2024. Attributing daily ocean temperatures to anthropogenic climate change. *Environmental Research: Climate* 3(3):035003, https://doi.org/10.1088/2752-5295/ad4815.

Gilford, D.M., A.J. Pershing, B.H. Strauss, K. Haustein, and F.E.L. Otto. 2022. A multi-method framework for global real-time climate attribution. *Advances in Statistical Climatology, Meteorology and Oceanography* 8:135–154, https://doi.org/10.5194/ascmo-8-135-2022.

Gilford, D.M., J. Giguere, and A.J. Pershing. 2024a. Human-caused ocean warming has intensified recent hurricanes. *Environmental Research: Climate* 3(4):045019, https://doi.org/10.1088/2752-5295/ad8d02.

Gilford, D.M., A.J. Pershing, J. Giguere, and F.E.L. Otto. 2024b. Human fingerprints on daily temperatures in 2022. *Bulletin of the American Meteorological Society* 105(7):E1365–E1370, https://doi.org/10.1175/BAMS-D-23-0264.1.

Glantz, M.H., and I.J. Ramirez. 2020. Reviewing the Oceanic Niño Index (ONI) to enhance societal readiness for El Niño's impacts. *International Journal of Disaster Risk Science* 11(3):394–403, https://doi.org/10.1007/s13753-020-00275-w.

Goreau, T., T. McClanahan, R. Hayes, and A.L. Strong. 2000. Conservation of coral reefs after the 1998 global bleaching event. *Conservation Biology* 14(1):5–15, https://doi.org/10.1046/j.1523-1739.2000.00011.x.

Heron, S.F., L. Johnston, G. Liu, E.F. Geiger, J.A. Maynard, J.L. De La Cour, S. Johnson, R. Okano, D. Benavente, and T.F.R. Burgess. 2016. Validation of reef-scale thermal stress satellite products for coral bleaching monitoring. *Remote Sensing* 8(1):59, https://doi.org/10.3390/rs8010059.

Hobday, A.J., L.V. Alexander, S.E. Perkins, D.A. Smale, S.C. Straub, E.C.J. Oliver, J.A. Benthuysen, M.T. Burrows, M.G. Donat, M. Peng, and others. 2016. A hierarchical approach to defining marine heatwaves. *Progress in Oceanography* 141:227–238, 10.1016/j.pocean.2015.12.014, https://doi.org/10.1016/j.pocean.2015.12.014.

Hoegh-Guldberg, O. 1999. Climate change, coral bleaching and the future of the world's coral reefs. *Marine and Freshwater Research* 50(8):839–866, https://doi.org/10.1071/MF99078.

Hope, P., J. Nahar, G.C. Tolhurst, S.P. Rauniyar, R.C. McKay, L. Zhou, M.R. Grose, B.C. Trewin, D.J. Martin, and S. Grainger. 2024. Lessons learnt from a real-time attribution and contextualisation trial in a national meteorological and hydrological service. *Environmental Research: Climate* 3(4):045014, https://doi.org/10.1088/2752-5295/ad7da8.

IPCC. 2021. *Climate Change 2021: The Physical Science Basis. Contribution of Working Group I to the Sixth Assessment Report of the Intergovernmental Panel on Climate Change*. V. Masson-Delmotte, P. Zhai, A. Pirani, S.L. Connors, C. Péan, S. Berger, N. Caud, Y. Chen, L. Goldfarb, M.I. Gomis, and others, eds., Cambridge University Press, Cambridge, United Kingdom and New York, NY, USA, 2,391 pp., https://doi.org/10.1017/9781009157896.

IUCN (International Union for Conservation of Nature). 2025. "Summary Statistics." IUCN Red List of Threatened Species, https://www.iucnredlist.org/resources/summary-statistics#Summary%20Tables.

Jacox, M.G. 2019. Marine heatwaves in a changing climate. *Nature* 571:485–487, https://doi.org/10.1038/d41586-019-02196-1.

Lange, S. 2019. Trend-preserving bias adjustment and statistical downscaling with ISIMIP3BASD (v1. 0). *Geoscientific Model Development* 12(7):3,055–3,070, https://doi.org/10.5194/gmd-12-3055-2019.

Laufkötter, C., J. Zscheischler, and T. Frölicher. 202. High-impact marine heatwaves attributable to human-induced global warming. *Science* 369:1,621–1,625, https://doi.org/10.1126/science.aba0690.

Liu, G., S.F. Heron, C.M. Eakin, F.E. Muller-Karger, M. Vega-Rodriguez, L.S. Guild, J.L. De La Cour, E.F. Geiger, W.J. Skirving, and T.F.R. Burgess. 2014. Reef-scale thermal stress monitoring of coral ecosystems: New 5-km global products from NOAA Coral Reef Watch. *Remote Sensing* 6(11):11,579–11,606, https://doi.org/10.3390/rs61111579.

Manzello, D.P., R. Cunning, R.F. Karp, A.C. Baker, E. Bartels, R. Bohnag, A. Borreil, A. Bourque, K.T. Brown, and A.W. Bruckner. 2025. Heat-driven functional extinction of Caribbean *Acropora* corals from Florida's coral reef. *Science* 390(6771):361–366, https://doi.org/10.1126/science.adx7825.

Morice, C.P., J.J. Kennedy, N.A. Rayner, J.P. Winn, E. Hogan, R.E. Killick, R.J.H. Dunn, T.J. Osborn, P.D. Jones, and I.R. Simpson. 2021. An updated assessment of near-surface temperature change from 1850: The HadCRUT5 data set. *Journal of Geophysical Research: Atmospheres* 126(3):e2019JD032361, https://doi.org/10.1029/2019JD032361.

Morley, J.W., R.L. Selden, R.J. Latour, T.L. Frolicher, R.J. Seagraves, and M.L. Pinsky. 2018. Projecting shifts in thermal habitat for 686 species on the North American continental shelf. *PLoS One* 13(5), https://doi.org/10.1371/journal.pone.0196127.

NOAA. 2025. ONI_v5. https://www.cpc.ncep.noaa.gov/products/analysis_monitoring/ensostuff/ONI_v5.php.

Norström, A.V., M. Nyström, J. Lokrantz, and C. Folke. 2009. Alternative states on coral reefs: Beyond coral-macroalgal phase shifts. *Marine Ecology Progress Series* 376:295–306, https://doi.org/10.3354/meps07815.

Otto, F.E.L. 2017. Attribution of weather and climate events. *Annual Review of Environment and Resources* 42:627–646, https://doi.org/10.1146/annurev-environ-102016-060847.

Pershing, A.J., M.A. Alexander, C.M. Hernandez, L.A. Kerr, A. Le Bris, K.E. Mills, J.A. Nye, N.R. Record, H.A. Scannell, J.D. Scott, and others. 2015. Slow adaptation in the face of rapid warming leads to collapse of the Gulf of Maine cod fishery. *Science* 350(6262):809–812, https://doi.org/10.1126/science.aac9819.

Pershing, A.J., N.R. Record, B.S. Franklin, B.T. Kennedy, L. McClenachan, K.E. Mills, J.D. Scott, A.C. Thomas, and N.H. Wolff. 2019. Challenges to natural and human communities from surprising ocean temperatures. *Proceedings of the National Academy of Sciences of the United States of America* 116(37):18,378–18,383, https://doi.org/10.1073/pnas.1901084116.

Reed, K.A., M.F. Wehner, and C.M. Zarzycki. 2022. Attribution of 2020 hurricane season extreme rainfall to human-induced climate change. *Nature Communications* 13(1):1905, https://doi.org/10.1038/s41467-022-29379-1.

Reynolds, R.W., T.M. Smith, C. Liu, D.B. Chelton, K.S. Casey, and M.G. Schlax. 2007. Daily high-resolution-blended analyses for sea surface temperature. *Journal of Climate* 20(22):5,473–5,496, https://doi.org/10.1175/2007JCLI1824.1.

Sheppard, C., A. Sheppard, A. Mogg, D. Bayley, A.C. Dempsey, R. Roache, J. Turner, and S. Purkis. 2017. Coral bleaching and mortality in the Chagos Archipelago. *Atoll Research Bulletin* (613):1–26, https://doi.org/10.5479/si.0077-5630.613.

Skirving, W.J., S.F. Heron, B.L. Marsh, G. Liu, J.L. De La Cour, E.F. Geiger, and C.M. Eakin. 2019. The relentless march of mass coral bleaching: A global perspective of changing heat stress. *Coral Reefs* 38(4):547–557, https://doi.org/10.1007/s00338-019-01799-4.

Spady, B.L., W.J. Skirving, J.L. De La Cour, E.F. Geiger, G. Liu, O. Hoegh-Guldberg, A. Norrie, S.F. Heron, M.W. Pomeroy, and G. Kolodziej. 2026. The 4th global coral bleaching event: Ushering in an era of near-annual bleaching. *Coral Reefs*, https://doi.org/10.1007/s00338-025-02810-x.

Spalding, M.D., H.E. Fox, G.R. Allen, N. Davidson, Z.A. Ferdaña, M.A.X. Finlayson, B.S. Halpern, M.A. Jorge, A.L. Lombana, and S.A. Lourie. 2007. Marine ecoregions of the world: A bioregionalization of coastal and shelf areas. *BioScience* 57(7):573–583, https://doi.org/10.1641/B570707.

Stott, P.A., D.A. Stone, and M.R. Allen. 2004. Human contribution to the European heatwave of 2003. *Nature* 432(7017):610–614, https://doi.org/10.1038/nature03089.

Strauss, B.H., P.M. Orton, K. Bittermann, M.K. Buchanan, D.M. Gilford, R.E. Kopp, S. Kulp, C. Massey, H. de Moel, and S. Vinogradov. 2021. Economic damages from Hurricane Sandy attributable to sea level rise caused by anthropogenic climate change. *Nature Communications* 12(1):2720, https://doi.org/10.1038/s41467-021-22838-1.

Swain, D.L., D. Singh, D. Touma, and N.S. Diffenbaugh. 2020. Attributing extreme events to climate change: A new frontier in a warming world. *One Earth* 2(6):522–527, https://doi.org/10.1016/j.oneear.2020.05.011.

UNEP WCMC (United Nations Environment Programme World Conservation Monitoring Centre). 2025. Ocean+ Habitats, https://doi.org/10.34892/fpe3-ar97.

Van Oldenborgh, G.J., K. van der Wiel, A. Sebastian, R. Singh, J. Arrighi, F. Otto, K. Haustein, S. Li, G. Vecchi, and H. Cullen. 2017. Attribution of extreme rainfall from Hurricane Harvey, August 2017. *Environmental Research Letters* 12(12):124009, https://doi.org/10.1088/1748-9326/aa9ef2.

Witman, J.D., A.J. Pershing, and J.F. Bruno. 2023. Smooth and spiky: The importance of variability in marine climate change ecology. *Annual Review of Ecology, Evolution, and Systematics* 54:129–149, https://doi.org/10.1146/annurev-ecolsys-022323-082123.

ACKNOWLEDGMENTS

This work synthesizes climate models and Earth system observations produced by agencies all over the world, but especially by NOAA in the United States. We are deeply grateful for these valuable contributions to our ability to track changes on the planet. This manuscript and the analysis were improved by helpful suggestions from Erick F. Geiger, Derek Manzello, Blake L. Spady, Alistair Hobday, and two anonymous reviewers. Financial support for this work was provided by the Bezos Earth Fund and the CO2 Foundation (AJP, JG).

AUTHORS

Andrew J. Pershing (apershing@climatecentral.org), Climate Central Inc., Princeton, NJ, USA. **John F. Bruno**, Department of Biology, University of North Carolina at Chapel Hill, Chapel Hill, NC, USA. **Joseph Giguere**, Climate Central Inc., Princeton, NJ, USA. **Alexandra Khrizman**, Department of Earth System Science, Doerr School of Sustainability, Stanford University, Stanford, CA, USA.

ARTICLE CITATION

Pershing, A.J., J.F. Bruno, J. Giguere, and A. Khrizman. 2026. Quantifying the role of climate change in driving mass coral bleaching. *Oceanography* 39(2):12–16, https://doi.org/10.5670/oceanog.2026.e210.

ECOLOGICAL BENTHIC UNITS

A NEW CHARACTERIZATION OF THE GLOBAL SEAFLOOR FOR OCEAN SPATIAL PLANNING AND MANAGEMENT

By Peter T. Harris, Dawn J. Wright, Kevin Butler, Keith VanGraafeiland, Mark John Costello, Kerry Howell, Gustav Kågesten, Vanessa Lucieer, Miles Macmillan-Lawler, and Roger Sayre

ABSTRACT. Effective management of deep-sea ecosystems and the high seas is hindered by the absence of a globally consistent framework for characterizing benthic habitats. Here we present the first global ecological classification of the seafloor, comprising 250 unique ecological benthic units (EBUs), distributed on the seafloor as nearly 700,000 EBU polygon occurrences, generated by intersecting a high-resolution geomorphic map with multivariate environmental seascapes. Using 17 million seafloor data points and 0.05° resolution biophysical datasets—including bottom temperature, dissolved oxygen, pH, carbon flux, sediment thickness, crustal age, and bottom currents—we identified 57 benthic regions across six major geomorphic groups (shelves, slopes, seamounts/guyots, spreading ridges, abyssal/hadal areas, plateaus). The resulting EBUs reveal previously unrecognized ecological gradients, quantify global patterns of benthic heterogeneity, and expose large-scale environmental vulnerabilities. Notably, we find that 95.6 million km^2 (26% of the ocean area) of abyssal seafloor lies below the carbonate compensation depth, that 4.16 million km^2 (1% of the ocean) of continental slopes intersect severe oxygen minima, and <1% of seamounts occur in seascapes most environmentally favorable to life. These insights provide a powerful basis for identifying rare habitat configurations, assessing exposure to climate-driven stressors, and prioritizing areas for high seas marine protected area planning, as well as a policy-relevant foundation for environmental impact assessment and biodiversity baseline proxies under the new United Nations High Seas Treaty.

INTRODUCTION

Society's interest in exploiting deep-sea resources is growing rapidly, but the same cannot be said for our ability to effectively conserve and manage the deep ocean (>500 m depth) and high seas (i.e., international waters beyond national jurisdiction). The recent ratification of the United Nations (UN) High Seas Treaty (formally the Agreement on Marine Biological Diversity of Areas Beyond National Jurisdiction or BBNJ Agreement; High Seas Alliance, 2025) indicates that there is a growing need to conserve the ocean's resources and protect the biodiversity that it contains. There have been discussions of what aspects should be considered when planning conservation strategies for the deep ocean realms (Ceccarelli et al., 2021), but there remains a lack of sufficient tools and data to guide decision-making processes (McQuaid et al., 2023; Misiuk and Brown, 2024).

Marine spatial planning in the ocean, including the high seas areas, involves making decisions about managing human activities in the ocean. For example:

1. Sustainable harvesting of living marine resources and conservation of biodiversity: There is growing interest in harvesting deep-sea biological resources for food and the genetic materials used in the development of pharmaceuticals (Bisson et al., 2023).
2. Understanding impacts of pollution: For example, deep-sea sediments are the final resting place for plastic pollution lost in the ocean. However, our understanding of pathways and what environments are most impacted is very poor (Harris et al., 2023). This includes creating more accurate environmental impact assessments for potential deep-sea resource extraction.
3. Establishment and monitoring of high seas marine protected areas: To create an ecologically representative global network of marine protected areas (MPAs) as per the new UN Highs Seas Treaty, we first need to understand the spatial distribution of different seabed environments and the biodiversity they contain. Our understanding of deep-sea habitats is still extremely limited, illustrated by the recent extraordinary discovery of the electrochemical production of "dark oxygen" on the abyssal seafloor by polymetallic nodules (Sweetman et al., 2024).
4. Understanding impacts of climate change: Research shows that global climate change is driving changes in deep ocean pH (Sulpis et al., 2018), bottom currents, and patterns of sedimentation. Further, the shape of the seafloor combines with these factors to influence the amount of heat flowing underneath ice shelves and contributing to melting (Richter et al., 2025). Deep-sea biota will respond to these ecosystem changes by moving and/or recolonizing different locations that suit their needs (Ramirez-Llodra et al., 2011).

In this paper, we present a new benthic classification that we call "ecological benthic units" (EBUs) for the world ocean. Our aim is to provide a new tool to improve global understanding and decision-making capability for a range of global issues, as listed above. EBUs build upon an earlier map of ecological marine units (EMUs) that characterizes the ocean water column as a proxy for pelagic ecosystems (Sayre et al., 2017). As abiotic surrogates for benthic biodiversity (McArthur et al., 2010; Astudillo-Scalia et al., 2021), the EBUs are environmentally distinct areas occurring within physiographically stratified geomorphic types, and they represent the ecological settings that control the distribution of benthic biota.

APPROACH TAKEN

The global map of seafloor geomorphic features (Harris et al., 2014) provides the basis for the present study. It contains 29 seafloor feature categories, such as submarine canyons, seamounts, mid-ocean ridges, troughs, rift valleys, escarpments, and basins. The map divides the global ocean floor into more than 120,000 separate polygons and provides the basis for quantitative classification of seafloor areas. Seafloor geomorphology, mapped and measured by marine scientists, has proven to be a very useful physical attribute for ocean management. This is because different geomorphic features (e.g., submarine canyons, seamounts, spreading ridges, escarpments, plateaus, trenches) are commonly associated with particular suites of habitats and biological communities (Harris and Baker, 2020). The features themselves, be they canyons, sea valleys, rocky reefs, or sand banks, become the shorthand descriptor (if not the direct focus) of conservation efforts and marine management processes because they are easily understood by the broader community and are commonly associated with a particular kind of benthic community.

To advance the science underpinning ocean conservation, better classification resolution and spatial resolution are needed to sub-classify geomorphic features into more meaningful EBUs. We used existing spatial datasets for environmental parameters relevant to the deep-sea ecosystem. For example, six ecologically relevant biophysical variables (depth, seabed slope, sediment thickness, primary production, bottom water dissolved oxygen, and bottom temperature) were used by Harris and Whiteway (2009) to classify the ocean into 53,713 separate polygons comprising 11 different categories called "seascapes." A similar approach was used by Sayre et al. (2017) to create the EMU ocean water column classification. In this paper, we subclassify the existing map of seafloor geomorphic features into different sub-units with existing spatial data using multivariate statistics.

ECOLOGICAL SIGNIFICANCE OF VARIABLES USED AND DERIVED

Reviews of the ecological significance of biophysical variables used for global seascape type analyses such as those conducted for the present study have been published previously (e.g., Harris and Whiteway, 2009). The input variables used may be grouped into four broad categories: (1) physical/structural (depth, seafloor gradient [slope)], feature height above seafloor, crustal age, spreading rate, sediment thickness); (2) chemical (water temperature, pH, dissolved oxygen, salinity); (3) biological (primary productivity, seafloor downward organic carbon flux); and (4) hydrodynamic (sea ice cover, significant wave height, tidal range, benthic current velocity).

The use of static variables (e.g., annual mean value when seasonal variations are present) to characterize the ocean has clear limitations. The occurrence of biota at any given location on the seafloor will not necessarily be in response to the mean value of any variable. Dynamic aspects of the benthic environment include natural changes in variables like current speed, temperature, dissolved oxygen, and food supply. It is now an established fact that there are "benthic storms" (e.g., Woodgate and Fahrbach, 1999) and seasons in the deep sea. Detrital-feeding fauna and suspension-feeding organisms have evolved to exploit the seasonal, vertical flux of surface matter sinking to the seabed. Seasons are recorded by moored sediment traps (e.g., Juniper et al., 2013) and in thick versus thin growth rings in the shells of small abyssal molluscs (Gage and Tyler, 1991). A key driver for longer-frequency (>1 year) variations is change in deep ocean (near bottom) current speed and/or direction. Because water properties are essentially carried passively over benthic habitats in the moving water column, changes in bottom currents can trigger changes in (for example) the quantity and quality of particulate organic carbon (POC) flux (food) to the abyssal seafloor (Smith et al., 2008). For this reason, we include modeled bottom water current speed and direction in our analysis.

Examples of derived variables include local benthic habitat heterogeneity (e.g., number of unique EBU types per neighborhood) and orientation of seafloor features to the prevailing current. Several authors have reported evidence that seafloor heterogeneity is an indicator of areas with high species richness (e.g., Harris, 2012; Zeppilli et al., 2016; Riehl et al., 2020; Zhao et al., 2020; Romoth et al., 2023). In this study, we quantify the number of polygons per unit area to compare the heterogeneity of seascapes and their associated geomorphic features.

Some seafloor features rise up prominently, providing a hard, rocky substrate that is habitat for sessile benthic animals that rely upon filter-feeding plankton and organic detritus from the water column for their food supply. The optimum orientation of such a substrate is one that faces into the prevailing current, thus bringing the most amount of suspended detritus (food) to the waiting tentacles (Baynes and Szmant, 1989). In this study we include an analysis of seafloor feature orientation relative to the modeled bottom current.

METHODS

CREATING SEAFLOOR GEOMORPHOLOGY AS A SINGLE MAP LAYER

The project builds upon the foundation of an existing 1 km global grid of seafloor geomorphic features (Harris et al., 2014) that was based on bathymetric data available at the time, in particular, the SRTM 30_PLUS model of Becker et al. (2009). Although the global bathymetry database is improving every year, it is beyond the scope of this project to produce a revised/updated version of the 2014 global seafloor geomorphic features map.

The geomorphic features were first "flattened" in ArcGIS Pro 3.6 to remove all areas of spatial overlap. This flattening was performed through a hierarchical overlay process in which the 28 geomorphic feature types were prioritized based on their logical order of superposition. Superimposed features were sequentially "burned into" those below them in the hierarchy. For example, a canyon cutting across a slope that ends on an abyssal plain would overwrite the slope and abyssal plain where it intersects them, while the slope and abyssal plain would remain elsewhere. This resulted in a single map layer where every grid point was allocated into a single geomorphic feature type. Table 1 lists the 28 feature categories used in this study. We did not include escarpments mapped by Harris et al. (2014) because these were measured from bathymetry (gradient exceeding 20°) and draped over other features (e.g., ridges with escarpment, canyons with escarpment). Hence "escarpment" is a secondary attribute of other features.

ESTABLISHING GEOMORPHIC GROUPS

The next step was to allocate relevant biophysical variables to each of the geomorphic features. Geomorphic feature types were grouped into six broad geomorphic groups—continental shelf, continental slope, seamounts and guyots, crust-forming, complex/deep seafloor, and plateaus—to reflect fundamental differences in ecological drivers and physical processes across the seafloor. This grouping allowed for a more targeted selection of environmental variables within each geomorphic group. Although a number of data layers covering the global ocean (or specific areas of the global ocean) are available, not every data layer is necessarily relevant to sub-classifying a given geomorphic feature. For example, ocean surface waves may impact the shallow continental shelf but have no impact on mid-ocean spreading ridges. Conversely, seafloor spreading rate is an important characteristic of mid-ocean rift valleys but is not relevant to shallow coral reefs. Therefore, relevant biophysical variables were allocated differently for each geomorphic group (Table 1). In short, we clipped the biophysical data to geomorphic group geographies, performed a cluster analysis within each geomorphic group, subdivided the geomorphic group into seascapes using the clustered biophysical data, and then summarized distribution of those seascapes among geomorphic feature types, as follows.

SEASCAPES

Within each of the six geomorphic groups (Groups A–F), a separate K-means clustering analysis was carried out based on the biophysical variables as they are aligned in Table 1. The main data source was Bio-Oracle (Assis et al., 2024), a gridded product at a pixel spacing of 0.05° (~6 km); all data sources are listed in Table 2. To prevent variables with a higher variance from having more influence in the clustering, we standardized each variable to a mean of zero and a standard deviation of one before clustering. We then created a regular global grid of points covering the seafloor at 0.05° resolution (approximately 5.5 km at the equator), yielding 17,034,951 points. This resolution was chosen to match the Bio-ORACLE v3.0 dataset, which provided most of the physiochemical variables used in the analysis. Each point of the global mesh was assigned to one of the six geomorphic groups based on its location within the flattened geomorphic layer. Environmental variables were extracted from a series of raster datasets (Table 2), some with differing cell sizes and spatial alignments.

TABLE 1. List of the geomorphic feature groups (A–F) and their associated biophysical variables used for sub-classification in this study. Seascapes were derived separately to match six different groups of seabed geomorphic features: (A) shelf, (B) slope, (C) seamounts and guyots, (D) spreading ridges and rift valleys, (E) other abyssal and hadal areas, and (F) plateaus. Variables common to all groups are shown in orange text.

	A. Shelf	B. Slope	C. Seamounts and Guyots	D. Spreading Ridges and Rift Valleys	E. Other Abyssal and Hadal Areas	F. Plateaus
GEOMORPHIC FEATURE GROUP	• Sill on shelf • Basin on shelf • Glacial trough • Shelf valley • Coral reef • Low relief shelf • Medium relief shelf • High relief shelf	• Basin on slope • Canyon - Shelf incising - Blind canyon • Terraces • Other continental slope	• Seamount • Guyot	• Mid-ocean ridge • Rift valley	• Fan • Continental rise • Bridge • Trough • Trench • Ridge • Abyssal plain • Abyssal hill • Abyssal mountain • Hadal	• Plateau
BIOPHYSICAL VARIABLES	• Tidal range • Wave Hsig • Depth • pH • Salinity • Dissolved O_2 • Primary productivity • Temperature • Sea ice cover	• Slope • Depth • Current velocity • pH • Dissolved O_2 • Temperature • Carbon flux	• Crust age • Height • Current velocity • pH • Dissolved O_2 • Temperature • Carbon flux	• Spreading rate • Slope • Depth • pH • Current velocity • Dissolved O_2 • Temperature • Carbon flux	• Crust age • Depth • pH • Sediment thickness • Current velocity • Dissolved O_2 • Temperature • Carbon flux	• Slope • Depth • pH • Sediment thickness • Current velocity • Dissolved O_2 • Temperature • Carbon flux

To ensure consistent attribution, values in Table 2 were assigned to points using nearest neighbor resampling, which assigns the value of the raster cell containing the point without interpolation. Importantly, the specific geomorphic feature type (e.g., "sill on shelf" or "guyot") was not included as an input variable, allowing the clustering to remain blind to the geomorphic feature type. For pixels with slope >3°, current direction was assessed relative to pixel aspect. Currents flowing from 90° to 270° relative to aspect were classified as high relief exposed, whereas currents flowing from 270° through 0° to 90° were classified as high relief sheltered.

For each geomorphic group, we constructed a cross-correlation matrix to assess redundancy among variables. Variables with correlations greater than 0.7 were removed to reduce redundancy and ensure that no single type of environmental condition was overrepresented in the analysis. This helped ensure that each variable contributed more equally to the clustering process.

Clustering was conducted separately for each geomorphic group using K-means clustering in SAS. The number of clusters tested ranged from 3 to 25. The optimal number of clusters for each group was selected using the "gap statistic" (Tibshirani et al., 2001), which compares the within-cluster dispersion to that expected under a null reference distribution. The optimal number corresponds to the highest significant peak in the gap statistic. Each point was labeled with its final cluster assignment, and these clusters—interpreted as distinct seascape types—were merged across all groups to produce the final global seafloor classification. All variables listed in Table 1 were used in the clustering; no variables were removed post hoc due to cross correlation.

TABLE 2. List of variables used in this study, with units, data source, and resolution. The variables "Escarpments" and "Orientation towards current" were not used as inputs to the K-means clustering. They are derived attributes added after clustering to provide additional environmental context for the resulting EBUs and to support future analyses by other researchers. They do not influence cluster assignments or polygon boundaries in this study.

NAME	UNITS	RESOLUTION	SOURCE	COMMENTS
Depth (mean)	m	0.05 degrees	Bio-ORACLE v3.0	Bio-Oracle data are documented by Assis et al. (2024); data are averaged over 2000–2018
Tidal range	m	0.05	FES (2022) (AVISO)	Model is a finite elements solution that has been interpolated to 0.05 degrees. https://www.aviso.altimetry.fr/en/data/products/auxiliary-products/global-tide-fes/release-fes22.html
Significant wave height	m	0.2	Copernicus Marine Service	Data averaged from 1980–2024 based on the Météo-France WAve Model (MFWAM)
pH (mean)	n/a	0.05	Bio-ORACLE v3.0	CCD at pH of 7.79 ± 0.014 was determined using data from Sulpis et al. (2018)
Slope	degrees	0.05	Bio-ORACLE v3.0	
Global sediment thickness	km	0.083	GlobSed v3.0	After Straume et al. (2019)
Primary production	mmol m^{-3}	0.05	Bio-ORACLE v3.0	
Current velocity (long-term mean)	m s^{-1}	0.05	Bio-ORACLE v3.0	
Sea ice cover	% per year	0.25	NOAA	NOAA High-resolution Blended Analysis of Daily SST and Ice (Huang et al., 2021). NOAA OI SST V2 high resolution dataset provided by the NOAA Physical Sciences Laboratory, Boulder, CO, USA, from their website at https://psl.noaa.gov
Bottom dissolved oxygen (long-term min)	mmol m^{-3}	0.05	Bio-ORACLE v3.0	
Bottom primary productivity (long-term mean)	mmol m^{-3}	0.05	Bio-ORACLE v3.0	
Bottom temperature (long-term max)	°C	0.05	Bio-ORACLE v3.0	
Seafloor downward organic carbon flux (2006-2015 average)	mmol/m^2/d	0.2	Brodeau et al. (2010)	Data averaged over 2006–2015
Salinity	Parts per thousand (ppt) long-term mean		Bio-ORACLE v3.0	
Crustal age	Ma			Muller et al. (2008)
Seafloor spreading rate	cm yr^{-1}			Muller et al. (2008)
Seamount height	m			Calculated in this study using the latest GEBCO
Escarpments	Present/absent	30 arc seconds (~1 km)	Harris et al. (2014)	Seafloor gradient exceeding 20 degrees; Added last as a qualifying attribute
Orientation towards current	Dimensionless Exposure index		This study	Added last as a qualifying attribute

NAMING OF SEASCAPES AND EBUs

Terminology and thresholds describing the environmental variables that establish the class names and value ranges for each class are based on the National Oceanic and Atmospheric Administration (NOAA) Coastal and Marine Ecological Classification Standard (CMECS) scheme, where relevant terms are available (US FGDC, 2012; see online supplementary Table S1). For each of the 57 seascape types identified, the mean value of each environmental variable used in the clustering (Table 1) was calculated, except in the case for temperature and dissolved oxygen, where long-term maximum and minimum values were used to better reflect biologically limiting values (e.g., Baker et al., 2024; Capotondi et al., 2024). Throughout this paper, the term "mean" is used for temperature calculated as the average temperature of the warmest month in the period 2000–2010 and for dissolved oxygen as the average level occurring in the month having the lowest average dissolved oxygen in the period 2000–2010; they are thus mean maximum and minimum values, respectively. All mean values were then assigned descriptive labels using existing thresholds (shown in Table S1), concatenated to form a short descriptive seascape name that summarizes the dominant environmental conditions represented by the cluster. For example, a high-latitude continental shelf seascape might be labeled as *Minimally Tidal, Moderately High Wave Energy, Mesobenthic to Shallow Infralittoral Depth, pH Above CCD, Euhaline, Highly Oxic, Very Low Productivity, Very Cold Temperature, with Moderate Ice*.

EBUs inherit the seascape name and append the corresponding geomorphic feature name. As a result, every location on the ocean floor represented in the EBU map is associated with an explicit descriptive label that captures both its environmental setting and its geomorphic context. These labels are provided with the publicly available EBU dataset.

EBU HETEROGENEITY

To identify areas where the greatest EBU heterogeneity occurs, a focal variety analysis of the data was undertaken in ArcGIS Pro 3.6. The focal variety tool determines the number of unique values (or the variety) for each cell location on an input raster within a specified neighborhood and sends it to the corresponding cell location on the output raster. In this study, we used a 100 km search radius (i.e., an area of 31,400 km^2) to define the neighborhood, reported here as polygons per 1,000 km^2. EBU heterogeneity used normalized numbers of EBUs in the neighborhood analysis window, thus taking into account any potential variation in the density of EBU types across the geomorphic groups that may have been caused by differing clustering approaches within the geomorphic groups.

RESULTS: SEASCAPES AND GEOMORPHIC FEATURE SUB-CLASSES

The global map of seascapes (Figure 1) produced in this study divides the ocean floor into 162,687 separate polygons. The following sections describe the 57 seascape types by geomorphic group and assess the intersection of seascapes with the previously mapped geomorphic features.

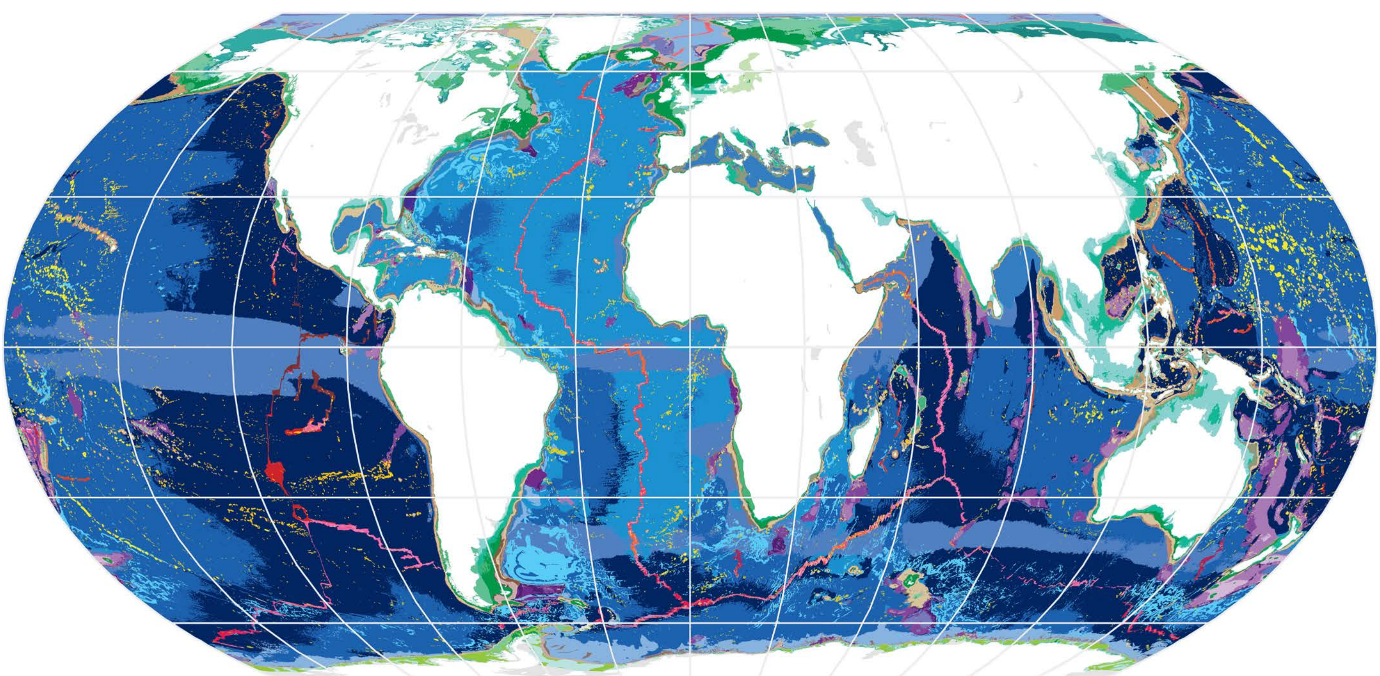

FIGURE 1. Map in Equal Earth projection of the global distribution of 57 seascapes derived for the present project.

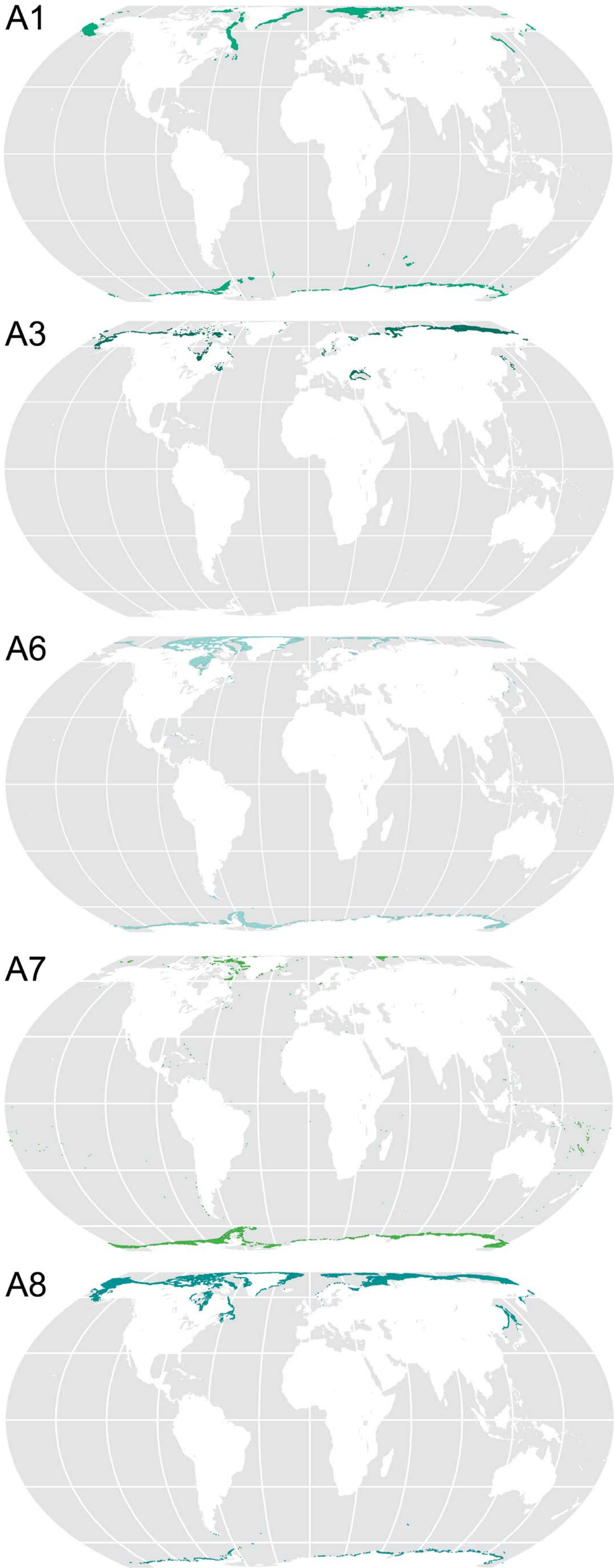

FIGURE 2. Polar shelf seascapes (A1, A3, A6, A7, and A8), mapped in the Equal Earth projection (as per all maps in this paper), derived in the present study. See Table 1 for the list of variables used in the cluster analysis. These seascapes have mean sea ice cover per day of greater than 70% and mean water temperature below 2.8°C. The geomorphic features associated with each seascape are illustrated in Figure 3.

SHELF SEASCAPES (GROUP A) AND GEOMORPHIC FEATURES

The 12 shelf seascapes fall into three broad categories based on sea ice cover and water temperature: polar, tropical, or temperate. The "polar" category (A1, A3, A6, A7, A8) is characterized by significant sea ice cover (grid cells are ice-covered >70% of the year), cold water (<2.8°C), generally very low to low primary productivity, and the occurrence of geomorphic glacial troughs (Figures 2 and 3). Seascape A1 contains only 0.46 polygons per 1,000 km^2, making it the least heterogeneous (greater number of large, continuous polygons) of all shelf seascapes.

Polar seascape A7 has the deepest mean water depth of all shelf seascapes (602 ± 186 m; 186 m is the standard deviation convention used throughout this paper). This great depth is associated with the greatest occurrence of shelf-perched basins, abundant glacial troughs, and the smallest area of low-relief shelf. A7 also has a low mean temperature (0.24°C), which explains the occurrence of this seascape at some higher latitudes (Figure 2) where the shelf extends deeper and intersects cold water masses.

Seascape A3 stands out with its very shallow mean water depth (15.6 ± 12.5 m), relatively low mean salinity (22 ppt), and very high dissolved oxygen 360 ± 33 mmol m^{-3}. This seascape is found close to the Arctic coastline and in the Black Sea (Figure 2), and it is the warmest and has the highest primary productivity of the polar seascapes.

There are two "tropical" shelf seascapes (A4 and A10) where mean temperature is over 20°C—this is where 85% of coral reefs occur (Figures 3 and 4). Seascapes A4 and A10 are the largest shelf seascapes by surface area, covering 5,615,274 km^2 and 6,073,758 km^2, respectively (Figure 3), totaling 36.7% of the

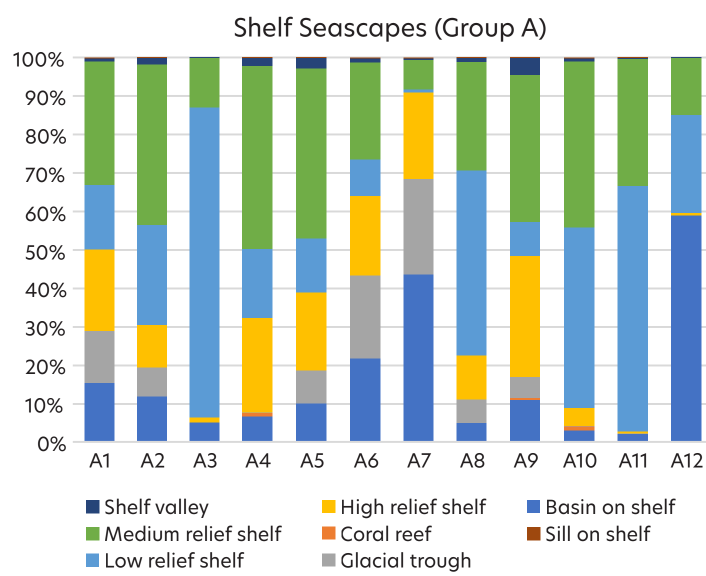

FIGURE 3. Intersection of different shelf geomorphic features with the seascapes, shown as a percent area. The graph shows that each seascape is dominated mainly by different percent areas of low (<10 m), medium (10–50 m), and high (>50 m) vertical relief shelf areas.

total shelf area (31,894,360 km^2). Seascape A10 has greatest area of all shelf seascapes and includes the largest area of coral reefs (57,543 km^2), largest area of low-relief shelf (2.8 million km^2), 46% of sills, and the second-highest mean tidal range of 2.37 m.

Seascape A4 is noteworthy for having the highest mean salinity (34.98 ppt) of all shelf seascapes. It also has the second greatest area of all shelf seascapes and includes the second-largest area of coral reefs (45,081 km^2) and the largest area of medium-relief shelf (2.6 million km^2), capturing some temperate regions as well (e.g., Stuart-Smith et al., 2017).

The five "temperate" seascapes (A2, A5, A9, A11, and A12) are broadly distributed geographically but have a generally moderate mean temperature range between 3.11°C and 17.97°C. In other respects, these seascapes each exhibit a unique, characteristic attribute. Seascape A2 is the only macrotidal seascape, having a mean, macrotidal range of 5.09 ± 2.06 m, the largest range of all shelf seascapes. This seascape is found on the west European shelf; in the Gulf of Alaska, eastern Canada, and the Sea of Okhotsk; and on the southern Argentine shelf and the Australian northwest shelf.

Seascape A5 exhibits the most energetic wave climate, with a mean significant wave height of 2.94 ± 0.75 m, found around the North Atlantic, Aleutian Islands, southern part of South America, New Zealand, and southern Australia (Figure 5). A5 is also characterized by a significant area of glacial trough.

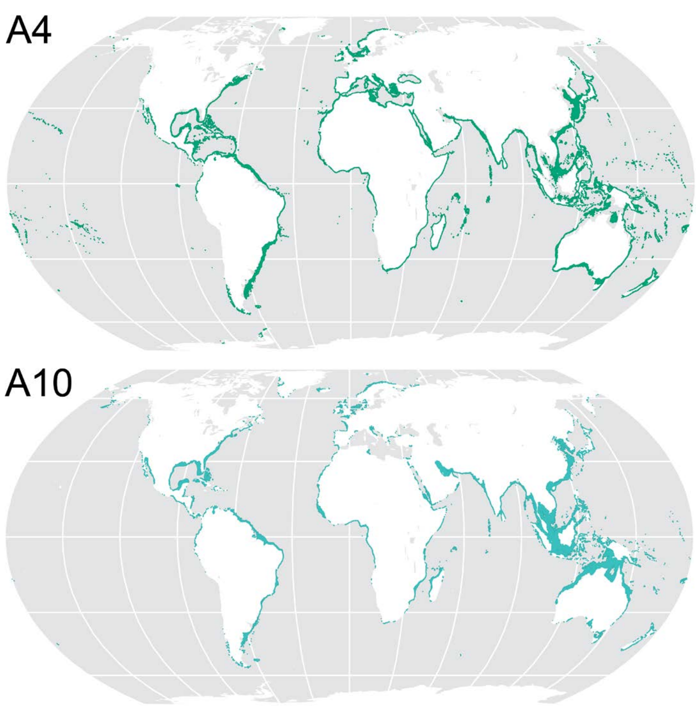

FIGURE 4. "Tropical" shelf seascapes (A4 and A10) derived in the present study are generally located near the equator but do extend to higher latitudes in some places. Seascapes A4 and A10 have mean water temperatures of 20.09° ± 5.75 ° C and 29.05° ± 4.71°C, respectively. The geomorphic features associated with each seascape are illustrated in Figure 5.

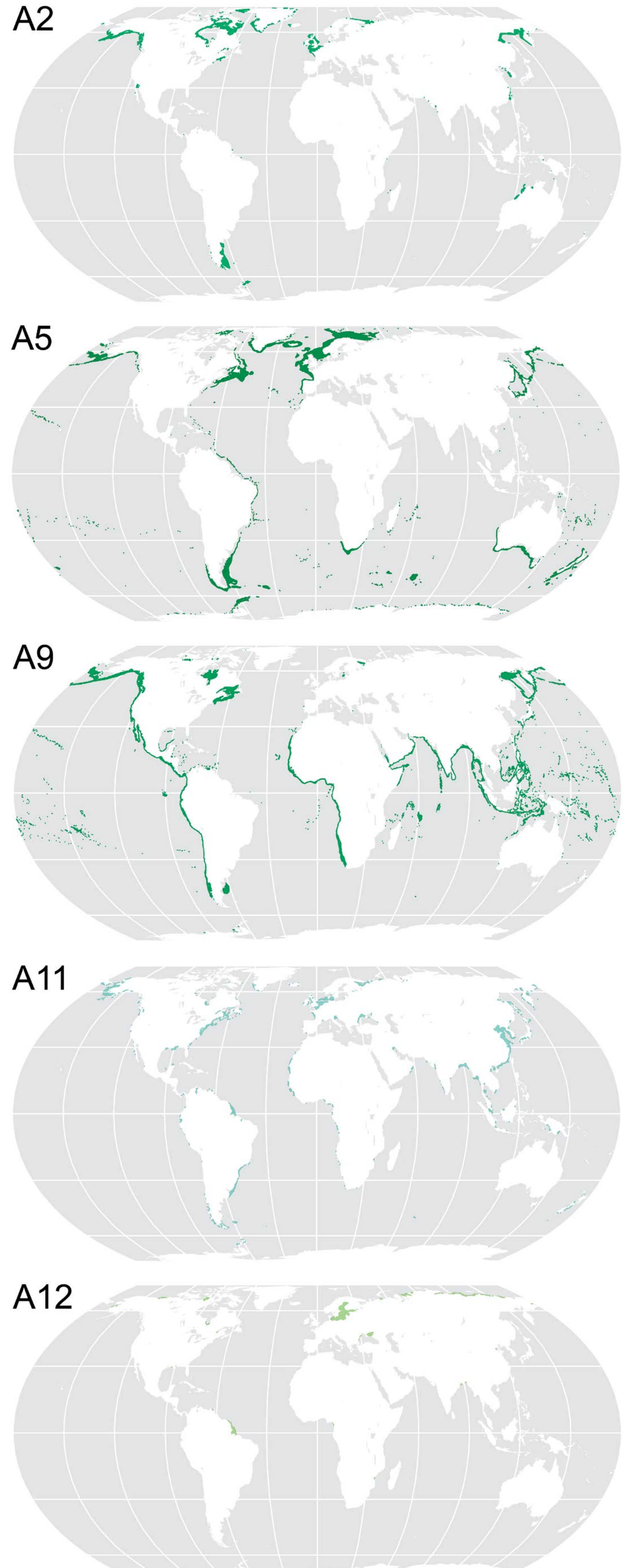

FIGURE 5. "Temperate" shelf seascapes (A2, A5, A9, A11, and A12) derived in the present study generally have mean water temperatures between 3.11°C and 17.97°C. The geomorphic features associated with each seascape are illustrated in Figure 3.

Seascape A9 is the only hypoxic shelf area with (long-term minimum) dissolved oxygen levels of 94.55 mmol m^{-3}. It is also characterized by relatively low pH (mean value of 7.7), compared to other shelf waters. This seascape is spatially very strongly associated with western continental margins (Figure 5), which are commonly known as upwelling zones. The upwelled water masses are commonly depleted of oxygen and have a lower pH. Upwelling of deep water depleted in oxygen has been documented in a number of locations associated with boundary currents, including off the coasts of Peru, California (USA), Chile, and West Africa (Chavez and Messié, 2009). The source of the deep water is not necessarily from abyssal depths, but rather mid-depth, oxygen minimum zones. However, there is also evidence that oxygen levels in the global ocean are decreasing in association with anthropogenic climate change and that mid-depth oxygen minimum zones are expanding (Grégoire al., 2021).

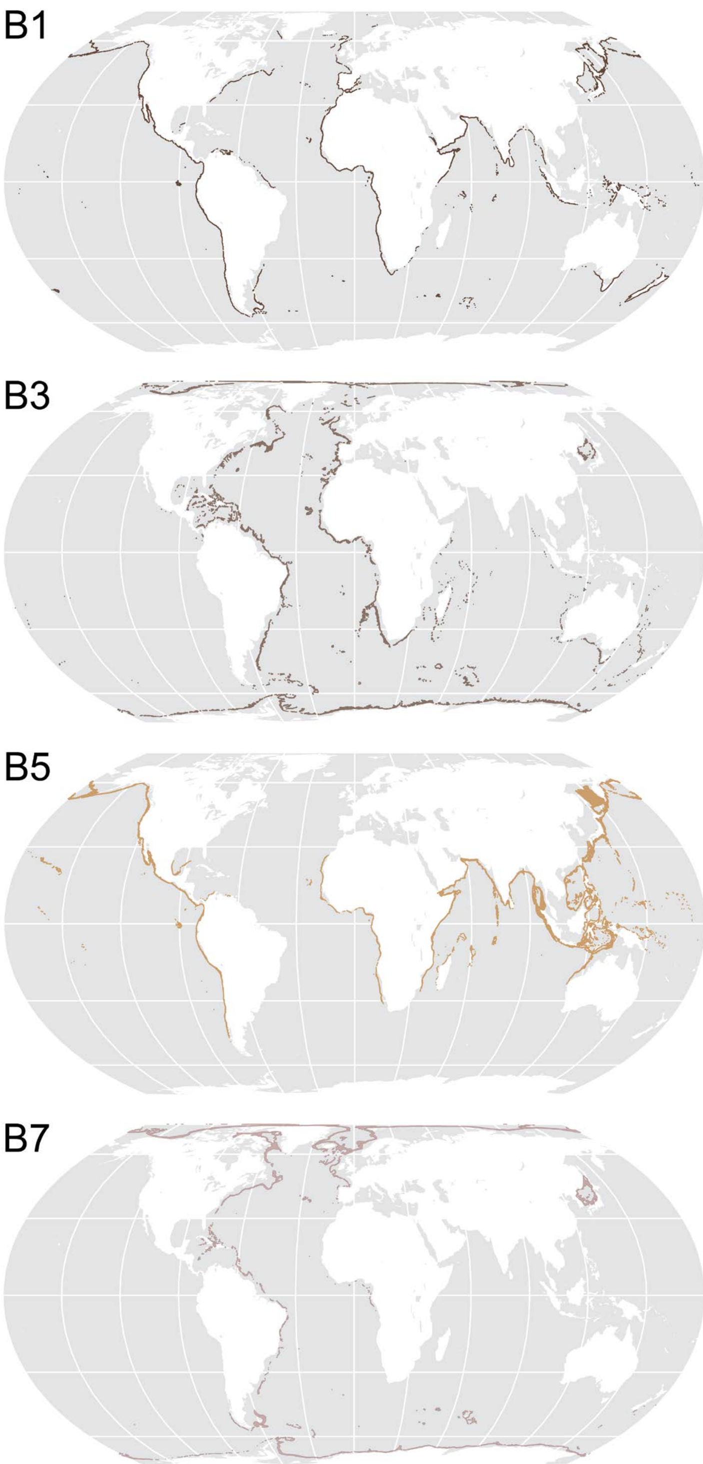

FIGURE 6. Hypoxic slope seascapes B1 and B5 versus highly oxic seascapes B3 and B7. In terms of the depth differences, the mean water depth is 285 m for B1, 895 m for B5, 2,752 m for B3, and 1,112 m for B7.

Seascape A11 is characterized by a very shallow mean depth of 15.86 m, the highest mean pH of 8.07 (most alkaline), and the highest primary productivity, 5.78 mmol m^{-3}, of all shelf seascapes. A11 is the most heterogeneous of all shelf seascapes, containing 2.57 polygons per 1,000 km^2. This seascape is broadly dispersed, occurring on the margins of most continents with the exceptions of Australia and the eastern shelf of Africa.

Finally, seascape A12 is classed as "Atidal," having a mean tidal range of only 0.0693 m; it also has low wave energy with mean significant wave height of 0.91 m, and it has the lowest salinity of all shelf seascapes, only 7.14 ppt. This seascape is geographically constrained to the Baltic Sea, the mouth of the Amazon River, and also adjacent to major Russian and Canadian river mouths that discharge into the Arctic Ocean.

SLOPE SEASCAPES (GROUP B) AND GEOMORPHIC FEATURES

Slope seascapes are mostly isobath parallel zones of continental margins. Among the most important variables for benthos is the dissolved oxygen regime of the water mass (e.g., Diaz and Rosenberg, 2008; Brietburg et al., 2009; Levin, 2018) impinging on the slope and geomorphic features found along it. Slope seascapes B1 and B5 are characterized by water containing (long-term minima) 72.2 and 52.5 mmol m^{-3} dissolved oxygen, making these seascapes hypoxic and severely hypoxic, respectively. Seascape B1 is located at the shallowest mean water depth (285 m) of all slope seascapes, and seascape B5 is the third most shallow seascape (895 m). The pH of bottom water in these two seascapes is also the lowest (most acidic) of all slope seascapes (mean pH of 7.67 and 7.64 for B1 and B5, respectively). Seascape B1 has the highest rate of particulate organic carbon flux (7.12 mmol/m^2/d), which is consistent with these areas' association with ocean upwelling and enhanced primary productivity. Hypoxic seascape geographic distribution is concentrated around the Pacific rim, along the eastern margin of North and South America, in the western Pacific along the coast of Asia, and around Africa, India, New Zealand, and Tasmania (Figure 6). Finally, seascape B1 has the greatest heterogeneity of slope seascapes, 6.7 polygons per 1,000 km^2, while B5 has the lowest heterogeneity, 0.80 polygons per 1,000 km^2.

In contrast, seascapes B3 and B7 are characterized by the most oxygen-rich waters, containing mean dissolved oxygen levels of 270 and 297 mmol m^{-3}, respectively. Seascapes B3 and B7 are also characterized by cold bottom water (mean temperatures of −0.07°C and 0.11°C, respectively) and high pH (mean pH values of 7.94 and 8.02, respectively). These well oxygenated seascapes occur at intermediate water depths (2,752 m and 1,112 m, respectively) and are located in both polar seas and along the margins of the Atlantic (Figure 2).

With regard to slope geomorphic features (Figure 7), one obvious association is that about 53.7% of slope-perched basins occur in seascape B9. The depth range of this seascape is 1,581 ± 576 m, and the gradient mean is 1.66°, which characterizes the common locations of slope basins. Submarine canyons occur in all nine seascapes but are most common in polar regions of seascape B3, which contains 32.1% of blind canyons and 22.3% of shelf incising canyons. This is consistent with the observation of Harris et al. (2014) that canyons in polar regions are the largest in the world ocean.

SEAMOUNTS AND GUYOTS (GROUP C)

The five seascapes created for seamounts and guyots suggest two main categories: Seascapes C1 and C3 (Figure 8) are characterized by warm waters (mean bottom water temperatures of 2.86°C and 8.31°C, respectively) and low to high organic matter flux (mean POC flux of 0.24 and 1.46 mmol/m^2/d, respectively). The other three seascapes (C2, C4, and C5) are colder (mean temperature <1.45°C) and exhibit very low POC flux (mean POC flux <0.08 mmol/m^2/d).

Seascape C3 has the greatest heterogeneity of seamount and guyot seascapes with 6.95 polygons per 1,000 km^2. Compared to deep, cold, low oxygen seascapes (Costello et al., 2023), this seascape appears to provide relatively more favorable conditions for species among seamounts and guyots with warm, oxygenated waters (mean dissolved oxygen is 185 mmol m^{-3}), good food supply (high POC flux), relatively strong bottom currents (maximum current speed of 0.58 m s^{-1}), and locations above the carbonate compensation depth (CCD; mean pH is 7.91). However, C3 is also the smallest seamount and guyot seascape at only 81,855 km^2, representing only 0.94% of the total area of 8,715,301 km^2 for seamounts and guyots.

Seascape C1 covers more area (1,260,146 km^2) but has colder water and low POC flux. Nevertheless, C1 still has oxygenated waters (mean dissolved oxygen is 243 mmol m^{-3}), relatively strong bottom currents (maximum current speed of 0.4 m s^{-1}), and is mainly located above the CCD (mean pH is 7.90).

The three cold/low POC flux seascapes (C2, C4, and C5) are generally much larger in area, overall comprising 72.1% of seamount and guyot seascapes. Seascape C4 is the largest among seamount and guyot seascapes at 2.95 million km^2, and it also has the lowest heterogeneity of 0.72 polygons per 1,000 km^2.

SPREADING RIDGES AND RIFT VALLEYS (GROUP D)

Multivariate analysis of spreading ridges and rift valleys within slower-spreading ridges identified 15 separate seascapes (Figure 9). Based on mean seafloor spreading rate, the group can be divided into three main categories: slow (<50 mm yr^{-1}), medium (55–100 mm yr^{-1}), and fast (>100 mm yr^{-1}). The "fast" category has only two members, seascapes D2 and D9, which are characterized by having the gentlest mean seafloor gradients (1.13° and 1.23°, respectively) and the lowest mean dissolved oxygen levels (136 mmol m^{-3} and 159 mmol m^{-3}, respectively) of all spreading ridge and rift valley seascapes. Seascape D2 has the lowest heterogeneity among spreading ridge and rift valley seascapes of 0.21 polygons per 1,000 km^2.

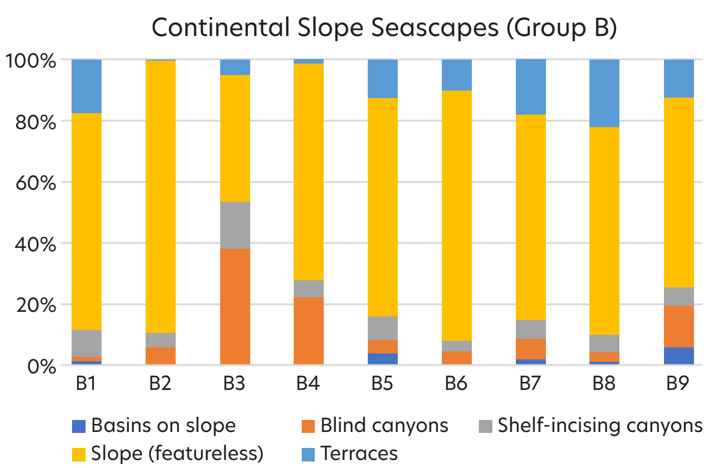

FIGURE 7. Intersection of different slope geomorphic features with the seascapes, shown as a percent area. The graph shows that featureless slope comprises the majority of slope area.

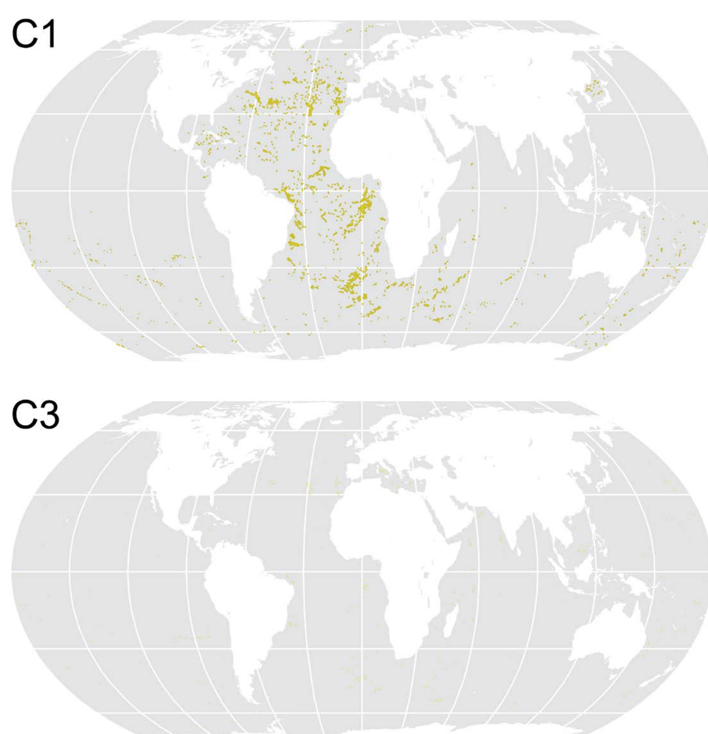

FIGURE 8. Maps show the locations of seascapes C1 and C3, characterized by warm waters and low (C1) to high (C3) organic matter flux.

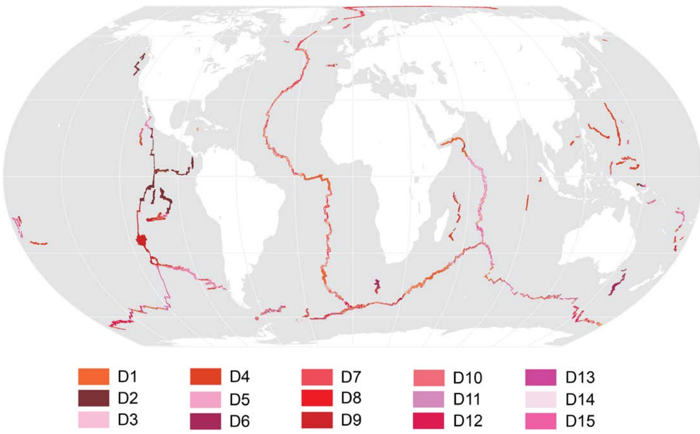

FIGURE 9. Map provides the locations of seascapes D1 to D15, which characterize the mid-ocean spreading ridges and rift valleys. Darker colors indicate faster spreading sub-classes.

The "medium" category includes four seascapes, D4, D5, D13, and D15, and all nine of the other seascapes are in the "slow" category. The "fast" and "medium" categories are located almost exclusively in the Pacific and Indian Oceans (Figure 9). The seascapes range in size from 20,572 km^2 (D14) to 1.023 million km^2 (D15) and have a total area of 6.166 million km^2. Seascape D3 in the "slow" category has the greatest heterogeneity among spreading ridge and rift valley seascapes of 8.53 polygons per 1,000 km^2.

ABYSSAL SEASCAPES (GROUP E) AND GEOMORPHIC FEATURES

Multivariate analysis of the abyssal to hadal ocean floor identified seven separate seascapes (Figures 10 and 11). Abyssal seascapes are generally characterized by their very large area (average size of 39.9 million km^2) and very low heterogeneity (average of 0.29 polygons per 1,000 km^2). Distinguishing and unique aspects that characterize each of the abyssal seascape are as follows:

- E1 4.6% of abyssal seascapes by area, has the greatest mean bottom current speed of 0.77 m s^{-1}.
- E2 10.9% of abyssal seascapes by area, has the greatest POC flux of 0.53 mmol/m^2/d.
- E3 31.9% of abyssal seascapes by area, has the youngest mean age of ocean crust (22.4 million years), the thinnest cover of sediment (mean thickness of 101 m), and the lowest mean dissolved oxygen (176 mmol m^{-3}). E3 has the largest areas of abyssal mountains, fans, ridges, and troughs (Figure 10). The age of ocean crust is inversely proportional to sediment cover (young crust has had less time for sediment to accumulate; Olson et al., 2016) and hence we expect a relationship between crustal age and the occurrence of rocky substrate versus thick sediment cover habitats.
- E4 13.4% of abyssal seascapes by area, has the highest dissolved oxygen of 250 mmol m^{-3}. E4 has the largest area of continental rise (Figure 10).
- E5 3.4% of abyssal seascapes by area, has the coldest mean water temperature of –0.55°C, the lowest mean POC flux of 0.01 mmol/m^2/d, and most alkaline waters with a mean pH of 7.93 (equal with E6).
- E6 1.5% of abyssal seascapes by area, has the oldest mean ocean crust age at 136.7 Ma, the thickest sediments (mean thickness 6,986 m), most shallow mean depth of 2,679 m, warmest mean water temperature of 3.95°C, and most alkaline waters with a mean pH of 7.93 (equal with E5).
- E7 34.3% of abyssal seascapes by area, has the greatest mean depth of 5,096 m, weakest mean bottom current speed of 0.08 m s^{-1}, and most acidic pH of 7.75, which is below the CCD. E7 has the largest areas of abyssal hills, abyssal plains, bridges, hadal zones, and trenches (Figure 10).

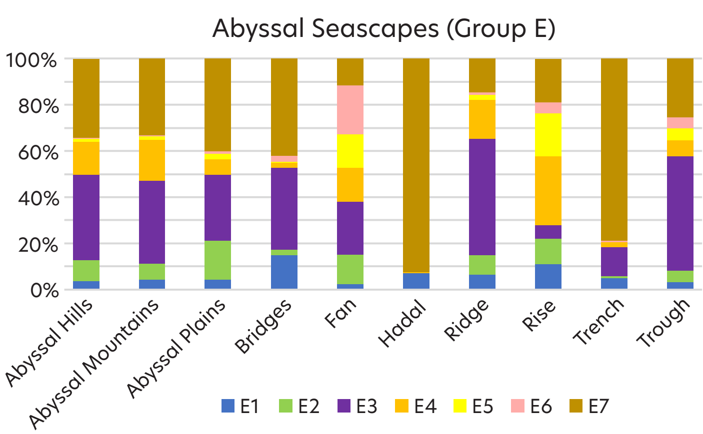

FIGURE 10. The distribution of geomorphic features by seascape as a percent of area is plotted in this bar graph.

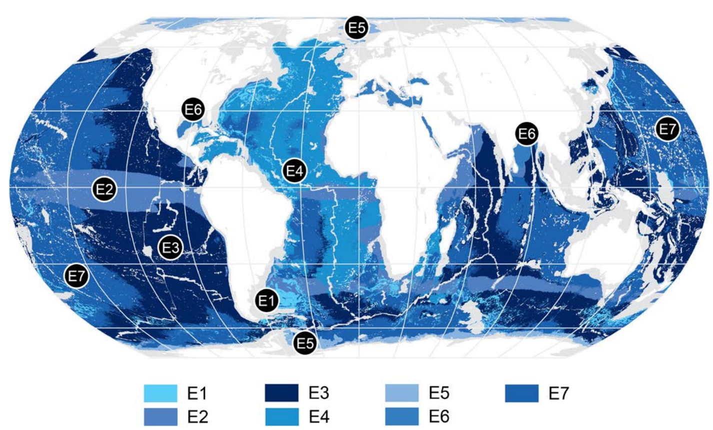

FIGURE 11. Map shows the locations of seascapes E1 to E7 that characterize the abyssal to hadal ocean floor.

By combining geomorphic structure with key biophysical drivers—including temperature, oxygen, pH, carbon flux, bottom currents, and sediment thickness—the EBU framework reveals previously unrecognized environmental gradients and boundaries across the global ocean floor.

PLATEAUS (GROUP F)

Multivariate analysis of the ocean floor having plateaus identified nine separate seascapes (Figure 12). Distinguishing and unique aspects that characterize plateau seascapes are as follows:

F1 6.4% of plateau seascapes by area, has the greatest mean sediment thickness of 4,168 m, located mainly in the Atlantic Ocean.

F2 1.6% of plateau seascapes by area, has very strong maximum bottom current speed of 0.44 m s^{-1} (nearly equal to F9), comprised of two plateaus located in the western Atlantic and one plateau off Norway. F2 has the lowest heterogeneity among plateau seascapes of 0.12 polygons per 1,000 km^2.

F3 8.0% of plateau seascapes by area, has the most alkaline mean bottom water pH of 8.02, located mainly in the Arctic Ocean and the North Atlantic.

F4 6.9% of plateau seascapes by area, deepest plateaus at mean depth of 3,074 m, lowest (most acidic) pH of 7.81, thinnest mean sediment cover of 518 m, broadly distributed but mainly located in the Pacific and Indian Oceans.

F5 34.9% of plateau seascapes by area, the largest seascape by area, similar to F4 as it is broadly distributed but mainly located in the Pacific and Indian Oceans.

F6 33.0% of plateau seascapes by area, has the lowest mean dissolved oxygen level of 156 mmol m^{-3}, broadly distributed.

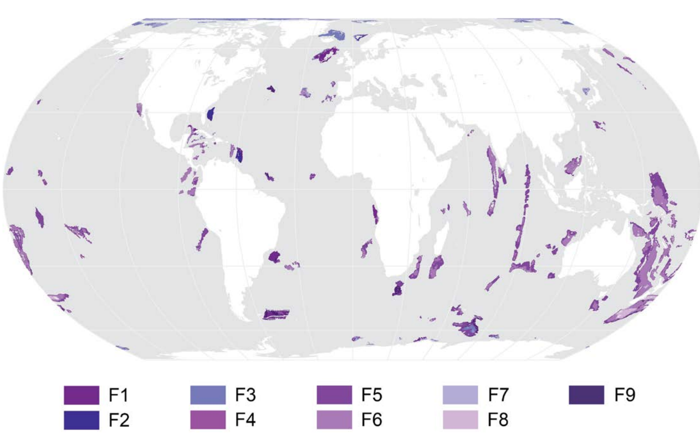

FIGURE 12. Seascapes F1 to F9 that characterize plateaus are plotted here.

F7 1.1% of plateau seascapes, the smallest plateau seascape by area, steepest seafloor gradient of 5.08°, coldest mean bottom water temperature of −0.5°C, and lowest mean POC flux of 0.01 mmol/m^2/d, located mainly in the Arctic and Southern Oceans. F7 has the greatest heterogeneity of 8.85 polygons per 1,000 km^2 (highest of all seascapes, globally).

F8 3.4% of plateau seascapes by area, most gentle seafloor slope of 0.39°, most shallow mean depth of 530 m, warmest mean bottom water temperature of 7.34°C, greatest mean POC flux of 1.87 mmol/m^2/d, located mainly adjacent to New Zealand.

F9 4.8% of plateau seascapes by area, has very strong maximum bottom current speed of 0.46 m s^{-1} (compare to F2), broadly distributed.

RESULTS: ECOLOGICAL BENTHIC UNITS

The individual polygons located within specific geomorphic feature polygons are termed ecological benthic units (EBUs). Each EBU is a unique combination of a biophysical (bottom water) seascape located within a particular geomorphic unit. A total of 697,235 EBUs have been identified in this study.

The characteristics of EBUs provide specific environmental context for the geomorphic feature in which they occur and provide a basis for distinguishing between features of the same type (i.e., differences among seamounts, submarine canyons, and deep ocean trenches). The information can be accessed through the online EBU Explorer created as an output of this project. The following section provides examples of specific geomorphic features and the EBUs they contain.

"THE GULLY" SUBMARINE CANYON

"The Gully" submarine canyon, located about 200 km off the coast of Nova Scotia, Canada, is 15–16 km wide and extends approximately 65 km downslope to a depth of over 3,000 m. It is a shelf-incising canyon carved into Tertiary bedrock draped by Quaternary glaciomarine sediments. The canyon was formed by combined mass wasting of the slope and turbidity currents during the Pleistocene. The Gully links the shallow banks of the continental shelf with deeper, steep canyon walls that support cold-water corals and other benthic fauna, while the canyon floor supports deep-water fish, invertebrates, and deep-diving cetaceans, linking surface, pelagic, and benthic ecosystems (Harrison and Fenton, 1998; Fisheries and Oceans Canada, 2025).

Figure 13 shows screenshots of information provided by the EBU Explorer tool for The Gully canyon. The dialogue box indicates that the highlighted feature is a shelf-incising submarine canyon and that there are 20 EBUs within the canyon polygon. The bar graph illustrates how The Gully compares globally with shelf-incising submarine canyons, indicating that The Gully has a relatively high proportion of seascape B3, with oxygen-rich waters. In contrast, there is an absence of seascapes B4, B5, and B9.

The panels below the bar graph contain information on the 20 EBUs, listed in order of decreasing percent area. The top EBU number, 157859 (seascape B3), covers 75.2% of The Gully, and it is located mainly on the lower continental slope. The second EBU number, 161480 (seascape B7), covers 10.2% of The Gully and is located mainly on the upper continental slope and across the shelf

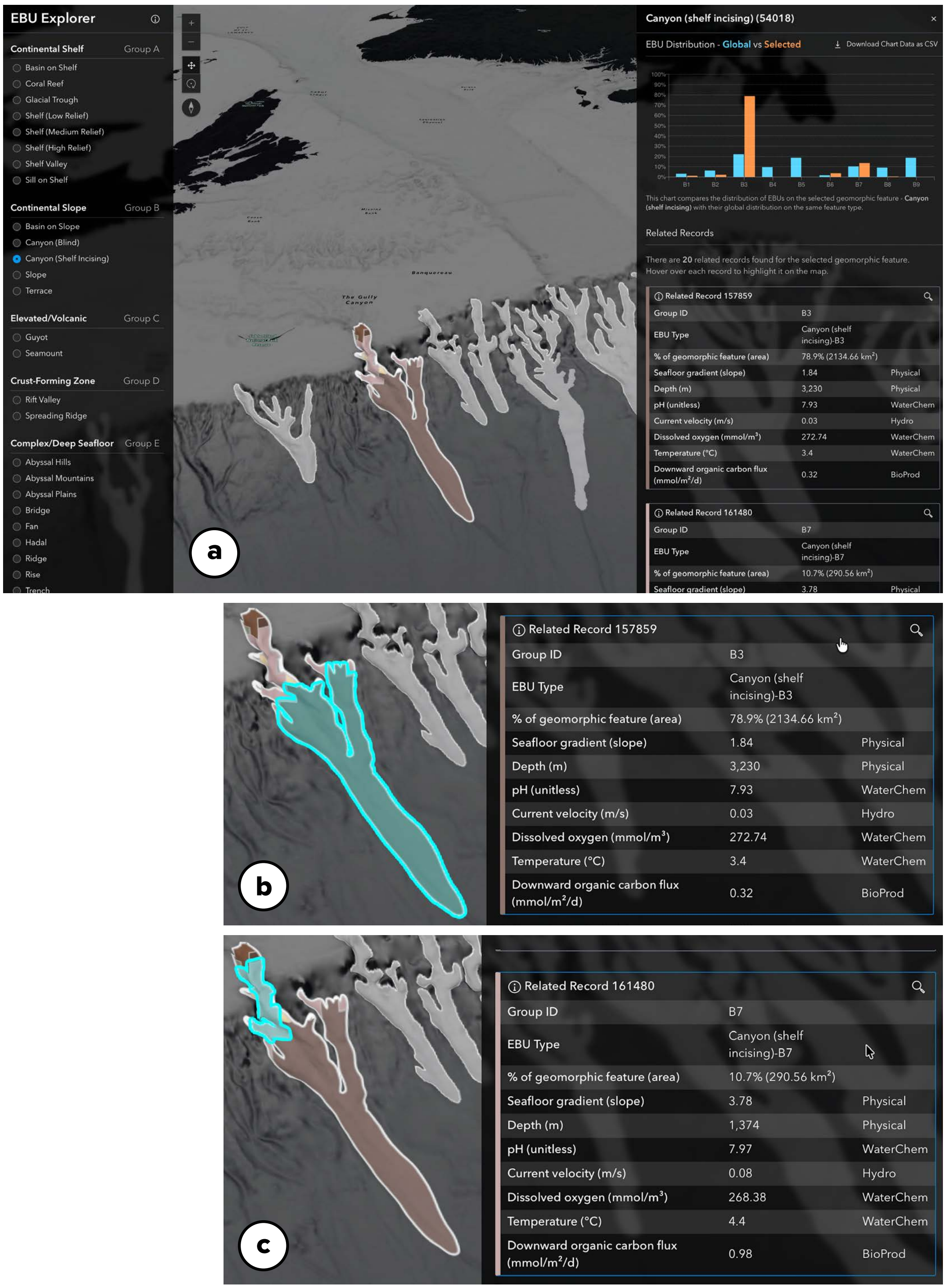

FIGURE 13. Screenshots taken from the EBU Explorer show the The Gully submarine canyon off Newfoundland, Canada. (a) Location of The Gully with bar graph showing the relative proportion of EBUs characterizing all shelf-incising canyons (in blue) versus the EBUs that characterize The Gully canyon (in orange). (b) Zoom-in view of EBU B3 with respective information panel. (c) Zoom-in view of EBU B7.

break. EBU B7 is 1°C warmer in mean temperature than B3 (4.4°C versus 3.4°C), illustrating the most significant difference in physical properties between the two (Figure 13).

MARIANA TRENCH

The Mariana Trench, the deepest part of the ocean, is located in the western Pacific Ocean, east of the Mariana Islands. It forms a long, narrow, crescent-shaped depression created where the Pacific Plate subducts beneath the smaller Philippine Sea Plate and the small, crescent-shaped Mariana microplate that broke off from it (van Rijsingen, 2019). It is ~2,500 km in length, 70–100 km in width, and reaches its deepest point at 10,935 m in the Challenger Deep (Greenaway et al., 2021). The Trench has steep, asymmetric sides, and the western wall is typically steeper due to tectonic forces that include the large age differential between the downgoing and overriding plates.

Figure 14 shows a segment of the Mariana Trench illustrating its composition relative to trenches globally. Seascape E7 is dominant in most trenches, as it is with the Mariana Trench, characterized by cold temperatures and acidic bottom waters (see also Figure 10). But in contrast to other trenches, the Mariana Trench does not contain any area of seascapes E2, E3, E4, or E6 (Figure 14).

GIFFORD GUYOT

Gifford Guyot is a flat-topped seamount located on the Lord Howe Rise plateau in the Coral Sea. The Gifford Marine Park is included within the Australian Government's national marine protected area network (Nanson et al., 2018). The Guyot formed as the Indo-Australian plate migrated north across a stationary magma source ("hotspot") during the Middle Miocene (about 15 million years ago) and has a depth range of approximately 3 km, rising from 3,400 m on the abyssal plain to as shallow as 250 at its summit (Nanson et al., 2018).

Figure 15 illustrates the dominance of seascape C5, characterized by warm water temperatures around the Gifford Guyot. In contrast, most guyots globally are dominated by seascape C4 with its colder water temperatures. Of particular significance is the above-average occurrence of seascape C3 on the Gifford since

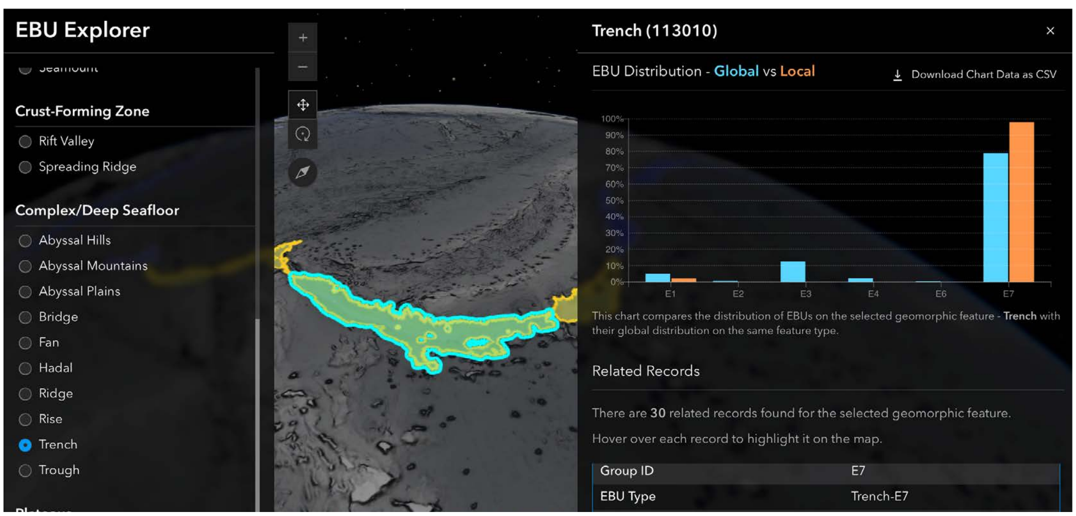

FIGURE 14. Screenshot taken from the EBU Explorer showing a section of the Mariana Trench in the Pacific Ocean. The bar graph plots the relative proportion of EBUs comprising the trench, which is dominated by seascape E7; seascape E1 covers less than 2%. The largest EBU, which covers 60.3% of the trench, is shown here.

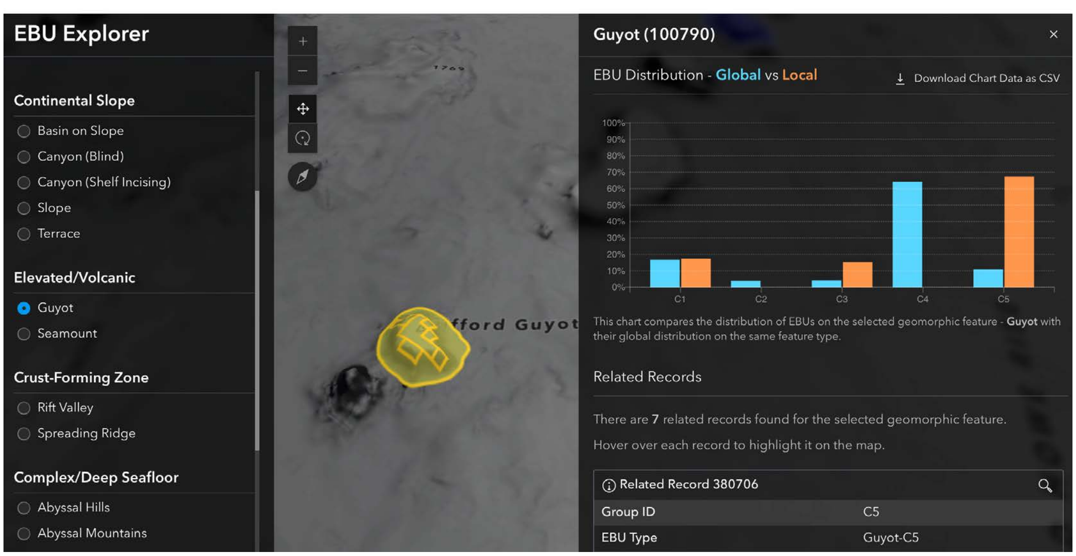

FIGURE 15. Screenshot taken from the EBU Explorer describes Gifford Guyot in the Coral Sea. The bar graph shows the relative proportion of EBUs comprising Gifford Guyot, which is dominated by seascape C5.

this seascape was noted above for its high heterogeneity and high potential for benthic productivity and biomass. Limited sampling of the Gifford suggests the presence of a relatively diverse, albeit sparse, epibenthic assemblage, including mixed cold-water coral and sponge assemblages (Nanson et al., 2018).

DISCUSSION

INSIGHTS INTO GLOBAL BENTHIC BIODIVERSITY FROM EBUs

The diversity of EBUs is an indicator of the diversity found in benthic ecosystems, and as such, it can also be considered to represent benthic biodiversity in terms of likely species richness for a given area (e.g., Harris and Baker, 2020; Almond et al., 2021; Girard et al., 2025). Our map of EBU heterogeneity (Figure 16) has direct applications in designing and cross-validating spatial conservation zones (i.e., marine protected areas, MPAs; Howell, 2010; Fischer et al., 2019); we note, for example, the close correspondence between our map of EBU diversity (Figure 16) and the map of MPA prioritized areas by Zhao et al. (2020, their Figure 4). The hotspots of heterogeneity (Figure 16) immediately suggest themselves within bioregions as candidates for MPAs, where the maximum biodiversity can be conserved in the smallest possible area (Roff and Taylor, 2000). They are also areas where targeted marine surveys could be optimized to investigate the regional diversity of environments.

CCD AND ACIDIFICATION

EBUs provide the first global, spatially explicit view of how seafloor habitats are distributed relative to the CCD and therefore quantify which benthic systems are already exposed—or will soon be exposed—to corrosive, low-pH bottom waters. Seascape E7, the most abundant seascape globally (95.6 million km^2), is characterized by a mean pH of 7.75, already below the modern CCD threshold used in this study. The extent of E7 highlights that a substantial fraction of the global abyss is currently bathed in waters corrosive to calcium carbonate ($CaCO_3$). This has direct ecological implications: the CCD has recently been demonstrated to act as a biological boundary that structures abyssal biogeography (Simon-Lledó et al., 2023), and experimental studies confirm that decreasing pH reduces fitness and survival in several abyssal taxa (Barry et al., 2013).

As the ocean continues to absorb anthropogenic CO_2, deep-water masses entering the global conveyor belt (thermohaline circulation system) will carry progressively lower pH and oxygen concentrations. Model and observational evidence indicate that the CCD is rising (Sulpis et al., 2018; Harris et al., 2023), resulting in increasing areas of the seafloor—particularly in older, sediment-starved basins—crossing into undersaturated conditions. EBUs therefore allow us to identify which geomorphic systems lie nearest to this chemical boundary and where upward shoaling of the CCD will most rapidly expose carbonate-dependent habitats and fauna to corrosive conditions.

EBUs offer a novel geospatial tool for quantifying ecosystem vulnerability to ocean acidification by mapping the intersection of benthic environments, geomorphic features, and evolving carbonate saturation horizons. This capability is directly relevant to global MPA planning, environmental impact assessment for deep-sea industries, and future biodiversity monitoring frameworks.

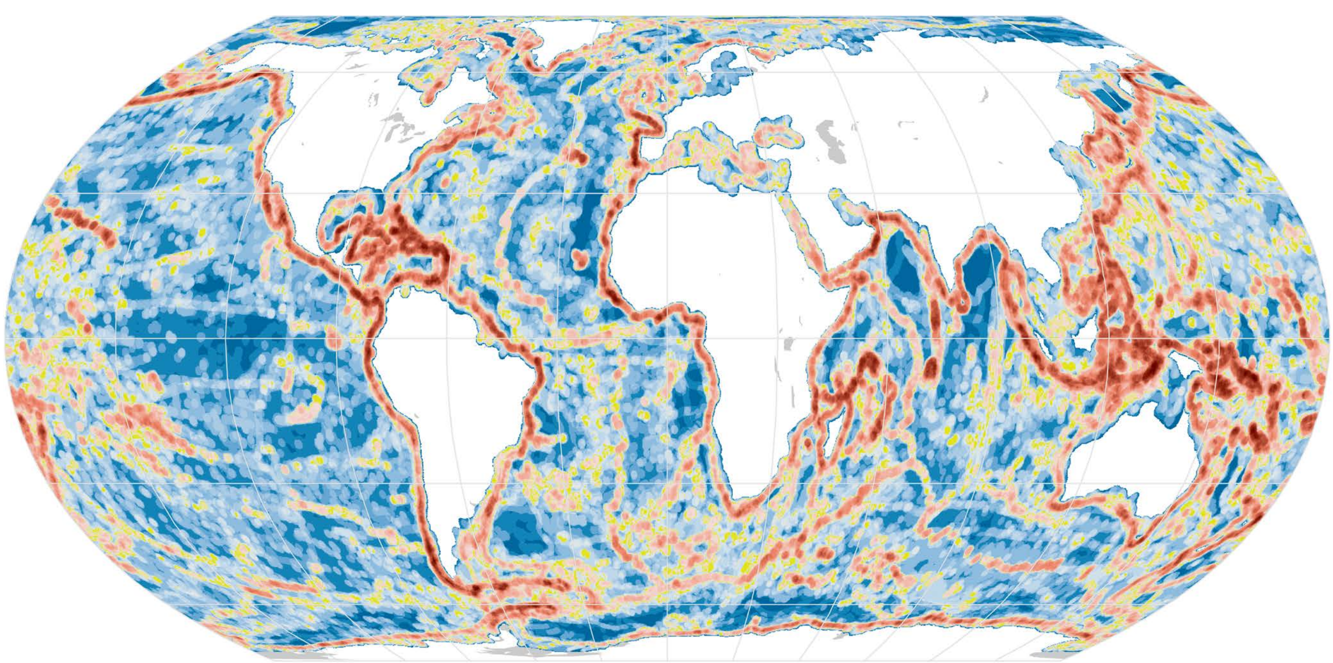

FIGURE 16. Map showing the heterogeneity of the global ocean based on focal variety analysis of EBU polygons within a 100 km search radius. Blue colors indicate heterogeneities as low as 1 and red colors heterogeneities as high as 50. Higher heterogeneity values identify broad transition zones where multiple EBU types occur together within a regional neighborhood.

OXYGEN DEAD ZONES

Oxygen minimum zones (OMZs) are expanding globally due to warming-driven stratification and reduced ventilation, and EBUs provide a new way to map where low-oxygen waters intersect specific geomorphic settings. Slope seascapes B1 and B5 represent the clearest expression of this phenomenon: they contain hypoxic (72.2 mmol m^{-3}) and severely hypoxic (52.5 mmol m^{-3}) bottom waters, respectively, and together cover 4.16 million km^2. Their distribution—along the continental margins of the Pacific Rim, western South America, North America, and parts of Asia, Africa, India, New Zealand, and Tasmania—closely matches known global OMZ cores (Paulmier and Ruiz-Pino, 2009).

These oxygen-depleted environments (oxygen dead zones) have well-documented ecological consequences, including reduced habitat suitability for metabolically sensitive taxa, compression of species' depth ranges, altered trophic structure, and enhanced vulnerability of demersal fisheries (Diaz and Rosenberg, 2008; Levin, 2018). Our results show that the most oxygen-stressed systems (and EBUs) occur on economically important slopes near productive shelf ecosystems, where many nations rely on fisheries resources.

The ability to quantify the areal extent and geomorphic context of hypoxic EBUs provides a practical tool for evaluating where deepening OMZs will next make contact with slope habitats, and which regions are most at risk of biodiversity loss or fisheries displacement. As oxygen minimum zones continue to intensify under climate change (Grégoire et al., 2021), EBUs offer a globally consistent spatial framework for monitoring, forecasting, and prioritizing management responses.

SEAMOUNT HABITAT AND CONSERVATION PRIORITIES

Seamounts and guyots host some of the most ecologically distinctive habitats in the deep ocean, yet they vary enormously in their environmental conditions and biodiversity potential (Rogers, 2000; Clark et al., 2011). EBUs allow these differences to be quantified globally for the first time. Among the five seamount and guyot seascapes, C3 stands out as a rare and highly favorable habitat type, combining warm, oxygenated bottom waters (mean 185 mmol m^{-3} dissolved oxygen), relatively strong currents, elevated POC flux, and pH values above the CCD. Together, these conditions promote enhanced suspension-feeding communities, greater metabolic scope for fauna, and increased ecological connectivity. Despite its favorable characteristics, C3 is extremely limited in extent, representing <1% of global seamount and guyot area. We note also that favorable environmental conditions may not always equate with higher biodiversity. While we can define relatively rare habitats, we cannot be certain that they are host to an especially unique community.

By contrast, the majority of seamounts occur within C2, C4, and C5, which are characterized by cold, low-productivity, low-POC-flux waters—conditions associated with sparse benthic assemblages and reduced potential for habitat-forming taxa such as corals and sponges. This global environmental pattern suggests that the vast majority of seamounts reside in ecological "cold spots," while a very small minority form important biodiversity reservoirs. The EBU framework therefore highlights two conservation priorities: (1) recognition of naturally rare, highly productive seamount habitats (e.g., C3 units) as critical areas for biodiversity protection, ecological monitoring, and potential MPA designation within a network of ecologically representative areas (Zhao et al. 2020); and (2) differentiation among superficially similar seamounts—allowing managers to move beyond treating all seamounts as equivalent, which has historically hindered ecologically representative and coherent conservation planning.

These insights align with previous biogeographic analyses demonstrating that seamounts cannot be managed as a single class of features. Clark et al. (2011), for example, identified 194 distinct seamount classes based on oxygen, depth, production regimes, and geographic context, and demonstrated their ecological relevance by comparing classes with distributions of octocoral assemblages. EBUs extend this approach globally and at higher spatial resolution, enabling direct integration of geomorphology, environmental regimes, and carbonate chemistry into conservation decision-making.

For high-seas MPA planning, fisheries management, and general ocean human-use and infrastructure management, EBUs therefore provide a transformative tool: they identify which seamounts host rare ecological configurations, which are exposed to hypoxia or acidification, and which exist within areas less suitable for benthic life. This differentiation is essential for prioritizing surveys, assigning conservation value, and evaluating the vulnerability of seamount systems in a rapidly changing ocean.

CONCLUSION

This study presents the first global benthic classification system that explicitly integrates seafloor geomorphology with environmental regimes to generate 250 unique EBUs distributed on the seafloor as nearly 700,000 EBU polygon occurrences. By combining geomorphic structure with key biophysical drivers—including temperature, oxygen, pH, carbon flux, bottom currents, and sediment thickness—the EBU framework reveals previously unrecognized environmental gradients and boundaries across the global ocean floor.

EBUs demonstrate that benthic habitats are far more heterogeneous than suggested by geomorphology or environmental variables alone. The resulting classification highlights important environmental patterns: the dominance of CCD-exposed abyssal plains (E7), the concentration of hypoxic environments along productive continental margins (B1, B5), and the extreme rarity of seamounts with high biodiversity potential (C3). These patterns underscore the uneven distribution of environmental vulnerability across the seafloor and show how different geomorphic settings mediate exposure to climate stressors such as acidification, deoxygenation, and shifting food supply.

As a global characterization of the seafloor for decision support, EBUs have direct application to high-seas MPA design, national assessments of the representativeness of MPA networks, environmental impact assessments, and biodiversity baseline proxies for emerging conservation frameworks under the UN High Seas Treaty, and more. Because EBUs operate at the scale of geomorphic features that are widely used in marine policy, they provide an intuitive and spatially resolved way to compare habitats within and among ocean basins, identify rare or vulnerable systems, and guide prioritization for exploration and protection. The ocean is vast, and grossly under-sampled. EBUs can help target exploration and sampling efforts by providing a framework for the design of a global sampling strategy.

While the present analysis offers the most comprehensive global benthic classification to date, further refinements will benefit from time-varying environmental datasets, higher-resolution bathymetry, and expanded biological observations to strengthen ecological validation. In this study we have delineated what we believe to be ecologically meaningful areas, but further study is needed to more fully understand the relationship between our complexes of unique physical environments and actual species distributions. As new global datasets emerge, EBUs can be dynamically updated, providing a living framework for monitoring environmental change in the deep sea. They may also provide a useful extension to the General Bathymetric Chart of the Oceans (GEBCO) grid of the UN Nippon Foundation–GEBCO Seabed 2030 program (Mayer et al., 2018), lending insight into the EBUs beyond just bathymetry.

In summary, EBUs offer a transformative step forward for global ocean management by linking where benthic habitats occur, what environmental regimes define them, and how vulnerable they are to future change. This integrative approach delivers a foundation for more informed and proactive stewardship of the world's largest, least understood biome. As a reproducible, data-driven, and updatable global classification, EBUs deliver a new decision-support resource that helps to power area-based management tools for understanding and managing the world's largest and least explored biome.

SUPPLEMENTARY MATERIALS

The supplementary materials are available online at https://doi.org/10.5670/oceanog.2026.e211.

REFERENCES

Almond, P.M., K. Linse, S. Dreutter, S.M. Grant, H.J. Griffiths, R.J. Whittle, M. Mackenzie, and W.D.K. Reid. 2021. In-situ image analysis of habitat heterogeneity and benthic biodiversity in the Prince Gustav Channel, Eastern Antarctic Peninsula. *Frontiers in Marine Science* 8:614496, https://doi.org/10.3389/fmars.2021.614496.

Assis, J., S.J. Fernández Bejarano, V.W. Salazar, L. Schepers, L. Gouvêa, E. Fragkopoulou, F. Leclercq, B. Vanhoorne, L. Tyberghein, and E.A. Serrão. 2024. Bio-ORACLE v3. 0: Pushing marine data layers to the CMIP6 Earth System Models of climate change research. *Global Ecology and Biogeography* 33(4):e13813, https://doi.org/10.1111/geb.13813.

Astudillo-Scalia, Y., F. Albuquerque, B. Polidoro, and P. Beier. 2021. Environmental diversity as a reliable surrogacy strategy of marine biodiversity. *Perspectives in Ecology and Conservation* 19(2021):429–434, https://doi.org/10.1016/j.pecon.2021.08.002.

Baker, E.K., K. Thygesen, and P.T. Harris. 2024. *Increase in Oxygen Depletion in the Marine Environment: Drivers and Recommendations*. Arendal, Norway, GRID-Arendal, 32 pp., https://grid-arendal.herokuapp.com/publications/1034.

Barry, J.P., K.R. Buck, C. Lovera, P.G. Brewer, B.A. Seibel, J.C. Drazen, M.N. Tamburri, P.J. Whaling, L. Kuhnz, and E.F. Pane. 2013. The response of abyssal organisms to low pH conditions during a series of CO_2-release experiments simulating deep-sea carbon sequestration. *Deep Sea Research Part II* 92:249–260, https://doi.org/10.1016/j.dsr2.2013.03.037.

Baynes, T., and A. Szmant. 1989. Effect of current on the sessile benthic community structure of an artificial reef. *Bulletin of Marine Science* 44:545–566.

Becker, J.J., D.R. Sandwell, W.H.F. Smith, J. Braud, B. Binder, J. Depner, D. Fabre, J. Factor, S. Ingalls, S.H. Kim, and others. 2009. Global bathymetry and elevation data at 30 arc seconds resolution: SRTM30_PLUS. *Marine Geodesy* 32(4):355–371, https://doi.org/10.1080/01490410903297766.

Bisson, K., H. McMonagle, I. Iglesias, S. Halfter, and N. Gallo. 2023. Five reasons to take the precautionary approach to deep sea exploitation. *Communications Earth & Environment* 4(1):152, https://doi.org/10.1038/s43247-023-00823-4.

Breitburg, D.L., D.W. Hondorp, L.A. Davias, and R.J. Diaz. 2009. Hypoxia, nitrogen, and fisheries: Integrating effects across local and global landscapes. *Annual Review of Marine Science* 1(1):329–349, https://doi.org/10.1146/annurev.marine.010908.163754.

Brodeau, L., B. Barnier, A.M. Treguier, T. Penduff, and S. Gulev. 2010. An ERA40-based atmospheric forcing for global ocean circulation models. *Ocean Modelling* 31:88–104, https://doi.org/10.1016/j.ocemod.2009.10.005.

Capotondi, A., R.R. Rodrigues, A. Sen Gupta, J.A. Benthuysen, C. Deser, T.L. Frölicher, N.S. Lovenduski, D.J. Amaya, N. Le Grix, T. Xu, and others. 2024. A global overview of marine heatwaves in a changing climate. *Communications Earth & Environment* 5(1):701, https://doi.org/10.1038/s43247-024-01806-9.

Ceccarelli, D.M., K. Davey, G.P. Jones, P.T. Harris, S.V. Matoto, J. Raubani, and L. Fernandes. 2021. How to meet new global targets in the offshore realms: Biophysical guidelines for offshore networks of no-take marine protected areas. *Frontiers in Marine Science* 8:634574, https://doi.org/10.3389/fmars.2021.634574.

Chavez, F.P., and M. Messié. 2009. A comparison of eastern boundary upwelling ecosystems. *Progress in Oceanography* 83(1):80–96, https://doi.org/10.1016/j.pocean.2009.07.032.

Clark, M.R., L. Watling, C. Smith, A. Rowden, and J.M. Guinotte. 2011. A global seamount classification to aid the scientific design of marine protected area networks. *Ocean & Coastal Management* 54(1):19–36, https://doi.org/10.1016/j.ocecoaman.2010.10.006.

Costello, M.J., R. Corkrey, A.E. Bates, M.T. Burrows, C. Chaudhary, G.C. Edgar, R.D. Stuart-Smith, M. Yasuhara, and C.-L. Wei. 2023. The universal evolutionary and ecological significance of 20°C. *Frontiers of Biogeography* 15(4):e61673, https://doi.org/10.21425/F5FBG61673.

Diaz, R.J., and R. Rosenberg. 2008. Spreading dead zones and consequences for marine ecosystems. *Science* 321(5891):926–929, https://doi.org/10.1126/science.1156401.

Fischer, A., D. Bhakta, M. Macmillan-Lawler, and P.T. Harris. 2019. Existing global marine protected area network is not representative or comprehensive measured against seafloor geomorphic features and benthic habitats. *Ocean & Coastal Management* 167:176–187, https://doi.org/10.1016/j.ocecoaman.2018.10.001.

Fisheries and Oceans Canada (DFO). 2025. "The Gully Marine Protected Area." Government of Canada, https://www.dfo-mpo.gc.ca/oceans/mpa-zpm/gully/index-eng.html.

FES Tide Product. 2022. The FES2022 Tide product was funded by CNES, produced by LEGOS, NOVELTIS and CLS and made freely available by AVISO. CNES, 2024. FES2022 (Finite Element Solution) Ocean Tide (Version 2022) [Data set], CNES, https://doi.org/10.24400/527896/A01-2024.004

Gage, J.D., and P.A. Tyler. 1991. *Deep-Sea Biology: A Natural History of Organisms at the Deep-Sea Floor*. Cambridge University Press, Cambridge, 504 pp., https://doi.org/10.1017/CBO9781139163637.

Girard, F., D.W. Caress, J.B. Paduan, L.A. Kuhnz, S.Y. Litvin, E. Flattery, A.S. Kahn, A. DeVogelaere, E.J. Burton, C. Lovera, and others. 2025. Habitat heterogeneity over multiple scales supports dense and diverse megafaunal communities on a northeast Pacific ridge. *Limnology and Oceanography* 70(2):377–392, https://doi.org/10.1002/lno.12766.

Greenaway, S.F., K.D. Sullivan, S.H. Umfress, A.B. Beittel, and K.D. Wagner. 2021. Revised depth of the Challenger Deep from submersible transects; including a general method for precise, pressure-derived depths in the ocean. *Deep Sea Research Part I* 178:103644, https://doi.org/10.1016/j.dsr.2021.103644.

Grégoire, M., V. Garçon, H. Garcia, D. Breitburg, K. Isensee, A. Oschlies, M. Telszewski, A. Barth, H.C. Bittig, J. Carstensen, and others. 2021. A global ocean oxygen database and atlas for assessing and predicting deoxygenation and ocean health in the open and coastal ocean. *Frontiers in Marine Science* 8:724913, https://doi.org/10.3389/fmars.2021.724913

Harris, P.T., and T. Whiteway. 2009. High seas marine protected areas: Benthic environmental conservation priorities from a GIS analysis of global ocean biophysical data. *Ocean and Coastal Management* 52:22–38, https://doi.org/10.1016/j.ocecoaman.2008.09.009.

Harris, P.T. 2012. Biogeography, benthic ecology, and habitat classification schemes. Pp. 61–91 in *Seafloor Geomorphology as Benthic Habitat: GeoHab Atlas of Seafloor Geomorphic Features and Benthic Habitats*. P.T. Harris and E.K. Baker, eds, Elsevier, Amsterdam, https://doi.org/10.1016/B978-0-12-385140-6.00004-9.

Harris, P.T., M. MacMillan-Lawler, J. Rupp, and E.K. Baker. 2014. Geomorphology of the oceans. *Marine Geology* 352:4–24, https://doi.org/10.1016/j.margeo.2014.01.011.

Harris, P.T., and E.K. Baker, eds. 2020. *Seafloor Geomorphology as Benthic Habitat: GeoHab Atlas of Seafloor Geomorphic Features and Benthic Habitats*. 2nd ed., Elsevier, Amsterdam, 1,076 pp., https://doi.org/10.1016/B978-0-12-814960-7.00060-9.

Harris, P.T., L. Westerveld, Q. Zhao, and M.J. Costello. 2023. Rising snow line: Ocean acidification and the submergence of seafloor geomorphic features beneath a rising carbonate compensation depth. *Marine Geology* 463:107121, https://doi.org/10.1016/j.margeo.2023.107121.

Harrison, W.G., and D.G. Fenton, eds. 1998. *The Gully: A Scientific Review of Its Environment and Ecosystem.* Canadian Technical Report of Fisheries and Aquatic Sciences 2245. Fisheries and Oceans Canada, Dartmouth, Nova Scotia, 282 pp.

High Seas Alliance. 2025. "High Seas Treaty Ratification Tracker," https://highseasalliance.org/treaty-ratification/.

Howell, K.L. 2010. A benthic classification system to aid in the implementation of marine protected area networks in the deep/high seas of the NE Atlantic. *Biological Conservation* 143(5):1,041–1,056, https://doi.org/10.1016/j.biocon.2010.02.001.

Huang, B., C. Liu, V. Banzon, E. Freeman, G. Graham, B. Hankins, T. Smith, and H.-M. Zhang. 2021. Improvements of the Daily Optimum Interpolation Sea Surface Temperature (DOISST) Version 2.1. *Journal of Climate* 34:2,923–2,939, https://doi.org/10.1175/JCLI-D-20-0166.1

Juniper, S.K., M. Matabos, S. Mihaly, R.S. Ajayamohan, F. Gervais, and A.O.V. Bui. 2013. A year in Barkley Canyon: A time-series observatory study of mid-slope benthos and habitat dynamics using the NEPTUNE Canada network. *Deep Sea Research Part II* 92:114–123, https://doi.org/10.1016/j.dsr2.2013.03.038.

Levin, L.A. 2018. Manifestation, drivers, and consequences of ocean deoxygenation. *Annual Review of Marine Science* 10:229–260, https://doi.org/10.1146/annurev-marine-121916-063359.

Mayer, L., M. Jakobsson, G. Allen, B. Dorschel, R. Falconer, V. Ferrini, G. Lamarche, H. Snaith, and P. Weatherall. 2018. The Nippon Foundation—GEBCO Seabed 2030 Project: The quest to see the world's oceans completely mapped by 2030. *Geosciences* 8(2):63, https://doi.org/10.3390/geosciences8020063.

McArthur, M., B. Brooke, R. Przeslawski, D. Ryan, V. Lucieer, S. Nichol, A. McCallum, C. Mellin, I. Cresswell, and L. Radke. 2010. On the use of abiotic surrogates to describe marine benthic biodiversity. *Estuarine, Coastal and Shelf Science* 88(1):21–32, https://doi.org/10.1016/j.ecss.2010.03.003.

McQuaid, K.A., A.E.H. Bridges, K.L. Howell, T.B.R. Gandra, V. de Souza, J.C. Currie, O.T. Hogg, T.R.R. Pearman, J.B. Bell, L.J. Atkinson, and others. 2023. Broad-scale benthic habitat classification of the South Atlantic. *Progress in Oceanography* 214:103016, https://doi.org/10.1016/j.pocean.2023.103016.

Misiuk, B., and C.J. Brown. 2024. Benthic habitat mapping: A review of three decades of mapping biological patterns on the seafloor. *Estuarine, Coastal and Shelf Science* 296:108599, https://doi.org/10.1016/j.ecss.2023.108599.

Muller, R.D., M. Sdrolias, C. Gaina, and W.R. Roest. 2008. Age, spreading rates, and spreading symmetry of the world's ocean crust. *Geochemistry, Geophysics and Geosystems* 9(4), https://doi.org/10.1029/2007GC001743.

Nanson, R., A. Carroll, Z. Huang, S. Nichol, and K. Miller. 2018. *An Eco-Narrative of Gifford Marine Park: Temperate East Marine Region.* Report to the National Environmental Science Programme, Marine Biodiversity Hub, Geoscience Australia Canberra, 17 pp.

Olson, P., E. Reynolds, L. Hinnov, and A. Goswami. 2016. Variation of ocean sediment thickness with crustal age. *Geochemistry, Geophysics, Geosystems* 17(4), https://doi.org/10.1002/2015GC006143.

Paulmier, A., and D. Ruiz-Pino. 2009. Oxygen minimum zones (OMZs) in the modern ocean. *Progress in Oceanography* 80(3–4):113–128, https://doi.org/10.1016/j.pocean.2008.08.001.

Ramirez-Llodra, E., P.A. Tyler, M.C. Baker, O.A. Bergstad, M.R. Clark, E. Escobar, L.A. Levin, L. Menot, A.A. Rowden, C.R. Smith, and C.L. Van Dover. 2011. Man and the last great wilderness: Human impact on the deep sea. *PLoS ONE* 6(8):e22588, https://doi.org/10.1371/journal.pone.0022588.

Richter, M.E., K.J. Heywood, R.A. Hall, and P.E. Davis. 2025. Observations of turbulent mixing in the Dotson Ice Shelf cavity. *Ocean Science* 21:3,341–3,359, https://doi.org/10.5194/os-21-3341-2025.

Riehl, T., A.-C. Wölfl, N. Augustin, C.W. Devey, and A. Brandt. 2020. Discovery of widely available abyssal rock patches reveals overlooked habitat type and prompts rethinking deep-sea biodiversity. *Proceedings of the National Academy of Sciences of the United States of America* 117(27):15,450–15,459, https://doi.org/10.1073/pnas.1920706117.

Roff, J.C., and M.E. Taylor. 2000. National frameworks for marine conservation – A hierarchical geophysical approach. *Aquatic Conservation: Marine and Freshwater Ecosystems* 10:209–223, https://doi.org/10.1002/1099-0755(200005/06)10:3<209::AID-AQC408>3.0.CO;2-J.

Rogers, A.D. 2000. The role of the oceanic oxygen minima in generating biodiversity in the deep sea. *Deep-Sea Research Part II* 47:119–148, https://doi.org/10.1016/S0967-0645(99)00107-1

Romoth, K., A. Darr, S. Papenmeier, M.L. Zettler, and M. Gogina. 2023. Substrate heterogeneity as a trigger for species diversity in marine benthic assemblages. *Biology* 12(6):825, https://doi.org/10.3390/biology12060825.

Sayre, R.G., D.J. Wright, S.P. Breyer, K.A. Butler, K. VanGraafeiland, M.J. Costello, P.T. Harris, K.L. Goodin, J.M. Guinotte, Z. Basher, and others. 2017. A three-dimensional mapping of the ocean based on environmental data. *Oceanography* 30(1):90–103, https://doi.org/10.5670/oceanog.2017.116.

Simon-Lledó, E., D.J. Amon, G. Bribiesca-Contreras, D. Cuvelier, J.M. Durden, S.P. Ramalho, K. Uhlenkott, P.M. Arbizu, N. Benoist, J. Copley, and others. 2023. Carbonate compensation depth drives abyssal biogeography in the northeast Pacific. *Nature Ecology & Evolution* 7(9):1,388–1,397, https://doi.org/10.1038/s41559-023-02122-9.

Smith, C.R., F.C. De Leo, A.F. Bernardino, A.K. Sweetman, and P.M. Arbizu. 2008. Abyssal food limitation, ecosystem structure and climate change. *Trends in Ecology & Evolution* 23(9):518–528, https://doi.org/10.1016/j.tree.2008.05.002.

Straume, E.O., C. Gaina, S. Medvedev, K. Hochmuth, K. Gohl, J.M. Whittaker, R. Abdul Fattah, J.C. Doornenbal, and J.R. Hopper. 2019. GlobSed: Updated total sediment thickness in the world's oceans. *Geochemistry, Geophysics, Geosystems* 20(4):1,756–1,772, https://doi.org/10.1029/2018GC008115.

Stuart-Smith, R.D., G.J. Edgar, and A.E. Bates. 2017. Thermal limits to the geographic distributions of shallow-water marine species. *Nature Ecology & Evolution* 1:1,846–1,852, https://doi.org/10.1038/s41559-017-0353-x.

Sulpis, O., B.P. Boudreau, A. Mucci, C. Jenkins, D.S. Trossman, B.K. Arbic, and R.M. Key. 2018. Current $CaCO_3$ dissolution at the seafloor caused by anthropogenic CO_2. *Proceedings of the National Academy of Sciences of the United States of America* 115(46):11,700–11,705, https://doi.org/10.1073/pnas.1804250115.

Sweetman, A.K., A.J. Smith, D.S.W. de Jonge, T. Hahn, P. Schroedl, M. Silverstein, C. Andrade, R.L. Edwards, A.J.M. Lough, C. Woulds, and others. 2024. Evidence of dark oxygen production at the abyssal seafloor. *Nature Geoscience* 17(8):737–739, https://doi.org/10.1038/s41561-024-01480-8.

Tibshirani, R., G. Walther, and T. Hastie. 2001. Estimating the number of clusters in a data set via the gap statistic. *Journal of the Royal Statistical Society: Series B* 63(2):411–423, https://doi.org/10.1111/1467-9868.00293.

US FGDC (United States Federal Geographic Data Committee). 2012. *Coastal and Marine Ecological Classification Standard (CMECS)* (FGDC-STD-018-2012). National Oceanic and Atmospheric Administration (NOAA), Washington, DC, 353 pp., https://repository.library.noaa.gov/view/noaa/27552.

van Rijsingen, E., F. Funiciello, F. Corbi, and S. Lallemand. 2019. Rough subducting seafloor reduces interseismic coupling and mega-earthquake occurrence: Insights from analogue models. *Geophysical Research Letters* 46(6):3,124–3,132, https://doi.org/10.1029/2018GL081272.

Woodgate, R.A., and E. Fahrbach. 1999. Benthic storms in the Greenland Sea. *Deep Sea Research Part I* 46(12):2,109–2,127, https://doi.org/10.1016/S0967-0637(99)00037-0.

Zeppilli, D., A. Pusceddu, F. Trincardi, and R. Danovaro. 2016. Seafloor heterogeneity influences the biodiversity-ecosystem functioning relationships in the deep sea. *Scientific Reports* 6(1):26352, https://doi.org/10.1038/srep26352.

Zhao, Q., F. Stephenson, C. Lundquist, K. Kaschner, D.R.M. Jayathilake, and M.J. Costello. 2020. Where marine protected areas would best represent 30% of ocean biodiversity. *Biological Conservation* 244:108536, https://doi.org/10.1016/j.biocon.2020.108536.

ACKNOWLEDGMENTS

The authors appreciate the helpful comments from Mark Wiltermuth (U.S. Geological Survey) and the insights of three anonymous reviewers. Any use of trade, firm, or product names is for descriptive purposes only and does not imply endorsement by the U.S. Government. We thank Esri for in-kind computational support and Andrew Skinner for additional cartographic help with Figures 1–2, 4–6, 8–9, 11–12, and 16. P.T.H., D.J.W., R.S., K.H., G.K., and M.J.C. participated in an introductory workshop to design the research; P.T.H., K.B., K.V., and D.J.W. performed the research; K.B. and K.V. analyzed the data and prepared the figures; K.V. developed the web app; and P.T.H., D.J.W., K.B., K.V., M.J.C., K.H., G.K., V.L., M.M.-L., and R.S. wrote the paper. The authors declare no competing interest.

AUTHORS

Peter T. Harris (p.harris@utas.edu.au), Institute for Marine and Antarctic Studies, University of Tasmania, Hobart, Australia. **Dawn J. Wright** (dwright@esri.com), Environmental Systems Research Institute, Inc. (Esri), Redlands, CA, USA, and College of Earth, Ocean, and Atmospheric Sciences, Oregon State University, Corvallis, OR, USA. **Kevin Butler** and **Keith VanGraafeiland**, Esri, Redlands, CA, USA. **Mark John Costello**, Nord University, Bodø, Norway. **Kerry Howell**, University of Plymouth, Plymouth, UK. **Gustav Kågesten**, HUB Ocean, Oslo, Norway. **Vanessa Lucieer**, Institute for Marine and Antarctic Studies, University of Tasmania, Hobart, Australia. **Miles Macmillan-Lawler**, GRID-Arendal, Arendal, Norway. **Roger Sayre**, United States Geological Survey, Reston, VA, USA.

ARTICLE CITATION

Harris, P.T., D.J. Wright, K. Butler, K. VanGraafeiland, M.J. Costello, K. Howell, G. Kågesten, V. Lucieer, M. Macmillan-Lawler, and R. Sayre. 2026. Ecological benthic units (EBUs): A new characterization of the global seafloor for ocean spatial planning and management. *Oceanography* 39(2):17–33, https://doi.org/10.5670/oceanog.2026.e211.

COPYRIGHT & USAGE

TOWARD OCEAN MODEL-DRIVEN ROBOTIC EXPLORATION

By Renato Mendes, Ana F. Duarte, Leonardo Azevedo, Lucrezia Bernacchi, João Borges de Sousa, João Pereira, Bernardo Gabriel, João Bogas, Marina Cunha, Clara F. Rodrigues, Ajit Subramaniam, Fernando Esteves, and Kanna Rajan

ABSTRACT. This interdisciplinary work demonstrates the viability of coupling ocean models with in situ robotic sampling in a dynamic coastal region as a means to increase model skill and prediction. Model-driven exploration closes the *sample-assimilate-predict-direct* loop within a virtuous cycle to refine prediction for a range of applications in a region characterized by harsh conditions, high variability, and diverse physical forcings, including bathymetry and coastal topography. By exploring the feasibility of coupling high-resolution autonomous underwater vehicle (AUV) sampling and data assimilation with a geostatistical model in a continuous loop, we aim to provide a new approach to understanding coastal dynamics and processes, while using modest computational resources. The novelty of this effort is threefold: the demonstration of coupling models with AUV sampling, the importance of targeted sampling, and the impact of loop closure toward model prediction.

INTRODUCTION

The marine areas extending from the coastline to the continental slope and encompassing the continental shelf, known collectively as the coastal ocean, constitute one of the most dynamic and complex regions of the ocean. These areas are characterized by high variability and intricate topographies and coastline geometries. They are forced by a wide range of physical and biogeochemical processes that occur across diverse spatial and temporal scales. They are among the most productive and economically significant areas of the world ocean, benefiting from terrestrial inputs via river discharges and nutrient renewal driven by upwelling processes. As a result, and in part, coastal areas concentrate a great proportion of human activities, including leisure, fisheries, offshore aquaculture, and renewable energy exploitation. The coastal ocean mediates interactions between deep-ocean processes and coastal environments, influencing how large-scale phenomena—such as climate-driven changes or extreme weather events—affect the coastal population. It also governs, for example, how anthropogenic influences originating on land are redistributed and affect marine ecosystems (Greene and Delaney, 2025).

Interactions among physical, chemical, and biological processes in the coastal ocean can amplify or mitigate the impacts of extreme events, including storms, flooding, and pollution. Furthermore, the coastal ocean serves as a key interface where large-scale oceanic and atmospheric changes manifest their consequences for coastal ecosystems. Accurately forecasting the state of the coastal ocean is therefore essential not only for safeguarding environmental and economic interests but also for enhancing resilience to climate variability, natural hazards, and anthropogenic stressors.

Ocean models have become essential tools for predicting ocean state, and they underpin a wide range of societal applications, from climate forecasting to pollution monitoring and resource management. However, these models are inherently imperfect representations of complex reality. Data assimilation techniques, where observational data are integrated to update models, play a critical role in correcting or adjusting model errors and improving their forecasting capabilities. Yet, the success of data assimilation depends heavily on the availability, quality, and relevance of observations.

Satellite remote sensing provides extensive spatial coverage but is generally limited to surface observations and constrained by atmospheric conditions. In situ observations from ships, moorings, or drifting platforms, although spatially sparse and logistically demanding, complement satellite data by providing higher spatial or temporal resolution and access to subsurface processes, adding a critical three-dimensional component to the observing system. Recent technological advances have enabled the use of autonomous underwater vehicles (AUVs) and other robotic platforms, offering flexible, mobile, and increasingly autonomous means of sampling ocean properties with high spatiotemporal resolution and low logistic footprints (Das et al., 2012, 2015; Graham et al., 2012; Fossum et al., 2018).

However, even with these new tools, efficiently collecting data for modeling at optimal spatial and temporal scales remains a complex challenge. AUVs are constrained not only by endurance and communication bandwidth but also by speed (typically on the order of 1–2 ms^{-1}), which is comparable to ambient current velocities and thus limits synopticity. This limitation is even more pronounced for gliders, as they operate at lower effective speeds. Operational risks that further restrict deployment include vessel traffic, fishing activity, strong currents, and complex bathymetry. In addition, the ocean itself remains highly dynamic, with key processes often evolving faster than traditional ship-based sampling strategies can capture. This opens the door to adaptive sampling strategies, where observation efforts are guided by model outputs and uncertainty estimates to maximize the relevance of collected data. Adaptive sampling (Zhang and Sukhatme, 2007; Singh et al., 2009; Fossum et al., 2019a) represents a fundamental shift: instead of executing pre-planned missions, autonomous vehicles dynamically prioritize areas for observation. Our approach combines model predictions with adaptive sampling using propelled AUVs. Lermusiaux (2007), Ford et al. (2022), and Wihsgott et al. (2026) explore such a concept, with Lermusiaux in simulation only. While Ford et al. (2022) focus a single glider on chlorophyll as a driver, and Wihsgott et al. (2026) multiple gliders on chlorophyll, temperature, and oxygen, we target temperature exclusively. The novelty of our work is in demonstrating the applicability of controlling the AUV's trajectory using onboard computation and articulating the importance of the larger *sample-assimilate-predict-direct* loop. Our setup is also simpler as we employ the Copernicus Marine Service (CMEMS) Nucleus for European Modelling of the Ocean (NEMO) numerical model, which is used to initiate the stochastic model, the primary model we use in our work. This is supplemented with practical ways to reduce operational costs using small boat operations and multiple in-house designed AUVs with our mature technology suite for command/control.

Model forecasts identify where spatial uncertainty is highest or where new observations are expected to have the greatest impact in reducing forecast errors. Vehicles are then directed to sample these areas, and their data are in turn assimilated back into the models, as a virtuous cycle. Data assimilation from these high uncertainty regions is then incorporated into the model so that new predictions benefit from improved in situ data. Such an approach promises to significantly enhance the skill of ocean forecasts, especially in the complex coastal environment where processes occur over a wide range of scales.

Our work has three significant results. First, it demonstrates the importance of coupling ocean models with high-resolution AUV sampling. Second, it highlights the importance of targeted adaptive sampling based on model uncertainty. Third, it demonstrates the importance of assimilation in predicting and closing the *sample-assimilate-predict-direct* loop (Figure 1). Additionally, sampling resolution with AUVs vastly outweighs that of the data obtained from traditional ship-based approaches. Using multiple

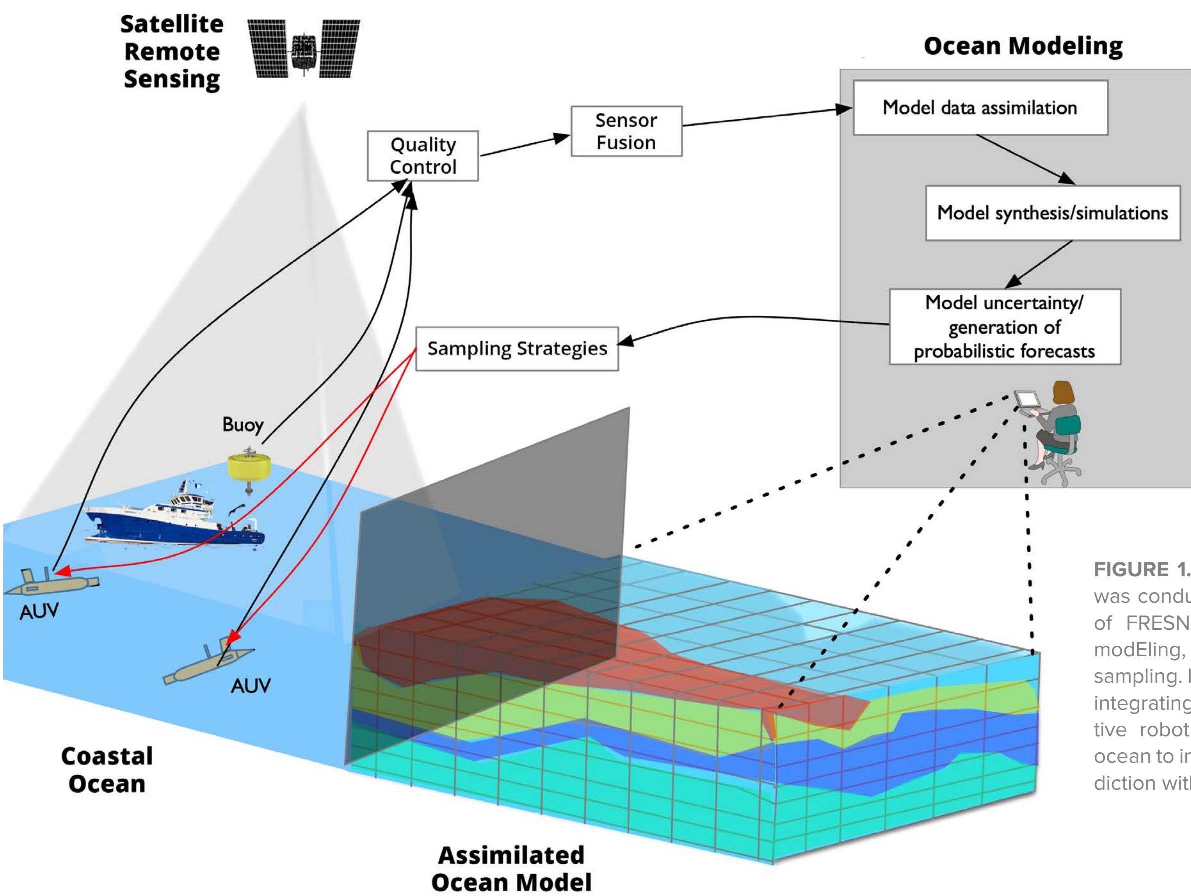

FIGURE 1. The work described here was conducted within the framework of FRESNEL (Field expeRiment for modEling, aSsimilatioN and adaptivE sampling. It demonstrates the value of integrating ocean models with adaptive robotic vehicles in the coastal ocean to increase model skill and prediction within a tight control loop.

AUVs sampling simultaneously, as we do here, also makes a dent in spatial as well as temporal coverage of dynamic environments at relatively moderate costs. Finally, AUVs can provide near-real-time data, allowing for their rapid re-tasking and potential placement in evolving spatially separated regions.

This manuscript is organized as follows. We first introduce the problem we are tackling, providing a motivation for the *sample-assimilate-predict-direct* loop. Next, we provide the environmental context and the challenge of modeling and operating robotic vehicles in a dynamic coastal region. Our Methods section then highlights the details of the forecasting, assimilation, sampling, and operational strategies that lie at the core of this paper. We next highlight the results of our experiment, followed by a discussion and analysis of these results. We wrap up with conclusions and propose future work.

STUDY AREA

In this study, we address the challenge of loop closure by implementing and evaluating a complete data cycle, from model prediction, to uncertainty generation, to adaptive sampling, to data assimilation. The work was conducted within the framework of FRESNEL (Field expeRiments for modEling, aSsimilatioN and adaptivE sampLing), specifically designed to explore and test model-driven robotic exploration strategies.

The study was conducted off central Portugal, focusing on the region influenced by the Nazaré Canyon (39.2°–39.9°N; Figure 2) during fall 2024. While the experiment considered the measurable impact of model-driven robotic sampling on the biogeochemistry of the canyon region, this manuscript focuses on the implications of closing the *sample-assimilate-predict-direct* loop closure.

Implementing such a closed-loop system in a dynamic coastal environment presents substantial challenges. These include the need for spatial high-resolution numerical models capable of rapidly generating uncertainty predictions, robust algorithms for exploration under a range of constraints, reliable communication links for mission updates, and assimilation frameworks that integrate heterogeneous real-time data streams. Furthermore, marine operations face logistical risks and communication limitations, such as intermittent connectivity, unpredictable weather, and vessel traffic, that further constrain the execution of robotic missions.

The Nazaré area features pronounced topographic contrasts: the transition from the wide Estremadura Plateau to the narrower northern shelf, the long and narrow Nazaré submarine canyon that incises the shelf and extends more than 200 km offshore, and the Berlengas archipelago, a UNESCO Biosphere Reserve with high ecological value. These features contribute to enhanced biological productivity and biodiversity and strongly modulate physical and biogeochemical processes in the region.

Freshwater inputs from major rivers, such as the Tagus, have only a limited direct impact on the area. In contrast, smaller rivers and the Óbidos lagoon, located south of Nazaré, can episodically

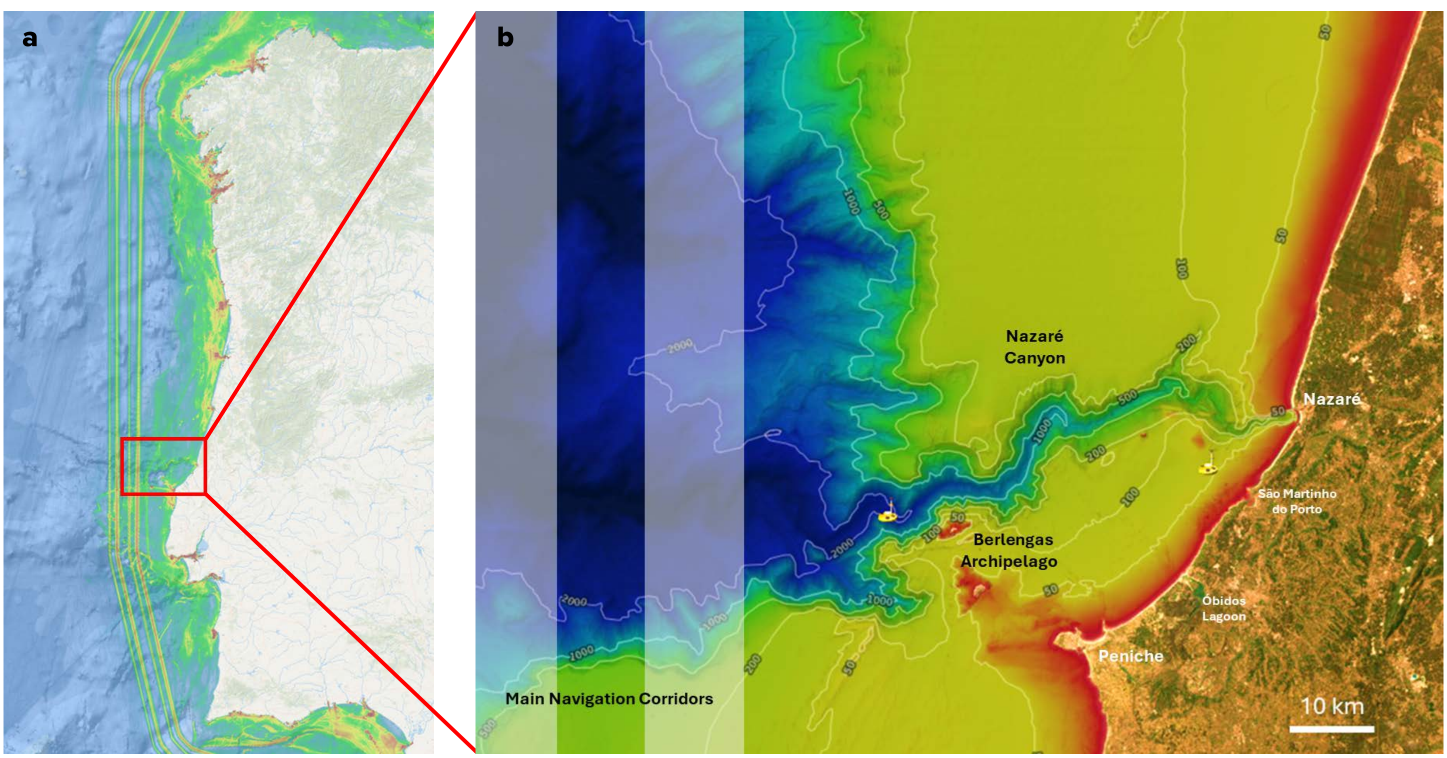

FIGURE 2. (a) Map of Portugal's west coast with the study area highlighted with a red rectangle. (b) The bathymetry of the FRESNEL study area includes the Nazaré Canyon-Berlengas area and its environment. The white bands indicate commercial shipping lanes. The two buoys drawn on the map are part of a coastal observing system. The Nazaré Canyon is a significant feature of this area and a driver for the biogeophysics of the domain (Tyler et al., 2009), along with other prominent features.

deliver low-salinity, nutrient-rich plumes to the shelf. Circulation is driven by seasonal wind forcing linked with the Azores High, with persistent upwelling-favorable northerly winds in summer and frequent downwelling episodes in winter under southerly winds. The interplay between canyon topography, shelf circulation, and atmospheric forcing generates complex mesoscale dynamics, intensified tidal currents, and internal wave activity that promote strong vertical mixing and cross-shelf exchanges (Quaresma et al., 2007; I. Martins et al., 2010).

The combination of sharp bathymetric gradients, variable forcing, and rich physical-biogeochemical interactions makes the Nazaré Canyon region an ideal natural laboratory for testing sampling strategies and evaluating how model-based uncertainty projections can guide sampling and assimilation to improve ocean model predictive skill.

METHODS

Our methodology is based on implementing a closed-loop data cycle to improve predictions from a coastal ocean model via robotic adaptive sampling and data assimilation. The approach consists of three fundamental steps, executed iteratively daily:

1. **MODEL FORECAST AND UNCERTAINTY PROJECTION.** An ocean model provides a daily step forecast $\hat{\theta}(k + 1, x, y)$ of a target oceanic variable θ, along with an associated uncertainty field $\sigma_{\hat{\theta}}(k + 1, x, y)$, where k represents the current day and (x, y) denote the geographical coordinates. These outputs are organized into discrete spatial maps, $M_{\hat{\theta}}(x, y)$ and $M_{\sigma_{\hat{\theta}}}(x, y)$, representing the predicted state and its uncertainty, respectively, over a predefined grid covering the study area.
2. **TARGETED SAMPLING.** We define areas of larger uncertainty predictions as areas of higher "reward" to bias where the AUVs sample. Using the uncertainty map $M_{\sigma_{\hat{\theta}}}(x, y)$ as input, the targeted sampling algorithm determines the set of trajectories for N AUVs for the next operational cycle, typically the following day. The goal is to maximize the accumulated uncertainty sampled along the vehicle trajectories.
3. **DATA COLLECTION AND ASSIMILATION.** Throughout the operational cycle, each AUV collects measurements of the target variable θ along its assigned path. After mission completion, the collected measurements are assimilated into the model using an appropriate data assimilation scheme. This updated model state serves as the new initial condition for the next forecasting cycle, closing the loop.

While previous efforts have concentrated on a form of embedded and automated decision-making for AUV-based adaptive sampling (McGann et al., 2008; Ryan et al., 2010; Garcia-Olaya et al., 2012; Rajan and Py, 2012), the trajectories in this work are generated offline, with adaptation focused on deployment based on $M_{\sigma_{\hat{\theta}}}(x, y)$. Here, loop closure refers to the *sample-assimilate-predict-direct* process.

MODEL FORECAST, UNCERTAINTY PROJECTION, AND DATA ASSIMILATION

Sampling strategies rely on timely information about the spatial variability of ocean properties. Conventional numerical ocean circulation models, based on the fluid dynamics, such as CMEMS NEMO (EU Copernicus Marine Service [CMEMS] Information Marine Data Store [MDS], 2024a), Regional Ocean Modeling System (ROMS; Shchepetkin and McWilliams, 2005), and Hybrid Coordinate Ocean Model (HYCOM; Wallcraft et al., 2009), for example, are widely used by the scientific community for operational forecasting and research. These models provide physically consistent simulations of ocean state variables (e.g., temperature, salinity, currents) and underpin applications ranging from climate prediction to coastal management. However, numerical ocean models are computationally intensive, and their runtime makes them impractical for use with high spatial resolution and in near-real-time mission planning (Agarwal et al., 2021). While assimilation-prediction cycles such as the one we propose could, in principle, be implemented within such models, it would require either substantially larger computational resources or longer execution times.

As a practical alternative, we use geostatistical simulation (i.e., direct sequential simulation; Soares, 2001) as a computationally efficient surrogate for short-term spatial predictions of ocean variables together with estimates of spatial uncertainty (Deutsch and Journel, 1992). This approach captures the essential spatio-temporal variability of local ocean dynamics, based on a prior numerical ocean model solution, at a fraction of the computational cost of numerical models, while remaining flexible enough to rapidly assimilate new in situ observations (Duarte et al., 2025). However, with these types of surrogate models, we are not explicitly considering the full physics of the system, and the quality of the predictions directly depends on the accuracy of the numerical model and the prediction time length. If the numerical model is unable to capture the true nature of the system, the geostatistical predictions will likely be inaccurate.

Our methodology relies on ensembles of geostatistical realizations, each representing a state of an ocean variable field conditioned *a priori* by the deterministic CMEMS NEMO model (Madec et al., 1997, 2015; EU Copernicus Marine Service [CMEMS] Information Marine Data Store [MDS], 2024a) using the Iberian Biscay Irish domain. In doing so we use a variogram model describing the temporal dependency between days over a 14-day period. Realizations are generated via stochastic sequential simulation: the grid is visited along a random path and, at each node, the local Kriging mean and variance are computed from the covariance/variogram model and the available conditioning data, from which a value is drawn from the corresponding conditional distribution. By computing the pointwise standard deviation across the ensemble, we obtain spatial uncertainty maps that highlight regions where predictions are more variable and therefore potentially a target for robotic sampling. These maps then, serve as the basis for identifying areas where new measurements are expected to maximize the reduction of forecast error.

Beyond uncertainty prediction, the statistical approach incorporates AUV data through sequential assimilation, refining forecasts for subsequent cycles. Data collected on a given day is used to update the ocean variable forecast for the following day by combining prior predictions with new measurements. The geostatistical simulation grid, in this case, includes two temporal layers: the first contains the AUV measurements at their spatial locations, and the second corresponds to the new prediction step. With AUV sampling denser than the model horizontal grid resolution (approximately 0.0035°, corresponding to about 300–400 m at the study latitude), measurements within the same grid cell are averaged as a form of arithmetic upscaling (Duarte et al., 2025). To incorporate spatial and temporal variability, we apply sequential simulation with local means (Soares, 2001),[1] where each simulated value is drawn from its conditional distribution, accounting for both prior simulated values and local mean models. Doing so enables consistent updating of the variable field while integrating both AUV observations and *a priori* information. The ensemble of realizations thus provides an updated ocean forecast and a quantitative measure of uncertainty.

The spatial and temporal continuity of the variable field is simultaneously characterized by variogram models fitted to long-term numerical ocean model data from CMEMS NEMO. For each depth layer of the numerical model where the AUV navigation is defined, geostatistical simulations are performed independently using a moving temporal window of the previous 14 days as conditioning data. This window length was selected through comparison with the numerical model's short-term evolution under similar seasonal conditions, striking a balance between forecast stability and computational cost. Spatial propagation occurs only horizontally within each depth level, while vertical consistency is implicitly maintained through the depth-specific variogram structures derived from the 3D numerical model (see Figure 3 of Duarte et al., 2025). This provides both a forecast of the ocean variables being simulated and a quantitative assessment of the prediction uncertainty. By updating the forecasts with new in situ measurements through sequential assimilation, the method progressively refines the variable field while maintaining consistency with prior model dynamics. The resulting forecast and uncertainty maps then form the input for the targeted sampling algorithm, guiding the allocation of AUV trajectories toward regions of greatest expected information gain. Duarte et al. (2025) provide a complete description of the methodology and implementation.

THE SAMPLING ALGORITHM

Our adaptive sampling problem involves the design of vehicle trajectories that maximize information gain (Eidsvik et al., 2015; Fossum et al., 2018) extracted from the uncertainty map provided by the model, while satisfying operational AUV constraints. Each day, the model provides both a forecast field and its associated uncertainty distribution, which together define the reward landscape for the trajectory planner. The task is to generate, for each vehicle, a tour that accumulates the highest possible uncertainty values. The tour is traveled at a prescribed AUV speed while the duration is bounded above by the assimilation period. The starting and ending points are selected to simplify logistics for launch and recovery.

Although the underlying numerical CMEMS NEMO model is fully three-dimensional and the statistical solution also provides predictions across multiple depth layers, in this work, the sampling algorithm operates on a two-dimensional (2D) horizontal field derived from the uncertainty structure of the statistical solution. This field is obtained by averaging the horizontal depth slices of uncertainty between the surface and 40 m depth, a depth interval chosen to represent the upper mixed layer in the Nazaré study region. Within this layer, turbulent mixing typically maintains relatively weak vertical gradients, and most of the temperature variability relevant for mission planning is concentrated near the surface and the upper thermocline. Averaging across this depth range, therefore, yields a stable and physically meaningful representation of the uncertainty field.

While the trajectory planning itself is carried out in two dimensions, the yo-yo motion executed by the AUVs along each transect naturally restores vertical sampling capability, compensating for the 2D approximation and enabling the acquisition of high vertical resolution profiles at all visited locations. This strategy also aligns with the dominant physical and biogeochemical processes occurring within the mixed layer, where air-sea interactions, nutrient entrainment, and local thermal structure exert primary control on short-term dynamics (Behrenfeld and Boss, 2014; Mahadevan, 2016).

The tour is formulated as a graph theoretic problem. The spatial uncertainty map is first pre-processed to remove obstacles and smoothed to highlight large-scale features. Candidate waypoints are then identified from the map and used to build a weighted graph, where nodes carry a reward proportional to their uncertainty value and edges represent travel costs. The trajectory planning task is posed as a multi-vehicle, multi-depot tour routing problem where routes must balance the rewards obtained from visiting nodes with associated costs of traveling between them (Vidal et al., 2013; Toth and Vigo, 2014). By solving this graph traversal problem, the algorithm returns a set of near-optimal trajectories that prioritize regions of greatest uncertainty while enforcing an effective travel budget (endurance) and an obstacle-masked admissible area (safety) (Bernacchi et al., 2025). This is illustrated by the boundaries in the uncertainty field shown in the zoomed area of Figure 4b.

[1] Defined by Kriging estimates and variances, which are conditioned to existing direct measurements and a spatial covariance matrix (Cressie, 1993).

OPERATIONS AND DATA COLLECTION

The in situ data collection process involved three upper water-column light autonomous underwater vehicles (LAUVs; XP2, XP3, and XP5)[2] that performed targeted sampling missions with durations of up to 60 hours over the Nazaré Canyon region, with all vehicles sampling the upper 100 m of the water column. These vehicles were designed and developed in-house at the University of Porto (Sousa et al., 2012) and are equipped with a range of sensors, including a CTD (Figure 3a), along with Wi-Fi and Iridium satellite communications. The CTDs mounted on the AUVs were cross calibrated to ensure consistency. In addition to the hardware involved, we used an extensive suite of mature mission planning and command/control tools whose discussion is outside the scope of this paper and can be found in Dias et al. (2005), R. Martins and Sousa (2010), and Pinto et al. (2013).

The experiment had a small human and support vessel footprint, demonstrating significant cost reduction in comparison to traditional ship-based methods while measuring at higher spatial and temporal resolution. Operations were conducted continuously by pairs of operators working six-hour shifts based in Porto as well as locally in Nazaré—small boat use was limited to the launch and recovery of AUVs, which operated unattended.

Challenging meteorological and ocean conditions constrained the number of consecutive iterations of the *sample-assimilate-predict-direct* loop to a three-day sequence of experiments (October 29–31, 2024; Figure 3b). Also for simplicity and clarity, we focused on a single variable: temperature measurements. As a consequence, this work is univariate in showing the impact of assimilated model-driven exploration. We believe that the experimental results presented in this paper are general enough to apply to other critical physical oceanographic variables, which would be modeled similarly. Therefore, the analysis presented here ultimately aims to quantify the impact of assimilating AUV-acquired temperature data on the predictive performance of the statistical model and to assess the operational feasibility of the data cycle approach in a coastal setting.

Each experimental day followed a structured cycle that involved (1) the generation of a statistical model forecast and its associated uncertainty field using the prior CMEMS NEMO model data available up to the previous day (Sotillo et al., 2021), (2) the execution of the target sampling algorithm to plan the next day mission, (3) in situ data collection by AUVs following the algorithmically determined tours, (4) and, finally, assimilation of data from the tour into the model.

A MULTI-SCENARIO FRAMEWORK

Given the logistical and weather-related challenges encountered, a number of scenarios contribute to the final solution set. The scenarios are labeled A through D (and their corresponding assimilation variants) in Table 1, which provides a compact, color-coded overview of all configurations (used in Figure 6), including statistical forecast dates, prior CMEMS NEMO fields, and the specific AUV datasets assimilated at each stage.

On October 29, 2024, the statistical model produced the initial forecast solution (A), which was used to plan the mission executed by XP2 (Figure 3b). The resulting data were assimilated offline to produce an updated statistical model solution (B1) for October 30.

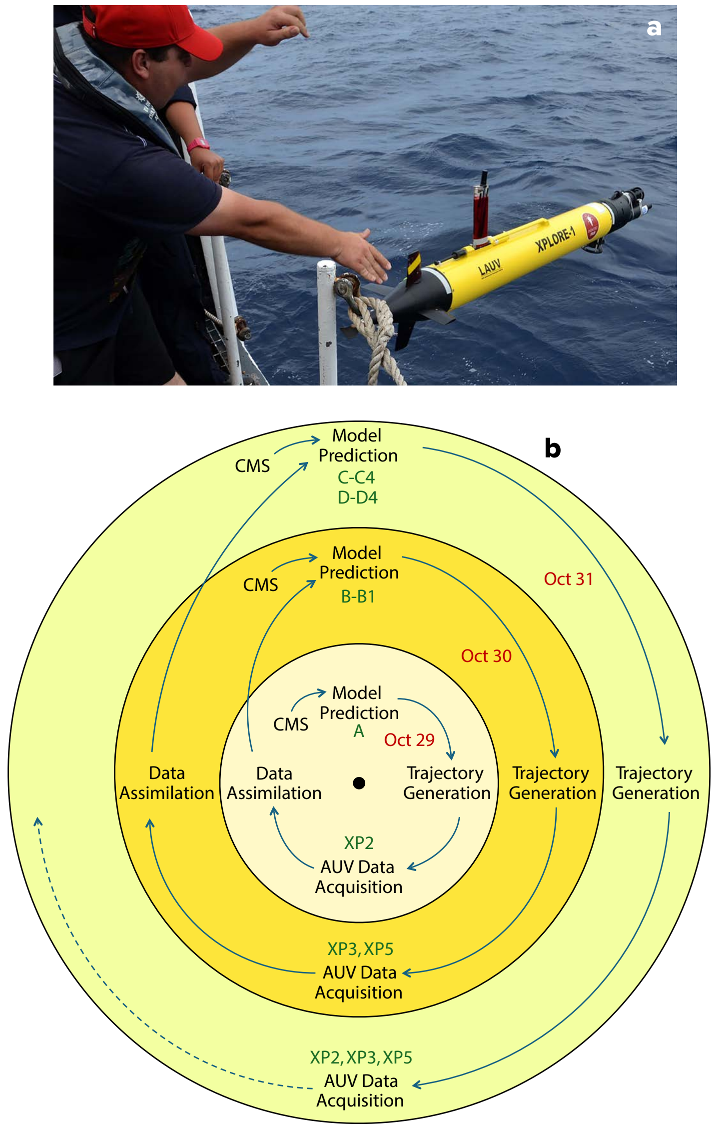

FIGURE 3. (a) Multiple light autonomous underwater vehicles (LAUVs), such as the one in this photo, were used in FRESNEL. This low-cost platform designed at the University of Porto has proven to be robust, is easily integrated with a number of oceanographic sensors, and comes with sizable open source command/control software. See the supplemental video for LAUV XP5 recovery at sea. (b) Three-day sequence (October 29–31, 2024) of the *sample-assimilate-predict-direct* loop in the FRESNEL experiment. Each cycle integrated statistical model predictions using the EU Copernicus Marine Service Information (CMEMS) Copernicus Marine Service Nucleus for European Modelling of the Ocean (NEMO) model as a prior, targeted sampling, AUV data acquisition, and subsequent assimilation for the following day's prediction.

[2] We will refer to these specific vehicles across the three-day period based on the diversity and specificity of their operating environments and measurements.

Although operational real-time assimilation was initially planned, logistical constraints prevented its implementation; consequently, all assimilations were performed offline after AUV mission completion. The targeted sampling algorithm, therefore, relied on statistical forecasts without assimilation (B), using pre-existing data as input for daily mission planning. This limitation is not expected to have significantly affected the experimental outcomes, as the operational area was compact and the predicted variability field remained consistent between consecutive days.[3]

For October 31, multiple assimilation configurations were tested to quantify how the information collected on previous days could influence short-term predictive skill. Measurements from XP3 and XP5 on October 30 were assimilated offline to generate scenarios C1–C4, complementing the non-assimilated reference case C. These cases progressively integrate different subsets of AUV observations, ranging from XP2-only data (C1) to the full multi-vehicle dataset from October 29 to 30 (C4).

A parallel set of scenarios (D and D1–D4) was generated to evaluate the sensitivity of the statistical model to the choice of prior CMEMS NEMO fields. The D-series uses CMEMS NEMO data available only up to October 29, thus representing a less favorable initial state, and applies the same assimilation configurations as in the C-series. This dual-series approach enables a controlled comparison of how data assimilation interacts with differences in model initialization. Model performance was evaluated by comparing predicted and observed temperature data along the AUV trajectories using root mean square error (RMSE) as the performance metric for October 31.

FRESNEL is part of a larger concept for multi-domain sensing, observation, and exploration that couples ocean models, autonomous robotics, artificial intelligence, and machine learning with a small satellite constellation. Our end goal is to democratize ocean model prediction using low-cost operations integrated with open-source software to enable spatio-temporal data assimilation from mobile or immobile robots across space, aerial, surface, and underwater domains (Rajan et al., 2021).

TABLE 1. Summary of scenarios and assimilation configurations. The color codes are referred to in Figure 6 to disambiguate root mean square error plots.

SCENARIO	FORECAST DATE	CMEMS NEMO PRIOR DATA UP TO	ASSIMILATED AUV DATASETS
A	29 Oct	28 Oct	None (baseline)
B	30 Oct	29 Oct	None (baseline)
B1	30 Oct	29 Oct	XP2 (29 Oct)
C	31 Oct	30 Oct	None (baseline)
C1	31 Oct	30 Oct	XP2 (29 Oct)
C2	31 Oct	30 Oct	XP2 (29 Oct), XP5 (30 Oct)
C3	31 Oct	30 Oct	XP5 (30 Oct)
C4	31 Oct	30 Oct	XP2, XP3, XP5 (29–30 Oct)
D	31 Oct	29 Oct	None (baseline)
D1	31 Oct	29 Oct	XP2 (29 Oct)
D2	31 Oct	29 Oct	XP2 (29 Oct), XP5 (30 Oct)
D3	31 Oct	29 Oct	XP5 (30 Oct)
D4	31 Oct	29 Oct	XP2, XP3, XP5 (29–30 Oct)

EXPERIMENTAL RESULTS

Figure 4a summarizes environmental conditions observed during the three-day experimental window considered in this study. The background fields correspond to the Level 3 sea surface temperature (SST) product (EU Copernicus Marine Service (CMEMS) Information Marine Data Store (MDS), 2024b). The operational area covers approximately 100 km^2 south of Nazaré Canyon. While all missions focused on temperature variability predicted by the model, on October 31, XP2 was deployed for a cross-shore transect of approximately 13 km to sample an internal wave hotspot; in this study, it serves as an independent ground-truth dataset. These observations are used as a reference for evaluating the forecast cases C1–C4 and D1–D4. See online supplementary material for more information regarding AUV paths.

During the experimentation, the coastal ocean was influenced by a late-season upwelling-relaxation cycle. At the beginning of the sequence (October 29), the SST field revealed the characteristic signature of coastal upwelling, with colder water masses extending offshore due to wind-driven Ekman transport that brings subsurface, nutrient-rich waters to the surface. In the following days, the weakening of upwelling-favorable winds led to a relaxation phase, during which warmer offshore waters gradually advanced toward the coast. This transition is reflected in the SST maps by an overall warming trend in the nearshore region, particularly evident on November 1 (Figure 4a).

It is important to note that the SST imagery is partially affected by cloud coverage, which limits the availability and accuracy of satellite-derived temperature data. Despite these limitations, the SST patterns clearly capture the dominant mesoscale features and coastal processes driving the observed variability during the experiment. The pronounced temperature gradients associated with the upwelling front generated well-defined spatial and temporal variability, making the impact of targeted in situ observations on predictive model skill visible.

Figure 4b shows the vertical temperature distribution measured by the AUVs between October 29 and 31. The panels illustrate the temporal and vertical structure of the coastal water column throughout the three-day period, and they highlight the complexity of logistics in multi-vehicle operations, where scheduling, resources, and environmental constraints together determine the actual temporal coverage of the vehicles.

XP2 operated on October 29 and 31, XP5 on October 29, 30, and 31, and XP3 on October 30 and 31. The temperature fields reveal a thermocline and a progressive warming of the surface layer down to approximately 40 m depth, with temperatures ranging from

[3] In future implementations, on-board or near-real-time assimilation would need to be considered to fully exploit the framework's adaptive potential.

~14°C in deeper layers to ~18°C near the surface, reaching their maximum on the afternoon of October 30 during XP5's mission.

In Figure 5, four scatter plots compare the measurements acquired in situ on October 31 against the corresponding geostatistical predictions derived under each scenario. They focus on the most contrasted scenarios: the baseline cases without assimilation (C and D) and those incorporating the full set of AUV observations from previous days (C4 and D4). The observations include all available data collected by the missions on that day (see Figure 4a,b). Colors indicate the depth layers associated with the vertical discretization used in the CMEMS NEMO model, which defines the vertical structure of the statistical model. This comparison illustrates the statistical model's ability to reproduce the observed temperatures at each measurement point accurately, contrasting the non-assimilated cases (C and D) with the partially and fully assimilated (C1–C4 and D1–D4).

In the baseline scenarios without assimilation (C and D), the plots exhibit a wide spread of points around the reference line, indicating substantial discrepancies between the model predictions and the observed AUV measurements. These deviations are particularly evident in XP3 and XP5 data, where temperatures around 20–30 m depth tend to be overestimated by almost 1°C (Figure 6b,c). This dispersion reflects the model's limited ability to accurately reproduce the vertical thermal structure when it relies solely on CMEMS NEMO data without incorporating in situ information.

In contrast, the fully assimilated scenarios (C4 and D4) show a much tighter clustering of points around the reference, especially within the studied upper layers, where the previous AUV missions provide dense and temporally relevant observations. This reduction in spread suggests a clear improvement in predictive accuracy, indicating that the assimilation of targeted measurements

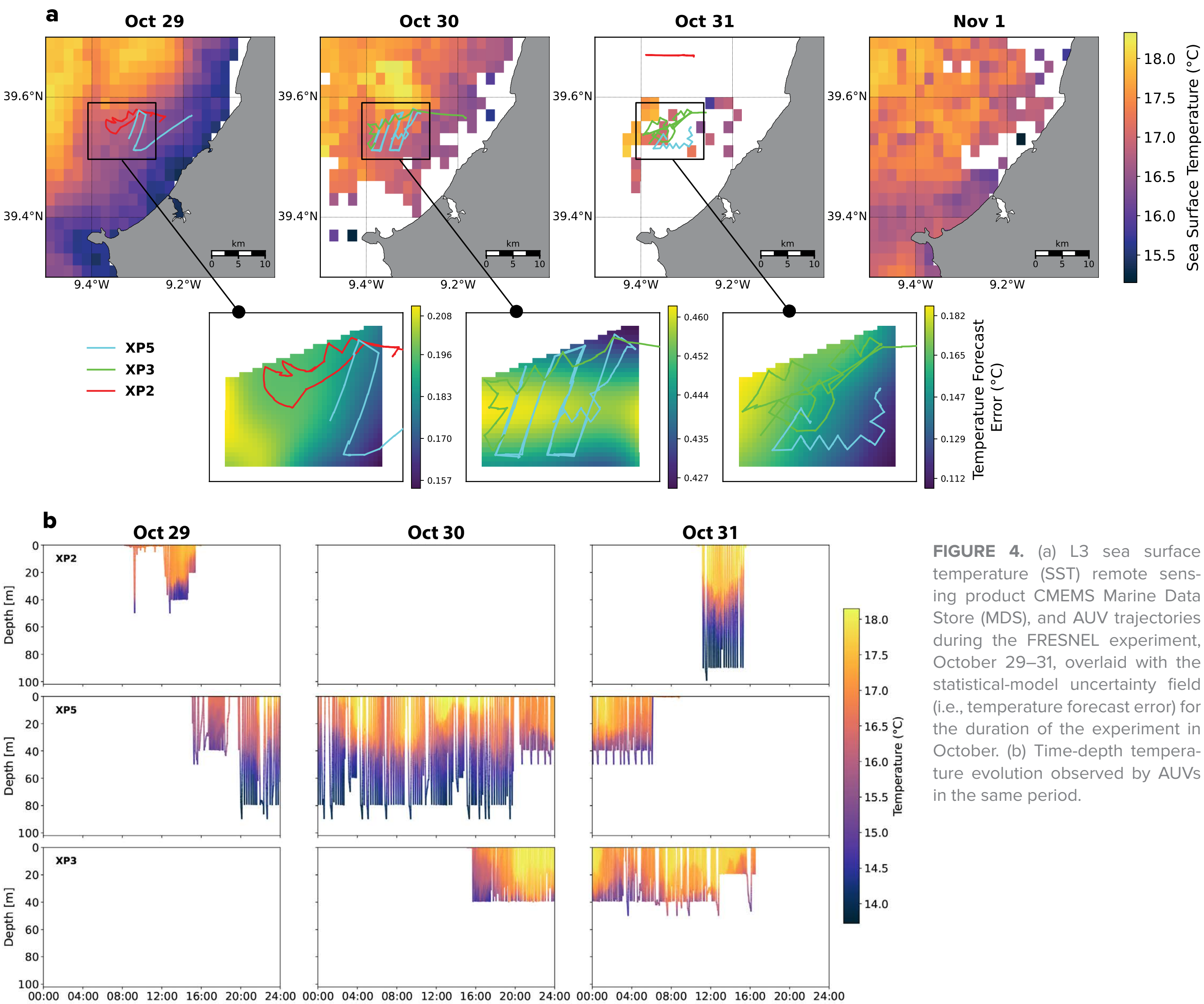

FIGURE 4. (a) L3 sea surface temperature (SST) remote sensing product CMEMS Marine Data Store (MDS), and AUV trajectories during the FRESNEL experiment, October 29–31, overlaid with the statistical-model uncertainty field (i.e., temperature forecast error) for the duration of the experiment in October. (b) Time-depth temperature evolution observed by AUVs in the same period.

effectively constrains the thermal structure and captures ongoing physical transitions in the water column. See the online supplementary material for a detailed comparison of SST fields across the CMEMS NEMO model products from C to C4 and from D to D4.

Figure 6 presents the RMSE between the statistical model forecasts and the in situ temperature observations collected by the AUVs. These figures cover all experimental configurations examined in this study. Figure 6a corresponds to the initial phase of the experiments on October 29 and 30. Scenario A represents the baseline statistical forecast based on CMEMS NEMO data. B and B1 scenarios correspond to forecasts for October 30 without and with the assimilation of in situ observations during the previous day (see Table 1). RMSE values in scenario A range from approximately 0.48°C near the surface to 1.33°C at 40 m, with a mean RMSE of about 0.74°C. The errors increase with depth, indicating reduced model skill in reproducing the subsurface thermal structure. The non-assimilated B scenario remains similar to A in the upper layers but diverges below 20 m. Assimilation in scenario B1 consistently improves predictions across the water column compared to the non-assimilated B scenario with RMSE values between 0.31°C and 0.55°C and an average of 0.39°C representing an overall reduction of nearly 50% relative to B. This improvement is most pronounced in the 5–20 m layers, coinciding with the strongest vertical temperature gradients and the region most densely sampled by the AUVs.

The results for October 31, summarized in Figure 6, correspond to the phase of the experiment in which multiple assimilation scenarios were tested. The C-series used CMEMS NEMO data up to October 30, whereas the D-series uses CMEMS NEMO up to October 29, representing a less favorable statistical initial state. In both cases, the assimilation scenarios (C1–C4 and D1–D4) correspond to the incorporation of AUV data collected during previous days (see Table 1).

A consistent reduction in statistical forecast error is observed across most vehicles and assimilation stages. In the C-series, the average RMSE across all AUVs decreases from approximately 0.40°C in C to 0.31°C in C4, while in the D-series, the mean RMSE drops from 0.55°C in D to 0.40°C in D4 (see Table 1). These improvements correspond to an average error reduction of 25%–30%, demonstrating that the assimilation of targeted observations can compensate for differences in the initial state and improve predictive accuracy.

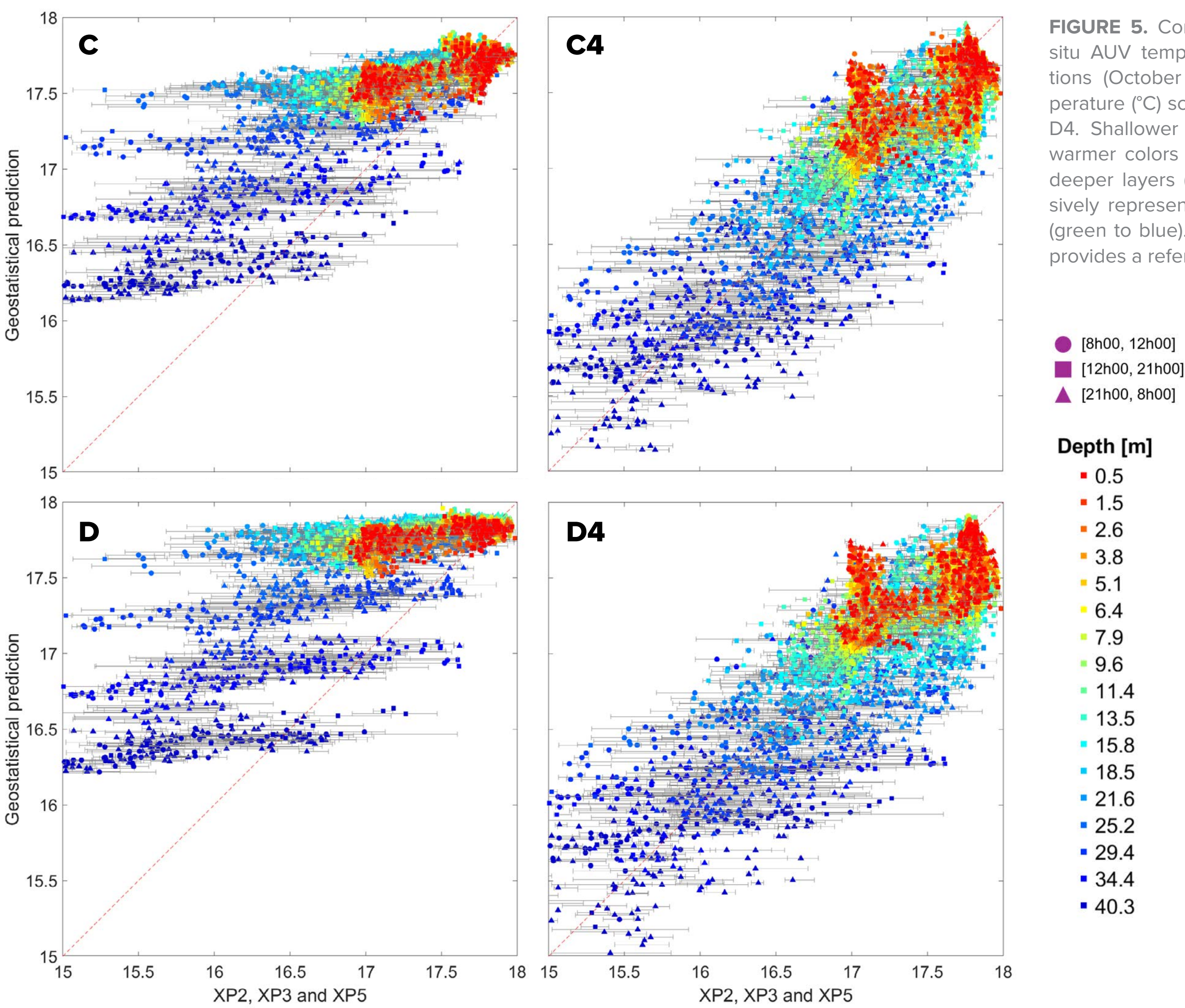

FIGURE 5. Comparison between in situ AUV temperature (°C) observations (October 31) and model temperature (°C) scenarios C, C4, D, and D4. Shallower layers are shown in warmer colors (red to yellow), while deeper layers (>30 m) are progressively represented in cooler shades (green to blue). The dashed red line provides a reference for correlation.

For XP3 and XP5, which performed targeted sampling in the same area where previous assimilation data were collected, RMSE values show a consistent reduction. In contrast, XP2, which on October 31 performed a cross-shore transect outside the main target region, exhibits a weaker response to assimilation. The implications of this behavior and its relevance for evaluating the predictive robustness of the framework are examined in the next section. Vertically, RMSE profiles show similar behavior in both experiment sets: errors tend to increase gradually below 25–30 m, where model uncertainty and unresolved variability are higher. However, this gradient weakens considerably in the fully assimilated cases (C4 and D4), particularly in the upper 30 m, where the assimilation of prior AUV data significantly improves the representation of the temperature structure and short-term thermal evolution probably associated with the upwelling-relaxation transition.

DISCUSSION

Assessing the impact of targeted AUV observations on short-term ocean forecasts requires evaluating both model-data agreement and how assimilation effects vary across regions and dynamical oceanographic regimes. Although assimilation generally improves model skill, vehicle-specific results highlight differences linked to sampling patterns and regional dynamics.

Figure 6b,c presents the RMSE predictions compared with in situ data under the different assimilation scenarios (C, C4, D, and D4) for October 31. The results are shown as a function of depth and vehicle, allowing a direct comparison with and without data assimilation. For XP3 and XP5, a clear and consistent trend is observed: the assimilation scenarios (C4 and D4) improve the model prediction skill, with RMSE decreasing across all depths, indicating that the assimilation procedure effectively constrains the local dynamics represented in the statistical model. Although small differences are present between C4 and D4, they are not statistically significant and confirm that assimilation results are robust with respect to initial configuration differences.

The situation for XP2 was different, however. The assimilation scenarios (C4 and D4) lead to higher prediction errors compared with the non-assimilation runs (C and D). This counterintuitive result reflects a spatial mismatch: on October 31, XP2 operated north of Nazaré Canyon, while assimilated data from the previous days (October 29 and 30) were collected south of it. Nazaré Canyon marks a transition zone between distinct oceanographic regimes, where circulation patterns are strongly influenced by the canyon's complex topography and the interaction between shelf and slope processes. Inside the canyon, residual currents are generally aligned along the canyon axis as a result of strong topographical forcing, and this alignment extends well above the canyon edges (~150 m depth), implying substantial disturbance of the predominant north-south circulation parallel to the general trend of the shelf and slope (Relvas et al., 2007; Tyler et al., 2009; Guerreiro et al., 2014). This topographic forcing not only alters circulation but also serves as a conduit for transporting organic matter and sediment from the shelf to the deep sea. The divergence in physical regimes at the canyon likely supports distinct biological assemblages, or "hotspots" of productivity that would be misrepresented by a model that fails to capture these subgrid dynamics (de Stigter et al., 2007; Cunha et al., 2011).

CMEMS NEMO fields (Figure 7) provide a broader context, comparing temperature distributions in northern and southern regions of the study area during the days preceding and during the experiment. Before October 26, although mean temperatures differ between the two regions, their variability is consistent, indicating

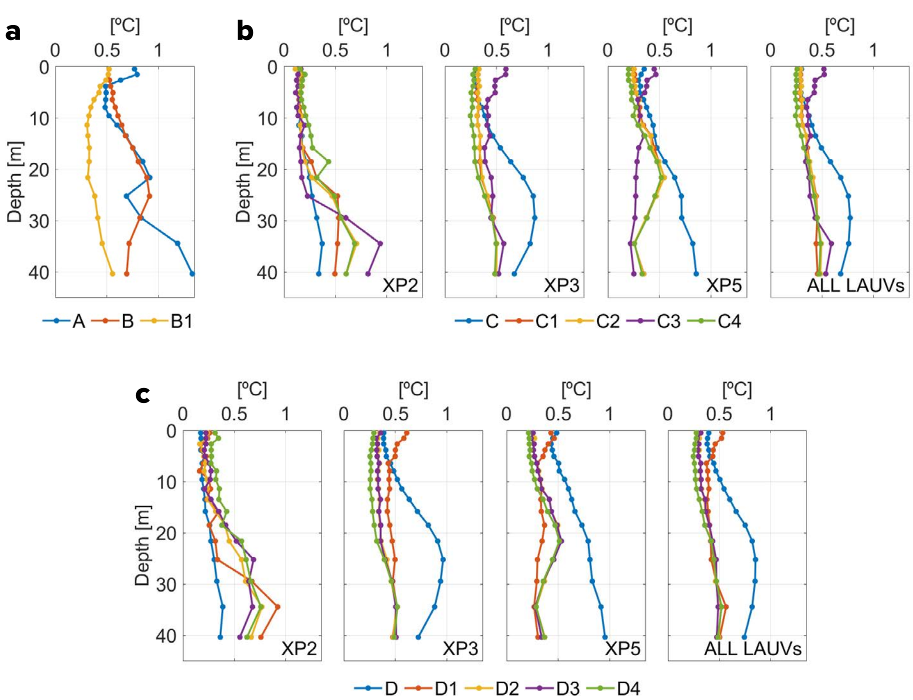

FIGURE 6. (a) Root mean square error (RMSE) in °C between model forecasts and in situ AUV temperature observations for October 29–30. Scenario A corresponds to the baseline statistical forecast generated based on CMEMS NEMO data up to October 29. Scenarios B and B1 represent forecasts for October 30 without and with, respectively, the assimilation of AUV observations collected by light autonomous underwater vehicle (LAUV) XP2. (b) RMSE, between the statistical model forecasts and in situ AUV temperature measurements for October 31, for scenarios C and C1–C4. These forecasts were initialized using Copernicus Marine Service Nucleus for European Modelling of the Ocean (CMEMS NEMO) data available up to October 30, and the assimilation steps progressively incorporate AUV observations collected on previous days. Results are shown for each vehicle and for the combined dataset ("All LAUVs"). (c) Same as (b), but for scenarios D and D1–D4, in which forecasts for October 31 were initialized using CMEMS NEMO data available only up to October 29. Assimilation configurations D1–D4 mirror those of the C-series but start from this less favorable prior state. Results are again presented per vehicle and for the aggregated dataset.

that the system was evolving coherently across the canyon, with systematically colder waters (by about 1°C) in the northern region. After October 26, the temperature evolution in the two regions diverges, with the CMEMS NEMO model showing relatively warmer conditions in the north compared to the south. This divergence coincides with the onset of the upwelling-relaxation transition and highlights a shift toward slightly distinct dynamical regimes on either side of the canyon. This transition can explain why assimilation of southern data, collected under a single dynamical regime, fails to improve and, in fact, degrades forecasts. An alternative explanation for the divergence of the results, which may also act in combination with previously explained factors, concerns the choice of covariance length scales. In our configuration, the estimated variogram range is approximately 70 km in the horizontal, with a temporal correlation scale of about one season. The variogram parameters are estimated using data from the entire domain of interest, which can be interpreted as capturing an "average" space-time behavior. As a consequence, this single, domain-wide covariance model cannot represent local heterogeneity, such as differences between the southern and northern sectors of the Nazaré Canyon region. Therefore, local over- and/or under-estimation of the variogram range may lead to overly broad or overly localized background corrections, which can in turn increase the RMSE in the assimilative experiments (C4 and D4) relative to the corresponding baseline runs (C and D) without assimilation.

This spatial mismatch underscores the need for trajectory-planning strategies that maximize class separation between distinct dynamical regimes, as proposed by Fossum et al. (2019b) using hierarchical clustering methods. Such approaches, based on criteria including variance reduction, mutual information, or entropy, could help identify routes that better discriminate between competing oceanographic states and mitigate situations where assimilation may propagate misleading information if relying solely on uncertainty fields.

Another highlight of this experiment was in showing the variability within the model grid, which provided additional insight into the subgrid-scale structure of the observed field. Figure 8 depicts the interquartile distance (IQD) of measurements recorded by the AUVs within the three-dimensional discretization of the statistical model. Each grid cell represents the maximum spatial resolution available in the model, while the IQD quantifies the local variability of in situ measurements acquired as the vehicles navigated through each cell.

This figure illustrates how robotic platforms can capture significant variability at scales smaller than the model resolution, revealing the existence of fine-scale gradients, in some locations greater than 1°C, as processes that are also unresolved by the model. Although the statistical model provides smoothed, grid-averaged predictions of ocean properties, AUV measurements highlight fluctuations that occur within individual cells, indicating the presence of subgrid-scale dynamics. Unresolved variability is a known source of error in data assimilation systems; numerical forecasts and statistical surrogates inevitably smooth or filter variability below grid scale, so observations that resolve submesoscale or turbulent features will often disagree locally with grid-averaged model fields (Oke and Sakov, 2008; Janjić et al., 2018). These considerations underscore that high-resolution observations from AUVs should not be interpreted solely through coarse model fields. Instead, subgrid variability itself provides valuable information about local forecast uncertainty and should be explicitly accounted for when assimilating observations into coarser-resolution predictive systems.

Across all missions, the AUVs sampled each grid cell with median values ranging from 9 to 14 measurements per cell and mean values between 19 and 26. These statistics indicate a relatively uniform and dense sampling pattern, sufficient to characterize the local variability of the water column at the subgrid level. The maximum number of samples per grid cell reached several

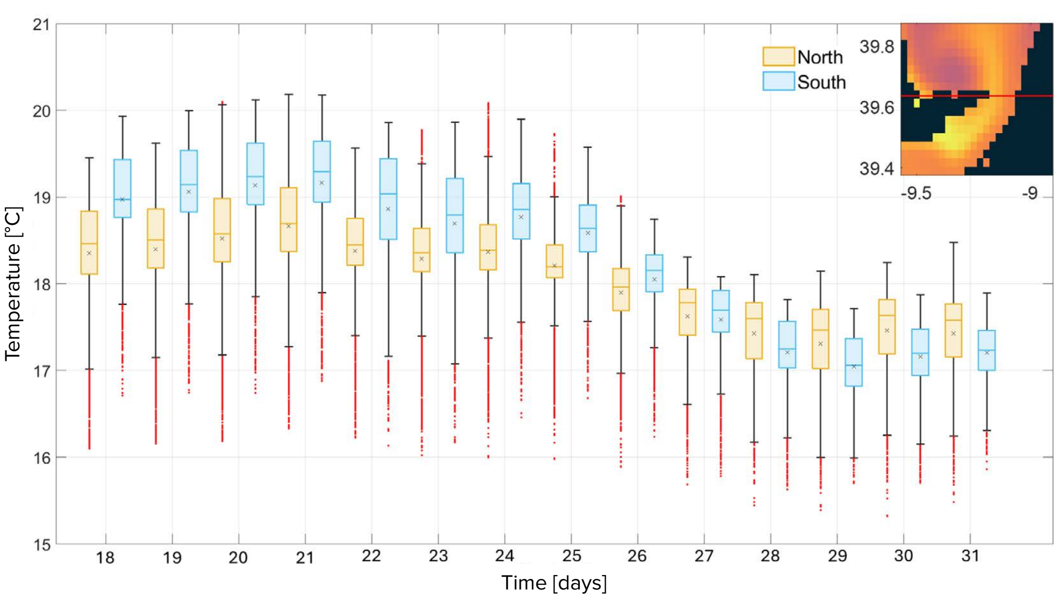

FIGURE 7. Temperature distributions from CMEMS NEMO for the northern and southern regions of the study area between October 18 and 31. The division between regions follows the line boundary shown in the inset map, top right. Only grid points shallower than 200 m were retained to avoid including the canyon interface. Boxplots show the spatial distribution of CMEMS NEMO temperature within each region, capturing both the median and the spread of variability.

thousand available to communicate and geolocate, though these values are biased by vehicle behavior near the surface.

Despite these localized biases, the overall sampling density achieved by the AUVs provides a detailed depiction of fine-scale ocean variability. The IQD distributions reveal higher variability near the thermocline (30–40 m), where vertical gradients are strongest, while in some instances increased variability could also appear near the surface, potentially corresponding to small-scale frontal zones or localized mixing events. Because AUVs sample continuously along their trajectories, they resolve spatial and temporal scales that often fall between CTD stations in traditional ship-based surveys, thereby capturing subgrid processes that remain unresolved in numerical models.

This subgrid variability is not observational noise; it provides valuable insight into local uncertainty and environmental heterogeneity. For example, quantifying this variability is essential for biological oceanography, as many marine organisms—from zooplankton to fish larvae—aggregate in micro-fronts or thermal patches that are often smaller than model resolution. Understanding this "noise" helps distinguish biological aggregations from physical turbulence (Visser and Stips, 2002). Incorporating both the variability (such as IQD) and the spatial sampling density into data assimilation frameworks enhances the model's ability to represent uncertainty at the subgrid scale and improve the realism of short-term forecasts.

This field study provides invaluable lessons in operational procedures, refinement of adaptive sampling and algorithms, and risk minimization for operating in an area with dense ship traffic and fishing nets. Our AUVs were occasionally affected by strong vertical currents that may have resulted from the impact of internal waves that are common in the area and that were observed with the help of remote-sensing imagery during the experiment.

Finally, the results achieved with this deployment provided additional insights and the motivation to further advance the state of the art in refining the *sample-assimilate-predict-direct* cycle with the goal of improving the skill of oceanographic models. Furthermore, dense grids of sampled oceanographic data have the potential to fuel developments that target existing gaps in modeling skill when different levels of spatial and temporal resolution are considered (Balaji et al., 2022).

CONCLUSIONS

This effort demonstrates the usefulness of overall integration to close the *sample-assimilate-predict-direct* cycle to improve oceanographic model skill by leveraging observations from robotic platforms. Figure 6 shows clear indications of an increase in predictive skill when high-resolution data from AUVs are assimilated in a geostatistical model. By choosing such a modeling approach, this effort offers a window into the rapid process of assimilating and predicting, the primary goal of FRESNEL, and doing so with minimal operational support. The accuracy of the predictions of the geostatistical

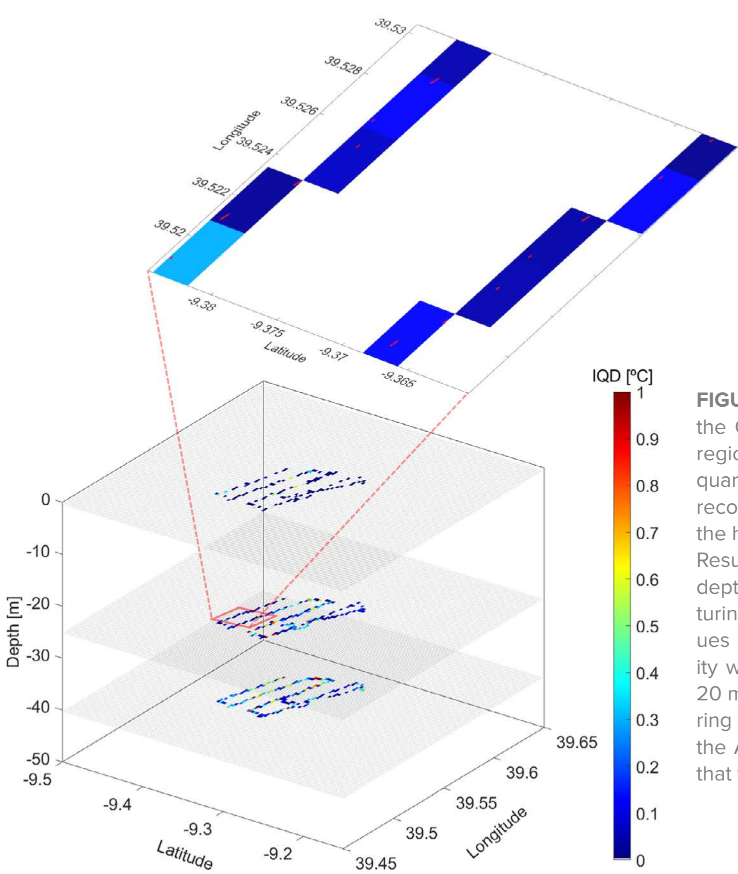

FIGURE 8. Trajectory of LAUV XP5, during the October 30 mission in the Nazaré Canyon region. The color shading represents the interquartile range (IQD) of temperature values recorded within each model grid cell, illustrating the horizontal resolution of the statistical model. Results are shown for three representative depth layers: near-surface, 20 m, and 40 m, capturing distinct vertical regimes. Higher IQD values indicate regions of higher thermal variability within the model grid. Close-up view of the 20 m layer reveals fine-scale fluctuations occurring inside single grid elements, illustrating that the AUVs are capturing subgrid-scale structure that the model does not resolve.

model increased after several cycles, while overall prediction errors decreased as noted. These results provide a foundation for continuous ocean prediction when obtaining high-resolution in situ data as conceptualized in the METEOR (A Mobile (Portable) ocEan roboTic ObsErvatORy) framework (Rajan et al., 2021).

A confluence of external factors reduced the observation period from the planned three weeks to three days, primarily due to weather, platform availability, and personnel constraints. Future work will extend the observation period to validate and expand upon these promising results.

Other challenges that remain to be addressed include near-real-time assimilation and continuous model prediction, especially to capture dynamic coastal events. While we are still lacking the desired statistical significance of a long series of consecutive cycles, our future work will target optimization of the parameters used for deeper integration of the algorithms used in the cycle. For instance, we hope to investigate the selection of representative depths for the application of the sampling algorithm used to find the horizontal projection of the AUV paths (Bernacchi et al., 2025). Another potential outcome to be investigated is the use of higher-resolution numerical models and longer prediction horizons, considering computational trade-offs. In doing so, we would also like to demonstrate the viability of portable low (computational) cost models running in the cloud, which can be initialized for any region rapidly to demonstrate the loop-closure we set out to validate.

Along these lines, an additional research direction involves encapsulating a model surrogate embedded within the control system of one or more AUVs to capture coastal dynamism at fine scales (Frolov et al., 2009; Fossum et al., 2019b), while complementing an increase in the assessment of shore-based model skill.

SUPPLEMENTARY MATERIALS

The supplementary materials are available online at https://doi.org/10.5670/oceanog.2026.e209.

REFERENCES

Agarwal, N., D. Kondrashov, P. Dueben, E. Ryzhov, and P. Berloff. 2021. A comparison of data-driven approaches to build low-dimensional ocean models. *Journal of Advances in Modeling Earth Systems* 13(9):e2021MS002537, https://doi.org/10.1029/2021MS002537.

Balaji, V., F. Couvreux, J. Deshayes, J. Gautrais, F. Hourdin, and C. Rio. 2022. Are general circulation models obsolete? *Proceedings of the National Academy of Sciences of the United States of America* 119(47):e2202075119, https://doi.org/10.1073/pnas.2202075119.

Behrenfeld, M.J., and E.S. Boss. 2014. Resurrecting the ecological underpinnings of ocean plankton blooms. *Annual Review of Marine Science* 6(1):167–194, https://doi.org/10.1146/annurev-marine-052913-021325.

Bernacchi, L., A.F. Duarte, R. Mendes, L. Azevedo, and J.B. de Sousa. 2025. Closing the data loop: Real-world AUVs adaptive sampling for improved ocean model predictions. Pp. 1–8 in *2025 Symposium on Maritime Informatics and Robotics (MARIS)*. June 26–27, 2025, Syros, Greece, IEEE, https://doi.org/10.1109/MARIS64137.2025.11139688.

Cressie, N.A.C. 1993. *Statistics for Spatial Data*. Revised Edition, Wiley, New York, 928 pp., https://doi.org/10.1002/9781119115151.

Cunha, M.R., G.L. Paterson, T. Amaro, S. Blackbird, H.C. de Stigter, C. Ferreira, A. Glover, A. Hilario, K. Kiriakoulakis, L. Neal, and others. 2011. Biodiversity of macrofaunal assemblages from three Portuguese submarine canyons (NE Atlantic). *Deep Sea Research Part II* 58(23–24):2,433–2,447, https://doi.org/10.1016/j.dsr2.2011.04.007.

Das, J., F. Py, T. Maughan, M. Messie, T. O'Reilly, J. Ryan, G.S. Sukhatme, and K. Rajan. 2012. Coordinated sampling of dynamic oceanographic features with AUVs and drifters. *International Journal of Robotics Research* 31(5), https://doi.org/10.1177/0278364912440736.

Das, J., F. Py, J.B. Harvey, J.P. Ryan, A. Gellene, R. Graham, D.A. Caron, K. Rajan, and G.S. Sukhatme. 2015. Data-driven robotic sampling for marine ecosystem monitoring. *International Journal of Robotics Research* 34:(12):1,435–1,452, https://doi.org/10.1177/0278364915587723.

de Stigter, H.C., W. Boer, P.A. de Jesus Mendes, C.C. Jesus, L. Thomsen, G.D. van den Bergh, and T.C. van Weering. 2007. Recent sediment transport and deposition in the Nazaré Canyon, Portuguese continental margin. *Marine Geology* 246(2–4):144–164, https://doi.org/10.1016/j.margeo.2007.04.011.

Deutsch, C.V., and A.G. Journel. 1992. GSLIB: *Geostatistical Software Library and User's Guide*. Oxford University Press, New York, first edition, 340 pp.

Dias, P.S., S.L. Fraga, R.M. Gomes, G.M. Goncalves, F.L. Pereira, J. Pinto, and J.B. Sousa. 2005. NEPTUS - A framework to support multiple vehicle operation. Pp. 963–968 in *Europe Oceans 2005*. June 20–23, 2005, Paris, France, IEEE, https://doi.org/10.1109/OCEANSE.2005.1513187.

Duarte, A.F., L. Bernacchi, R. Mendes, J.T. Sousa, and L. Azevedo. 2025. Geostatistical uncertainty maps for real-world efficient AUV data collection. *Frontiers in Marine Science* 12:1674989, https://doi.org/10.3389/fmars.2025.1674989.

EU Copernicus Marine Service (CMEMS) Information Marine Data Store (MDS). 2024a. *Atlantic-Iberian Biscay Irish-Ocean Physics Analysis and Forecast*, https://doi.org/10.48670/moi-00027.

EU Copernicus Marine Service (CMEMS) Information Marine Data Store (MDS). 2024b. *European North West Shelf/Iberia Biscay Irish Seas – High Resolution ODYSSEA Sea Surface Temperature Multi-sensor L3 Observations Reprocessed*, https://doi.org/10.48670/moi-00311.

Eidsvik, J., T. Mukerji, and D. Bhattacharjya. 2015. *Value of Information in the Earth Sciences: Integrating Spatial Modeling and Decision Analysis*. Cambridge University Press, 400 pp., https://doi.org/10.1017/CBO9781139628785.

Ford, D.A., S. Grossberg, G. Rinaldi, P.P. Menon, M.R. Palmer, J. Skákala, T. Smyth, C.A. Williams, A. Lorenzo Lopez, and S. Ciavatta. 2022. A solution for autonomous, adaptive monitoring of coastal ocean ecosystems: Integrating ocean robots and operational forecasts. *Frontiers in Marine Science* 9:1067174, https://doi.org/10.3389/fmars.2022.1067174.

Fossum, T.O., J. Eidsvik, I. Ellingsen, M. Alver, G. Fragoso, G. Johnsen, R. Mendes, M. Ludvigsen, and K. Rajan. 2018. Information-driven robotic sampling in the coastal ocean. *Journal of Field Robotics* 35(7):1,101–1,121, https://doi.org/10.1002/rob.21805

Fossum, T.O., G.M. Fragoso, E.J. Davies, J. Ullgren, R. Mendes, G. Johnsen, I. Ellingsen, J. Eidsvik, M. Ludvigsen, and K. Rajan. 2019a. Toward adaptive robotic sampling of phytoplankton in the coastal ocean. *Science Robotics* 4(27), https://doi.org/10.1126/scirobotics.aav3041.

Fossum, T.O., J. Ryan, T. Mukerji, J. Eidsvik, T. Maughan, M. Ludvigsen, and K. Rajan. 2019b. Compact models for adaptive sampling in marine robotics. *International. Journal of Robotics Research* 39(1), https://doi.org/10.1177/0278364919884141.

Frolov, S., A.M. Baptista, T.K. Leen, Z. Lu, and R. van der Merwe. 2009. Fast data assimilation using a nonlinear Kalman filter and a model surrogate: An application to the Columbia River estuary. *Dynamics of Atmospheres and Oceans* 48(1–3):16–45, https://doi.org/10.1016/j.dynatmoce.2008.10.004.

Garcia-Olaya, A., F. Py, J. Das, and K. Rajan. 2012. An online utility-based approach for sampling dynamic ocean fields. *IEEE Journal of Oceanic Engineering* 37(2):185–203, https://doi.org/10.1109/JOE.2012.2183934.

Graham, R., F. Py, J. Das, D. Lucas, T. Maughan, and K. Rajan. 2012. Exploring space-time tradeoffs in autonomous sampling for marine robotics. Pp. 819–839 in *Experimental Robotics: The 13th International Symposium on Experimental Robotics*. J.P. Desai, G. Dudek, O. Khatib, and V. Kumar, eds, vol. 88 in Springer Tracts in Advance Robotics, https://doi.org/10.1007/978-3-319-00065-7_55.

Greene, H.G., and J.R. Delaney. 2025. Urban sea systems and why they are important: A preliminary characterization. *Estuarine, Coastal and Shelf Science* 322:109274, https://doi.org/10.1016/j.ecss.2025.109274.

Guerreiro, C., C. Sá, H. de Stigter, A. Oliveira, M. Cachão, L. Cros, C. Borges, L. Quaresma, A.I. Santos, J.-M. Fortuño, and others. 2014. Influence of the Nazaré Canyon, central Portuguese margin, on late winter coccolithophore assemblages. *Deep Sea Research Part II* 104:335–358, https://doi.org/10.1016/j.dsr2.2013.09.011.

Janjić, T., N. Bormann, M. Bocquet, J. Carton, S.E. Cohn, S.L. Dance, S.N. Losa, N.K. Nichols, R. Potthast, J.A. Waller, and others. 2018. On the representation error in data assimilation. *Quarterly Journal of the Royal Meteorological Society* 144(713):1,257–1,278, https://doi.org/10.1002/qj.3130.

Lermusiaux, P.F. 2007. Adaptive modeling, adaptive data assimilation and adaptive sampling. *Physica D: Nonlinear Phenomena* 230(1–2):172–196, https://doi.org/10.1016/j.physd.2007.02.014.

Madec, G., P. Delecluse, M. Imbard, and C. Levy. 1997. *Ocean General Circulation Model Reference Manual*. Note du Pôle de modélisation, Institut Pierre-Simon Laplace (IPSL), France, No. 11, 91 pp.

Madec, G., and the NEMO team. 2015. *NEMO ocean engine*. Note du Pôle de modélisation, Institut Pierre-Simon Laplace (IPSL), France, No 27, 391 pp.

Mahadevan, A. 2016. The impact of submesoscale physics on primary productivity of plankton. *Annual Review of Marine Science* 8(1):161–184, https://doi.org/10.1146/annurev-marine-010814-015912.

Martins, I., J. Vitorino, and S. Almeida. 2010. The Nazaré Canyon observatory (W Portugal) real-time monitoring of a large submarine canyon. Pp. 1–7 in *OCEANS'10 IEEE SYDNEY*. May 24–27, 2010, Sydney, Australia, IEEE, https://doi.org/10.1109/OCEANSSYD.2010.5603854

Martins, R., and J. Sousa. 2010. Concepts and tools for coordination and control of networked ocean-going vehicles. Pp. 1–6 in *2010 IEEE/OES Autonomous Underwater Vehicles*. September 1–3, 2010, Monterey, California, IEEE, https://doi.org/10.1109/AUV.2010.5779672.

McGann, C., F. Py, K. Rajan, J.P. Ryan, and R. Henthorn. 2008. Adaptive control for autonomous underwater vehicles. Pp. 1,319–1,324 in *AAAI'08: Proceedings Association for the Advancement of Artificial Intelligence*, vol. 3.

Oke, P.R. and P. Sakov. 2008. Representation error of oceanic observations for data assimilation. *Journal of Atmospheric and Oceanic Technology* 25(6):1,004–1,017, https://doi.org/10.1175/2007JTECHO558.1.

Pinto, J., P.S. Dias, R. Martins, J. Fortuna, E. Marques, and J. Sousa. 2013. The LSTS toolchain for networked vehicle systems. Pp. 1–9 in *2013 MTS/IEEE OCEANS - Bergen*. June 10–14, 2013, Bergen, Norway, IEEE, https://doi.org/10.1109/OCEANS-Bergen.2013.6608148.

Quaresma, L.S., J. Vitorino, A. Oliveira, and J. da Silva. 2007. Evidence of sediment resuspension by nonlinear internal waves on the western Portuguese mid-shelf. *Marine Geology* 246(2–4):123–143, https://doi.org/10.1016/j.margeo.2007.04.019.

Rajan, K., and F. Py. 2012. T-REX: Partitioned inference for AUV mission control. Chapter 9 in *Further Advances in Unmanned Marine Vehicles*. G.N. Roberts and R. Sutton, eds, The Institution of Engineering and Technology (IET), https://doi.org/10.1049/PBCE077E_ch9.

Rajan, K., F. Aguado, P. Lermusiaux, J. de Sousa, A. Subramaniam, and J. Tintore. 2021. METEOR: A Mobile (Portable) ocEan roboTic ObsErvatORy. *Marine Technology Society Journal* 55(3), https://doi.org/10.4031/MTSJ.55.3.42.

Relvas, P., E.D. Barton, J. Dubert, P.B. Oliveira, Á. Peliz, J.C. da Silva, and A.M.P. Santos. 2007. Physical oceanography of the western Iberia ecosystem: Latest views and challenges. *Progress in Oceanography* 74(2–3):149–173, https://doi.org/10.1016/j.pocean.2007.04.021.

Ryan, J.P., S. Johnson, A. Sherman, K. Rajan, F. Py, H. Thomas, J. Harvey, L. Bird, J. Paduan, and R. Vrijenhoek. 2010. Mobile autonomous process sampling within coastal ocean observing systems. *Limnology & Oceanography: Methods* 8:394–402, https://doi.org/10.4319/lom.2010.8.394.

Shchepetkin, A.F., and J.C. McWilliams. 2005. The regional oceanic modeling system (ROMS): A split-explicit, free-surface, topography-following-coordinate oceanic model. *Ocean Modelling* 9(4):347–404, https://doi.org/10.1016/j.ocemod.2004.08.002.

Singh, A., A. Krause, and W.J. Kaiser. 2009. Nonmyopic adaptive informative path planning for multiple robots. Pp. 1,843–1,850 in *IJCAI'09: Proceedings of the 21st International Joint Conference on Artificial Intelligence*. Morgan Kaufmann Publishers Inc., Pasadena, California.

Soares, A. 2001. Direct sequential simulation and cosimulation. *Mathematical Geology* 33(8):911–926, https://doi.org/10.1023/A:1012246006212.

Sotillo, M.G., F. Campuzano, K. Guihou, P. Lorente, E. Olmedo, A. Matulka, F. Santos, M.A. Amo-Baladrón, and A. Novellino. 2021. River freshwater contribution in operational ocean models along the European Atlantic facade: Impact of a new river discharge forcing data on the CMEMS IBI regional model solution. *Journal of Marine Science and Engineering* 9(4):401, https://doi.org/10.3390/jmse9040401.

Sousa, A., L. Madureira, J. Coelho, J. Pinto, J. Pereira, J. Sousa, and P. Dias. 2012. LAUV: The man-portable autonomous underwater vehicle. *Navigation, Guidance and Control of Underwater Vehicles* 3(1):268–274, https://doi.org/10.3182/20120410-3-PT-4028.00045.

Toth, P., and D. Vigo, eds. 2014. *Vehicle Routing: Problems, Methods, and Applications*. SIAM, 449 pp., https://doi.org/10.1137/1.9781611973594.

Tyler, P., T. Amaro, R. Arzola, M.R. Cunha, H. de Stigter, A. Gooday, V. Huvenne, J. Ingels, K. Kiriakoulakis, G. Lastras, and others. 2009. Europe's grand canyon: Nazaré Submarine Canyon. *Oceanography* 22(1):46–57, https://doi.org/10.5670/oceanog.2009.05.

Vidal, T., T.G. Crainic, M. Gendreau, and C. Prins. 2013. A hybrid genetic algorithm with adaptive diversity management for a large class of vehicle routing problems with time-windows. *Computers & Operations Research* 40(1):475–489, https://doi.org/10.1016/j.cor.2012.07.018.

Visser, A.W., and A. Stips. 2002. Turbulence and zooplankton production: Insights from PROVESS. *Journal of Sea Research* 47(3–4):317–329, https://doi.org/10.1016/S1385-1101(02)00120-X.

Wallcraft, A., E. Metzger, and S. Carroll. 2009. *Software Design Description for the Hybrid Coordinate Ocean Model (HYCOM), Version 2.2*. Technical report, Naval Research Laboratory, Stennis Space Center, MS, https://doi.org/10.21236/ADA494779.

Wihsgott, J., T. Mansfield, S. Kay, J. Skakala, D. Partridge, D. Ford, G.H. Tilstone, T. Jordan, P. Land, K. Wang, and others. 2026. Improving predictions of coastal marine ecosystem forecasts through a digital twin ocean approach. Paper presented at the 2026 Ocean Sciences Meeting, February 22–27, 2026, Glasgow, Scotland.

Zhang, B., and G.S. Sukhatme. 2007. Adaptive sampling for estimating a scalar field using a robotic boat and a sensor network. Pp. 3,673–3,680 in *Proceedings of the IEEE International Conference on Robotics and Automation*, April 10–14, 2007, Rome, Italy, https://doi.org/10.1109/ROBOT.2007.364041.

ACKNOWLEDGMENTS

This work was carried out with the support of the US Office of Naval Research (ONR), contract N00014-22-1-2796. We are grateful to Tom Drake (Code 32) for his support. RM and JBS acknowledge the support of Fundação para a Ciência e a Tecnologia (FCT) for its financial support to LAETA via the project UID/50022/2025. LA and AD gratefully acknowledge the support of CER-ENA (UID/04028/2025). MC and CR thank UID Centro de Estudos do Ambiente e Mar (CESAM) + LA/P/0094/2020 for support. AD is funded by the Fundação para a Ciência e a Tecnologia (FCT, Portuguese Foundation for Science and Technology) through project PRT/BD/154661/2023. The work was also partially supported by JUNO—Robotic Exploration of Atlantic Waters project—Refa 2021/0008 from FLAD, by the DiverSea project (grant # 101082004) supported by the European Commission and the TRAINEE project (2024.07606. IACDC) supported by FCT. Finally, we would like to thank the two anonymous reviewers whose comments and critique have contributed substantially to strengthening this manuscript.

AUTHORS

Renato Mendes (rpmendes@inegi.up.pt), Laboratório de Sistemas e Tecnologia Subaquática (LSTS), Faculdade de Engenharia da Universidade do Porto, and Laboratório Associado de Energia, Transportes e Aeronáutica (LAETA), Instituto de Ciência e Inovação em Engenharia Mecânica e Engenharia Industrial (INEGI), Porto, Portugal. **Ana F. Duarte** and **Leonardo Azevedo**, Centro de Recursos Naturais e Ambiente (CERENA), DER/Instituto Superior Técnico, Universidade de Lisboa, Portugal. **Lucrezia Bernacchi**, LSTS, Faculdade de Engenharia da Universidade do Porto, Portugal. **João Borges de Sousa**, LSTS, Faculdade de Engenharia da Universidade do Porto, and LAETA, INEGI, Porto, Portugal. **João Pereira**, LAETA, INEGI, Porto, Portugal. **Bernardo Gabriel**, LSTS, Faculdade de Engenharia da Universidade do Porto, Portugal. **João Bogas**, LSTS, Faculdade de Engenharia da Universidade do Porto, and LAETA, INEGI, Porto, Portugal. **Marina Cunha**, Departamento de Biologia, Universidade de Aveiro, Portugal. **Clara F. Rodrigues**, Departamento de Biologia and Centro de Estudos do Ambiente e do Mar, Universidade de Aveiro, Portugal. **Ajit Subramaniam**, Lamont-Doherty Earth Observatory of Columbia University, Palisades, NY, USA. **Fernando Esteves**, RAND Corporation, Santa Monica, CA, USA. **Kanna Rajan**, LSTS, Faculdade de Engenharia da Universidade do Porto, Portugal.

ARTICLE CITATION

Mendes, R., A.F. Duarte, L. Azevedo, L. Bernacchi, J.B. de Sousa, J. Pereira, B. Gabriel, J. Bogas, M. Cunha, C.F. Rodrigues, A. Subramaniam, F. Esteves, and K. Rajan. 2026. Toward ocean model-driven robotic exploration. *Oceanography* 39(2):34–47, https://doi.org/10.5670/oceanog.2026.e209.

COPYRIGHT & USAGE

THE QUEST TO MAP THE GLOBAL OCEAN

By Larry Mayer

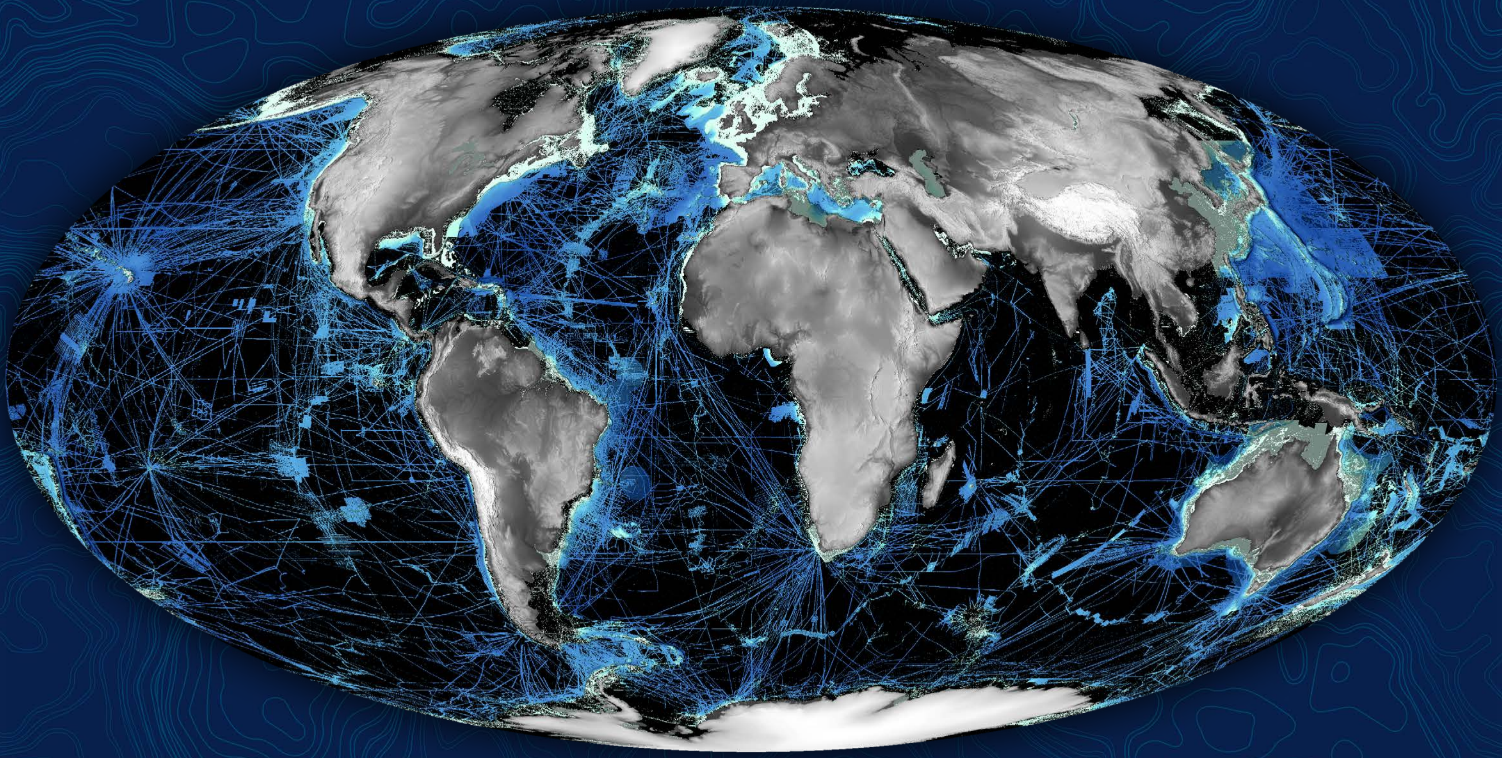

Current global bathymetric coverage in the GEBCO 2025 grid (blue) displayed on Mollweide projection. Black areas have no bathymetric coverage. *Web service created by Paul Johnson, Center for Coastal and Ocean Mapping, University of New Hampshire,* https://gis.ccom.unh.edu/portal/apps/instant/basic/index.html?appid=2cd9ce9dd37c48bf9036d102b6f32485

The Roger Revelle Commemorative Lecture Series was created by the Ocean Studies Board of the National Academies of Sciences, Engineering, and Medicine in honor of Roger Revelle to highlight the important links between ocean sciences and public policy. Dr. Larry Mayer, the twenty-seventh annual lecturer, spoke on March 17, 2026, at the National Academy of Sciences.

INTRODUCTION: MAPPING AS EXPLORATION

When asked to give the Revelle Lecture—and come up with a catchy title that would capture the essence of my talk—we came up with "The Quest to Map the Global Ocean." That sounded good, but it also led me to delve deeper into what a "quest" really is. Drawing on several formal definitions, I arrived at "A long, adventurous search or journey undertaken to find or achieve something important involving challenges and obstacles." I felt that was an accurate description of what I would talk about, but, in all honesty, I would have to say that when I first entered this field, I was driven less by the altruistic goal of "achieving something important" and more by the more selfish desire of searching for adventure.

From my earliest days growing up in an apartment building in the Bronx, I wanted to be an ocean explorer. Like many of my generation, I was inspired by Jacques Cousteau, and while it was the spectacular images of macrofauna and wrecks that folks like Cousteau and Bob Ballard produced that caught my imagination, I also recognized that these images were only minuscule snapshots of a vastly unknown ocean system—true exploration begins with mapping. This is what the early explorers did as they ventured into the unknown—Lewis and Clark, Magellan, and Captain Cook all started by making maps, establishing the spatial framework for all else that they and others would discover.

HUMAN PERCEPTION, IMAGERY, AND THE PRIMACY OF VISION

Mapping, in the context of exploration, is the process of creating a visual representation of spatial data. Visual representation is central to mapping because spatial exploration is fundamentally a sensory process and, among the human senses, vision dominates both perceptually and neurologically. Approximately 30% of the neurons in the human brain are devoted directly to visual processing, and over 60% of the brain is involved in vision directly or indirectly (Billinghurst and Thomas, 2016). Throughout history, exploration has therefore been closely tied to imagery: telescopes pointed skyward, maps sketched from elevated vantage points, and, more recently, satellites imaging Earth from space with remarkable resolution.

Our modern approaches to understanding Earth's processes reflect this visual bias. Satellite imagery, digital terrain models, and geospatial visualization tools allow researchers to "see" processes unfolding across the continents. High-resolution imagery reveals glacier retreat, forest loss, urban expansion, and geomorphic change with unprecedented clarity. Mapping does not merely document these processes; it provides the spatial context necessary to interpret them quantitatively. Modern satellite-based digital elevation models provide the spatial framework upon which interpretation, navigation, governance, and both resource exploitation and environmental protection depend. Today, for the terrestrial components of Earth, advances in remote sensing, geodesy, and computing have produced near-global, meter-scale representations of Earth's surface. These datasets now underpin climate science, hydrology, ecology, hazard mitigation, and land-use planning. With a few keystrokes, anyone can extract this remarkable imagery for any terrestrial location with readily available applications like Google Earth. In stark contrast, when focused on the ocean's surface, the same sensors that spectacularly map terrestrial components provide little information about our ocean, which represents 71% of Earth's surface and the largest continuous environment on the planet. This disparity is striking and frightening as the ocean exerts a disproportionate influence on our planet. Ocean circulation regulates climate; the seafloor controls deep-water pathways and mixing; maritime trade sustains the global economy; fisheries feed and support hundreds of millions of people; and submerged landscapes host ecosystems, resources, and cultural heritage (Figure 1).

FIGURE 1. Some of the many reasons why ocean maps are important to understanding Earth processes. How do we manage and protect what we do not know and understand?

THE PHYSICAL CONSTRAINT: WHY THE OCEAN RESISTS OPTICAL MAPPING

The principal barrier to comprehensive ocean mapping is physical rather than conceptual. The sensors used for satellite remote sensing typically rely on electromagnetic radiation—visible light, infrared, or radar—that propagates efficiently through air. In seawater, however, absorption and scattering dramatically reduce penetration depth. Even in the clearest open-ocean waters, visible light rarely penetrates beyond ~200 m; in most coastal waters, penetration is typically less than 50 m.

This limitation renders optical imaging ineffective for the vast majority of the seafloor and water column. The mean depth of the global ocean is approximately 3,700–4,000 m, with large areas exceeding 5,000 m; 94% of the world's seafloor is deeper than 200 m. Beyond these depths (and typically much shallower) the seafloor lies permanently beyond the reach of light-based remote sensing. This does not mean deep-sea optical imaging is impossible; rather, it requires placing sensors very close to the seafloor to overcome rapid light attenuation. As outlined by Chris Scholin in last year's Revelle Lecture (Scholin, 2025), this can be accomplished using cabled remotely operated vehicles (ROVs) or free-swimming autonomous underwater vehicles (AUVs) that can be operated close to the seafloor and collect high-resolution optical imagery. Unfortunately, these vehicles move very slowly and, given the rapid attenuation of light, can only image a very small portion of the seafloor at a time.

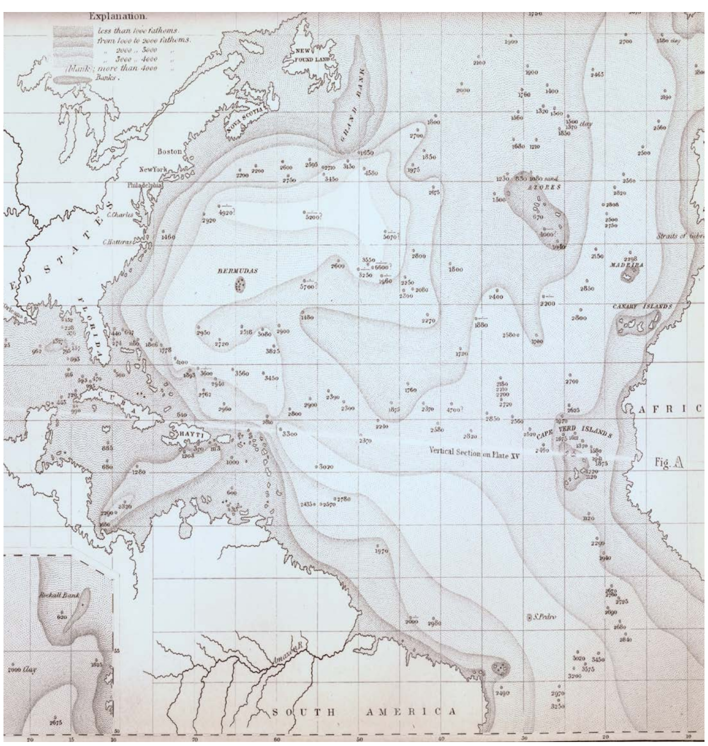

FIGURE 2. This early contour map of the Atlantic Ocean is based on lead-line soundings undertaken and recorded by Lt. Matthew Fontaine Maury in 1854. *Credit: NOAA Central Library Historical Collection, https://www.noaa.gov/noaa-collections/photo-library/map00002jpg*

A thought experiment underscores the magnitude of this constraint. What would it take to create a "Google Ocean" of optical images with resolution analogous to that of Google Earth? To collect the optical imagery necessary to obtain the resolution provided by Google Earth, cameras would need to operate within roughly 10–20 m above the seafloor with a very limited field of view (~10 m). Given this limited field of view and the enormous area of the ocean floor, such an effort would require on the order of 34×10^9 images and, given the very slow rate of coverage for these vehicles, tens of millions of years to completely capture these images at realistic acquisition rates. Supporting these estimates, Bell et al. (2025) estimated that, to date, all efforts to image the deep seafloor since 1958 have covered only .001% of the deep seafloor. These order-of-magnitude estimates make clear that optical mapping of the complete deep ocean is not merely impractical, it is physically untenable.

FROM TOUCH TO SOUND: EARLY SEAFLOOR MAPPING

LEAD-LINE SOUNDINGS AND MILLENNIA OF CONTINUITY

Given the limits of optical imagery—and thus the inability to use our sense of vision for mapping the seafloor—we had to turn to other senses, initially touch. For most of human history, seafloor depth measurements were made by direct physical contact. Weighted ropes or wires—lead lines—were lowered until they touched the bottom. This method, depicted in artifacts from Egyptian tombs dating back to at least 2000 BCE, remained essentially unchanged for nearly 4,000 years. Even as ship design, navigation, and seafaring expanded dramatically, the fundamental approach to measuring depth did not. Lead-line soundings can be accurate in shallow water under calm conditions, but they are slow, labor-intensive, and spatially very sparse. As water depth increases, uncertainty grows due to ship motion, current-induced line deflection, and difficulty in detecting bottom contact. Consequently, lead-line datasets provide only the coarsest representations of seafloor morphology (Figure 2).

SINGLE BEAM ECHO SOUNDING

Because sound waves propagate efficiently through seawater unlike electromagnetic waves, efforts to use sound (and thus the engagement of another sense: hearing), to measure depth and to identify icebergs accelerated in the early 1900s and marked a turning point in ocean mapping (NOAA, n.d.). Perfected through the Second World War, "single beam" echosounders were developed that allowed the rapid measurement of depth in any depth of water (assuming the frequency of the echosounder is low enough to allow it to travel to the deepest part of the ocean; for full-ocean depth measurements, echosounders typically use frequencies of 12,000 cycles/sec or 12 kHz). Single beam echosounders transmit an acoustic pulse downward and then measure the time required for the echo to return to the vessel. If the speed of sound in the

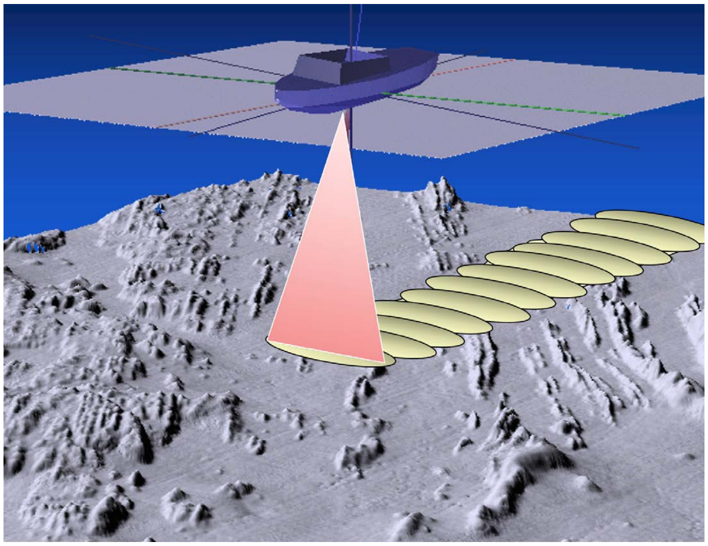

FIGURE 3. Geometry of a single beam sonar. The beam widens as it propagates from a narrow ping emitted from the vessel to insonify a large area on the seafloor. However, only a single reading of the shallowest depth the sonar encounters is returned to the ship, and it does not provide any information about the location in the footprint that depth occurred. *Source: John Hughes Clarke, Center for Coastal and Ocean Mapping, University of New Hampshire*

water column is known, then the travel time can be converted to depth. This approach dramatically increased data acquisition rates and accuracy of depth measurements relative to lead lines.

Using an average speed of sound in seawater of 1,500 ms^{-1}, a single measurement of depth with an echosounder in the approximately 11,000 m Challenger Deep of the Mariana Trench (the deepest place in the ocean) would take approximately 14.7 seconds for a sound wave to travel from the vessel to the seafloor and back to the vessel. A lead-line measurement in these water depths would take many hours, and it would likely be inaccurate.

While representing a tremendous leap with respect to the rate at which depth measurements could be made (and thus the number of measurements made on a given mission), single beam echosounders have limited spatial resolution on the seafloor. As the sound pulse leaves the echosounder on the ship, it expands much like a beam of light leaving a flashlight. By the time the sound pulse reaches the seafloor, it has insonified a broad conical footprint that increases in size with increasing water depth. In deep water, this footprint can be kilometers wide, but the returned signal is a single depth measurement representing the shallowest feature within that footprint rather than the point directly beneath the vessel. As a result, single beam data are spatially ambiguous and require extensive interpolation between widely spaced tracks (Figure 3). The result is a rather defocused representation of the seafloor, averaged over the spatial footprint of the sonar (usually about one-third to one-half the water depth). Typically, to visualize these data, measured points of equal depth are connected with "contour" lines, offering a crude and widely interpolated representation of the distribution of depths in a region.

SATELLITE ALTIMETRY: A GLOBAL, BUT COARSE VIEW

In the late 1990s, Smith and Sandwell (1997) introduced an approach to estimating seafloor depths (bathymetry) from satellite altimetry measurements. Satellite radar altimetry introduced a fundamentally different approach to seafloor mapping. Rather than measuring the depth of the seafloor directly, altimeters measure the height of the sea surface with centimeter-scale precision. Variations in sea surface height reflect gravitational anomalies caused by changes in seafloor mass distributions: the excess mass of seamounts produces positive anomalies and a slight elevation of the sea surface, while the missing mass of trenches produce negative ones and a slight depression of the sea surface. By relating the dense gravity anomaly measurements to sparse known depth measurements, Smith and Sandwell (1997) were able to produce a global interpolated grid of predicted depths. These predictions work best for long-wavelength features (~10–15 km) and are particularly good at revealing large features like mid-ocean ridges, fracture zones, and trenches on a planetary scale (Figure 4). Satellite altimetry provided the first truly global view of the ocean basins and played a critical role in advancing plate tectonic theory but is inherently coarse. Typical spatial resolution is on the order of 10–15 km, though a new satellite mission, Surface Water and Ocean Topography (SWOT), is providing resolution as fine as 4–5 km (Sandwell et al., 2025). Even this improved scale, however, is insufficient for resolving geomorphic features, habitat heterogeneity, or seafloor roughness relevant to ocean circulation and ecosystems. Satellite altimetry therefore provides a remarkable global perspective for understanding tectonic processes but is not a substitute for direct mapping.

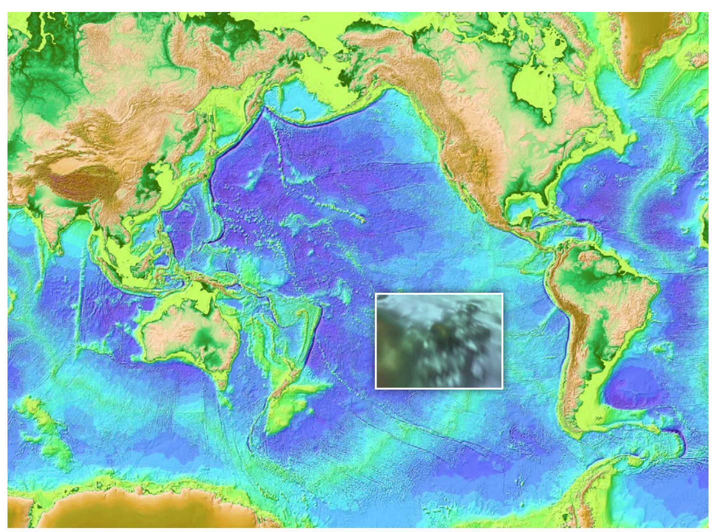

FIGURE 4. Global predicted bathymetry from satellite altimetry provides an excellent estimate of global bathymetry at low spatial resolution that is useful for understanding tectonic-scale features but of limited use for understanding many ocean processes. Inset zooms into a 200 × 200 km area at the scale of satellite-altimetry-derived bathymetry. *Map from https://www.star.nesdis.noaa.gov/socd/lsa/AltBathy/*

MULTIBEAM SONAR: A REVOLUTION IN OCEAN MAPPING

The most transformative advance in ocean mapping came with the development of multibeam echosounders (MBES), which evolved out of classified military systems in the mid-1970s and 1980s. Unlike single beam systems, multibeam sonars use a separate transmitter and receiver. The transmitter produces a fan of sound that is thin in the along-track direction and wide—typically five to seven times the water depth—in the across-track direction. The receiver simultaneously creates many, often hundreds, of small fans that are narrow in the across-track direction and wide in the along-track direction. The intersection of the transmit and receive pulses on the seafloor results in hundreds of small insonified areas on the seafloor (beams), each producing a highly accurate depth measurement (Figure 5). Typical swath widths are four to seven times the water depth (>20 km in 4,000 m of water), and the size of the beam footprint (controlling the lateral resolution of features on the seafloor) is typically on the order of 0.017% of the water depth (for a 1° beam), and thus, the spatial resolution of features in 4,000 m of water is on the order of 70 m. Hundreds of these high-resolution soundings are collected with each "ping" of the sonar (which takes place at rates ranging from many tens per second to once every 5–10 seconds depending on water depth), enabling thousands of highly accurate soundings to be collected each hour over a relatively wide swath of the seafloor. This dramatic increase in data density represented a fundamental change in our ability to map the seafloor and revolutionized the use of bathymetric data to understand ocean processes.

The introduction of multibeam sonar would not, on its own, have resulted in a revolution in ocean mapping. Fortunately, as these new sonar technologies were developed, there were concomitant advances in precise navigation, high-quality motion sensors, accurate sound-speed profiles, advanced computing, and sophisticated visualization tools. It is only through the careful integration of these components that the thousands to millions of raw acoustic travel times collected by multibeam sonars can be converted into accurate high-resolution digital terrain models. The density of data acquired by multibeam sonar allows us to return to the central role that vision plays in exploration, as the high density of multibeam sonar data support the use of modern visualization techniques that allow the production of realistic looking sun-illuminated three-dimensional (3-D) images that allow scientists to recognize patterns, infer processes, and generate hypotheses in ways that were impossible with sparse datasets (Figure 5), including details of volcanic constructs, fault scarps, submarine landslides, channels, sediment waves, and flat-topped seamounts (guyots) that record past sea level exposure. Such features provide direct evidence of tectonic, volcanic, and sedimentary processes and inform models of crustal formation, slope stability, and sediment transport. Equally important, detailed bathymetry enables quantitative analyses of seafloor roughness and slope, parameters that strongly influence ocean circulation and mixing. Seamounts and rough terrain enhance turbulence and energy dissipation, affecting deep-water stratification and heat transport—key components of climate models.

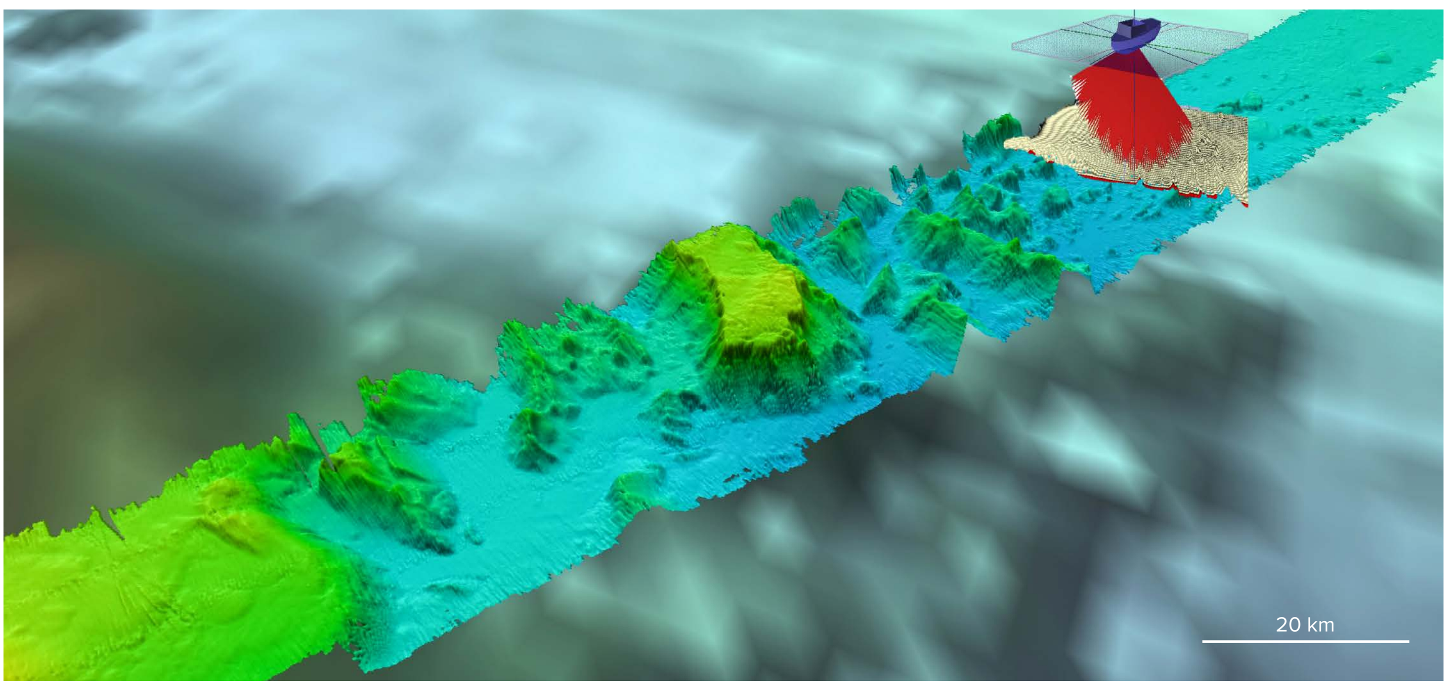

FIGURE 5. A single swath in 4,000 m of water north of Hawai'i shows the difference between the resolution of multibeam sonar data (detailed swath in bright colors) and single beam and satellite-altimetry-derived bathymetry (underlying image). The top right illustration on the sonar data shows the geometry of a multibeam sonar swath, where hundreds of individual high-resolution depths are measured simultaneously across a swath that typically measures five to seven times the water depth. *Source: Larry Mayer, top right image of ship and multibeam sonar from John Hughes Clarke, Center for Coastal and Ocean Mapping, University of New Hampshire*

BEYOND DEPTH: ACOUSTIC BACKSCATTER AND SEAFLOOR CHARACTERIZATION

Modern multibeam systems record not only depth but also the intensity of the returned acoustic signal, known as backscatter. Backscatter varies with the properties of the seafloor, most importantly its roughness and hardness. Thus, careful mapping of seafloor backscatter provides insights into the nature of the substrate. When combined with bathymetry, backscatter allows scientists to move from identifying *where* the seafloor is (from the bathymetry) to inferring *what* it is composed of. Applications include identification of seafloor type and items on the seafloor (e.g., wrecks [Box 1] and other infrastructure), benthic habitat mapping (Box 2), detection of anthropogenic disturbances such as dredge spoil disposal (Figure 6), and many more.

BOX 1. MAPPING AND MARITIME HERITAGE

As many as three million underwater wrecks are estimated to be preserving a remarkable record of the history of civilization (Croome, 1999). While some shallow-water marine cultural heritage sites are reachable by divers, the advent of new sonar and imaging technologies offers the possibility of discovering and exploring wrecks at all ocean depths. Recently, a powerful combination of sonar and uncrewed systems technologies was used to explore the historic wrecks of "Iron Bottom Sound," where five naval battles took place off Guadalcanal in the Solomon Islands over the course of several months in 1942. The Battle of Guadalcanal resulted in the tragic loss of more than 100 vessels, 1,200 aircraft, and over 20,000 Japanese, American, Australian, and New Zealand sailors. With many of the wrecks lying in water depths between 600 m and 1,000 m, the traditional search method for these wrecks would be a serial process in which a large crewed surface vessel maps the seafloor using multibeam or side-scan sonar, identifies potential targets, stops searching, and then launches a remotely operated vehicle to determine if the potential target is a wreck and if so, then conducts a detailed visual survey of the wreck. Instead, the Guadalcanal search took advantage of a small uncrewed surface vessel equipped with a multibeam sonar optimized for mapping in the water depths of Iron Bottom Sound and perfected a parallel process where the uncrewed surface vessel was operated from shore to continuously map and locate potential targets. As the uncrewed vessel identified targets (Figure B1-2), their locations were transmitted to a large vessel whose crew would drop a remotely operated vehicle (ROV) on the target in order to image the wreck in detail (Figure B1-2). In this way, many tens of targets could be identified independently of the expensive crewed surface vessel, and the crew aboard the surface vessel could quickly move the ROV from one target to the next, a tremendously more efficient mode of operation. With the addition of real-time high-resolution telemetry, naval historians around the world could participate in the exploration and—based on many surprising results—literally re-write history in real time.

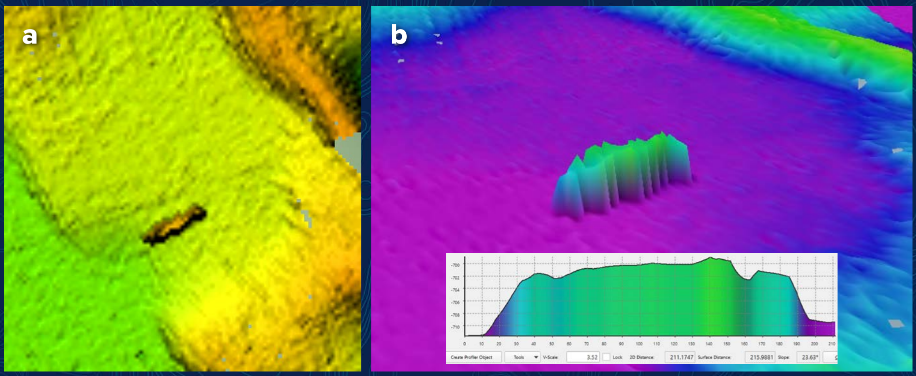

FIGURE B1-1. (a) His Majesty's Australian Ship (HMAS) *Canberra* is clearly seen lying at 700 m in this multibeam sonar bathymetric map derived from data collected by the uncrewed surface vessel DriX in Iron Bottom Sound, off Guadalcanal, Solomon Islands. (b) HMAS *Canberra* is further delineated in a three-dimensional view and profile derived from DriX multibeam sonar.

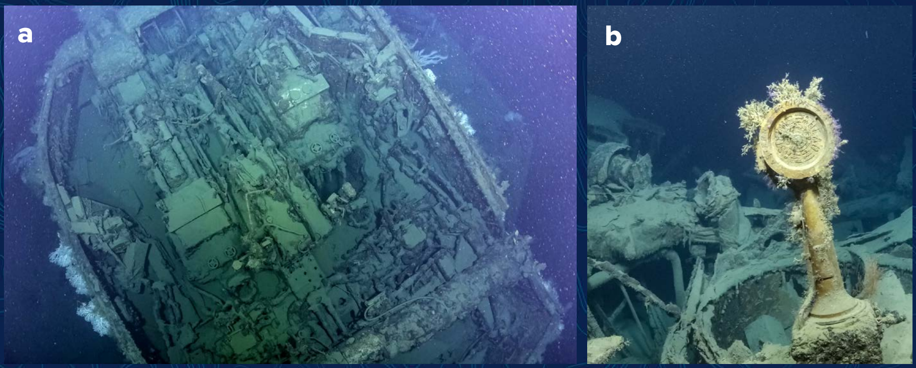

FIGURE B1-2. (a) A camera pass over HMAS *Canberra* by ROV *Hercules* provides further detail. (b) An image of the bridge telegraph on HMAS *Canberra* collected by *Hercules* shows the telegraph setting at full astern. Images like this help naval historians better understand the details of the Battle of Savo Island, the first major naval confrontation of the Guadalcanal campaign, on August 9, 1942. *Photos courtesy of Ocean Exploration Trust*

BOX 2. MAPPING FINDS THE LARGEST KNOWN DEEP-SEA COLD CORAL REEF PROVINCE

An increasingly important application of seafloor mapping is the identification of benthic habitats, in both shallow and deep waters. Historically, habitat has been defined by diver observations and cameras systems—both severely limited in their fields of view. Sonars, however, can cover much larger areas of the seafloor, and as sonar systems begin to achieve higher resolution along with the ability to extract information beyond just depth, acoustic mapping systems have become important contributors to benthic habitat studies. As part of NOAA Ocean Exploration's efforts to map and characterize the US exclusive economic zone, as well as to establish the limits of the US Extended Continental Shelf as defined by the UN Convention on the Law of the Sea, thousands of square kilometers of seafloor off the US East Coast were mapped with multibeam sonar. While the existence of some cold-water coral mounds in the region have been known since the early 1960s, the mapping, combined with new automated analytical techniques that can quantitatively identify the morphology of small features, identified 83,908 individual coral mounds over an area up to 500 km long and 110 km wide on Blake Plateau (Sowers et al., 2024; Figures B2-1 and B2-2). The analysis also documented the variations in the distribution of coral communities, including their density and height. This vast coral province is thought to be the largest deep-sea coral reef habitat discovered to date.

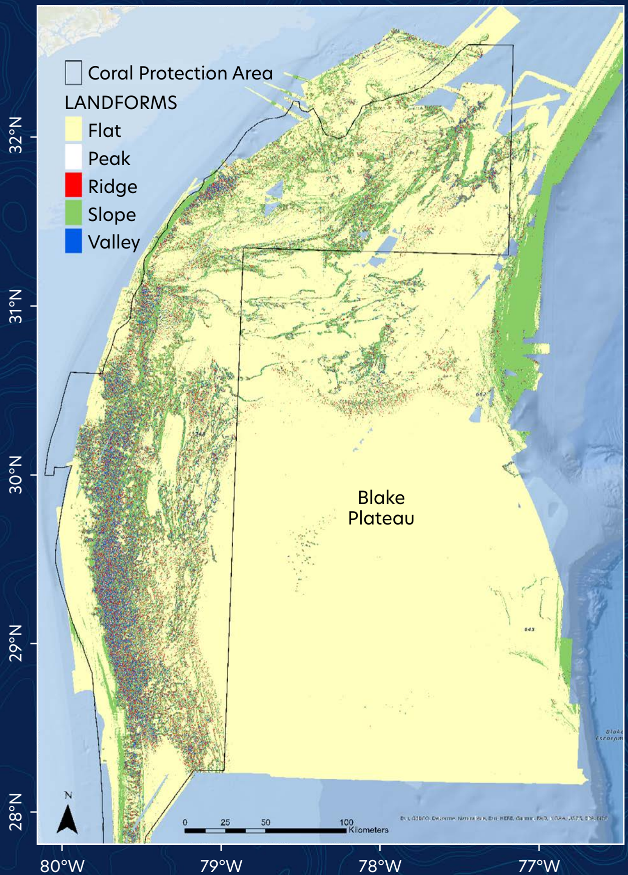

FIGURE B2-1. More than 80,000 of cold-water coral mounds were mapped on Blake Plateau. *Figure modified from Sowers et al. (2024)*

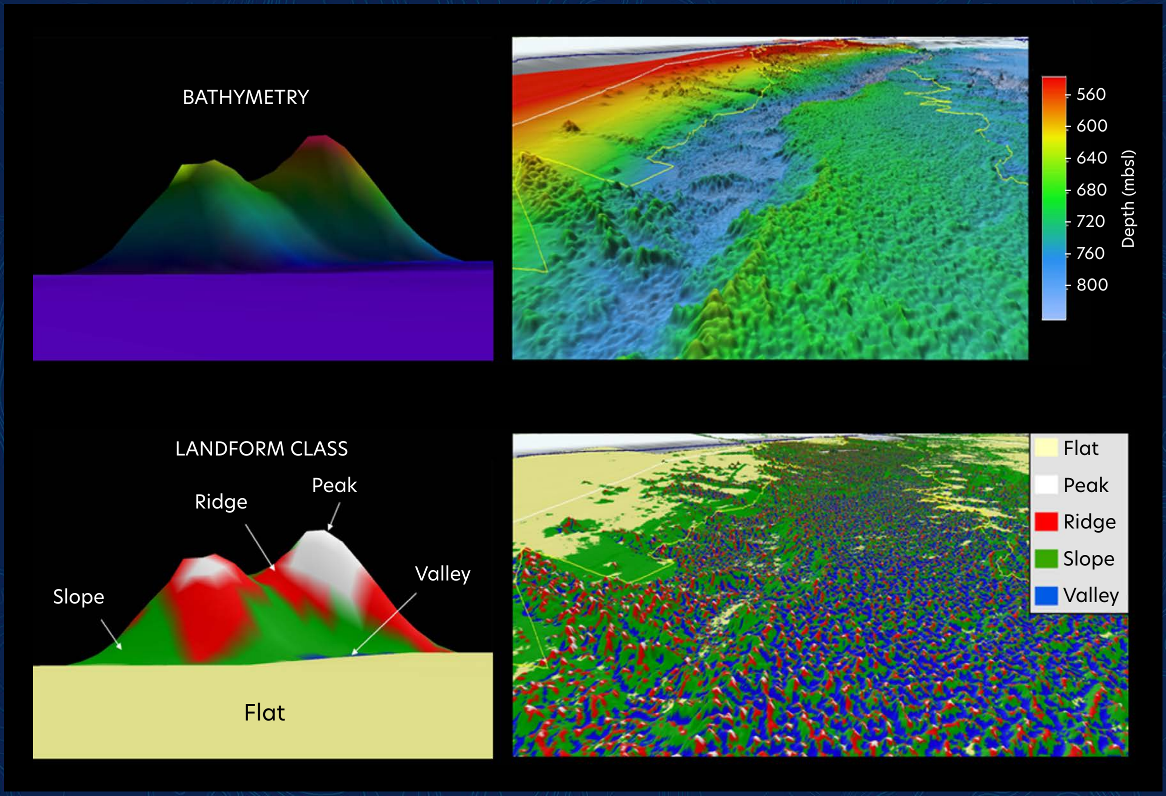

FIGURE B2-2. "Geomorphons" (descriptions of morphological elements) automatically extracted from multibeam sonar data allowed quantification of cold-water coral reefs on Blake Plateau. *Figure modified from Sowers et al. (2024)*

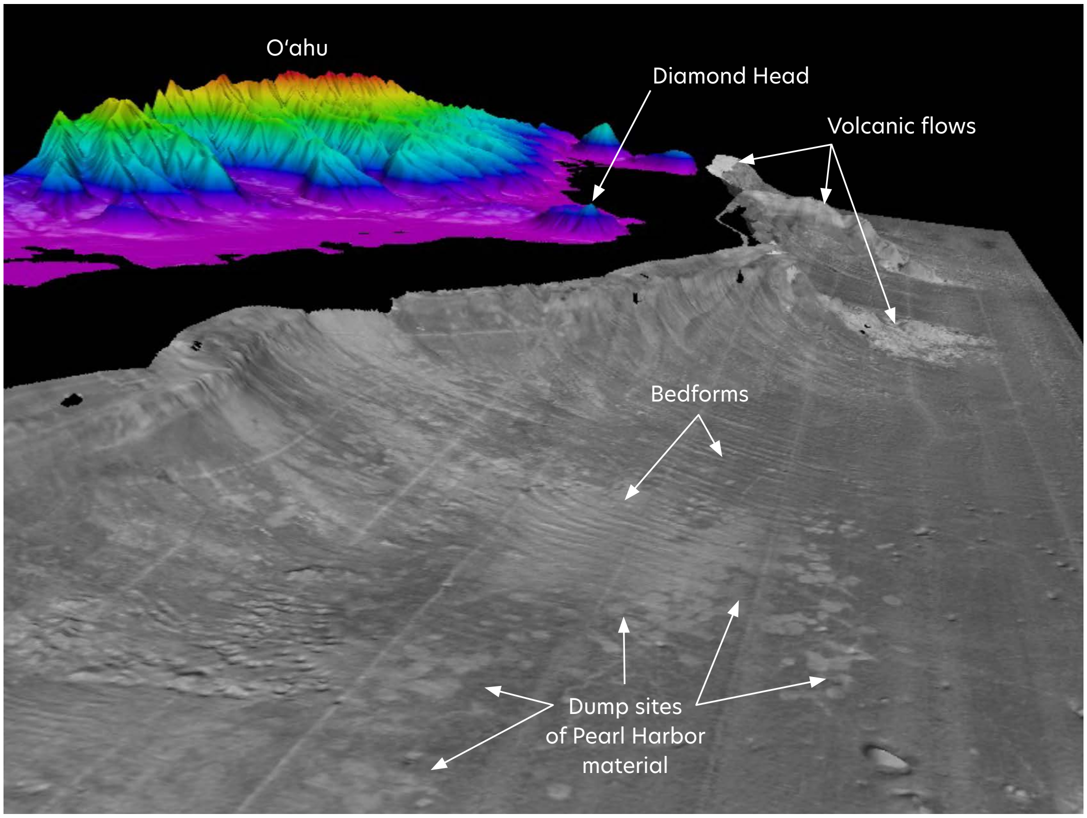

FIGURE 6. Multibeam sonar backscatter data draped on top of bathymetry data off the island of O'ahu, Hawai'i. Bright white (high-backscatter) regions off Diamond Head (top right of figure) indicate volcanic flows, while more subtle, rounded, lighter areas near the bottom of the image indicate dredge material that was removed from Pearl Harbor and dumped in 400–600 m of water offshore. Bedforms running through them indicate some dispersal of material. *Source: James Gardner, Center for Coastal and Ocean Mapping, University of New Hampshire*

IMAGING THE WATER COLUMN: A SECOND ACOUSTIC REVOLUTION

From their inception, multibeam sonars were focused on the return from the seafloor, originally only collecting depth data and then, as the systems became more sophisticated, adding seafloor backscatter measurements. To collect seafloor data, the acoustic wave had to travel through the water column, and, as computational and data storage capabilities improved, multibeam sonars began to offer the option of acquiring data in the water column. While immensely increasing data volumes, water column data also offered tremendous new insights into processes both at and near the seafloor and in the ocean's volume. Fish schools, zooplankton layers, and other biological aggregations produce strong acoustic scattering signals in the water column. Fishery sonars had been imaging the water column for years; however, these were single beam sonars insonifying only a narrow sector of the water column. In contrast, water column data from multibeam sonars offered the opportunity to see the distribution and behavior of fish schools and other targets simultaneously over a wide area, addressing the important question of whether fish were avoiding the sonar vessel and thus biasing biomass estimates (Soria et al., 1996; Mayer et al., 2002). Similarly, gas seeps produce strong acoustic targets; the ability for multibeam sonars to visualize gas seeps was clearly demonstrated during the test of a newly installed water column-capable multibeam sonar on NOAA Ship *Okeanos Explorer* off the coast of northern California where natural methane gas seeps were clearly seen rising more than 1,400 m from the seafloor (Gardner et al., 2009; Figure 7).

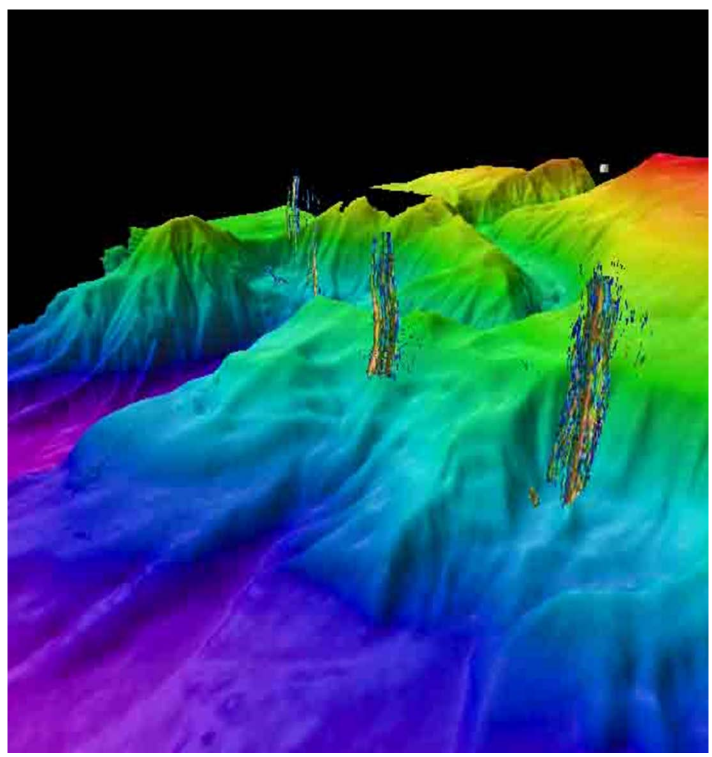

FIGURE 7. Natural gas seeps, each about 1,400 m high, off Mendocino, California, were detected during early testing of multibeam sonar water column data collection on NOAA Ship *Okeanos Explorer*. *Source: James Gardner, Center for Coastal and Ocean Mapping, University of New Hampshire*

Water column mapping proved invaluable in 2010 during the Deepwater Horizon incident, where acoustic monitoring was used following explosion of the drill rig to assess wellhead integrity after capping (Hickman et al., 2013; Box 3). These observations demonstrated the ability of multibeam systems to detect even small leaks and distinguish them from background noise, and they have led to the use of multibeam sonars to broadly map and estimate the distribution of both natural and human-made gas seeps in the ocean—underestimated contributors to ocean acidification and in some cases atmospheric CO_2 (Weber et al., 2012; Ruppel et al., 2024).

Perhaps one of the most exciting applications of midwater mapping is the ability of our sonar systems to reveal physical oceanographic changes in the water column. Internal waves, pycnoclines, turbulence, thermohaline staircases, mixed-layer depth, and anoxic layers have all been imaged acoustically (some with

BOX 3. WATER-COLUMN MAPPING AND DEEPWATER HORIZON

After many attempts, including a containment dome, "top kill" and "junk shot" procedures, and a cap for funneling oil and gas to a surface ship, all failed to stop the leaking Macondo wellhead during the aftermath of the Deepwater Horizon explosion, a three-ram capping stack was installed in July 2010, nearly three months after the spill began, with the hope of finally stopping the leak. As plans for this installation were being made, concern grew that if there were issues with the subsurface drilling infrastructure, the cap could lead to a sidewall blowout and an oil spill that would be unstoppable. Engineers predicted that such a blowout would be preceded by significant gas expulsion and if this could be seen as soon as it happened, the cap could be removed before a sidewall blowout occurred. The question was posed to the acoustic mapping team as to whether they could "guarantee" that they would see gas leaking from the wellhead. "Guarantee" is a scary word for scientists, but our understanding of the very large acoustic response of gas bubbles led us to say we could. The cap was installed, and an acoustic mapping vessel was positioned directly over the wellhead. The sonar imagery quickly revealed a gas plume rising from the wellhead (Figure B3-1), and BP immediately sent remotely operated vehicles (ROVs) down to the wellhead to see what was happening. The ROVs revealed that the large acoustic plume seen on the sonar imagery was the result of just a few bubbles per second coming from a scratch on a cap stack flange (Figure B3-2). Thus, there was no danger of a blowout, and the capping process leading to the eventual kill of the well proceeded successfully. The process revealed, however, just how sensitive acoustic mapping can be in defining both natural gas seeps and leaking infrastructure. Since then, the water column mapping techniques developed during Deepwater Horizon have been used to map natural gas seeps in many areas of the world and have added significantly to our understanding of the widespread nature of gas seeps and their impact on the global methane budget.

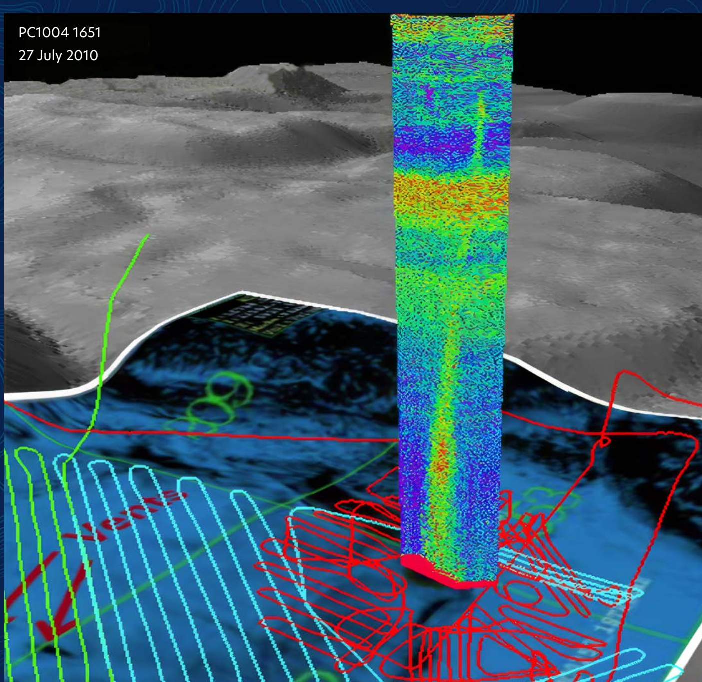

FIGURE B3-1. A sonar water column image captured over the Macondo wellhead after installation of the cap stack shows a gas plume rising from the wellhead. *Image credit: Tom Weber*

FIGURE B3-2. ROV image of gas bubbles coming from the Macondo wellhead cap stack. The large acoustic target seen in Figure B3-1 was the result of only a few bubbles a second leaking from a scratch on a flange in the cap.

multibeam sonar and some with single beam fisheries sonars), in each case revealing fine-scale structure previously accessible only through direct point measurements with conductivity, temperature, depth sensors (CTDs) or microturbulence sensors (Colbo et al., 2014; Stranne et al., 2017, 2018; Weidner et al., 2020; Figure 8). These observations are opening new horizons for the understanding of mixing processes and stratification in both polar and temperate oceans.

HOW MUCH IS MAPPED?

We have come a long way, from 4,000 years of measuring depth with lead lines to modern multibeam sonars capable of covering wide swaths of the seafloor with high resolution. Most modern research vessels and many commercial and military vessels carry multibeam sonars, and these vessels have been collecting mapping data for the past 40 years. Despite these efforts, by 2017, only approximately 6% of the global seafloor had been mapped using modern techniques (i.e., single beam or multibeam sonars). Recognizing the critically important roles that mapping plays in understanding our ocean, the Nippon Foundation established an ambitious and aspirational international mission to inspire ocean mapping and deliver a complete seabed map for the benefit of people and the planet. This effort, the Nippon Foundation/GEBCO Seabed 2030 program, comprises a series of regional centers that have discovered unpublished data and facilitated collection of new data, all of which are added to the publicly available GEBCO global bathymetric grid. Since its inception in 2017, global coverage of modern bathymetric data has increased from 6% to 28.7% in 2026 (Seabed 2030, 2026).

The United States also recognized the critical importance of mapping data for managing and protecting its offshore resources by establishing the National Ocean Mapping, Exploration, and Characterization (NOMEC) Council under a 2019 Presidential Memorandum. NOMEC contributes to the global Seabed 2030 initiative and calls for the complete mapping of the deeper waters of the US exclusive economic zone by 2030 and the shallow waters by 2040.

While these efforts have greatly accelerated the rate of seafloor mapping, almost 75% of the global seafloor remains unmapped. How long would it take to map the remaining 75%? Using our best estimate of the distribution of depths (the mapping effort changes radically with water depth as the swath width changes) and assuming the use of current technology (large research vessels with deep-water multibeam systems), it has been estimated that it would take between 200 and 350 ship-years to map the ocean deeper than 200 m at the resolutions specified by Seabed 2030

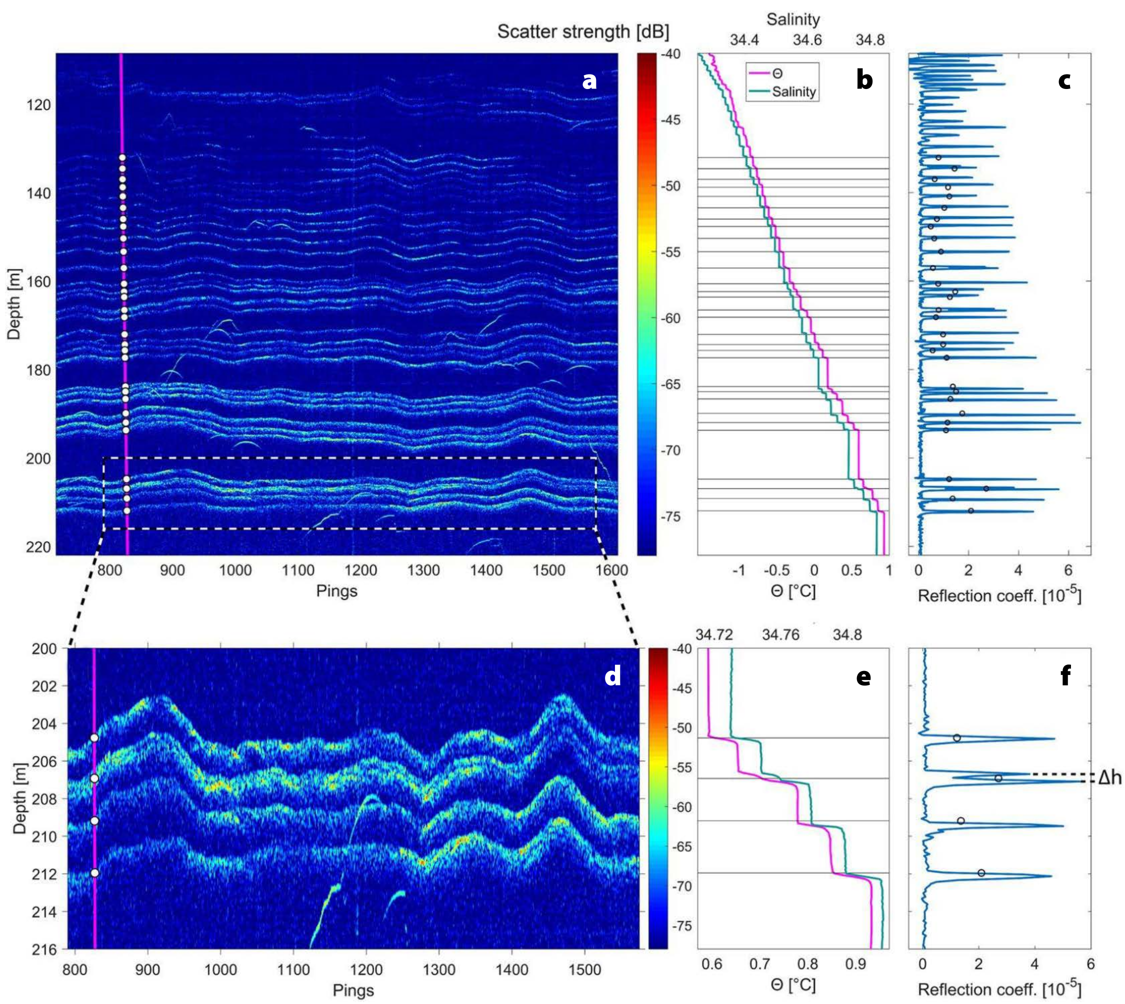

FIGURE 8. Fine-scale thermohaline structure (thermohaline staircases) revealed by broad-band single beam sonar in the high Arctic (a and d). Temperature and salinity profiles were collected at the location of the purple line in a and d (plotted in b and e). Reflection coefficients (changes in acoustic response) were calculated from the temperature and salinity profile (blue line) and calculated from the acoustic response (black circles) as shown in c and f. *Source: Stranne et al. (2017), by* CC BY 4.0

(Mayer et al., 2018). Assuming an average day rate of $50,000 for a large research vessel, the estimated cost would be between three and five billion dollars.

While it might seem unrealistic to spend several billion dollars to completely map the ocean, the reality is that we have spent much more than that to map other planets. To date, the global community has launched 18 orbiters to Mars, resulting in the near complete mapping of that planet at a resolution of 6 m or better (Zurek et al., 2024). Each mission costs somewhere between $300M and $1B, and thus more than approximately $11B has already been spent to map Mars. This is not to demean the tremendous technological achievement of mapping Mars nor the importance of these maps in understanding planetary origins and planning future missions; however, one cannot help but ask why we are not willing to put a similar level of investment into mapping our own planet. The typical response is that it is actually harder to map the deep ocean than it is to remotely map Mars from an orbiter (which is true), but as has been demonstrated above, even with current technology, we have the ability to map the entire ocean, and, for the same (or less of an) investment than we have put into mapping Mars, it can be done.

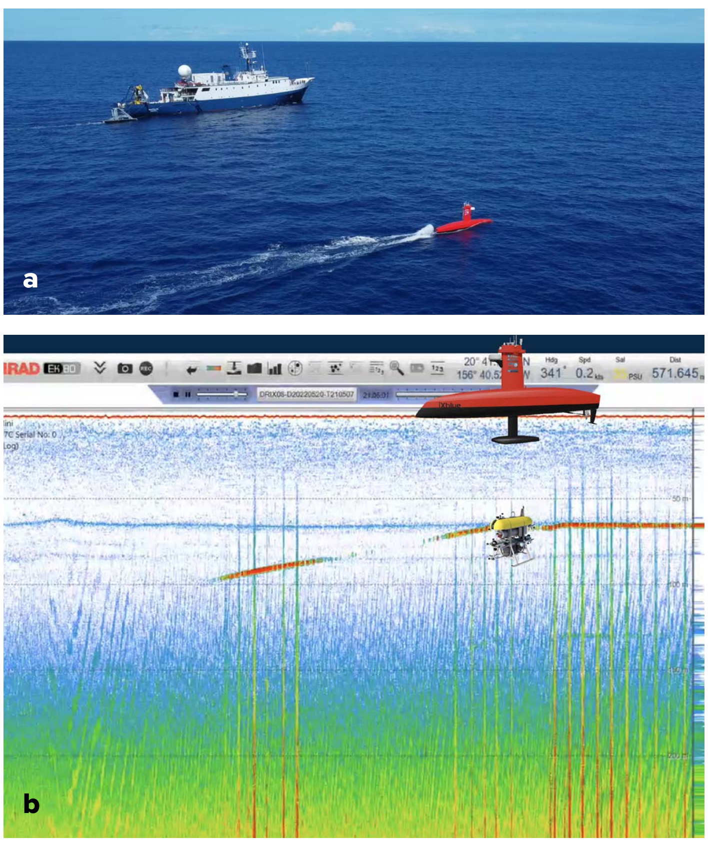

FIGURE 9. (a) DriX, a bright red 7.7 m long uncrewed vessel capable of mapping to 3,000 m is shown acting as a force multiplier while operating in parallel with E/V *Nautilus*. *Photo courtesy of Ocean Exploration Trust* (b) DriX is used to direct the Woods Hole Oceanographic Institution autonomous underwater vehicle (AUV) *Mesobot* to a mid-water acoustic target layer and to turn on its video and environmental DNA samplers when the AUV's arrival at the at the target layer is verified.

CAN TECHNOLOGICAL INNOVATION REDUCE THE COST AND EFFORT?

The cost and time estimates discussed above assume the use of current technologies for ocean mapping—that is, the use of large multibeam-sonar-equipped research vessels. Can technical innovations reduce these costs and make the goal of complete mapping of the ocean more obtainable? There are a limited number of large research vessels with many demands on their time beyond mapping. If we are to achieve comprehensive coverage, we must find means to scale ocean mapping beyond the use of traditional research vessels.

UNCREWED OR MINIMALLY CREWED SURFACE VESSELS

One of the largest expenses associated with traditional research vessels is the cost of the crew. If we can eliminate or minimize crew costs, significant savings can be had. AUVs have matured greatly over the past 60 years and are now available in a range of sizes serving many applications (Wynn et al., 2014; Ma et al., 2025). These vehicles typically operate near the bottom (and thus cannot use GPS for navigation), have limited endurance, and move rather slowly (in efforts to extend endurance). They present the only means to collect extremely high-resolution mapping data in very deep waters, as their sonars are near the bottom; however, their slow speed, limited endurance, small area of coverage (because they are near the bottom), and navigational challenges make them less than ideal for comprehensive mapping of the global ocean at this time.

In contrast to fully crewed research vessels, uncrewed or minimally crewed surface vessels (USVs or MCSVs) offer the possibility to field platforms of sufficient size to carry the large sonars needed to map in deep water and potentially to provide the speed and endurance that will allow efficient scaling of the ocean mapping problem. Small uncrewed vessels have proven effective force-multipliers for shallow water mapping (e.g., *Journal of Petroleum Geology*, 2023), and medium-to-small USVs have proven remarkably valuable for expanding the footprint of ocean exploration by monitoring the activities of AUVs and, in real time, directing these vehicles to specific targets in the water column. For example, recently in the mid-Pacific, a 7.7 m USV deployed from a mother ship was used to map mid-water acoustic targets (scattering layers) and was able to track and direct a small AUV (*Mesobot*) directly into the scattering layer before turning on environmental DNA samplers and high-resolution video, all while the mother ship was free to carry on other activities. This new approach to "Verified Directed Sampling" promises capability for estimating biodiversity in the mesosphere and improving our understanding of the nature of mid-water scattering layers (Mayer, 2023; Govindarajan, 2025; Figure 9). We are, however, still in the early days of development of USVs that are large enough and have the endurance to carry out long-range deep-ocean mapping missions. Challenges include operations in extreme environments, long-term reliability, and truly autonomous behaviors that include obstacle avoidance and dynamic decision-making (Norazaruddin et al., 2024).

Several vendors are bringing to market large uncrewed vessels designed to carry deep-water sonars that may have the speed, range, and endurance to potentially provide a scalable and cost-effective alternative to traditional research vessels (e.g., Exail, Ocean Infinity). Addressing the other major costs associated with traditional research vessels, large sail-powered uncrewed vessels have been developed and are currently collecting mapping data while exploring the trade-offs between slower rates of coverage and potentially extended endurance (Figure 10). Because there is still much to be learned about the best operational modes for these vessels and their shore-based crewing requirements, questions remain about the overall cost-effectiveness of their operation. As experience is gained and lessons are learned from operating these systems, their viability and the role they can play in the complete mapping of the global ocean will be better understood (Mayer, 2023).

Mindful of the tremendous technological and safety concerns of operating USVs on the open seas, ocean, land, and ice explorer and venture capitalist Victor Vescovo is constructing a small (24 m), minimally (one- or two-person) crewed vessel whose only purpose would be to map. This "Ocean Mapper" is estimated to be an order of magnitude cheaper to operate than a traditional ocean-going research vessel, and serves as a challenge to others to build similar vessels so that a fleet of these relatively inexpensive to operate vehicles can address the goal of completely mapping the oceans (Dunn, 2025; Figure 10).

OTHER INNOVATIONS

While the efforts described above have focused on decreasing the cost of collecting multibeam sonar data, deep-water multibeam sonars are inherently large and expensive. To supplement multibeam sonar data, others are looking at ways to increase the use of simpler and cheaper single beam sonars and to find ways to deploy them in remote areas of the ocean.

One approach to this is to engage the "crowd," the millions of recreational and commercial vessels that carry echosounders but do not commonly record the depth information. To address this, efforts are now underway to create very inexpensive devices that are easily attached to most any vessel's echosounder, perform internal calibrations, and even transmit those data to the national data archive (Calder et al., 2020). This approach has proven successful when applied to the commercial fishing sector (Novaczek et al., 2019), and its expansion to the broader community can add important new data to the global database.

Crowd-sourced bathymetry tends to focus on shallow water areas and regions that are well traveled by commercial vessels. To address the issue of collecting data in the most remote regions, specialized profiling floats have been designed that use the thermal difference in the upper part of the water column to supply power to drive a buoyancy engine and a narrow beam echosounder. These floats can be deployed in the most remote regions of the ocean to drift for many years while moving up and down in the water column to harvest power as they collect several soundings a day, each time surfacing and sending data back to shore-based repositories via satellite (Mayer, 2023; Figure 11).

Recently, researchers at MIT/Lincoln Labs have proposed a truly innovative way to address seafloor mapping. Their approach uses the concept of a sparse array where many small autonomous vessels move together to create a very large (e.g., 40 km × 40 km) array, with some of the vessels sending out sonar pings that are

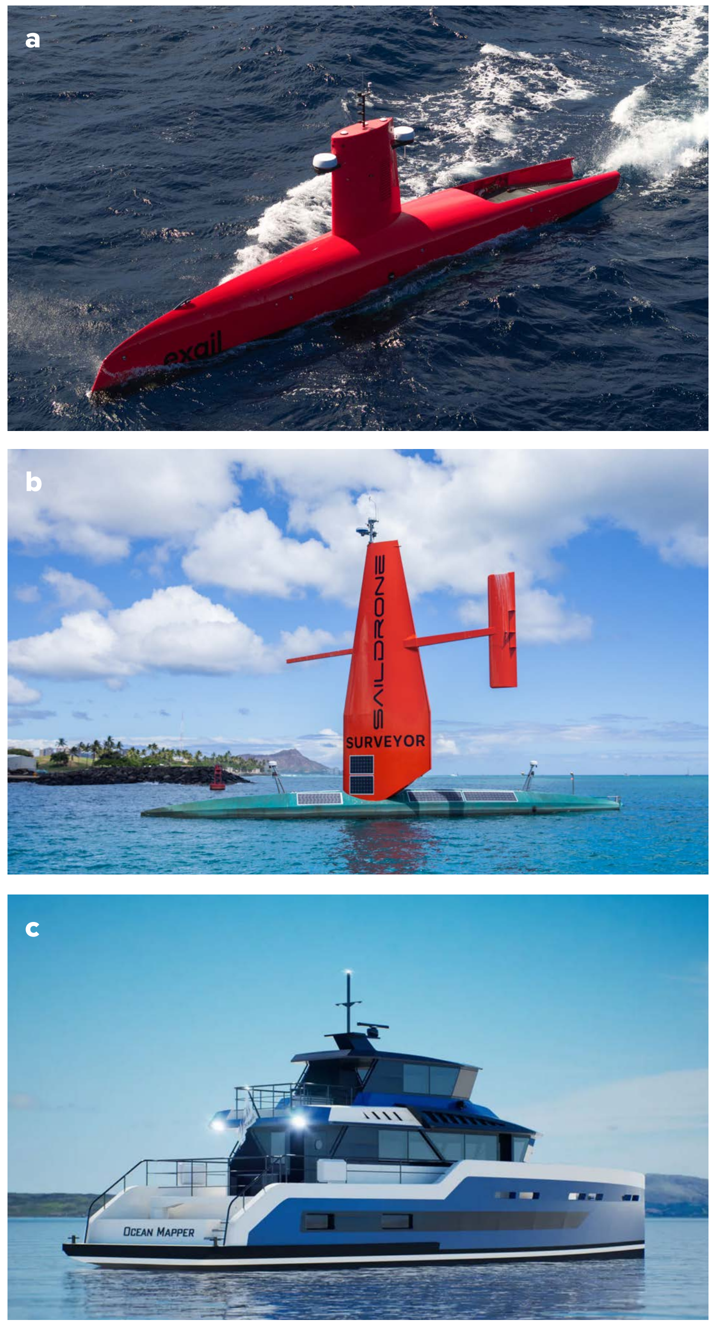

FIGURE 10. (a) The photo shows a 16 m long DriX O-16 long-endurance, deep-mapping uncrewed surface vehicle (USV). *Source: Exail* (b) The photo captures a 21 m long Saildrone Surveyor, a sail-powered, deep-water mapping USV. *Source: Saildrone* (c) Artist's depiction of Victor Vescovo's "Ocean Mapper"—a 24 m minimally crewed vessel. *Credit: Espen Øino International*

FIGURE 11. This concept graphic shows a specialized profiling float that employs the thermal difference in the upper part of the water column to supply power for a buoyancy engine and a narrow beam deep-water echosounder. *Image courtesy of Yi Chao, SeaTrec Inc.*

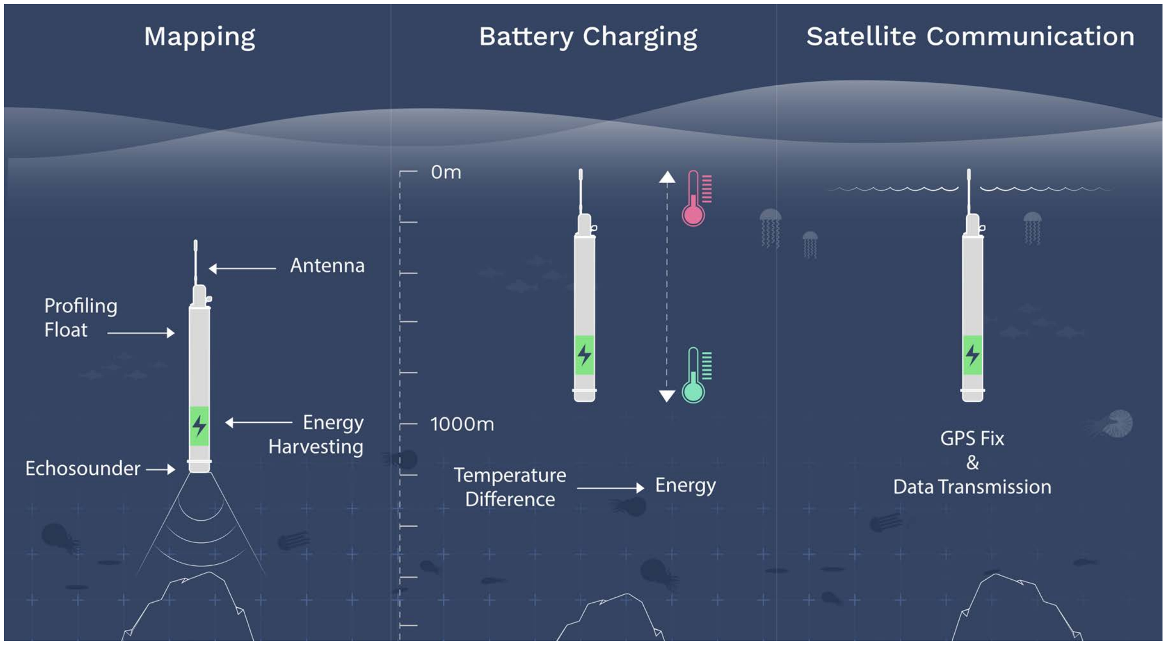

then received by the rest of the vessels. Smaller prototypes have been built and tested, but, working at full scale, the approach has the potential to achieve both much better resolution and greater coverage than a conventional multibeam sonar (Ryu et al., 2023). Together, these approaches suggest that complete mapping of the global ocean may be technically achievable within decades.

FROM QUEST TO PLANETARY RESPONSIBILITY

For me, the pursuit of ocean mapping began as an adventure, driven by curiosity and the desire to explore. As the field has progressed to the point where we can, at relatively high-resolution, visualize the fine-scale features of the deep-sea floor, I have learned that the information provided by detailed ocean mapping represents a foundational requirement for managing the Earth system, and my adventure-driven quest has evolved into a quest to achieve something important. The remaining unmapped ~75% of the seafloor represents not merely unexplored territory but unresolved risks to navigation, climate prediction, hazard mitigation, resource exploration, environmental stewardship, and the potential for yet-unknown discoveries. The tools to complete a map of the global ocean now exist or are rapidly emerging. What remains is the need for a collective decision (and the fiscal will) to recognize that the complete mapping of the ocean is essential to understanding—and responsibly managing—our planet. The quest continues.

REFERENCES

Bell, K.L.C., K.N. Johannes, B.R.C. Kennedy, and S.E. Poulton. 2025. How little we've seen: A visual coverage estimate of the deep seafloor. *Science Advances* 11(19), https://doi.org/10.1126/sciadv.adp8602.

Billinghurst, M., and B. Thomas. 2016. *Lecture 3: Human perception (COMP4010—Virtual Reality)* [Lecture slides]. University of South Australia, https://www.slideshare.net/slideshow/comp-4010-lecture3-human-perception/64827753.

Calder, B.R., S.J. Dijkstra, S.K. Hoy, K. Himschoot, and A.P. Schofield. 2020. A design for a trusted community bathymetry system. *Marine Geodesy* 43:327–358, https://doi.org/10.1080/01490419.2020.1718255.

Colbo, K., T. Ross, C. Brown, and T. Weber. 2014. A review of oceanographic applications of water column data from multibeam echosounders. *Estuarine, Coastal and Shelf Science* 145:41–56, https://doi.org/10.1016/j.ecss.2014.04.002.

Croome, A. 1999. Sinking fast. *New Scientist* 161(2169):49, https://www.newscientist.com/article/mg16121696-000-sinking-fast/.

Dunn, L. 2025. Victor Vescovo on enlisting Espen Øino to design a new $6M ocean-mapping vessel. *Boat International*, August 19, 2025, https://www.boatinternational.com/luxury-yacht-life/owners-experiences/victor-vescovo-mapping-ocean-floor-espen-oino.

Gardner, J.V., M. Malik, and S. Walker. 2009. Plume 1400 meters high discovered at the seafloor off the northern California margin. *Eos, Transactions American Geophysical Union* 90(2):275, https://doi.org/10.1029/2009EO320003.

Govindarajan, A., J. Fahy, E. Hayden, L. Mayer, C. Roman, V. Schmidt, N. Yang, and D. Yoerger. 2025. Combining multi-vehicle operations, autonomous sampling, and environmental 'omics for surface to seafloor biodiversity assessments of the Geologists Seamounts. OS-51A-05, AGU Fall Annual Meeting, New Orleans, LA, December 15–19, 2025.

Hickman, S.H., P.A. Hsieh, W.D. Mooney, C.B. Enomoto, P.H. Nelson, L.A. Mayer, T.C. Weber, K. Moran, P.B. Flemings, and M.K. McNutt. 2013. Scientific basis for safely shutting in the Macondo well after the April 20, 2010 *Deepwater Horizon* blowout. *Proceedings of the National Academy of Sciences of the United States of America* 109(50):20,268–20,273, https://doi.org/10.1073/pnas.1115847109.

Journal of Petroleum Technology. 2023. "Uncrewed Vessels Survey the Seafloor." *Journal of Petroleum Technology (Robotics/Unmanned Systems)*, January 11, 2023, https://jpt.spe.org/uncrewed-vessels-survey-the-seafloor.

Ma, D., Y. Li, T. Ma, and A.M. Pascoal. 2025. The state of the art in key technologies for autonomous underwater vehicles: A review. *Engineering*, https://doi.org/10.1016/j.eng.2025.08.002.

Mayer, L.A., M. Jakobsson, G. Allen, B. Dorschel, R. Falconer, V. Ferrini, G. Lamarche, H. Snaith, and P. Weatherall. 2018. The Nippon Foundation—GEBCO Seabed 2030 Project: The quest to see the world's oceans completely mapped by 2030. *Geosciences* 8(2):63, https://doi.org/10.3390/geosciences8020063.

Mayer, L.A., Y. Li, and G. Melvin. 2002. 3-D visualization for pelagic fisheries assessment and research. *ICES Journal of Marine Science* 59:216–225, https://doi.org/10.1006/jmsc.2001.1125.

Mayer, L. 2023. Uncrewed surface systems facilitating a new era of global ocean exploration. *International Hydrographic Review* 29(1), https://doi.org/10.58440/ihr-29-a05.

NOAA. n.d. "History: Timeline: NOAA Office of Ocean Exploration and Research." NOAA Ocean Exploration, https://oceanexplorer.noaa.gov/history/timeline-the-breakthrough-years-1866-1922/.

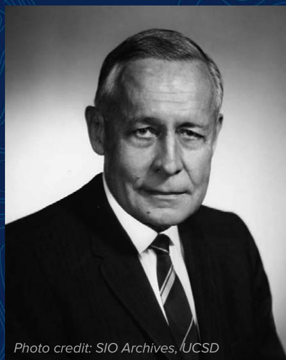

Photo credit: SIO Archives, UCSD

Roger Revelle

Revelle was a pioneer in oceanography who over his 50-year career pursued innovative research and created a vision that still influences the field of oceanography to this day. A strong proponent of science communication and public policy, Revelle was a leader in encouraging the scientific community to devote time to address the "long-range problems of society" (Day, 2000, quoting Revelle, 1957). For his contributions to geophysics, Revelle was elected to membership in the National Academy of Sciences (NAS). Revelle's commitment to science policy is evident in his extensive contributions to the work of the NAS. Revelle served as a member of the Ocean Studies Board and its predecessor (Ocean Sciences Board) from 1983 to 1987. He also served on the Board on Atmospheric Sciences and Climate (1982–1986) and as a committee member for several influential National Academies' studies.

Norazaruddin, M.A., Z.Z. Abidin, and M.I. Hamza. 2024. Unmanned surface vessels in hydrographic surveying: Exploring technological progressions and development challenges. *Indian Journal of Geo-Marine Sciences* 53(7), https://doi.org/10.56042/ijms.v53i07.10419.

Novaczek, E., R. Devillers, and E. Edinger. 2019. Generating higher resolution regional seafloor maps from crowd-sourced bathymetry. *PLOS ONE* 14(6):e0216792, https://doi.org/10.1371/journal.pone.0216792.

Ruppel, C.D., A.D. Skarke, N.C. Miller, M.W. Kidiwela, J. Kluesner, and W. Baldwin. 2024. Methane seeps on the U.S. Atlantic margin: An updated inventory and interpretative framework. *Marine Geology* 471:107287, https://doi.org/10.1016/j.margeo.2024.107287.

Ryu, P., D. Brown, K. Arsenault, B. Cho, A. March, W.H. Ali, A. Charous, and P.F.J. Lermusiaux. 2023. A wide-area deep ocean floor mapping system: Design and sea tests. *Geomatics* 3(1):290–311, https://doi.org/10.3390/geomatics3010016.

Sandwell, D.T., B.J. Phrampus, F. Salajegheh, B. Nilsson, B. Lu, Y. Yu, H. Harper, O.B. Andersen, W.H.F. Smith, P.A. Elmore, and others. 2025. Bathymetry prediction with SWOT gravity anomaly using machine learning methods: Paper 1—Model development. *ESS Open Archive*, preprint, https://doi.org/10.22541/essoar.176339961.11752151/v1.

Scholin, C. 2025. Oceanography in the age of intelligent robots and a changing climate. *Oceanography* 38(3):60–74, https://doi.org/10.5670/oceanog.2025.e310.

Seabed 2030. 2026. Global seabed mapping reaches new mileston as five million square kilometers added in a year. Media release, April 20, 2026, https://seabed2030.org/2026/04/20/global-seabed-mapping-reaches-new-milestone-as-five-million-square-kilometres-added-in-a-year/.

Smith, W.H.F., and D.T. Sandwell. 1997. Global sea floor topography from satellite altimetry and ship depth soundings. *Science* 277(5334):1,956–1,962, https://doi.org/10.1126/science.277.5334.1956.

Soria, M., P. Fréon, and F. Gerlotto. 1996. Analysis of vessel influence on spatial behaviour of fish schools using a multi-beam sonar and consequences for biomass estimates by echo-sounder. *ICES Journal of Marine Science* 53(2):453–458, https://doi.org/10.1006/jmsc.1996.0064.

Sowers, D.C., L.A. Mayer, G. Masetti, E. Cordes, R. Gasbarro, E. Lobecker, K. Cantwell, S. Candio, S. Hoy, M. Malik, and others. 2024. Mapping and geomorphic characterization of the vast cold-water coral mounds of the Blake Plateau. *Geomatics* 4(1):17–47, https://doi.org/10.3390/geomatics4010002.

Stranne, C., L.A. Mayer, T.C. Weber, B.R. Ruddick, M.J. Jakobsson, K. Jerram, E. Weidner, J. Nilsson, and K. Gårdfeldt, 2017. Acoustic mapping of thermohaline staircases in the Arctic Ocean. *Scientific Reports* 7:15192, https://doi.org/10.5194/os-14-503-2018.

Stranne, C., L. Mayer, M. Jakobsson, E. Weidner, K. Jerram, T.C. Weber, L.G. Anderson, J. Nilsson, G. Björk, and K. Gårdfeldt. 2018. Acoustic mapping of mixed layer depth. *Ocean Science* 14:503–514, https://doi.org/10.5194/os-14-503-2018.

Weber, T.C., L.A. Mayer, J. Beaudoin, K. Jerram, W. Shedd, and G. Rice. 2012. Mapping gas seeps with the deepwater multibeam echosounder on *Okeanos Explorer*. Pp. 54–55 in *New Frontiers in Ocean Exploration: The E/V* Nautilus *and NOAA Ship* Okeanos Explorer *2011 Field Season*. K.L.C Bell, K. Elliott, C. Martinez, and S.A. Fuller, eds., *Oceanography* 25(1), supplement, https://doi.org/10.5670/oceanog.2011.supplement.01.

Weidner, E., C. Stranne, J. Sundberg, T. Weber, L. Mayer, and M. Jakobsson. 2020. Tracking the spatiotemporal variability of the oxic–anoxic interface in the Baltic Sea with broadband acoustics. *ICES Journal of Marine Science* 77(7–8):2,814–2,824, https://doi.org/10.1093/icesjms/fsaa153.

Wynn, R.B., V.A.I. Huvenne, T.P. Le Bas, B.J. Murton, D.P. Connelly, B.J. Bett, H.A. Ruhl, K.J. Morris, J. Peakall, D.R. Parsons, and others. 2014. Autonomous underwater vehicles (AUVs): Their past, present and future contributions to the advancement of marine geoscience. *Marine Geology* 352:451–468, https://doi.org/10.1016/j.margeo.2014.03.012.

Zurek, R., L. Tamppari, M.D. Johnston, S. Murchie, A. McEwen, S. Byrne, R. Seu, N. Putzig, D. Kass, M. Malin, and B. Cantor. 2024. MRO overview: Sixteen years in Mars orbit. *Icarus* 419:116102. https://doi.org/10.1016/j.icarus.2024.116102.

AUTHOR

Larry Mayer (larry.mayer@unh.edu), Center for Coastal and Ocean Mapping, University of New Hampshire, Durham, NH, USA.

ARTICLE CITATION

Mayer, L. 2026. The quest to map the global ocean. *Oceanography* 39(2):48–61, https://doi.org/10.5670/oceanog.2026.e205.

THE PACE DATA HACKWEEK LAUNCHES A NEW WAVE OF OPEN SCIENCE

HOW WE DID IT (TWICE), AND WHY

By Anna E. Windle, Ian Carroll, Carina Poulin, Skye Caplan, and P. Jeremy Werdell

ABSTRACT. PACE Data Hackweeks bring together student, early-career, and senior scientists to work hands-on with data from NASA's Plankton, Aerosol, Cloud, ocean Ecosystem (PACE) mission. During two past events, participants collaborated in small teams to explore scientific questions, develop reproducible workflows, and gain experience working with large, cloud-hosted datasets. Leveraging community-supported cloud infrastructure, the hackweeks lowered technical barriers and emphasized modern tools, open-source practices, and FAIR data principles. The events fostered interdisciplinary collaboration and led to tangible outcomes, including new analyses, shared code, and ongoing collaborations. Overall, the PACE Data Hackweeks demonstrate that mission-focused hackweeks are an effective way to build community capacity and support adaptation to evolving data and computing environments.

NASA DOES HACKWEEKS

The NASA Plankton, Aerosol, Cloud, ocean Ecosystem (PACE) Data Hackweek builds on a growing ecosystem of geoscience hackweeks that leverage NASA Earth Observing System datasets, including Geohackweek, OceanHackWeek, and mission-specific events like ICESat-2 and SnowEx hackweeks (Huppenkothen et al., 2018; Mitchell et al., 2026). Unlike traditional workshops or competitive hackathons, hackweeks emphasize participant-driven learning through a mix of coding tutorials and group projects in a collaborative setting. Demand for these events has grown alongside major shifts in Earth science data access, including the migration of petabyte-scale data to NASA's Earthdata Cloud, hosted on Amazon Web Services (AWS), and the launch of new satellite missions that introduce novel, complex data products. Launched in February 2024, the PACE mission carries a three-instrument payload that collects synergistic oceanic, atmospheric, and terrestrial observations that extend Earth system data records for the next generation of scientists. Details on PACE data file formats, types, and volumes can be found at the Ocean Biology Distributed Active Archive System (OB.DAAC) and PACE websites. The OB.DAAC provides processed data along with publicly available processing and visualization tools, enabling researchers to quickly engage in exploring applications and interpretations of PACE data products. However, the user community still faces the dual challenge of becoming familiar with new data products while adapting workflows to cloud-based computing environments, including the use of community-supported software and cloud infrastructure.

Hackweeks provide an effective mechanism for helping researchers adapt to these evolving data environments by promoting open-source tools, FAIR (findable, accessible, interoperable, reusable) data practices, reproducible workflows, and cloud-based collaboration in support of NASA's open science goals (Scheick et al., 2026). Here, we describe the goals and outcomes of the PACE Data Hackweeks, highlight participant experiences, and identify remaining challenges. We conclude that sustained investment in hackweeks and community-maintained cloud infrastructure is essential for maximizing scientific and applied value of NASA's evolving Earth science systems.

GOALS OF A PACE DATA HACKWEEK

From organizing and leading two successful in-person hackweeks, we have gained valuable insights and refined a suite of goals for teams interested in hosting similar events. During early planning stages, our team consulted with the ICESat-2 Hackweek organizers, whose experience and resources proved instrumental in shaping our approach. Members of our team have also participated in and organized a multitude of short-format trainings, some within the Carpentries or eScience Institute hackweek frameworks. These experiences allowed us to formulate the goals below as a high-level strategy for achieving a research-focused event that generates tangible scientific outputs.

GOAL 1: KICKSTART NOVEL RESEARCH AND NEW COLLABORATIONS

PACE Data Hackweek participants arrive with diverse research ideas and are expected to depart with well-defined projects, collaborative teams, and a foundation for sustained remote collaboration. Developing effective group projects is one of the primary organizational challenges, requiring early alignment of research goals and active guidance from both scientific and technical mentors. Daily science lectures and tutorials, modeled after the ICESat-2 Hackweek, helped shape projects while providing exposure to current PACE research across oceanic, atmospheric, and terrestrial domains, as well as a break from intensive coding.

To promote continuity beyond the hackweek, teams were encouraged to develop projects into conference presentations, manuscripts, or proposal concepts, with continued support through cloud computing resources, Slack communication, technical guidance, and funding and publication advice. Structured social activities were also integral to fostering collaboration, helping participants build networks, exchange feedback across teams, and sustain a balanced, collaborative environment.

GOAL 2: DEMONSTRATE THE VALUE AND LIMITS OF CLOUD COMPUTING

The transition of NASA's Earthdata archive to the commercial cloud encourages researchers to adopt cloud-based data analysis (Gentemann et al., 2021). Earthdata Cloud provides free access to datasets stored in AWS and discoverable through NASA's Common Metadata Repository, but it does not currently offer compute resources; however, efforts are underway to expand access to integrated cloud-based computing environments that would allow users to analyze data without needing to manage cloud infrastructure. Cloud-based analysis requires separate compute infrastructure, most commonly AWS Elastic Compute Cloud (EC2). This architecture supports high-throughput, data-intensive workflows by enabling direct access to large datasets within the same AWS region, reducing data movement and speeding up processing.

An emerging model for accessing EC2 instances is through community-maintained cloud-based JupyterHubs. Co-locating hackweek compute and data in the cloud lowers barriers to working with large datasets without duplication, supports data streaming and reproducible workflows, enables real-time collaboration, and allows users to scale seamlessly from simplified tutorials to full-mission workflows (Box 1; Martin et al., 2025). For the PACE Data Hackweek, we used CryoCloud, a JupyterHub maintained by a broad Earth science community, and we collected participation feedback on usability during the event (online supplementary Box S1).

GOAL 3: GROW A PERSISTENT ONLINE RESOURCE

To extend the reach of the hackweeks, we created a public website using an open-source website template and the GitHub Pages hosting service. The PACE Data Hackweek website includes a single-page landing site for logistics and a detailed JupyterBook with recorded lectures, coding tutorials, schedules, and preparation materials. Participants found it intuitive and helpful, reducing pre-event questions.

Hackweek content is preserved as static archives and incorporated into NASA's Ocean Ecology Lab Help Hub, which provides

BOX 1. Summary of the value and limitations of using a cloud-based community-maintained JupyterHub for the PACE Data Hackweek.

+ VALUE	– LIMITATIONS
MANAGED COMPUTE ENVIRONMENT	
• Eliminates the need for individual software configuration, allowing participants to begin productive work immediately • Can be reused on other local or remote platforms beyond the hackweek • Reduces technical barriers and inequalities among participants • Fosters a community of support and collaboration	• Restricted control over resources and system configuration • Limited available memory (Box S3) • Unfamiliar development environment and operating system (i.e., JupyterLab, Linux, S3 bucket storage and access, commonly owned "shared" file system)
DIRECT DATA ACCESS	
• Reduces latency through storage-adjacent compute resources • Supports collaborative workflows with high-bandwidth connections and unlimited concurrency • Removes dependencies on local storage or network limitations	• Lack of cloud optimization for data products stored as NetCDF4/HDF5 reduces performance • Data products from different agencies (e.g., NASA, USGS, NOAA, ESA) are not all co-located in the same commercial cloud
FACILITATED COLLABORATION	
• Encourages reproducible research by standardizing the computing environment with access to datasets • Supports generation of preliminary analyses and hypothesis testing that can be built into future research proposals • Promotes sharing of code, workflows, and results with the broader community, accelerating scientific discovery	• Reproducing the compute environment outside a managed JupyterHub requires additional training • Limits and "best effort" restrictions on per-user and shared file storage (Figure S4)
COMMERCIAL CLOUD SCALABILITY	
• Supports both simple tutorials and computationally intensive projects • Enables seamless scaling for larger datasets or complex analyses	• Reliance on S3 over local or network file systems for persistent storage is unfamiliar and less widely supported

reproducible Jupyter Notebook tutorials combining code, text, and visualizations. Tutorials are collaboratively developed, peer-reviewed, and regularly updated using hackweek feedback to ensure relevance and usability. Hackweeks play a critical role in motivating the continual updating of Help Hub tutorials by serving as development sandboxes where project activities and participant feedback feeds directly into new or improved notebooks. Since its launch, the Help Hub has grown from 48 to over 6,200 weekly page views, with usage spikes following trainings and events (Figure S1).

GOAL 4: LEVERAGE PRIOR EXPERTISE

Hackweeks, workshops, and short courses are common in academic and open-source communities, often implicitly adopting the Openscapes program's flywheel approach: leveraging momentum toward greater outcomes (Robinson and Lowndes, 2022). Organizing a hackweek raises many questions about costs and execution, and planners are encouraged to consult multiple past event managers for guidance, as it is unlikely that any one approach can be exactly replicated. The PACE Data Hackweeks draw on two key sources of momentum: the CryoCloud community and the Ocean Carbon and Biogeochemistry (OCB) Project Office.

Participants receive access to CryoCloud (Snow et al., 2022), a cloud-based JupyterHub managed by the International Interactive Computing Collaboration (2i2c), originally developed for NASA cryosphere research but now serving a broader Earth science community. To reflect this expansion, the platform will soon be rebranded (Tasha Snow, Earth System Science Interdisciplinary Center, University of Maryland and NASA Goddard Space Flight Center, *pers. comm.*, 2025). Access during and after the hackweek is supported by NASA funding and AWS cloud credits.

Professional logistics support from the OCB Project Office assisted with funding, contracts, and travel, allowing the core organizing team to focus on participant recruitment, instructional design, and tutorial development. Other hackweeks have successfully partnered with the University of Washington eScience Institute for similar logistical coordination.

We also built on prior expertise by empowering past participants to take on leadership roles in subsequent events. These mentors brought valuable participant perspectives and offered practical feedback that helped improve the overall participant experience.

EXPERIENCE AT A PACE DATA HACKWEEK

The PACE Data Hackweeks, held in August 2024 and 2025, aimed to broaden access to PACE data, enhance data-access tools, promote open-source workflows, and support integration with other Earth observation datasets. Each five-day, in-person workshop brought together 40–50 participants, with all instructional materials released and new code and analyses shared across the community. Project teams were first organized around research interests identified in participants' applications and then grouped into broad themes. Mentors worked with groups to refine project scope, align goals with available datasets, and ensure that proposed analyses were feasible within the week-long program. This structure enabled teams to quickly coalesce around focused research questions while remaining flexible to emerging ideas. Through these collaborative efforts, participants explored novel applications of PACE data, developed reproducible workflows, and generated preliminary analyses that seeded new collaborations, informed future research directions, and in some cases, supported early-stage proposal development.

Of the 88 total participants across both years, 36 completed a post-event feedback survey and a separate demographic survey (41% response rate). Highlights from the surveys are included in the following summary of the hackweek experience and in the online supplementary material (Boxes S1–S3, Figures S2–S4). We also show data on cloud computing resource usage and costs that were derived from EC2 activity logs during the 2025 event.

LOGISTICS

Each five-day, in-person event was held at the University of Maryland, Baltimore County (UMBC) and funded through OCB Training Activity grants. OCB covered travel, lodging, and meals for US-based participants, while international participants received partial travel stipends, with remaining expenses supported by the participants or their home institutions. Accommodations were provided in UMBC dormitories, and meals were served at the university cafeteria. To support participants with family or dependent care responsibilities, additional funding was available to offset caregiver costs or to allow for customized travel arrangements.

SCHEDULE

Each day combined scientific lectures with hands-on coding tutorials and demonstrations designed to build skills in data accession, Python programming, and cloud computing (Figure 1). Both science lectures and coding tutorials were highly rated (based on 1–5 ranking scores collected in feedback surveys), and 100% of survey respondents reported increased confidence in working with PACE data (Figure S2). Daily check-ins supported collaboration and progress, and on the final day teams presented their projects and shared code via public GitHub repositories, with most planning continued collaboration (Box S2). Feedback was overwhelmingly positive, with participants describing the hackweek as fun, engaging, and collaborative (Figure S3). Social events, including a Bob Ross paint night, a fireside chat with NASA program managers, a local crab feast, a PACE Nerd Night, and a themed trivia exercise, were frequently cited as essential for community building and sustained engagement:

> "Best part of the day! Every night was so great and the energy was great."

> "I loved the intentional inclusion of social activities. It helped people meet and have fun while maintaining work-life balance and camaraderie."

DEMOGRAPHICS

The respondents represented a diverse international community spanning 15 countries (Figure 2). Most were graduate students or early career researchers, with the majority holding master's or doctoral degrees (Figure 2). Notably, 74% reported that the PACE Data Hackweek was their first hackweek experience.

CODING ENVIRONMENT

PACE Data Hackweek participants onboarded to CryoCloud benefited from a fully configured, cloud-based software environment with direct access to all PACE datasets and no local setup required. The hub launched Docker containers, running on adjustable hardware configurations (2–29 GB RAM and 0.2– 4 CPUs), that

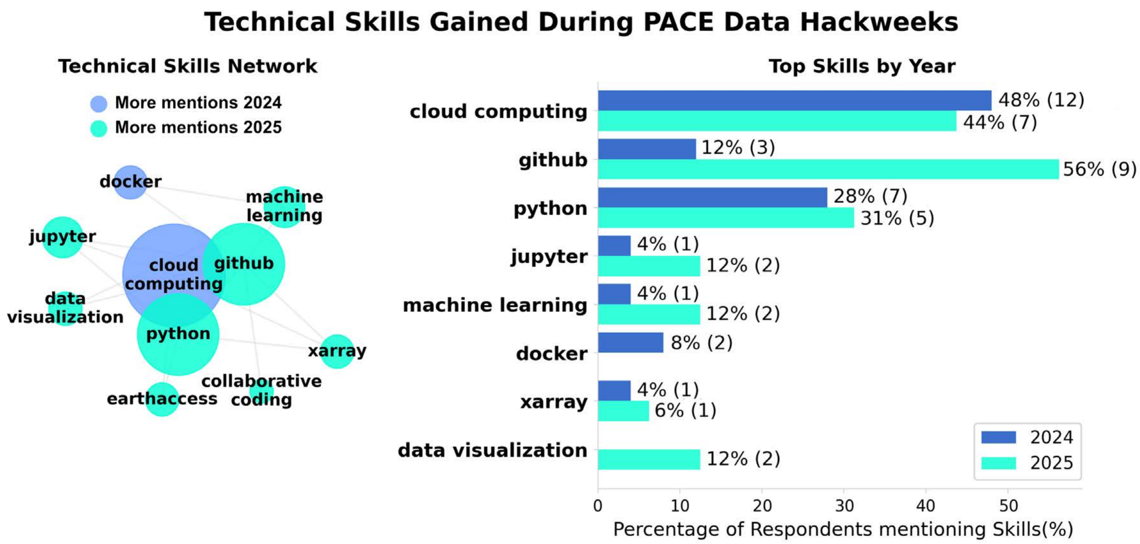

FIGURE 1. Most common technical skills, and associations among technical skills, mentioned in responses to the feedback survey question "What technical skills did you gain this week?" Node size in the technical skills network represents the number of times a skill was mentioned, while proximity indicates how frequently skills were co-mentioned by the same participant. Node coloring is based on the year in which the skill was mentioned most often.

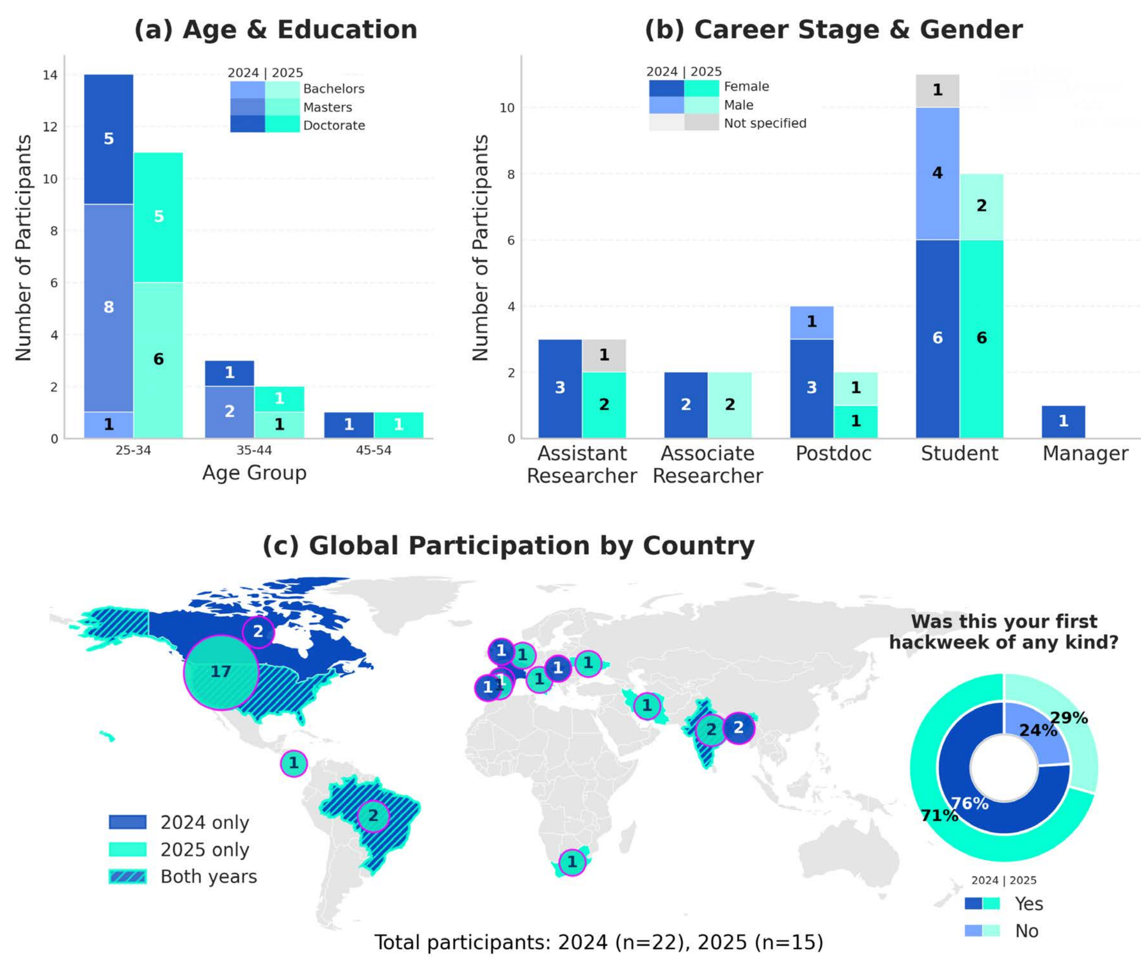

FIGURE 2. Responses to the demographic survey showing (a) age and education level, (b) career stage and gender, and (c) country of residence and first-time hackweek participation. Providing gender was optional and open-ended, with a non-response tagged as "Not specified."

included required Python packages and the NASA Ocean Biology Processing Group's Ocean Color Science SoftWare (OCSSW); this container is available on CryoCloud as the "Ocean Biology Python Image" (Figure S5). Participants were able to begin running tutorials and regenerating PACE data products in the commercial cloud almost immediately, all through a web browser.

Using the community-maintained JupyterHub, participants could execute tutorial and group-project notebooks, while experiencing both the benefits and limitations of cloud-based workflows (Box 1). Overall, CryoCloud played a central role in reducing technical barriers, fostering collaboration, and supporting open, reproducible workflows (Box S1). Feedback indicated that the majority of participants intend to continue using cloud computing in their research, although some concerns remain (Box S3, Figure S4).

COMMERCIAL CLOUD USAGE AND COSTS

Using Grafana dashboards developed by 2i2c, we charted EC2 usage and costs for all participants during the 2025 PACE Data Hackweek (Figure 3). Daily memory usage per user ranged from 155 KB to 29.4 GB, with an average of 1.79 GB, while CPU usage peaked at ~3.7 CPUs per user and averaged 0.6 CPUs per day (Figure 3). Peak memory and CPU demand occurred late in the week during intensive group project development.

CryoCloud costs include user-dependent expenses (e.g., compute and personal storage) and user-independent infrastructure costs that run continuously. Compared to the previous model of launching a dedicated hackweek JupyterHub that incurred ~$2,250 in startup and ~$2,250 in monthly infrastructure costs (Tasha Snow, Earth System Science Interdisciplinary Center, University of Maryland and NASA Goddard Space Flight Center, *pers. comm.*, 2025), maintaining a shared hub is substantially more cost-effective. For the full week, total EC2 compute costs were $367.99, with $36.36 in individual storage and $19.49 in shared storage, for a combined total of $423.84. Individual daily costs peaked on Day 4, with the highest single-user daily cost at $7.31 and a maximum single-user weekly cost of $22.61 (Figure 3). Uncertainty around these costs was a commonly raised concern among participants (Box S3), who did not have real-time access to the Grafana dashboards.

OPPORTUNITIES FOR IMPROVEMENT

While cloud computing is essential for processing large PACE datasets and enabling hackweeks, several challenges remain. (1) CryoCloud provides user home directories backed by Amazon Elastic Block Store (EBS) but limits storage to 50 GB due to per-user costs, creating constraints for users and the community. (2) Configuring and maintaining compute environments remains a technical challenge. Guidance on defining and running reproducible workflows, for example, binder-ready repositories, is often perceived as technically advanced by hackweek participants. (3) Data-adjacent computing requires co-located datasets, which is often not the case across agencies, and user-contributed data archives, making temporary data transfer, storage, and remote execution necessary even when working in a commercial cloud. (4) Performance limitations occur when accessing data not optimized for S3 (McNally et al., 2026). (5) Growing the CryoCloud

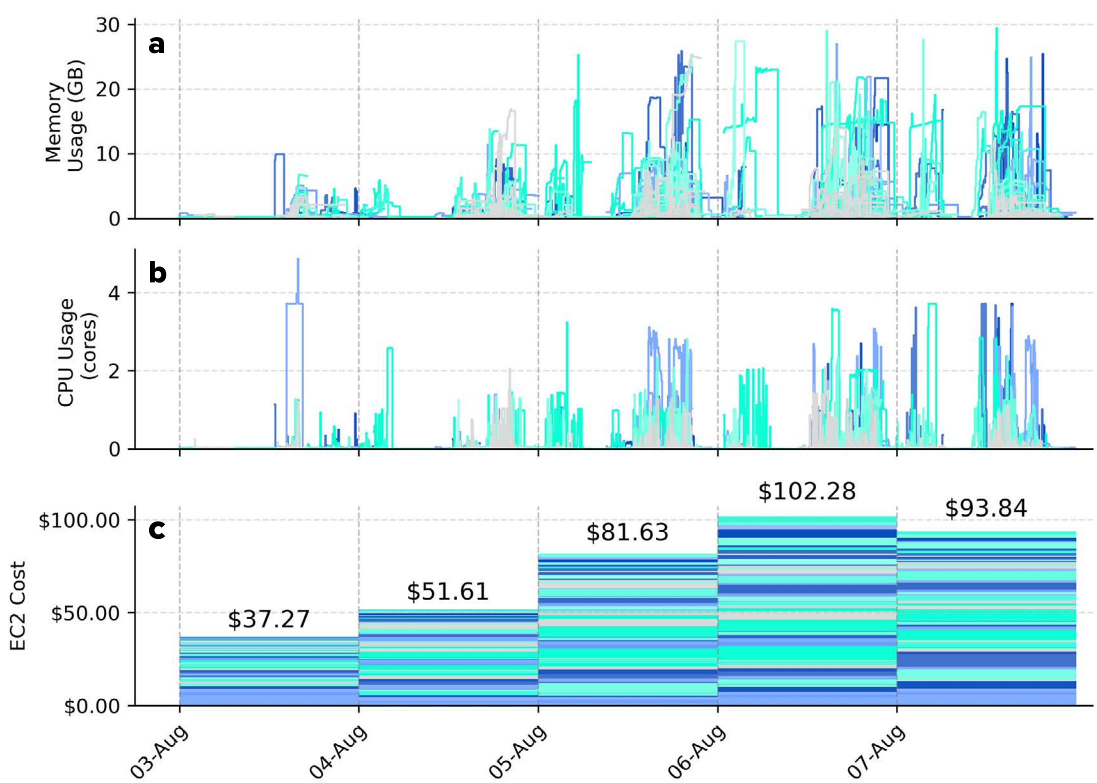

FIGURE 3. Graphs show (a) memory usage (GB) in CryoCloud for each PACE Data Hackweek participant over the five-day 2025 event, (b) central processing unit (CPU) usage (cores) in CryoCloud for each participant, and (c) Elastic Compute Cloud (EC2) cost incurred by each participant over the five-day event. Colors denote individual participants.

community requires additional funding, but clear mechanisms for contributions from grants, institutions, or agencies are not yet established. Future collaboration between hackweek organizers, data engineers, and cloud system administrators would help prioritize and address these challenges, with benefits extending beyond future hackweeks.

While PACE Data Hackweeks have been highly effective in building skills and community, opportunities exist to improve their reach, structure, and long-term impact. (1) Although PACE Data Hackweeks have primarily attracted early-career scientists, they also offer valuable opportunities for late-career researchers to update their skills in modern, cloud-based workflows. Future hackweeks will aim to increase participants from this group to broaden impact across the community. (2) Participant feedback also points to challenges with project development and completion. To address this issue, future PACE Data Hackweeks may adopt a more structured approach, with pre-defined project topics, participant matching, and dedicated mentors to support progress during and after the event.

CONCLUDING REMARKS

Hackweeks have become an effective mechanism for advancing scientific work, in large part because they bring together researchers who might not otherwise collaborate. Interactions often continue after the event, leading to new ideas and follow-on projects. By combining different areas of expertise over an intense but short research sprint, hackweeks provide space to experiment with new approaches and to take risks on novel or uncertain research directions.

PACE Data Hackweek participants not only explored new data products but also developed familiarity with cloud-based workflows and joined a larger community of Earth science researchers working to maximize the benefits of NASA's Earthdata Cloud. Leveraging an established, cloud-based JupyterHub for hackweeks is practical and cost-effective, and provides a nexus for continued interactions. Continued investment in hackweeks and shared cloud resources will be critical for sustaining these benefits, and we plan on hosting PACE Data Hackweeks in the future.

As NASA's Earth Observing System evolves, hackweeks are well positioned to serve as catalysts for skill-building and community formation. The oceanography community faces a mix of opportunities and challenges as it advances open science. Participants in the PACE Data Hackweeks are empowered to translate broad shifts in the data and computational landscape into meaningful, lasting impacts for the community.

SUPPLEMENTARY MATERIALS

The supplementary materials are available online at https://doi.org/10.5670/oceanog.2026.e204.

REFERENCES

Gentemann, C.L., C. Holdgraf, R. Abernathey, D. Crichton, J. Colliander, E.J. Kearns, Y. Panda, and R.P. Signell. 2021. Science storms the cloud. *AGU Advances* 2(2):e2020AV000354, https://doi.org/10.1029/2020AV000354.

Huppenkothen, D., A. Arendt, D.W. Hogg, K. Ram, J.T. VanderPlas, and R. Rokem. 2018. Hack weeks as a model for data science education and collaboration. *Proceedings of the National Academy of Sciences of the United States of America* 115(36):8,872–8,877, https://doi.org/10.1073/pnas.1717196115.

Martin, P.E., E. Eli Holmes, E. Mayorga, J.K. Ansong, U. Bhaskar, J. Cornejo-Donoso, D. Correa-Chilón, R. Damoah, D. Fierro-Arcos, L. Gómez-Navarro, and others. 2025. Harnessing marine open data science for ocean sustainability in Africa, South Asia, and Latin America. *Oceanography* 38(1):59–66, https://doi.org/10.5670/oceanog.2025.121.

McNally, A., L. Sterzinger, and I. Carroll. (2026). Producing Earth science data for impact: Improved commercial cloud usability of archive model data. *Environmental Modelling & Software* 197(106846), https://doi.org/10.1016/j.envsoft.2025.106846.

Mitchell, C., W.-J. Lee, F. Fernandes, J. Gum, A. Kerney, E. Mayorga, T. Moore, N. Mortimer, N. Ribeiro, and V. Staneva. 2026. OceanHackWeek: An inclusive, collaborative approach to developing oceanography data science skills. *Oceanography* 39(1):50–55, https://doi.org/10.5670/oceanog.2026.e104.

Robinson, E., and J. Stewart Lowndes. 2022. The Openscapes Flywheel: A framework for managers to facilitate and scale inclusive open science practices. *Earth ArXiv* preprint, https://doi.org/10.31223/x5cq02.

Scheick, J., A. Barrett, Z. Fair, Z. Katz, L. Lopez, A. Neeley, C. Roberts, B. Smith, T. Snow, R. Wegener, and A. Arendt. 2026. Ten simple rules to increase the usability of Earth observation mission datasets. *ESS Open Archive* preprint, https://doi.org/10.22541/essoar.176892205.56393151/v1.

Snow, T., J. Millstein, J. Scheick, W. Sauthoff, W.J. Leong, J. Colliander, F. Pérez, J. Munroe, D. Felikson, T. Sutterley, and M. Siegfried. 2023. "CryoCloud JupyterBook." Zenodo, https://doi.org/10.5281/ZENODO.7576601.

ACKNOWLEDGMENTS

We gratefully acknowledge the PACE Data Hackweek mentors, tutorial contributors, and science presenters. We thank Tasha Snow for guidance and support with CryoCloud, Eli Holmes for advice on hackweek organization, and Jenny Wong (2i2c) for assistance in analyzing CryoCloud costs and usage statistics. We also acknowledge the ICESat-2 Hackweek team for early scoping support, as well as the OCB Project Office, NASA Ocean Biology Biogeochemistry Program Managers, and the UMBC staff for funding, logistical, and technical assistance. We thank Anthony Arendt and Catherine Mitchell for their thoughtful and constructive reviews of this manuscript. And lastly, we thank all hackweek participants for their enthusiastic engagement.

FUNDING SUPPORT

The PACE Data Hackweek was established with the support of the Ocean Carbon & Biogeochemistry Project Office, which receives funding from the National Aeronautics & Space Administration (NASA 80NSSC25K7397) and the National Science Foundation (NSF OCE-2445578).

AUTHORS

Anna E. Windle (anna.windledipaola@nasa.gov), Ocean Ecology Lab, NASA Goddard Space Flight Center, and Science Systems and Applications Inc., Greenbelt, MD, USA. **Ian Carroll**, Ocean Ecology Lab, NASA Goddard Space Flight Center, Greenbelt, MD, USA, and GESTAR II, University of Maryland Baltimore County, Baltimore, MD, USA. **Carina Poulin** and **Skye Caplan**, Ocean Ecology Lab, NASA Goddard Space Flight Center, and Science Systems and Applications Inc., Greenbelt, MD, USA. **P. Jeremy Werdell**, Ocean Ecology Lab, NASA Goddard Space Flight Center, Greenbelt, MD, USA.

ARTICLE CITATION

Windle, A.E., I. Carroll, C. Poulin, S. Caplan, and P.J. Werdell. 2026. The PACE Data Hackweek launches a new wave of open science: How we did it (twice), and why. *Oceanography* 39(2):62–67, https://doi.org/10.5670/oceanog.2026.e204.

UNLOCKING A FISH FINDER FOR BENTHIC HABITAT CHARACTERIZATION

By Michael P. Scherer and Val Schmidt

ABSTRACT. Single beam sonars can provide valuable acoustic information on the structure of benthic habitats and the contents of the water column. Nominally, acoustic sensors that provide water column data in scientific applications can cost tens or hundreds of thousands of dollars. In contrast, consumer grade fish finders that are mass produced are very inexpensive, costing only tens or hundreds of dollars. Unlocking a fish finder for scientific use could increase access to low-cost sensing methods for coastal communities that are historically underserved. The principal challenge with using a fish finder for benthic habitat classification is that the sonars are generally not interoperable and are often limited to visualization on a display or chart plotter made by the sonar manufacturer. This vendor lock prevents the sonar data, and in particular water column data, from being stored and processed to create mapping products. In this project, "SonarPhony" was developed to provide interoperability software to enable the real-time visualization and logging of water column data from a low-cost fish finder. A machine learning approach was used to demonstrate that the logged data could be used to estimate bottom type and identify the presence of seagrasses. This solution thus provides a low-cost means for both benthic habitat classification and bathymetric mapping.

INTRODUCTION

Understanding the location and character of benthic habitats is critical for people to understand their fisheries. US laws such as the Magnuson–Stevens Fishery Conservation and Management Act (2007) require the definition and management of essential fish habitat, such as seagrasses, which in turn requires sensing that can be deployed on large scales to manage fisheries (Federal Register, 2013). Coastal communities around the world depend on fish stocks whose habitats are easily misunderstood for lack of visibility without expensive tools (Harden-Davies and Snelgrove, 2020). These economic barriers to entry prevent local, distributed, independent access to ocean data.

Existing data pipelines for crowdsourced bathymetry using low-cost sensors have been proven to expand access and detect changes to charted bathymetry, in particular, after natural disasters (Gilbert et al., 2025). Low-cost fish finders have been used for bathymetric studies and habitat mapping to create gridded digital elevation models (DEM; Gomes et al., 2025). Benthic acoustic classification has been thoroughly studied, but largely with significantly more expensive sensor systems (Anderson et al., 2008; Gumusay et al., 2019). Commercial solutions exist for processing higher end consumer grade fish finder data that rely on licensing models (Helminen et. al., 2019). Underwater video has been used to relate seafloor characteristics to acoustic data (Rooper and Zimmermann, 2007; Sánchez-Carnero, 2023). With added open interface water column data, consumer fish finders could be used to map beyond bathymetry to include seafloor and habitat characterization, at a cost that is accessible for citizen science.

Small uncrewed systems also benefit from low-cost sensing with open interfaces. Sensors incorporated on an uncrewed platform can cost as much or more than the vehicle itself. Because no people are on board, and uncrewed systems may operate completely over the horizon (Scherer and Chance, 2023; Cross et al., 2025), an open interface is required to collect and visualize data remotely.

To address this gap, we introduce SonarPhony, an open-source interoperability software that unlocks an off-the-shelf fish finder for data logging, remote or autonomous operation, and collection of water column data. The usefulness of these data is further demonstrated with the development of a machine learning classifier of benthic habitat type from the SonarPhony software.

MATERIALS AND COST

The benthic characterization system consists of three subsystems: the sonar itself, a GPS and sonar data logger, and a drop camera (Table 1). The Vexilar SP100 sonar is an off-the-shelf product that can be operated from any computer with the SonarPhony software. The data logger was based on a Raspberry Pi running SonarPhonyD. The integrated Wi-Fi on the Pi connects to the sonar. A USB GPS receiver was used to georeference the soundings. The drop camera was used to validate the bottom type.

ASSEMBLY

SOFTWARE. Two applications were created. SonarPhony has a graphical user interface that can be used to drive and visualize the sonar data (see Figure 1) or to play back log files. SonarPhonyD is a daemon that can log the water column data and output

NMEA0183 sentences. The NMEA0183 output is useful for interfacing with a chart plotter or other data acquisition system. An alternate daemon was also developed to control and transmit over ROS2 for robotics applications.

SONAR. The sonar was installed as specified by the manufacturer. When submerged in water, the sonar created a Wi-Fi access point for computer connection. The SonarPhony software was run to visualize and record the data. The T-Pod (SP100) model used for this study operates at 125 kHz and 30° beam, pinging 28–29 times per second with 302 samples per ping. The SP200 could reduce uncertainty due to its fixed mounting, though it operates at different frequencies.

DATA LOGGER. The portable charger was plugged into the input USB power port of the Raspberry Pi. Raspberry Pi OS Lite was installed on the Pi. A daemon version of SonarPhony, called SonarPhonyD, was initiated by a systemd script to run on the Pi to log sonar data. In addition to logging sonar data, it published a NMEA0183 string of the depth to a configured network port. OpenRVDAS (Agarwal and Cohn, 2020) was installed to log the GPS data and validate the logging of the sonar data, reading the NMEA0183 strings from both.

DROP CAMERA. The GoPro used for this study was chosen because it was on hand. With the waterproof enclosure, the camera is rated to 60 m of water depth. The light was attached to the base of the camera using the provided mount. The end of the diving reel line was then tied to the combined system. Additional weight could be added for a faster descent rate.

TABLE 1. Material costs for the SonarPhony acquisition system.

ITEM	COST
SONAR	
Vexilar SP100 or SP200	$59.95
Total	**$59.95**
DATA LOGGER	
Raspberry Pi 3 model B	$35.00
USB Wi-Fi Dongle	$20.00
USB GPS	$20.00
Portable USB Charger	$10.00
Watertight Enclosure	$10.00
Total	**$95.00**
DROP CAMERA	
Diving Reel (or thin line)	$20.00
GoPro HERO11 Black	$299.99
GoPro Enclosure	$49.99
Light – Movo LED-WP	$29.95
Total	**$399.93**
TOTAL COST	**$554.88**

CODE

The sonar, which also acts as the Wi-Fi access point, always assigns itself the IP of 192.168.1.1, and accepts UDP traffic on port 5000. The client first issues a handshake message to establish itself as the leader. Upon acceptance by the sonar, the client can then begin issuing commands to direct the sonar to begin transmitting pings and to select the requested range of the water column data. The commands are issued once per second to keep the sonar alive. If the commands stop, the sonar will cease transmitting after several seconds. Each returned ping contains the battery voltage, state of charge, water temperature, range of the water column (minimum and maximum), detected depth, and water column data that is a raster array of intensities with values between 0 and 255. Altering the gain had no effect on the returned raster intensities, so it is assumed that the gain is for visualization. The source code can be found on Github.

FIELD APPLICATION EXAMPLE

The usefulness of the sensor for bottom type characterization was assessed. Data were collected at Bonita Bayou in St. Petersburg, Florida, USA, on December 1, 2024, and March 2, 2025. The bay has a largely sandy seafloor with patches of seagrass, rocks, and fan corals. A third dataset was collected in Lake Martin, Louisiana, on November 17, 2024. Lake Martin is a freshwater lake with a silted mud bottom. The data logger was fixed to a kayak, and the sonar was towed by a short, fixed line behind it. A cell phone was used to connect to the OpenRVDAS instance running on the data logger to verify that the sonar and GPS were both collecting data. For the purposes of this study, a fixed sonar range of 0–9 ft was used at all times to reduce variability, making each sample in the

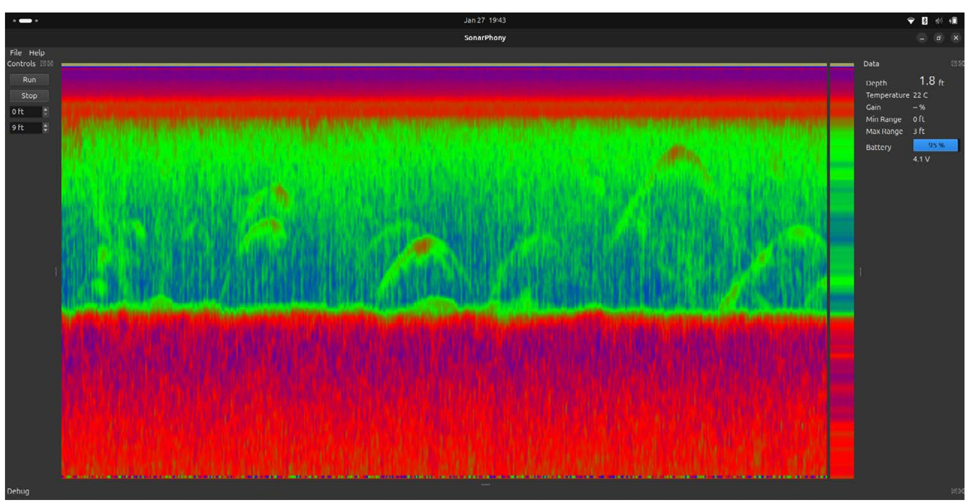

FIGURE 1. This image shows the SonarPhony app displaying a waterfall of water column data collected in Lake Martin, Louisiana.

water column approximately 7 cm high. Periodically, the camera was dropped from the kayak, logging the time of each deployment, shown in Figure 2.

The data logs were converted from NMEA0183 data and raw sonar data, respectively, into Python pickle format. Time was corrected by comparing the offset between GPS time and the system clock in the logs, and the corrected timestamps were used thereafter.

Each drop camera video segment was reviewed to determine the bottom type at the drop location. The timestamp recorded in the handwritten log for each camera drop was then used to associate the bottom type with a GPS coordinate. Training and test data were then extracted by first selecting the soundings within a 5-second neighborhood of each drop camera location and tagging those soundings based on the bottom type. Within each

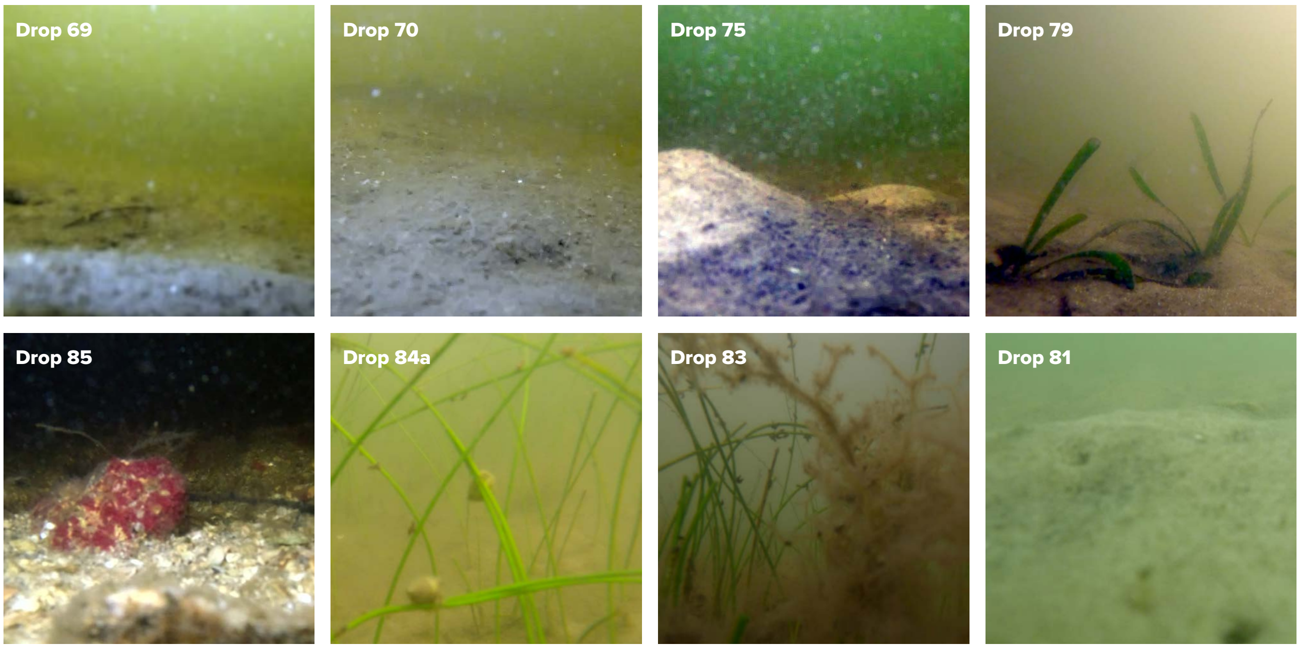

FIGURE 2. Imagery obtained from the drop camera at selected sites in Bonita Bayou, FL. Drop locations are shown in Figure 3.

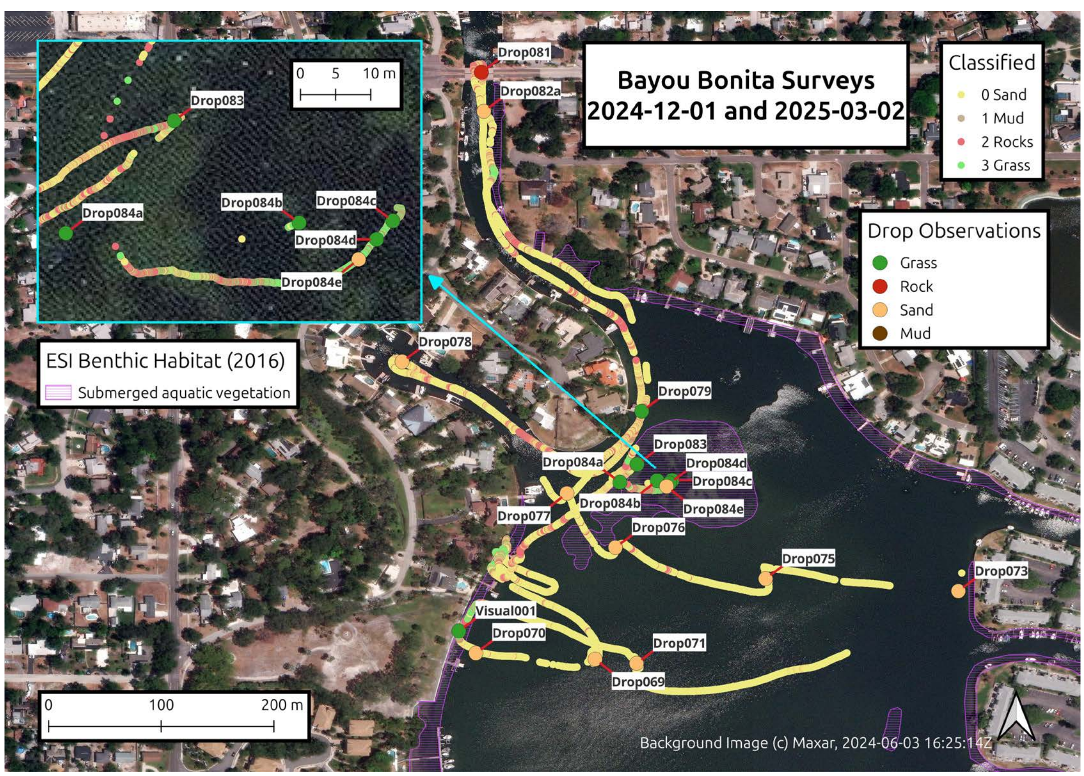

FIGURE 3. Survey region in Bayou Bonita, drop camera locations, and resultant classification of bottom type using sonar data. Detail shows classified seagrass correlated over the region where seagrass can be seen in a satellite image from six months prior. *Background image source: Maxar 2024-06-03*

sounding's water column data, the 16 samples on either side of the detected hard bottom were extracted, including the center sample at the hard bottom, resulting in a window of 33 samples. All other samples in the water column for each sounding were discarded to focus on bottom type classification. Thirty-three percent of the tagged and extracted soundings, randomly selected, were allocated to test data, and the remainder were used for training.

To increase model accuracy and generalization (Bishop, 2006), a set of basic statistical and power spectra features were extracted from each sounding's sample window (Preston et al., 2001). Basic features included mean, standard deviation, skew, and kurtosis. Power spectra features were quantified using the periodogram method from SciPy (Virtanen et al., 2020). Features were calculated on both the entire window and on the samples directly above the hard bottom to increase the discriminating ability of seagrass.

Many implementations use unsupervised clustering algorithms to detect bottom type (Gumusay et al., 2019), so initial trials were done with K-Means. Unsupervised learning methods are capable of discovering categorizations of data that might not be known a priori; however, these clusters may have no physical meaning (Mitchell, 1997). Thus, it was difficult to validate that the clusters were correlated to any particular bottom type.

Because the target classes (bottom types) were known for this study, a supervised learning algorithm was chosen. AdaBoost was selected after trialing a selection of supervised learning algorithms implemented in scikit-learn (Pedregosa et al., 2001). AdaBoost is an ensemble method that uses many so-called "weak" classifiers whose results are combined to get a more accurate result (Freund and Schapire, 1997). The AdaBoost classifier was trained on the data using 200 estimators, because additional estimators did not appreciably increase the accuracy of the model. When only considering classes of sand, mud, and rocks, the classifier performed very well with 96% accuracy and a Matthews correlation coefficient of 0.92. Considering all four classes of sand, mud, rocks, and seagrass, the quantitative scores reduced to 87% accuracy and a Matthews correlation coefficient of 0.79 (Figure 4). The greatest confusion in classification was between sand and grass. Because the identified grass lived in sand, it is reasonable that a broad swath would have poor discriminating ability between the two bottom types. As a notable example, location 79 was sparse in seagrass compared to locations 83 and 84, as shown in Figure 2. The results of the classification on the dataset can be found in Figure 3, demonstrating correlation of seagrass presence with both satellite imagery from 2024 and from NOAA Environmental Sensitivity Index (ESI) Benthic Habitats established in 2016. The machine learning code can be found on Github.

FUTURE DEVELOPMENT

Machine learning models could be improved by collecting training datasets with higher data density, such as by collecting persistent camera data during the entire collection process.

Further experimentation could be done using the SP300 model of sonar, which supports higher frequencies of 200 kHz that may have better discriminating ability for thin seagrasses. The SP300 also supports 80 kHz operation, so multiple frequencies could be collected to better characterize bottom type. Of additional interest is full characterization of the acoustic properties of the sonar, such as target strength calibration, which might allow the sonar to be used in more traditional processing pipelines for biomass estimation or classification.

A practical limitation in this solution is that it provides a fixed number of samples for any range setting. Therefore, increasing the range of the sensor reduces the resolution of the water column data. A future study could evaluate the reasonable maximum range

Class	Precision	Recall	F1-Score	Support
0. SAND	0.97	0.85	0.91	549
1. MUD	0.99	0.99	0.99	139
2. ROCKS	0.72	0.88	0.79	107
3. GRASS	0.65	0.80	0.72	186
Macro Avg	0.83	0.88	0.85	981
Weighted Avg	0.88	0.87	0.87	981
			Matthews Correlation Coefficient	0.79
			Accuracy	0.87

Confusion Matrix

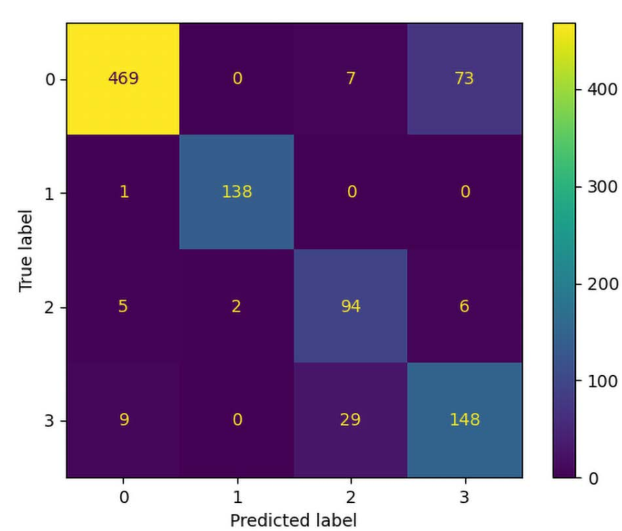

FIGURE 4. Classification statistics for a four-class machine learning model.

of the sonar, or if the minimum range could be modified to move the window of water column data to a region of interest without losing resolution.

CONCLUSION

Seafloor classification, and in particular seagrass identification, is valuable for communities where seagrasses are measured and protected. Low-cost tools for measuring seagrass abundance enable citizen scientists to track changes to essential fish habitat. SonarPhony was shown to be effective in a region for characterizing bottom type, and it was stable over two data collection excursions. Bottom type classification of sand, mud, and rocks was demonstrated in addition to identification of seagrasses, which could serve as a useful tool for understanding habitat. This low-cost methodology further enables crowdsourcing of seafloor classification.

REFERENCES

Agarwal, A., and D. Cohn. 2020. A novel data acquisition solution to expedite global oceanographic research. Pp. 1–6 in *Global Oceans 2020: Singapore–US Gulf Coas*t. Biloxi, MS, USA, October 5–30, 2020, https://doi.org/10.1109/IEEECONF38699.2020.9389328.

Anderson, J.T., D. Van Holliday, R. Kloser, D.G. Reid, and Y. Simard. 2008. Acoustic seabed classification: Current practice and future directions. *ICES Journal of Marine Science* 65(6):1,004–1,011, https://doi.org/10.1093/icesjms/fsn061.

Bishop, C.M. 2006. *Pattern Recognition and Machine Learning*. Springer, New York, New York, USA,738 pp.

Cross, R., D.R. Neff, and M.P. Scherer. 2025. Mission capable: A contrasting analyses of an uncrewed surface vehicle for extended duration offshore hydrographic survey. Pp. 1–5 *OCEANS 2025 - Great Lakes,* Chicago, IL, USA, September 29–October 2, 2025, https://doi.org/10.23919/OCEANS59106.2025.11245139.

Federal Register. 2013. Amendment 4 to the Fishery Management Plan for Corals and Reef Associated Plants and Invertebrates of Puerto Rico and the US Virgin Islands: Seagrass Management. NOAA (National Oceanic and Atmospheric Administration), https://www.federalregister.gov/documents/2013/03/06/2013-05067/amendment-4-to-the-corals-and-reef-associated-plants-and-invertebrates-fishery-management-plan-of.

Freund, Y., and R.E. Schapire. 1997. A decision-theoretic generalization of on-line learning and an application to boosting. *Journal of Computer and System Sciences* 55(1):119–139, https://doi.org/10.1006/jcss.1997.1504.

Gilbert, S., S.A. Murawski, M.E. Luther, A. Silverman, M. Hommeyer, R. Vistocci, S. Chernoch, H. Clark, S. Grasty, and K. Erickson. 2025. Partnering with the "Crowd": Development of a Community Bathymetry Program in Tampa Bay, Florida, USA. *Marine Technology Society Journal* 59(2), pp. 51–61, https://doi.org/10.4031/MTSJ.59.2.9.

Gomes, P.T., R. Henriques, M. Rubal, D. Azevedo, and D. Carreira-Flores. 2025. Assessing the potential of consumer-grade fish finders to improve coastal habitat mapping in data-poor areas. *Continental Shelf Research* 296:105590, https://doi.org/10.1016/j.csr.2025.105590.

Gumusay, M.U., T. Bakirman, I. Tuney Kizilkaya, and N.O. Aykut. 2019. A review of seagrass detection, mapping and monitoring applications using acoustic systems. *European Journal of Remote Sensing* 52(1):1–29, https://doi.org/10.1080/22797254.2018.1544838.

Harden-Davies, H., and P. Snelgrove. 2020. Science collaboration for capacity building: Advancing technology transfer through a treaty for biodiversity beyond national jurisdiction. *Frontiers in Marine Science* 7:40, https://doi.org/10.3389/fmars.2020.00040.

Helminen, J., T. Linnansaari, M. Bruce, R. Dolson-Edge, and R.A. Curry. 2019. Accuracy and precision of low-cost echosounder and automated data processing software for habitat mapping in a large river. *Diversity* 11(7):116, https://doi.org/10.3390/d11070116.

Mitchell, T.M. 1997. *Machine Learning*. McGraw Hill, New York, New York, USA, 432 pp.

Pedregosa, F., G. Varoquaux, A. Gramfort, V. Michel, B. Thirion, O. Grisel, M. Blondel, P. Prettenhofer, R. Weiss, V. Dubourg, and others. 2011. Scikit-learn: machine learning in Python. *Journal of Machine Learning Research* 12:2,825–2,830.

Preston, J.M., A.C. Christney, S.F. Bloomer, and I.L. Beaudet. 2001. Seabed classification of multibeam sonar images. Pp. 2,616–2,623 in *MTS/IEEE Oceans 2001*: *An Ocean Odyssey. Conference Proceedings*, Honolulu, HI, USA, November 5–8, 2001, (IEEE Cat. No. 01CH37295), https://doi.org/10.1109/OCEANS.2001.968411.

Rooper, C.N., and M. Zimmermann. 2007. A bottom-up methodology for integrating underwater video and acoustic mapping for seafloor substrate classification. *Continental Shelf Research* 27(7):947–957, https://doi.org/10.1016/j.csr.2006.12.006.

Sánchez-Carnero, N., D. Rodríguez-Pérez, S. Llorens, V. Orenes-Salazar, A. Ortolano, and J.A. García-Charton. 2023. An expeditious low-cost method for the acoustic characterization of seabeds in a Mediterranean coastal protected area. *Estuarine, Coastal and Shelf Science* 281:108204, https://doi.org/10.1016/j.ecss.2022.108204.

Scherer, M.P., and T.S. Chance. 2023. Enabling over the horizon operation on a line-of-sight uncrewed surface vehicle. Pp. 1–5 in *OCEANS 2023 - MTS/IEEE U.S. Gulf Coast*. Biloxi, MS, September 25–28, 2023, https://doi.org/10.23919/OCEANS52994.2023.10337131.

Virtanen, P., R. Gommers, T. Oliphant, M. Haberland, T. Reddy, D. Cournapeau, E. Burovski, P. Peterson, W. Weckesser, J. Bright, and others. 2020. SciPy 1.0: Fundamental Algorithms for Scientific Computing in Python. *Nature Methods* 17:261–272, https://doi.org/10.1038/s41592-020-0772-5.

ACKNOWLEDGMENTS

Seed funding for this project was provided by the Brook Byers Institute for Sustainable Systems at the Georgia Institute of Technology. Thank you to Joseph P. Montoya for his help in getting this effort sponsored. Thank you to Matthew Hommeyer and Alex Silverman at the University of South Florida Center for Ocean Mapping & Innovative Technologies (COMIT) for conducting additional beta testing of this system, and to two peer reviewers who helped improve this manuscript. Finally, thank you to the first author's sister, Rachel Scherer, for assisting with data collection efforts.

AUTHORS

Michael P. Scherer (michael.p.scherer@ieee.org), Georgia Institute of Technology, Atlanta, GA, USA. **Val Schmidt**, Center for Coastal and Ocean Mapping, University of New Hampshire, Durham, NH, USA.

ARTICLE CITATION

Scherer, M.P., and V. Schmidt. 2026. Unlocking a fish finder for benthic habitat characterization. *Oceanography* 39(2):68–72, https://doi.org/10.5670/oceanog.2026.e201.

COPYRIGHT & USAGE

STUDENTS CO-CREATING THEIR COMMUNITY OF INQUIRY

By Mirjam S. Glessmer, Anne Digranes Årvik, and Kjersti Daae

The Community of Inquiry is a well-established framework developed for online education (Garrison et al., 2010). It is often used by teachers to plan, evaluate, or reflect on teaching. The framework consists of three overlapping "presences" that teachers bring to the educational experience (Figure 1). The *cognitive presence* relates to how teachers can help students learn to think about concepts and make sense of them. Teachers can consider which concepts are relevant, what might be difficult for students to understand about these concepts, and why. They can listen to student expressions to understand their levels of comprehension or where there are currently challenges in order to respond in ways that help students connect, apply new ideas, and learn. The *teaching presence* involves developing activities that support practicing relevant skills, structuring lessons, and facilitating discussions in the classroom or online. The *social presence* includes becoming visible and connecting as a person. A teacher can show interest in and care for students and create environments in which students feel welcome and that they matter.

In the pairwise overlap between these main presences, we find ways the teacher can regulate learning by helping students focus on useful tasks and goals, supporting discussions both inside and

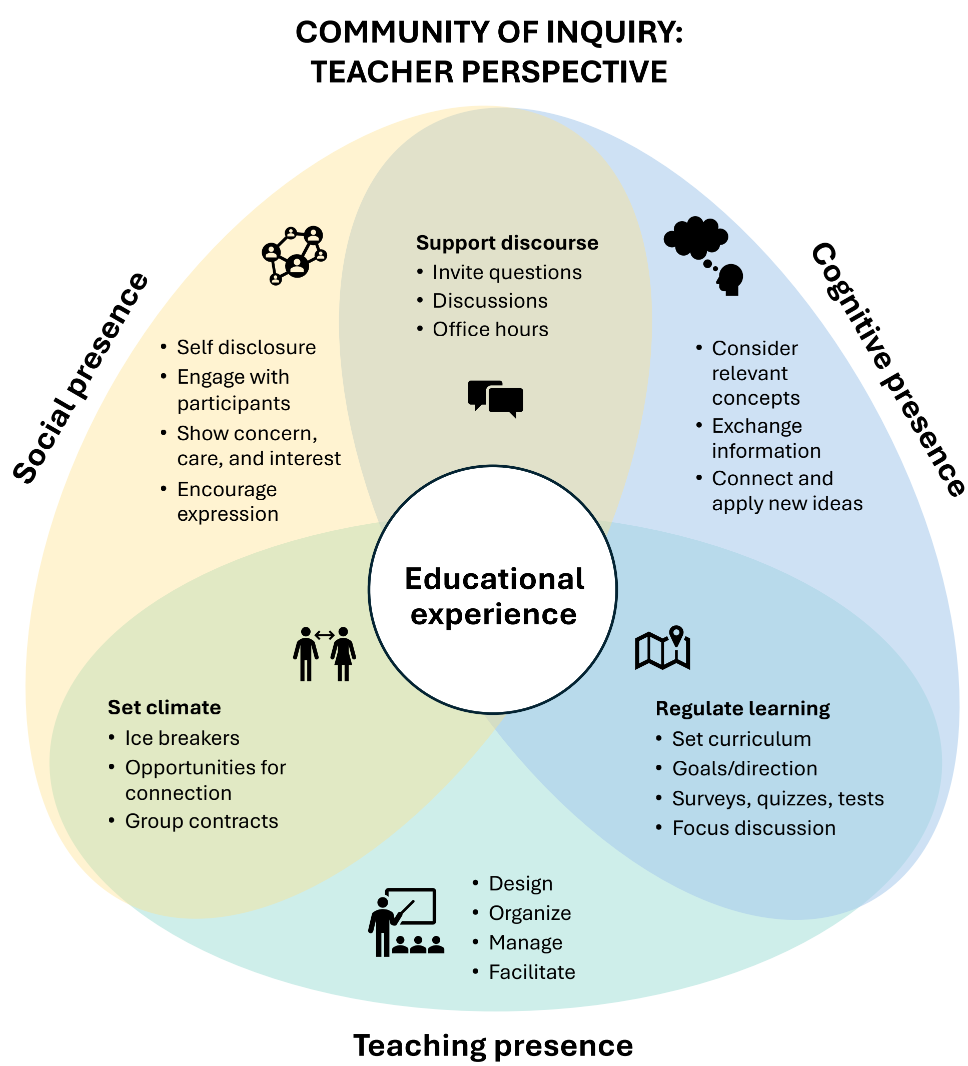

FIGURE 1. Activities that can be useful for creating a Community of Inquiry, from a teacher's perspective.

outside of class, and setting the climate by encouraging students to connect with their peers and providing structure and scaffolding for collaborative work. The total of all these presences forms the *educational experience* in a Community of Inquiry.

The Community of Inquiry framework is also a helpful tool for diagnosing which area of the educational experience might benefit from more attention and provides ideas of what that might look like. Mendoza et al. (2026), for example, use the framework to populate the three presences and their overlap with examples of strategies for creating an inclusive and accessible hybrid classroom. Just how important it is to have all three presences combined became very clear during the COVID-19 pandemic when there was an abrupt shift to online teaching. Many teachers instinctively focused on *cognitive presence*, followed by *teaching presence*. Maintaining sufficient *social presence* was very difficult, especially at the beginning, as everyone had to adjust to the new situation and had to figure out what it was that was actually missing. The experience during the pandemic renewed interest in relationships in learning and teaching, and a lot of advice for building trust with, and showing care for, students exists (e.g., Anderson et al., 2020; Felten and Lambert, 2020; Gravett et al., 2021, Glessmer et al., 2024, Hamshire et al., 2025), often with the goal of working with students as partners to co-create learning and teaching (Cook-Sather et al., 2014; Bovill, 2020).

Co-creation is also where our interest lies. Even though the Community of Inquiry framework is traditionally used to shape student experiences, it considers those experiences from the teacher's perspective. And while teachers can do a lot, we have previously argued that responsibility for learning should be a shared with students (Glessmer and Daae, 2021). What happens if we look at the Community of Inquiry framework from a student's perspective? We share the following thoughts based on our conversation between a student (AÅ), a teacher (KD), and a colleague (MSG) to inspire other teachers not only to think about their own practice but also to consider using the Community of Inquiry framework to talk with students about how they can take responsibility for their own learning and make it more meaningful and enjoyable (see Figure 2).

From a student's perspective, *cognitive presence* involves actively engaging in learning, both during scheduled teaching sessions and outside of them. This includes asking themselves questions, trying

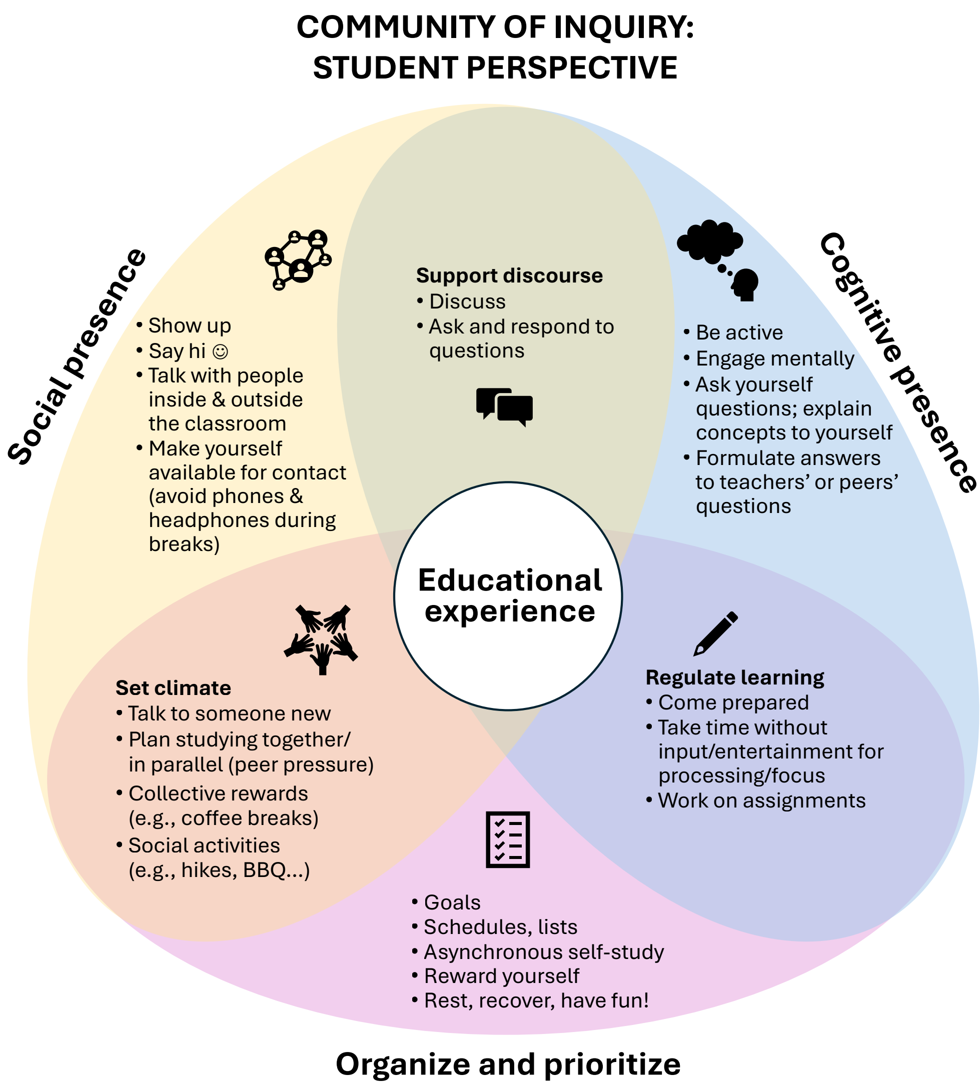

FIGURE 2. Activities that can be useful for creating a Community of Inquiry, from a student's perspective.

to explain concepts to themselves, predicting what a teacher might do next in an explanation, and formulating answers to teachers' or peers' questions. It can also mean taking notes, even though lecture notes or slides may be provided, and writing up a summary of the learning session.

The *teaching presence* is, from a student's perspective, better described as *organizing and prioritizing*, for example, by setting learning goals (in terms of outcomes, time spent on studying, content worked through); using schedules, lists, and asynchronous self-study time; and last but not least, rewarding oneself: rest, recover, and have fun!

From a student's perspective, *social presence* means first showing up and then engaging with peers and teachers: saying "hi," talking with people inside and outside of the classroom, and making themselves available for contact, for example, by putting away phones and headphones during breaks. However, some students may also wish to take a break from social interactions during break time, which is valid.

In the overlap between *social presence* and *organizing and prioritizing* presence, it becomes clear that, for a meaningful and rewarding educational experience, we cannot rely solely on in-class, facilitated interactions. Here, we find ways students can collaborate and integrate meaningful interactions into their lives and learning outside of class—for example, by creating accountability systems such as sticker charts for studying a certain amount of time, where the competitive element with peers might be an extra incentive to show up, or by organizing social events and activities with their peers.

It is, however, important to remember that some students, for whatever reasons, might not want to have relationships with their peers in the course but instead prefer a network separate from the course, with people they meet in other contexts or online. That is also valid, but then it becomes even more important for those students to figure out how to cultivate those relationships and use them for learning.

The other two overlaps between presences from the students' perspective are similar to those from the perspective of teachers. Students can regulate learning by coming prepared, working on assignments, and ensuring a good learning environment, free from disruptions. They can also discuss classroom material with their peers in various settings and visit their teachers during office hours to examine difficult concepts.

So, how can teachers make use of the students' perspectives on the Community of Inquiry framework? From our discussions, we suggest teachers consider the following steps:

1. Present the framework: Explicitly point out the importance of all three presences, alone and in combination, for learning. It is not just about cognitive engagement but also about being organized and doing things with others. The teacher can also create conditions that align with the Community of Inquiry framework and highlight how the methods used are designed to help students in different ways. However, most of the strategies depend on students actively choosing to adopt them.
2. Collect and share stories from older students or alumni regarding how they have organized their work alone and together, and how it has helped them. Learning always happens in a context, and examples from "close to home" tend to be accepted more easily than those that come from an article written by a team on the other side of the world.
3. Talk to students about the model. Do they recognize themselves in it? What strategies do they use that could be added, and which of the ideas presented might they want to try? How can they use the model together with their peers and the teacher to co-create learning and teaching?

We found our discussions between teachers and students meaningful and relevant to help shape better educational experiences. We hope that other teachers and students can build on our ideas and co-create valuable learning experiences in a Community of Inquiry in their own contexts.

REFERENCES

Anderson, V., R. Rabello, R. Wass, C. Golding, A. Rangi, E. Eteuati, Z. Bristowe, and A. Waller. 2020. Good teaching as care in higher education. *Higher Education* 79:1–19, https://doi.org/10.1007/s10734-019-00392-6.

Bovill, C. 2020. *Co-creating Learning and Teaching: Towards Relational Pedagogy in Higher Education*. Critical Publishing, 81 pp.

Cook-Sather, A., C. Bovill, and P. Felten. 2014. *Engaging Students as Partners in Learning and Teaching: A Guide for Faculty*. John Wiley & Sons, 304 pp.

Felten, P., and L.M. Lambert. 2020. *Relationship-Rich Education: How Human Connections Drive Success in College*. Johns Hopkins University Press, 208 pp.

Garrison, D.R., T. Anderson, and W. Archer. 2010. The first decade of the community of inquiry framework: A retrospective. *The Internet and Higher Education* 1(1–2):5–9, https://doi.org/10.1016/j.iheduc.2009.10.003.

Glessmer, M.S., and K. Daae. 2021. Co-creating learning in oceanography. *Oceanography* 34(4):81–83, https://doi.org/10.5670/oceanog.2021.405.

Glessmer, M.S., P. Persson, and R. Forsyth. 2024. Engineering students trust teachers who ask, listen, and respond. *International Journal for Academic Development* 30(1):106–119, https://doi.org/10.1080/1360144X.2024.2438224.

Gravett, K., C.A. Taylor, and N. Fairchild. 2021. Pedagogies of mattering: Re-conceptualising relational pedagogies in higher education. *Teaching in Higher Education* 29(2):388–403, https://doi.org/10.1080/13562517.2021.1989580.

Hamshire, C., R.G. Wilkinson, R. Forsyth, and A. Abdi. 2025. From belonging to mattering to trust: The experiences of minoritised ethnic students in UK higher education. *Higher Education Research & Development* 45(3):572–585, https://doi.org/10.1080/07294360.2025.2552319.

Mendoza, A., A. Venables, and T. Linden. 2026. Inclusive curricula: A framework and recommendations to promote students' sense of belonging in blended-learning environments. *International Journal of Learning, Teaching and Educational Research* 25(4), https://doi.org/10.26803/ijlter.25.4.27.

AUTHORS

Mirjam S. Glessmer (mirjam.glessmer@uib.no) is a senior lecturer at the Centre for Engineering Education, Faculty of Engineering, Lund University, Sweden. **Anne Digranes Årvik** is a master's student in physical oceanography at the Geophysical Institute, University of Bergen, Norway, and a student collaborator on a co-creation project at the Geophysical Institute. **Kjersti Daae** is Associate Professor in physical oceanography and Head of Education at the Geophysical Institute, University of Bergen, Norway.

ARTICLE CITATION

Glessmer, M.S., A.D. Årvik, and K. Daae. 2026. Students co-creating their Community of Inquiry. *Oceanography* 39(2):73–75, https://doi.org/10.5670/oceanog.2026.e208.

COPYRIGHT & USAGE

CAREER PROFILES Options and Insights

Gabby Ahmadia, Vice President, Seascapes and Science, World Wildlife Fund Oceans — gabby.ahmadia@wwfus.org

Degree: When, where, what, and what in?

I took a bit of a long and winding path through my degrees. It began at Humboldt State University, where I took five years to earn a degree in zoology, in part because I was also playing college soccer—a big part of my identity at the time. From there, I went to the University of West Florida for my master's degree in marine biology. That was where I was first exposed to international research, which really shaped what I wanted to do next. I then went on to Texas A&M Corpus Christi for my PhD in coastal and marine systems science, focusing on coral reef fish ecology. I was lucky to work with my advisor, Frank Pezold, who was incredibly supportive. He encouraged me to follow my own interests and career path rather than steering me toward his, which made a lasting impact.

Did you stay in academia at all, and if so, for how long?

Not at all. Toward the end of my PhD, I applied broadly to jobs both within and outside academia. I ended up landing a reef monitoring postdoc at World Wildlife Fund (WWF) right after graduating and have stayed ever since. I am now coming up on 14 years with the organization.

How did you go about searching for a job outside of the university setting?

This was a while ago, and the landscape has changed a lot since then. At the time, I relied heavily on listservs and word of mouth. I remember several people forwarding me the WWF job, thinking it would be a good fit. I also tried to be intentional about timing. I started my job search about six months before graduating and did not rush to finish my degree because I still had funding and health insurance. That extra time allowed me to focus on both the job search and wrapping up manuscripts from my PhD research.

Is this the only job (post-academia) that you've had? If not, what else did you do?

Yes, this has been my only role since finishing my PhD. That said, during my academic years I did a wide range of jobs. I washed athletes' laundry, which was not glamorous, did some consulting on data analysis, helped run a research station, and organized the local Ocean Sciences Bowl. Those experiences, even the less exciting ones, all added something along the way.

What is your current job? What path did you take to get there?

I am currently the VP of Seascapes and Science at WWF Oceans. My interest in this field really started early. I grew up in Hawaiʻi and took a marine biology class as a kid that involved going down to the shoreline to learn about the organisms there. That experience stuck with me. Even though I mostly saw myself as an athlete growing up, I always worked hard in school. As an undergraduate, I did not follow the typical path that many science students take. While others were doing internships, I was working for a local baseball team, spending time at the multicultural center, and picking up whatever jobs I could, including washing some very smelly laundry.

I went on to a master's program focused on marine ecophysiology, but over time I realized I was more drawn to ecology and fisheries science. I enjoy working with data and thinking about systems at a larger scale. For my PhD, I shifted into coral reef fish ecology, which gave me the opportunity to conduct research across the Pacific and Indian Oceans. I had to be resourceful in finding funding, piecing together small grants and AmeriCorps support to make that work.

After finishing my PhD, I joined WWF in a role focused on designing a monitoring program in Indonesia. Helen Fox, who was the Director of Marine Science at WFF, played a key role in mentoring me during that time, especially in helping me understand how to be a strong and respectful partner to local scientists. Over the years, I have had the opportunity to work with an incredible range of partners and teams, helping to connect solid science with conservation in practice. While my role now leans more toward the conservation side, I still rely heavily on scientific thinking and on the scientists on my team when designing and implementing programs.

What did your oceanographic education (or academic career) give you that is useful in your current job?

My academic training gave me a strong foundation in understanding what good science looks like and how to apply it in real-world settings. It also built resilience. Research comes with a lot of ups and downs, and learning how to navigate that has been invaluable. It also instilled in me a sense of curiosity and a habit of questioning assumptions. That mindset has carried through into my career and has helped me stay open to learning and adapting as I take on new challenges.

Is there any course or other training you would have liked to have had as part of your graduate education to meet the demands of the job market?

I think having a well-rounded academic experience is really important. Taking courses that span both policy and the natural sciences can make a big difference. Increasingly, scientists want their work to inform decisions, which means understanding the political and social context in which that work sits and being able to communicate effectively with a wide range of audiences.

I was also taught at one point that scientists should not be advocates. In practice, I do not think that fully holds. If you are not advocating for your work and its relevance, it is unlikely that others will step in to do that for you.

Is the job satisfying? What aspects of the job do you like best/least?

I find the job very satisfying. Being part of a mission-driven organization and working alongside smart, motivated colleagues is incredibly rewarding. One of the best parts of the role is the opportunity to travel and see conservation work firsthand, and to meet the people who are driving that work on the ground. At the same time, travel has become more complicated now that I have a young child at home. Another challenging aspect of the role is the amount of time spent on fundraising. While it is essential to sustaining the work, it does take time away from the parts of the job that I most enjoy.

Do you have any recommendations for new grads looking for jobs?

Persistence is critical. You will hear "no" many times but continuing to put yourself out there and staying open to opportunities both make a difference. It is also important to apply for roles even if you do not meet every listed qualification.

From a hiring perspective, I look not only at experience but also at whether someone is adaptable, curious, and willing to take on new challenges. Those qualities often matter just as much as checking every box on a job description.

ARTICLE DOI. https://doi.org/10.5670/oceanog.2026.e202

Shane Guan, Oceanographer, Bureau of Ocean Energy Management, and Adjunct Assistant Professor, Department of Mechanical Engineering, The Catholic University of America – guan@cua.edu

Degree: When, where, what, and what in?

I received my BSc degree in fisheries science from Nagasaki University, Japan, in 1993, where I was first exposed to marine bioacoustics during a study of humpback whale song structures off Okinawa. Following that experience, I enrolled in the Grice Marine Biology Program at the College of Charleston and earned an MSc degree in marine biology in 1998. My thesis research was on acoustic behavior of free-ranging bottlenose dolphins in the Charleston estuaries. After about 10 years working with the US Fish and Wildlife Service (USFWS) and the National Oceanic and Atmospheric Administration (NOAA), I pursued a PhD degree in underwater acoustics at the Catholic University of America (CUA), where I graduated in 2016. My dissertation research focused on anthropogenic underwater sound and marine soundscape characterization.

Did you stay in academia at all, and if so, for how long?

I always thought that I would like to stay in academia studying marine bioacoustics. But when I completed my MSc degree in the late 1990s, there were very few graduate programs offering that field (my thesis major advisor was an ornithologist!). So, I accepted a job offer as a government biologist, which led to a different career path. However, after completing my PhD, I was offered an adjunct assistant professor position teaching graduate-level classes in ocean acoustics, marine bioacoustics, and computational methods, which I gladly accepted and continue to this day. Though this is a part-time position beside my full-time career with the Bureau of Ocean Energy Management (BOEM), I enjoy the campus atmosphere and scholarly discussion with university faculty and students.

How did you go about searching for a job outside of the university setting?

By the time I completed my MSc degree, the Internet was just becoming a great place to look for jobs beyond the local commuting area. The US government employment website was launched in 1996, and I was able to find many opportunities there. I focused my search on marine biology/zoology related fields and was able to land a job as a biologist at the headquarters of the USFWS Fisheries Program in the Washington, DC, metro area.

Is this the only job (post-academia) that you've had? If not, what else did you do?

No. After six years with the USFWS working on native freshwater fish conservation, which also included a six-month temporary assignment with the US Coral Reef Task Force, I took a job with

NOAA Fisheries. My duties at NOAA were to assess anthropogenic noise effects on marine mammals for the issuance of incidental take authorization (ITA) under the Marine Mammal Protection Act. Utilizing my expertise on underwater acoustics and marine bioacoustics, I provided technical advice to the ITA program. In this capacity, I also developed many noise impact assessment tools and guidelines, and mentored colleagues who did not have acoustics backgrounds. While at NOAA Fisheries, I also took two short-term assignments at other NOAA line offices. One was with the US Integrated Ocean Observing System (IOOS), where I led the development of a metadata convention for underwater passive acoustic recording. The other was with the NOAA Office of Ocean Exploration Research, where I led the environmental assessment for the operations of NOAA Ship *Okeanos Explorer*. Due to my expertise in underwater noise effects on marine species, I was also invited to Taiwan many times to advise on monitoring and mitigation strategies to protect the critically endangered Taiwanese humpback dolphin from underwater noise exposure generated from offshore wind farm development.

What is your current job? What path did you take to get there?

I started my current job with BOEM in 2020 as an oceanographer in the Environmental Studies Program (ESP). My roles are to develop, fund, and manage underwater acoustics, acoustical oceanography, and marine bioacoustics studies that support BOEM's mission to assure that offshore energy, mineral, and geological resources are developed in an environmentally responsible way, and to ensure that BOEM's regulatory decisions are informed by the best available science and are fully compliant with statutory obligations. I work closely with external and internal scientists to conceptualize and formulate research ideas and turn them into studies that advance BOEM's mission. In the years since I joined the bureau, I have participated in research projects, led workshops, and collaborated on papers and reports. As with my previous government positions, I simply applied for the job on https://www.usajobs.gov/ and went through the competitive hiring process.

What did your oceanographic education (or academic career) give you that is useful in your current job?

I took quite extensive oceanographic and marine science courses—ranging from physical and biological oceanography, marine geology, ichthyology, marine zoology, and botany to aquaculture and even maritime affairs—both in my undergraduate and postgraduate (master's) years. These classes provided me with broad knowledge and appreciation of topics related to ocean science and technology that are critical in pursuing my career as an ocean acoustician.

Is there any course or other training you would have liked to have had as part of your graduate education to meet the demands of the job market?

Machine learning, geospatial tools, and software developer platforms. Though I am a proficient MATLAB user, which enables me to perform a variety acoustic signal processing tasks and analyses at work, I wish that I had had more training in information technology early on.

Is the job satisfying? What aspects of the job do you like best/least?

Absolutely! Being able to connect with academia and actively participate in research is the best part of my job. It is satisfying to know that the study results are valuable to resource managers for environmental compliance and science-informed decision-making. However, the ever-shifting change in priorities can sometimes be challenging to ensure the continuity of studies.

Do you have any recommendations for new grads looking for jobs?

Be flexible and look beyond your field of study. Oceanography is an interdisciplinary field, and I have observed that graduate students with cross-disciplinary knowledge and expertise are more likely to land jobs than those who only focus on their specific fields. Additionally, networking during conferences and workshops and being active in professional societies are great ways to establish connections that could lead you to your dream job.

ARTICLE DOI. https://doi.org/10.5670/oceanog.2026.e203